Short-term health effects of air pollution and viral exposure

Lammers, A.

Publication date
2021
Document Version
Final published version

Short-term health effects of air pollution and viral exposure

Ariana Lammers

Short-term health effects of air pollution and viral exposure

Ariana Lammers

ISBN	978-94-93270-11-4
Cover	Guus Gijben & Elke Smit
Layout	Guus Gijben
Print	Proefschrift-aio.nl

The work described in Part II of this thesis was funded by the Netherlands Ministry of Infrastructure and Water Management, as part of grant M240045 and commissioned to the National Institute for Public Health and the Environment. The work described in Part III of this thesis was supported by an unrestricted grant from Chiesi Pharmaceuticals, institutional funding from the Amsterdam UMC location AMC, Amsterdam UMC, University of Amsterdam (IA601011).

Financial support for the publication of this thesis was kindly provided by: Stichting Astma Bestrijding, Chipsoft, Chiesi Pharmaceuticals and Boehringer Ingelheim.

Short-term health effects of air pollution and viral exposure

ACADEMISCH PROEFSCHRIFT

ter verkrijging van de graad van doctor
aan de Universiteit van Amsterdam
op gezag van de Rector Magnificus
prof. dr. ir. K.I.J. Maex
ten overstaan van een door het College voor Promoties ingestelde commissie,
in het openbaar te verdedigen in de Agnietenkapel
op donderdag 28 oktober 2021, te 10.00 uur

door Ariana Lammers

geboren te Seria

Promotiecommissie

Promotor:	prof. dr. A.H. Maitland – van der Zee	AMC-UvA
Copromotores:	dr. S.J. Vijverberg	AMC-UvA
	dr. A.H. Neerincx	AMC-UvA
Overige leden:	prof. dr. E.H.D. Bel	AMC-UvA
	prof. dr. P.J. Sterk	AMC-UvA
	dr. J. Altenburg	AMC-UvA
	prof. dr. ir. R.C.H. Vermeulen	Universiteit Utrecht
	prof. dr. F.J. van Schooten	Universiteit Maastricht
	dr. S.M. Cristescu	Radboud Universiteit Nijmegen

Faculteit der Geneeskunde

Table of contents

Part I.

Introduction

Chapter 1.
General introduction

General introduction

Environmental exposure

It has been established that our health is not only determined by our genome, but also by environmental factors (also known as the exposome), such as lifestyle, socioeconomic status and environmental exposure. An important part of our environmental exposure is the air we breathe, as it is in direct contact with our respiratory system. Although environmental air consist of oxygen, an essential component for our body cells to function, it can also consists of hazardous agents, like air pollutants, cigarette smoke, and bacterial and viral components. These environmental substances can have a major impact on human health, that include but not limit to our respiratory system.

With the abundance of road traffic and the increasing number of aviation, air pollution is one of the major concerns regarding environmental exposure. Short-term and long-term exposure to air pollution can induce both acute and chronic health effects. These effects range from upper respiratory irritation to chronic respiratory and cardiovascular disease, and have been linked to premature mortality and reduced life expectancy [1]. This makes air pollution an important factor with respect to both personal and public health. Another important external exposure are viral components, as clearly demonstrated by the corona pandemic. The most common viral infectious agent in humans, is the rhinovirus. It is the predominant cause of a common cold [2] and comes with a great economic burden in terms of absenteeism and medical visits [3]–[5]. Yet, certain aspects about the health effects of air pollution and rhinoviruses remain unanswered and require further research and/or new methods of assessment, as will be described in more detail below.

Air pollution

Air pollution is a complex mixture of solid and gaseous components, such as nitrogen oxides (NOx, NO2), ozone (O3), sulphur dioxide (SO2) and particulate matter (PM). It has been established that exposure to air pollution is associated with adverse health effects, in which especially PM exposure has shown to increase morbidity and mortality due to pulmonary and cardiovascular events (e.g. asthma exacerbations, bronchitis, cardiac arrhythmias) [1], [6]–[8]. PM consists of carbonaceous particles together with organic chemicals and reactive metals, mainly originating from fossil fuel combustion [9]. These particulates can be inhaled, in which their size determines where they deposit in the respiratory tract; coarse particles (PM10, diameter 2.5–10 μm) do not pass the upper airways, whereas fine particles (PM2.5, diameter <2.5 μm) deposit in the smaller airways

and ultrafine particles (UFP or PM0.1, diameter <0.1 μm) reach the alveoli **(Figure 1)**. Concerns about UFP are rising, as these particles are potentially more toxic, due to their high surface-to-mass ratio and their ability to pass the alveolar wall and enter the blood stream [10]–[12].

Short-term exposure to UFP have shown to induce oxidative stress, and pulmonary, as well as, systemic inflammation [13]–[17], and to increase blood pressure and heart rate [18], [19], however, the causality between UFP exposure and cardiorespiratory effects remain inconclusive or insufficient [8], [20]. On top of that, most studies focus on UFP from road traffic [20], while aviation is also an important source of UFP and a major contributor to elevated UFP levels around large airports [21], [22]. Moreover, aviation-related UFP have a different chemical composition and tend to be smaller (mainly 10-20 nm) [21], [23] when compared to road traffic-related UFP (mainly >50 nm) [24], [25], and therefore the toxicity between these UFP sources may differ. This not only raises concerns for airport workers, but also for residents that live in the proximity of major airports. Altogether, this emphasizes the importance of studies investigating the possible health effects of exposure to aviation-related UFP, in which this thesis focusses on the short-term health effects in healthy adults **(Part II)**.

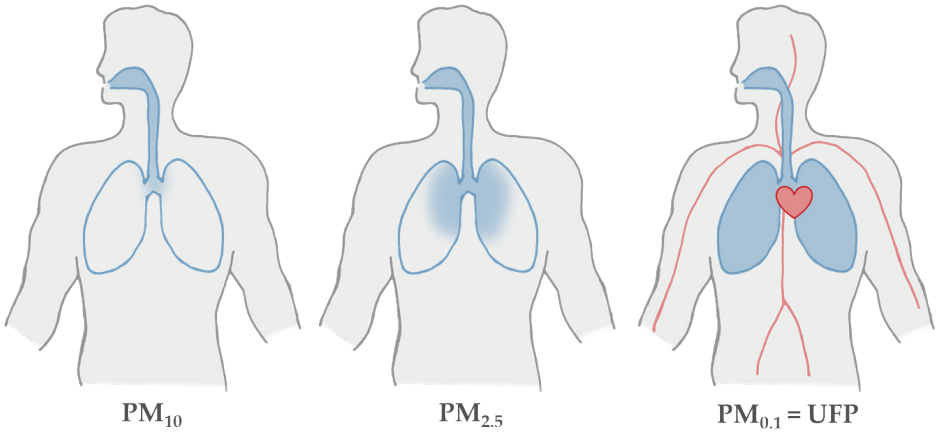

Figure 1. Through inhalation, particulate matter can enter the respiratory tract, in which particulates penetrate deeper into the lungs with decreasing size. Particles 2.5 – 10 μm (PM10) deposit in the upper airways, particles < 2.5 μm (PM2.5) in the smaller airways and particles <0.1 μm (PM0.1 = UFP) in the alveoli, but can diffuse over the alveolar wall and enter the circulation. This makes UFP potentially more toxic, as it can possibly induce reactions throughout the body.

Viral exposure

Other environmental exposures that are of importance for our health, are infectious diseases. Among viral infections in human, the rhinovirus (RV) is the most prevalent one, especially during fall and spring [26], [27]. It is transmitted through aerosols of respiratory droplets and contaminated surfaces, including direct person-to-person contact [28]. RV infections are the predominant cause of a common cold, and have socioeconomic consequences due to absenteeism from school and work [3]–[5]. Moreover, RV infections are also allied with the disease burden of asthma, as they are the primary cause of virus-induced worsening of asthma symptoms (i.e. exacerbations), such as wheezing, chest tightness and breathlessness, in both children [29], [30] and adults [31]. These exacerbations can lead to emergency visits and hospitalizations, making it a major burden for asthmatic patients [32], [33].

As treatment is modestly effective during such episodes [34], early detection or prediction of exacerbations could play an essential role in timely treatment or interventions, in order to prevent an exacerbation or reduce its progression. This would require a better understanding and assessment of biological processes during both stable and unstable states of asthma. It is believed that biological processes continuously fluctuate (i.e. homeokinesis), even under resting conditions, and that these fluctuations play a key role in the adaptive capacity of physiological systems in response to changing environmental conditions [35]. In chronic diseases, including asthma, such fluctuations may be either too rigid or overly unstable [36] and can be altered by external triggers like a rhinovirus [37], possibly leading to exacerbations.

Monitoring of these fluctuations could potentially enable early detection and prediction of disease instability, however, would require the assessment of biomarker-based metrics. Biomarkers are biological components, including proteins, genes and metabolites, that are indicative of e.g. a disease state or treatment response [38] and can be used to identify biological processes involved in pathogenesis. To make biomarkers feasible for clinical practice, especially with respect to home monitoring purposes, they need to be non-invasive, cheap and easy-to-collect. This could facilitate more direct feedback on disease control for patients and possibly lead to fewer hospital visits. Therefore, this thesis focusses on fluctuations in non-invasive biomarkers for the detection of a rhinovirus infection in both healthy and asthmatic adults **(Part III)**.

Metabolomics

As mentioned above, one of the methods to discover new biomarkers is through the study of metabolites in biological samples, i.e. metabolomics. Metabolites are small molecules, that are (end) products of metabolic processes and are present in biological specimens such as urine, exhaled breath, plasma, serum and feces. When compared to other biological measurements (e.g. genomics, transcriptomics and proteomics), the metabolome is uniquely suited for distinguishing phenotypes and capturing the impact of environmental factors on metabolic processes [39] **(Figure 2)**. The latter makes it hold promise for the assessment of air pollution exposure and rhinovirus infections. Of the different metabolic specimens that can be assessed, exhaled breath and urine are of high interest, as they are non-invasive and easily accessible samples.

Exhaled breath consists of volatile organic compounds (VOCs), that either have an exogenous (from the environment) or endogenous (from metabolic processes) origin. The VOC metabolites are of interest regarding biomarker discovery, as they can reflect local respiratory, as well as, systemic pathological processes [40]. They particularly have shown increased clinical potential in chronic airway diseases, including but not limited to the detection of phenotypes, disease activity and infectious diseases [40], [41], as described thoroughly in **Chapter 2**.

Urine is the primary route of excretion for cellular waste and therefore a biofluid rich in metabolites. These metabolites mostly originate from the circulation, through filtration of the blood by the kidneys, and therefore hold great potential for detection of pathway dysfunction from across the body [42]. They can reflect changes in pathological, pharmacological and physiological conditions, ranging from inflammation [43] and infectious diseases [44], to diabetes [45] and cancer [46].

Despite the increasing number of studies investigating metabolites in breath and urine, the number of clinically validated and implemented metabolites is modest. Further research in biomarker discovery and validation is required to expand the use of biomarkers for diagnostic purposes, health and disease monitoring, and treatment response detection or prediction. In this thesis, we focussed on how metabolites in exhaled breath and urine are affected by environmental exposures.

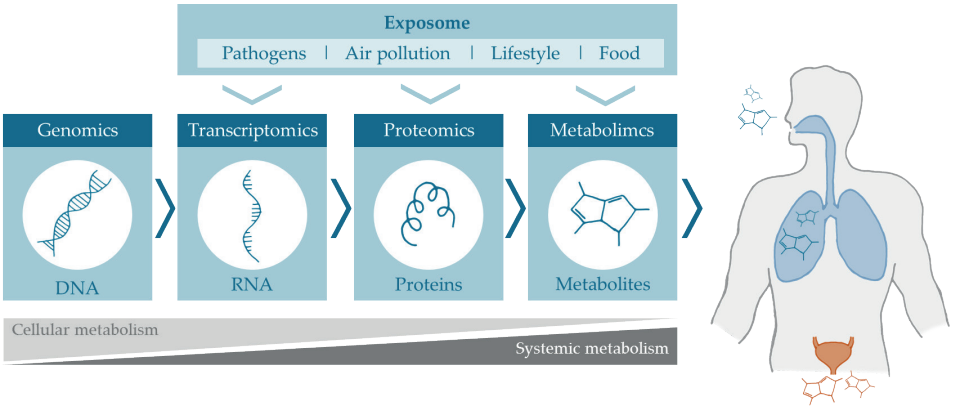

Figure 2. Omics aims to characterize and quantify the function and dynamics of an organism through the assessment of biological molecules. Genomic, transcriptomics and proteomics mainly reflect the cellular metabolism, and are of interest for the assessment of hereditary and acquired factors. Metabolomics reflects the systemic metabolism, and is highly suitable for distinguishing phenotypes, as well as, for the assessment of environmental influences. Therefore, this thesis has focused on the influences of the exposome (i.e. air pollution and rhinoviruses) on the metabolic content in easily accessible biological specimen; exhaled breath and urine.

Objectives and outline of this thesis

The overall aim of this thesis was to investigate how environmental exposures, more specifically air pollution and rhinoviruses, have short-term health effects in healthy and asthmatic adults, through the assessment of both commonly used cardiorespiratory function measurements, and novel biomarkers (i.e. metabolites) in breath and urine.

1. The first objective of this thesis was to investigate the short-term effects of 5h-exposures to air pollution, focused on ultrafine particles, near a major airport and two highways in healthy subjects on cardiorespiratory function, the exhaled breath profile and the metabolites in urine.

2. The second objective was to investigate the effect of a rhinovirus-16 challenge on the fluctuations in the exhaled breath profile of healthy volunteers and mild asthmatic patients.

This thesis consists of four parts, in which **Part I** is the introduction of this thesis. It consists of a general introduction describing how environmental exposure, more specifically air pollution and rhinoviruses, can effect health and/or disease stability and how more insight into these effects is needed, that can possibly be gained through biomarkers in exhaled breath and urine **(Chapter 1)**. Furthermore, it consists of an extensive review on exhaled breath analysis, including different exhaled breath detection techniques and the potential of exhaled breath analysis in respiratory diseases **(Chapter 2)**. **Part II** focusses on air pollution and describes the effects of short-term exposures to air pollution near a major airport on cardiorespiratory function **(Chapter 3)**, exhaled breath profiles **(Chapter 4)** and metabolites in urine **(Chapter 5)**. Next, **Part III** focusses on the effects of a rhinovirus-16 challenge on the fluctuations in exhaled breath profiles of mild asthmatics and healthy volunteers **(Chapter 6)**. Lastly, **Part IV** contains a summary of the main findings of this thesis and a general discussion describing the methodological challenges in and future perspectives of environmental exposure research **(Chapter 7)**.

References

[1] M. Kampa and E. Castanas, "Human health effects of air pollution," *Environmental Pollution*. 2008.

[2] H. A. Rotbart and F. G. Hayden, "Picornavirus infections: A primer for the practitioner," *Archives of Family Medicine*. 2000.

[3] K. L. Nichol, S. D'Heilly, and E. Ehlinger, "Colds and influenza-like illnesses in university students: Impact on health, academic and work performance, and health care use," *Clin. Infect. Dis.*, 2005.

[4] J. S. Bertino, "Cost burden of viral respiratory infections: Issues for formulary decision makers," in *American Journal of Medicine*, 2002.

[5] A. M. Fendrick, A. S. Monto, B. Nightengale, and M. Sarnes, "The economic burden of non-influenza-related viral respiratory tract infection in the United States," *Arch. Intern. Med.*, 2003.

[6] R. D. Brook *et al.*, "Particulate matter air pollution and cardiovascular disease: An update to the scientific statement from the american heart association," *Circulation*, vol. 121, no. 21, pp. 2331–2378, 2010.

[7] H. Khreis, C. Kelly, J. Tate, R. Parslow, K. Lucas, and M. Nieuwenhuijsen, "Exposure to traffic-related air pollution and risk of development of childhood asthma: A systematic review and meta-analysis," *Environment International*. 2017.

[8] U.S. EPA, "Integrated Science Assessment (ISA) for Particulate Matter (Final Report, 2019).," *U.S. Environ. Prot. Agency*, 2019.

[9] F. J. Kelly and J. C. Fussell, "Size, source and chemical composition as determinants of toxicity attributable to ambient particulate matter," *Atmos. Environ.*, vol. 60, pp. 504–526, 2012.

[10] K. S. Hougaard *et al.*, "A perspective on the developmental toxicity of inhaled nanoparticles," *Reprod. Toxicol.*, 2015.

[11] M. R. Miller *et al.*, "Inhaled Nanoparticles Accumulate at Sites of Vascular Disease," *ACS Nano*, 2017.

[12] H. J. Heusinkveld *et al.*, "Neurodegenerative and neurological disorders by small inhaled particles," *NeuroToxicology*. 2016.

[13] M. Khatri *et al.*, "Nanoparticles from photocopiers induce oxidative stress and upper respiratory tract inflammation in healthy volunteers," *Nanotoxicology*, 2013.

[14] K. Donaldson and V. Stone, "Current hypotheses on the mechanisms of toxicity of ultrafine particles," *Ann. Ist. Super. Sanita*, vol. 39, no. 3, pp. 405–410, 2003.

[15] K. Donaldson, V. Stone, A. Seaton, and W. MacNee, "Ambient particle inhalation and the cardiovascular system: Potential mechanisms," *Environ. Health Perspect.*, 2001.

[16] N. Li *et al.*, "Ultrafine particulate pollutants induce oxidative stress and mitochondrial damage," *Environ. Health Perspect.*, 2003.

[17] V. Stone *et al.*, "Ultrafine particle-mediated activation of macrophages: Intracellular calcium signaling and oxidative stress," in *Inhalation Toxicology*, 2000.

[18] K. J. Chuang, C. C. Chan, G. M. Shiao, and T. C. Su, "Associations between submicrometer particles exposures and blood pressure and heart rate in patients with lung function impairments," *J. Occup. Environ. Med.*, vol. 47, no. 11, pp. 1093–1098, 2005.

[19] R. Vora *et al.*, "Inhalation of ultrafine carbon particles alters heart rate and heart rate variability in people with type 2 diabetes," *Part. Fibre Toxicol.*, 2014.

[20] S. Ohlwein, R. Kappeler, M. Kutlar Joss, N. Künzli, and B. Hoffmann, "Health effects of ultrafine particles: a systematic literature review update of epidemiological evidence," *Int. J. Public Health*, vol. 64, no. 4, pp. 547–559, 2019.

[21] M. P. Keuken, M. Moerman, P. Zandveld, J. S. Henzing, and G. Hoek, "Total and size-resolved particle number and black carbon concentrations in urban areas near Schiphol airport (the Netherlands)," *Atmos. Environ.*, vol. 104, pp. 132–142, 2015.

[22] N. Hudda, T. Gould, K. Hartin, T. V. Larson, and S. A. Fruin, "Emissions from an international airport increase particle number concentrations 4-fold at 10 km downwind," *Environ. Sci. Technol.*, vol. 48, no. 12, pp. 6628–6635, 2014.

[23] B. Stacey, "Measurement of ultrafine particles at airports: A review," *Atmos. Environ.*, vol. 198, no. October 2018, pp. 463–477, 2019.

[24] L. Liu, B. Urch, R. Poon, M. Szyszkowicz, M. Speck, and D. R. Gold, "Ambient particle sizes and systemic biomarkers," vol. 534, no. 6, p. 6, 2015.

[25] R. M. Harrison, D. C. S. Beddows, and M. Dall'Osto, "PMF analysis of wide-range particle size spectra collected on a major highway," *Environ. Sci. Technol.*, 2011.

[26] E. Arruda, A. Pitkäranta, T. J. Witek, C. A. Doyle, and F. G. Hayden, "Frequency and natural history of rhinovirus infections in adults during autumn," *J. Clin. Microbiol.*, 1997.

[27] M. J. Mäkelä *et al.*, "Viruses and bacteria in the etiology of the common cold," *J. Clin. Microbiol.*, 1998.

[28] S. E. Jacobs, D. M. Lamson, S. Kirsten, and T. J. Walsh, "Human rhinoviruses," *Clin. Microbiol. Rev.*, 2013.

[29] N. W. Johnston *et al.*, "The September epidemic of asthma exacerbations in children: A search for etiology," *J. Allergy Clin. Immunol.*, 2005.

[30] G. P. Rakes *et al.*, "Rhinovirus and respiratory syncytial virus in wheezing children requiring emergency care: IgE and eosinophil analyses," *Am. J. Respir. Crit. Care Med.*, 1999.

[31] K. G. Nicholson, J. Kent, and D. C. Ireland, "Respiratory viruses and exacerbations of asthma in adults," *Br. Med. J.*, 1993.

[32] H. K. Reddel *et al.*, "An official American Thoracic Society/European Respiratory Society statement: Asthma control and exacerbations - Standardizing endpoints for clinical asthma trials and clinical practice," *Am. J. Respir. Crit. Care Med.*, vol. 180, no. 1, pp. 59–99, 2009.

[33] R. Y. Suruki, J. B. Daugherty, N. Boudiaf, and F. C. Albers, "The frequency of asthma exacerbations and healthcare utilization in patients with asthma from the UK and USA," *BMC Pulm. Med.*, 2017.

[34] R. J. B. Loymans *et al.*, "Comparative effectiveness of long term drug treatment strategies to prevent asthma exacerbations: Network meta-analysis," *BMJ*, 2014.

[35] A. L. Goldberger, L. A. N. Amaral, J. M. Hausdorff, P. C. Ivanov, C. K. Peng, and H. E. Stanley, "Fractal dynamics in physiology: Alterations with disease and aging," *Proc. Natl. Acad. Sci. U. S. A.*, 2002.

[36] U. Frey, G. Maksym, and B. Suki, "Temporal complexity in clinical manifestations of lung disease," *Journal of Applied Physiology*. 2011.

[37] A. Sinha *et al.*, "Loss of adaptive capacity in asthmatic patients revealed by biomarker fluctuation dynamics after rhinovirus challenge," *Elife*, vol. 8, 2019.

[38] A. J. Atkinson *et al.*, "Biomarkers and surrogate endpoints: Preferred definitions and conceptual framework," *Clinical Pharmacology and Therapeutics*. 2001.

[39] F. R. Pinu *et al.*, "Systems biology and multi-omics integration: Viewpoints from the metabolomics research community," *Metabolites*, 2019.

[40] M. P. Van Der Schee, T. Paff, P. Brinkman, W. M. C. Van Aalderen, E. G. Haarman, and P. J. Sterk, "Breathomics in lung disease," *Chest*, 2015.

[41] P. Brinkman, A. H. M. Van Der Zee, and A. H. Wagener, "Breathomics and treatable traits for chronic airway diseases," *Current Opinion in Pulmonary Medicine*. 2019.

[42] S. Bouatra *et al.*, "The Human Urine Metabolome," *PLoS One*, 2013.

[43] A. Julià *et al.*, "Urine metabolome profiling of immune-mediated inflammatory diseases," *BMC Med.*, 2016.

[44] H. Lv, C. S. Hung, K. S. Chaturvedi, T. M. Hooton, and J. P. Henderson, "Development of an integrated metabolomic profiling approach for infectious diseases research," *Analyst*, 2011.

[45] R. M. Salek *et al.*, "A metabolomic comparison of urinary changes in type 2 diabetes in mouse, rat, and human," *Physiol. Genomics*, 2007.

[46] L. Yu, C. Jiang, S. Huang, X. Gong, S. Wang, and P. Shen, "Analysis of urinary metabolites for breast cancer patients receiving chemotherapy by CE-MS coupled with on-line concentration," *Clin. Biochem.*, 2013.

Chapter 2.

Breathomics in chronic airway diseases

Lammers A *
Van Bragt JJMH *
Brinkman P
Neerincx AH
Bos LD
Vijverberg SJH
Maitland-van der Zee AH

Systems Medicine, Elsevier, 2021: 244-255

** both authors contributed equally to this work.*

Abstract

Chronic airway diseases cause a large burden for patients and caregivers and have large economic impact. Moreover, the burden is expected to increase with an increasing life expectancy of the world population. Therefore, there is a need for new biomarkers that can guide diagnosis, monitoring and the treatment of chronic airway diseases.

Exhaled breath contains a complex mixture of volatile organic compounds (VOC) that can reflect local, systemic and exogenous (patho)physiological processes in the airways and alveoli and may thus be a promising target for biomarker discovery. Furthermore, breathomics holds the potential for non-invasive, easy, safe and point-of-care analysis. Several techniques for exhaled breath analysis exist that can be distinguished by three main aspects; the ability to detect individual VOCs or VOC patterns, real-time or offline measurements, and targeted or untargeted approaches. Available techniques have different advantages and limitations regarding sensitivity, specificity, costs and complexity. Multiple clinical studies already show the many opportunities of exhaled breath analysis regarding disease diagnosis, monitoring and prediction in diseases like asthma, chronic obstructive pulmonary disease (COPD) and cystic fibrosis (CF).

To allow for implementation of exhaled breath in clinical practice, limitations of current detection techniques (e.g., the need for highly specialized personnel and machinery or sensitivity to detect very low concentrations of molecules in exhaled breath) should be overcome and results should be validated. Breathomics has large potential to make more personalized treatment possible in chronic airway diseases.

Introduction

Respiratory diseases are among the leading causes of death worldwide [1]. In European Union countries, one in eight deaths and 7% of all hospital admissions are due to respiratory conditions [1]. In general, chronic airway diseases affect the lungs as well as other parts of the respiratory system. They usually develop slowly and sometimes progress over time. Not all chronic lung diseases have a clear cause, however, some are known to be hereditary (e.g., cystic fibrosis), triggered by smoking tobacco (or second-hand smoke) or associated with different forms of air pollution.

In this article we will explain what breathomics is and what its value can be in several chronic airway diseases, focussing on asthma, chronic obstructive pulmonary disease (COPD) and cystic fibrosis. Therefore, we first discuss disease characteristics and current burdens and challenges in diagnostics and treatment, for which breathomics might be of use.

Asthma and COPD

The most frequent chronic airway diseases are asthma and COPD. Asthma is known for variable bronchoconstriction, airway hyper responsiveness, mucus secretion and a chronic inflammation of the airways. The hallmark trait of COPD is chronic inflammation, leading to structural changes and a loss of alveolar attachments. Asthma and COPD are expected to cause an increasing burden with aging of the world population [2], already causing 0.4 and 3.2 million global deaths in 2015 [3], respectively. Direct health care expenses in the US alone totalled 32.1 billion for COPD in 2010 [4] and 56 billion dollars for asthma in 2006 [5].

Over the past decades it has become clear that the “old” definitions of asthma and COPD seem to be an oversimplification of reality as both diseases are complex and heterogeneous conditions, expressed in a multitude of different phenotypes that often share overlapping traits. A precise characterization of these different phenotypes is key in the development and identification of new (precision) therapies that are suitable for a specific group of patients. Disease control is an important factor in the quality of life of patients and caregivers, therefore easy applicable and non-invasive monitoring tools are essential to detect deterioration early on. This can lead to more timely (and better targeted) treatment and consequently, to less lung damage.

Cystic fibrosis

A more rare, however life-shortening, chronic airway disease is cystic fibrosis (CF), with around 70,000 patients worldwide. It is an incurable, genetic disorder that mostly affects the lungs, but also the pancreas, intestines, liver and kidneys. It is characterized by thick mucus production due to a deficiency in the cystic fibrosis transmembrane conductance regulator (CFTR) protein, leading to difficult breathing, coughing and recurrent respiratory infections.

One of the major issues in CF is that patients are prone to acquire bacterial respiratory infections. Early in life, CF patients are most frequently infected with *Staphylococcus aureus* (*S. aureus*) (60–70%), whereas later in life *Pseudomonas aeruginosa* (*P. aeruginosa*) (70–80%) becomes more prevalent [6], [7]. Respiratory infections, especially with *P. aeruginosa*, lead to worsening of symptoms (i.e., exacerbations), hospitalizations, and lung function decline [8]. Currently, lung infections are mostly detected using sputum cultures, however, this method lacks both sensitivity and specificity. Furthermore, coughing up sputum is unpleasant for patients and sometimes difficult to perform, especially for kids. This causes treatment delay, leading to failure of eradication treatment and eventually chronic infections. For this reason, there is a need for a more accurate and easy way of detecting respiratory infections in CF.

Biomarkers in breath

To enable improvement in management and control of chronic airway diseases, it is needed to capture the complexity of the biological pathways involved in the disease. Instead of using a single biomarker, this complexity might be better captured by multiple biomarkers using so-called omics techniques. One of these omics techniques is metabolomics; the study of metabolic content of a cell, organ system, or organism. It can be performed in various samples such as blood, sputum, urine and exhaled breath. Analysis of the exhaled breath's metabolic content, is called breathomics. The advantage of breath over other biomarker samples, is its non-invasive nature. In addition, the collection of exhaled breath is safe as well as easy to perform for patients and caregivers. It is of special interest in pulmonary medicine, because of the intensive contact of breath with the respiratory tract.

Volatile organic compounds

Exhaled breath mainly contains nitrogen (~75%), oxygen (~13%), carbon dioxide (~6%) and water (~5%), however about 1% consists of volatile organic compounds (VOCs). These compounds are gaseous organic molecules that can either be of exogenous or endogenous origin. Exogenous VOCs are inhaled

from the environment with some VOCs having no interaction with human tissue, whereas others do interact and can sometimes be stored inside the body. Endogenous VOCs are produced by all metabolic processes of or in the body, either locally (i.e., in the lungs) or systemically (i.e., elsewhere in the body). This also includes VOCs of microbial origin such as bacteria, fungi and viruses. Therefore, exhaled VOCs do not exclusively represent pulmonary metabolism, but include all inhaled VOCs and those diffusing from the tissue and circulation into the alveoli and airways [9]. Moreover, reactions between these VOCs can occur.

The VOC composition of breath changes with various pathophysiological processes and could therefore contain useful information and be of added value for chronic airway diseases regarding diagnostics, phenotyping, exacerbation prediction, treatment stratification and treatment response [9]. Therefore, breathomics may help in providing a more personalized approach in respiratory medicine.

Outline of this article

In this article, we first describe exhaled breath sampling methods. Hereafter, the techniques for detection of VOCs in exhaled breath will be explained as well as their advantages and challenges. Finally, the clinical implications and opportunities in chronic airway diseases will be discussed, followed by future perspectives of breathomics.

Sampling of exhaled breath

In general, exhaled breath analysis starts with breath sample collection, with samples being either stored and/or pre-concentrated before detection (offline) or measured directly (online). The method of sampling exhaled breath can have profound effects on the obtained results due to several factors, as will be described below. Harmonization is therefore necessary and the European Respiratory Society (ERS) issued a special task force to provide recommendations for standardization of sampling, analyzing and reporting of exhaled breath (data) [10]. The information in the following paragraphs is largely based on the technical standard created by this task force.

Collection and storage

Most equipment is not able to perform analysis in real-time (there are some exceptions, as will be mentioned later), thus exhaled breath needs to be collected, stored and transported before analysis is possible. Collection of exhaled breath requires a device that is inert, meaning the device is made from a material that does not emit VOCs itself (or only a very minimum amount). Furthermore, as cleaning agents might also emit VOCs and pose a risk for carry-over effects, the collection device is preferably disposable. Another option is the use of Tedlar (polyvinyl fluoride) bags where washings with ultra-pure nitrogen after use have shown to deliver acceptable repeatability. Due to the low concentrations of VOCs that are present in exhaled breath (parts per billion (ppb) to parts per million (ppm) range), pre-concentration is often necessary before analysis. Therefore, the exhaled air in the collection device is pumped over sorbent traps or coated fibers, causing the VOCs the be adsorbed on sorbent material. Different sorbents have different affinities for specific VOCs and will thus have an influence on the results. Sorbents with low water-binding affinity are preferred, because water vapor can affect the results of certain analytical methods.

Maneuvers and ambient VOCs

Besides the need for the proper equipment to collect exhaled breath, the exhalation maneuver and correction for ambient air VOCs are equally important. Roughly, exhaled breath can be collected by two different ways. By expiratory sampling, which uses total breath, and by alveolar sampling, where the dead space is discarded first. By making a distinction between alveolar and total breath, it is possible to collect air from different compartments and thus to focus on different disease areas. For different compounds in exhaled breath, an exhalation flow-dependency has been reported. This implies that alteration in flow can affect the patterns that eNose sensors can detect. Correcting for ambient air VOCs is necessary to isolate the signals that arise from the VOCs that originate from processes in the patient itself. In general there are two ways of doing this. First, in- and exhalation filters can be applied to let patients breathe VOC-free air during a wash-in period, before measurement. Second, VOCs in ambient air can be measured simultaneously to the exhaled breath measurement and hereafter ambient VOCs concentrations will be deducted from exhaled breath VOCs.

Exhaled breath detection methods

Methods for detection of VOCs in exhaled breath already exist for several decades, originating from the 1950s. However, since the 1990s several new methods have been developed. This section starts with a broad explanation of exhaled breath detection methods followed by a more detailed description about the techniques that are commonly used for exhaled breath analysis.

Different approaches for VOC detection

Techniques for exhaled breath analysis can be distinguished by three main aspects (see Table 1). First, the method of detection, which can be based on individual VOC detection and/or patterns of VOC mixtures. Secondly, measurements of the exhaled breath can be either real-time or offline, requiring exhaled breath sampling and storage. Finally, an important aspect is the ability for a targeted or untargeted approach. Untargeted approaches are always hypothesis generating and should be followed by targeted approaches to confirm and validate the results. Eventually, this could mean it is better to go from a highly sensitive, complex and/or possibly expensive technique, towards a cheaper, easier, faster and/or bed-side suitable approach.

Other important characteristics are the sensitivity and specificity for VOC detection. Sensitivity is the ability to measure small quantities of the volatiles of interest and is usually expressed in parts per billion or trillion of volume (ppbv or pptv, respectively). Specificity is the ability to relate the measurement signal to only the volatiles of interest and not to other compounds. Moreover, aspects such as costs, complexity, and the size of the devices are also important, especially for clinical applicability. The detection principle and characteristics of several detection techniques will be described extensively below and are depicted in Figure 1.

Spectrometry: offline method

Before all new technologies were developed, gas chromatography combined with mass spectrometry (GC-MS) was the gold standard for exhaled breath analysis, existing since 1959. It allows for separation and identification of individual chemical compounds for both targeted and untargeted analysis, however always in an offline manner. The first part of the device is a gas chromatograph, consisting of a column that enables separation of different volatiles due to the differences in chemical properties between molecules and their relative affinity for the stationary phase of the column. The second part is a mass spectrometer

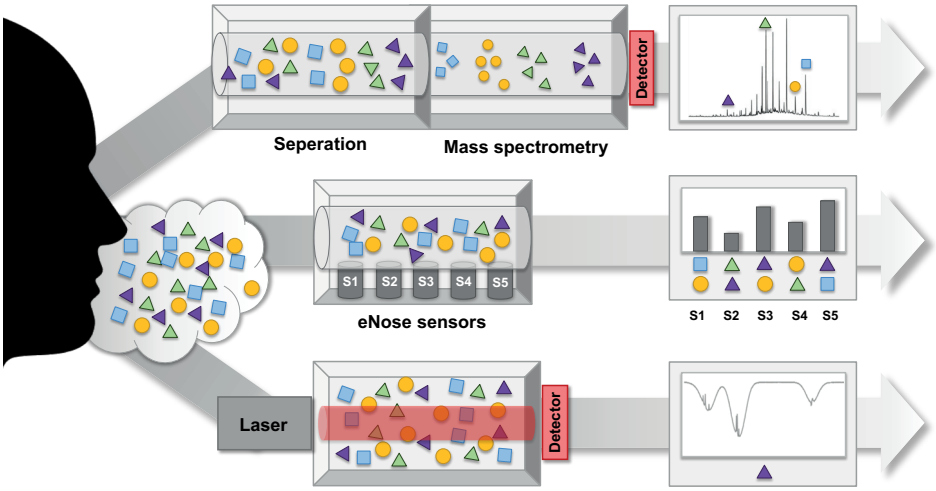

Figure 1. Schematic overview of different approaches for detection of VOCs (depicted by the coloured triangles, circle and square) in exhaled breath. The top part represents techniques that are based on chemical separation, with or without physical detection, of VOCs. This approach starts with a form of separation, based on e.g., GC, PTR, SIFT or ion mobility, followed by MS, that measures specific mass-to-charge ratios for each compound. The middle part represents eNose technology, which is based on cross-reactive chemical sensors followed by pattern recognition. The bottom part represents physical detection of VOCs using laser light, which allows for quantification of specific compounds. This could be only one compound, as depicted in the figure, but may also be several compounds.

Table 1. Overview of the different aspects of exhaled breath detection techniques

	Detection		Measurement		Approach	
	Molecule	**Pattern**	**Real-time**	**Offline**	**Targeted**	**Untargeted**
GC-MS	Y	~	N	Y	Y	Y
PTR-MS SIFT-MS	Y	~	Y	~	Y	~
IMS	~	Y	Y	~	~	Y
eNose	N	Y	Y	~	N	Y
LAS	Y	~	Y	~	Y	N

Y stands for yes, meaning the technique is suitable for this purpose. N stands for no, indicating that the technique cannot be used for this purpose. The symbol ~ means that it is possible, but that the technique is not per se meant and/or often used for this purpose. GC-MS, gas chromatography-mass spectrometry; PTR-MS, proton-transfer reaction mass spectrometry; SIFT-MS, selected ion flow tube mass spectrometry; IMS, ion mobility spectrometry; eNose, electronic nose; LAS, laser absorption spectroscopy.

that captures, ionizes (commonly by electric ionization), accelerates, deflects and detects the ionized molecules by breaking each molecule into ionized fragments and detecting these ionized fragments using their mass-to-charge (m/z) ratio.

Major advantages of GC-MS are its high sensitivity (pptv-ppbv) and specificity for compound identification and the possibility to detect multiple compounds at the same time. An extensive library exists for GC-MS detected volatiles, enabling linkage of the VOCs to molecular and biological pathways. It is an excellent technique for both exploratory untargeted, as well as targeted analysis in airway disease. To increase the separation resolving power and the resolution in mass data, the GC-Ms can be extended to a 2-dimensional GC (GC x GC) and a time of flight (TOF) mass spectrometry, respectively [11].

The main disadvantages of GC-MS are the necessity of breath collection and pre-concentration, combined with the long analysis time (about an hour). This makes GC-MS time consuming, and prone to significant losses of compounds or contamination of the sample [12]. Especially small highly volatile compounds are challenging to store, making the detectable mass to charge range of the GC-MS method only between 30 and 500 Da. Secondly, quantification of the VOCs is difficult and the mass spectra are rather complex. Therefore, GC-MS is, in its current state, unsuitable for direct findings during consultation or bed-side measurements [13]. Finally, GC-MS is a costly technique with high acquisition (about $100–200k) and maintenance costs and requires well-trained personnel, making it less feasible for clinical implementation.

Spectrometry: online methods

In order to allow real-time, rapid and sensitive analysis in a clinical setting, extensive research has been conducted to develop alternative spectrometry methods. The most commonly used in exhaled breath analysis include proton-transfer reaction mass spectrometry (PTR-MS), selected ion flow-tube mass spectrometry (SIFT-MS) and ion mobility spectrometry (IMS). There are different pros and cons for all three techniques, as will be described below.

PTR-MS and SIFT-MS

Compared to GC-MS, relatively new techniques are proton-transfer reaction mass spectrometry (PTR-MS) and selected ion flow tube mass spectrometry (SIFT-MS), originating from around 1995 [14], [15]. Both techniques allow detection, as well as quantification of VOCs in an online and real-time manner and are mainly suitable for a targeted approach. These techniques are based on so-called soft chemical ionization; meaning there is little fragmentation of the molecules [16].

For PTR-MS, volatiles in the exhaled breath are ionized using gas phase H_3O^+ ions, which are subsequently separated using a mass spectrometer based on their m/z ratio. A disadvantage of this technique, is that only molecules with a proton affinity higher than water can be detected. To overcome this limitation, SIFT-MS was developed [17]. This technique is based on the same principle as PTR-MS, however, the use of three reagent ions (i.e., H_3O^+, NO^+ and $O2^+$) makes it suitable for detection of volatiles with lower proton affinities than water [18].

The main advantage of both techniques are the ability to quantify exhaled volatiles. Absolute concentrations can be obtained without previous calibration measurements. Secondly, these techniques are fast (i.e., milliseconds time range) and online, enabling real-time measurements in exhaled breath. They eliminate the need for sample preparation [18], [19], pre-concentration and chromatography or other forms of separation [17], making them more applicable for clinical implementation. Furthermore, both techniques are very sensitive, with detection limits ranging from ppbv to pptv [20]. Finally, these methods are associated with less fragmentation when compared to GC-MS, making the interpretation of the mass spectra easier.

Unfortunately, identification of VOCs by these techniques is not always possible [12], since characterization is merely based on m/z ratios and, unlike GC-MS, no extensive compounds library exists [16]. Just like GC-MS, these techniques are associated with high costs, require trained personnel and are mainly suitable for a laboratory setting.

Ion mobility spectrometry

A different technique is ion mobility spectrometry (IMS), first developed in the 1950s and 1960s [21]. It allows for real-time measurements and is suitable for untargeted analysis using pattern recognition. It is a separation method based on differences in gas-phase ion mobilities [22], [23]. The ionized analytes migrate through an electric field at characteristic velocities according to their mass, charge, size, shape and interaction with collision gas [22].

The main advantage of IMS is that it is a simple and inexpensive technique working at ambient pressures and temperatures [23], [24]. In the last decade, the devices have become smaller and in some cases even portable. Furthermore, IMS enables fast (i.e., milliseconds time range) and sensitive (ppbv) detection of VOCs in exhaled breath [24].

However, IMS alone will likely not be sufficient for the identification of each volatile. Volatiles in exhaled breath frequently have similar or even the same mobility and can therefore not be distinguished. To overcome this problem, IMS can be linked to a MS to further separate the volatiles based on mass and charge [21]. However, this also means that the technique would become more complex and expensive, nullifying some of the advantages of IMS regarding clinical applicability.

eNose technology

Even though direct and online (mass) spectrometry methods have been developed, there is still a need for smaller devices that are affordable, accurate, user-friendly, fast and preferably real-time. A method that might fulfill these criteria is electronic nose (eNose) technology. In this section, the general principle of eNose technology is explained followed by a summary of the different eNose devices that have been used most in exhaled breath research.

The methodology of eNose technology is very different from MS methods, since it is an approach based on chemical sensors. The method of eNose technology resembles the human olfactory system; a system not based on highly specific receptors, but on a combination of broad sensitive receptors with the brain serving as a reference database. Electronic noses consist of cross-reactive sensor arrays in which the sensor properties change due to VOC exposure [25], [26]. The cross-reactive nature of the sensors allows for multiple volatiles to interact with the same sensor and *vice versa*, depending on the affinity of the VOC for the sensor and its substrate [27]. This results in a pattern of sensor signals, a so-called "breathprint", that can be analyzed using pattern recognition algorithms.

The main advantages of eNose technology is that it is a fast, simple, cheap and easy technique. It is useful for real-time point-of-care probabilistic diagnostic and monitoring purposes [28]. For this purpose, identification of individual molecular compounds is not always necessary.

However, the inability to detect and identify individual compounds remains the major limitation of eNose technology [29]. Therefore, it can be useful to combine GC-MS and eNose technology in research. With GC-MS the specific compounds can be detected and compared with the eNose sensors, to eventually allow for implementation of more specific eNose sensors [30]. Next to the lack of specificity, generally, eNose sensors tend to have limited sensitivity; mainly ppmv, however sometimes also ppbv. In addition, most sensors are unstable and are prone to baseline drift, depending on the sensing material. This causes issues with repeatability [31] and inter-device reproducibility [16].

eNose sensors and devices

Different types of sensors have been applied in different eNoses. Table 2 indicates different eNoses devices that have been/are being used in clinical studies and used different eNose sensor arrays.

Conducting polymer composite sensors change in electrical resistance after exposure to gases due to VOC induced expansion of the polymer composite [32]. The sensitivity to detect VOCs depends on the vapor pressure of the specific compounds. Low vapor pressure compounds have a higher tendency to stay in the composite polymer, thus causing easier expansion and are therefore able to be detected in the low ppb range. High vapor pressure compounds need concentrations in the high ppm range. An example eNose that uses these sensors is the Cyranose® 320 (Sensigent, CA, USA), applying an array that consists of 32 sensors. This eNose is already being used for quality control in diverse (petrochemical/food) industries and in medical research.

Table 2. An overview of different eNose types that have been used in clinical research.

Name eNose	Sensor type	Disease areas
Cyranose 320	32 conducting polymer composite sensors	Asthma, COPD
Tor Vergata enose prototype	Quartz crystal microbalance gas sensors	Asthma, COPD
Aeonose	Arrays of 3 metaloxide sensors	Asthma, and CF (children), COPD
SpiroNose	Arrays of 7 metaloxide sensors	Asthma, COPD, CF
Owlstone Lonestar	Field asymmetric ion mobility spectrometry	Asthma

COPD, Chronic Obstructive Pulmonary Disease; CF, Cystic Fibrosis.

Another type of sensors are quartz crystal microbalance gas sensors that are coated by molecular films of metalloporphyrins. This technique is based on the proportionality of the frequency of the quartz crystals to adsorbed mass and therefore the change of resonant frequency caused by the absorption of molecules by the films. These sensors have a fast response time, but poor signal to noise ratio [32]. An eNose (proto)type using these sensors was developed by Tor Vergata University (Rome, Italy).

Metal oxide sensors have been used in multiple eNoses. These sensors obtain semiconducting characteristics under high temperatures and are able to interact with reducing/oxidizing VOCs in a gas. This affects the resistance of the oxide, and therefore affects the conductance. Metal oxide sensors are used by

the Aeonose® (eNose company, Zutphen, the Netherlands) and SpiroNose® (Breathomix B.V., Reeuwijk, the Netherlands). The Aeonose uses three different sensors in its array and heating cycles to generate signals that are captured and pre-processed according to an algorithm named Tucker3. The SpiroNose uses arrays of seven different metal oxide sensors and is integrated with advanced cloud-based software that automatically corrects for ambient room VOCs. Furthermore the SpiroNose is able to provide immediate feedback, signifying an important step forward in the applicability of eNose technology in the point-of-care.

Laser absorption spectroscopy

Although pattern recognition by eNose technology could be sufficient for some purposes, it may be necessary to not only specifically but also quantitatively measure certain compounds. For this purpose, laser absorption spectroscopy (LAS) is very suitable. It is the foremost used technique to assess gas phase atoms and molecules quantitatively (i.e., concentration or amount), and is mainly used for detection of only one or a few compounds in a real-time and targeted manner. The method is based on the absorption of light by VOCs in the breath sample. Each molecule has its own unique absorption fingerprint, since they absorb very specific wavelengths. The amount of absorbed light is related to the concentration of the target VOC in the sample [16].

Important properties of LAS is its high sensitivity (ppbv-ppmv), specificity and selectivity in complex gas mixtures [33]–[35]. Furthermore, the ability to provide absolute quantification of a VOC in exhaled breath down to below parts-per-billion by volume levels is a major advantage [36]. The LAS-based methods are suitable for real-time measurements and can be made into compact sensors requiring low maintenance, as desired for medical implementation.

Unfortunately, LAS is only suitable for detection of small molecules and cannot characterize a large number of molecules at the same time [37]. Furthermore, any noise in the optical system can affect deteriorate the sensitivity of the technique.

Summary of detection methods

Overall, GC-MS could be seen as the foremost technique for identification of multiple VOCs in an exhaled breath sample. For quantification of multiple VOCs with a broad size range, the previously mentioned online MS techniques would be more optimal, whereas for quantification of one specific and small volatile, LAS techniques could be preferred. Currently, eNose technology seems to be the

most suitable for online and bed-side monitoring since the devices tend to be small, portable and inexpensive. However, this might change in the future, since new compact and real-time detection techniques are being developed.

Clinical implications

Various groups have been working on exhaled breath analysis in a clinical setting, mainly in differentiating between patients with an established diagnosis and healthy controls or differentiating between various diseases. Early studies have aimed to prove that these groups are being reflected by distinct VOC patterns. Later research has shifted to the applicability of breathomics in phenotyping and the identification of sub phenotypes that are susceptible to certain treatment. Other applications are thought to be in phenotyping and eventually the ability to predict exacerbations. Throughout the following chapters the terms phenotype and endotype will be used. With phenotype we mean a (sub)group that shares common characteristics (of disease), while endotype indicates the biological pathway, and corresponding cells and molecules, that result in a phenotype.

Asthma

Diagnosis of Asthma

One of the first studies that aimed to discriminate patients with an established asthma diagnosis from healthy controls based on exhaled VOCs has been performed by Dragonieri *et al.* in 2007 [38]. They used the Cyranose 320 to show that different exhaled VOC mixtures ("smellprints" as they were called in this study or "breathprints" as we tend to call them now) exist between both mild and severe asthmatics and controls. However, a difference between mild and severe asthma could not be found. Later studies with various eNoses confirmed the differences in breathprints between patients with different severities of asthma and healthy controls [39], [40]. A study with 27 asthmatics and 24 (healthy) controls, that used a prototype eNose from Tor Vergata university, was able to correctly classify patients with asthma compared with controls in 87.5% of the cases when alveolar air was sampled and in 72.5% of cases when total air was sampled [39] In this study, the eNose was able to outperform the more traditional fraction of exhaled Nitric Oxide (FeNO) measurements and spirometry, even when those were used in combination with each other. A more recent study found that another eNose, the Aeonose, was able to discriminate between children with asthma and controls with an AUROC of 0.87 [40].

Phenotyping in Asthma

It has become clear that the current taxonomy in respiratory disease is an oversimplification of reality. To properly treat patients, it is important to classify patients according to their phenotype of disease and exhaled breath is a promising, quick and non-invasive biomarker to achieve this. Volatiles identified by GC-MS, in combination with clinical features and asthma therapy, have already identified different distinct endotype clusters [41]. Later research used breathomics to identify different clusters in patients with chronic respiratory diseases, without using the labels asthma or COPD. The clusters that were found differed in inflammatory pattern and clinical characteristics, but interestingly all clusters included both asthma and COPD patients [42] It has also been shown that significant differences exist between cluster-stable and cluster-migrating patients [43]. The study by *De Vries et al*. made use of the SpiroNose, *Brinkman et al*. used a platform of different eNoses (using metal oxide-, quartz-microbalance- and organic polymer sensors and field asymmetric ion mobility spectrometry) to identify 3 eNose driven clusters with differences in circulating blood eosinophil and neutrophil percentages and differences in ratios of patients that were using systemic corticosteroids. Eosinophils in sputum were found to be associated with the difference in cluster-stable and -migrating patients. Taken together, these results show a large potential of breathomics in asthma phenotyping and in the identification of distinct inflammatory processes. The Cyranose could also discriminate between different inflammatory phenotypes in asthma [44] and another recent, large study showed that VOCs identified by GC-MS in exhaled breath are able to discriminate between two important inflammatory phenotypes in asthma; eosinophilic asthma and neutrophilic asthma [45]. In the latter study, GC-MS samples were obtained from 276 asthma patients and several compounds were identified able to discriminate between the phenotypes. A later validation set of 245 asthma patients confirmed 4 of these VOCs. When these VOCs are combined with FeNO and blood eosinophils a very high accuracy was achieved to predict eosinophilic asthma (AUROC = 0.9). In conclusion, breathomics research has provided very promising evidence for (sub)phenotyping of asthma patients, what might be of importance for its application in monitoring of asthma and in predicting treatment response. Fields with an unmet need for quick, and non-invasive biomarkers.

Monitoring and personalizing treatment of Asthma

The use of systemic corticosteroids (i.e., prednisone) causes a huge burden on patients and not all patients benefit from its use. Therefore, as a step towards the ability to personalize asthma treatment, the ability to predict systemic steroid responsiveness has been studied in 25 asthma patients using a Cyranose. The

results of this study showed that exhaled breath was able to predict treatment response in patients with established asthma and was able to identify patients that experience loss of control after they stop the use of systemic corticosteroids [46]. More recent research further confirms that exhaled breath could be a very valuable tool in the monitoring of loss of control in asthma [47]. Both GC-MS and the eNose platform (see "Phenotyping in asthma" section) proved able to correctly classify baseline measurements versus loss of control and loss of control versus patients that recovered. The eNose platform, in this instance most significantly driven by the ion mobility spectrometer (IMS), showed a higher accuracy than GC-MS. These two studies provide evidence that breathomics is able to retrospectively discriminate between responders/non-responders and that longitudinal monitoring of exhaled breath can be applicable to detect clinical instability in asthma patients.

Exacerbations are periodical flare-ups of disease, commonly characterized by an acute worsening of symptoms, requiring an increase in treatment or start with systemic immunosuppressants or antibiotics. Exacerbations can be triggered by a variety of stimuli (e.g., virus infections, exposure to noxious gasses, stress, etc.), therefore a quick and proper characterization of its origin can be very helpful to start adequate treatment on time. A combination of six or seven VOCs measured by GC/MS has already proven able to predict an asthma exacerbation in children with high specificity and sensitivity [48]. The same study showed that specific VOCs are able to monitor the course of an exacerbation.

COPD

Diagnosis and phenotyping of COPD

The ability to discriminate between healthy controls and patients was not only found in asthma, but also in COPD patients. GC-MS has been used to detect 1179 different VOCS between 50 COPD patients and 29 controls [49]. Further analysis revealed that 13 VOCs were needed to classify all 79 subjects in the study correctly. Six out of these 13 VOCs were still able to correctly classify 92% of the patients and later 29 out of 32 subjects in the independent validation population. Interestingly, 14 out of 15 steroid naive COPD patients were correctly classified, what seemed to exclude treatment influence. A study with 30 patients assessed the ability of the Cyranose to discriminate between patients with COPD and patients with lung cancer by examining the difference in VOC patterns [50]. This study showed a distinct difference and discriminant analysis provided a cross-validation value of 90% correctly classified.

Exhaled breath not only proved able to distinguish between respiratory patients and healthy controls, but is more importantly also able to discriminate between different respiratory diseases. The Cyranose was tested in 90 patients and proved able to discriminate between asthma and COPD with a very high accuracy (cross-validated accuracy = 96% correctly classified) [51]. However, this very high accuracy to discriminate between asthma and COPD was not confirmed in the BreathCloud cohort that de Vries *et al.* used for their study. This is not surprising however, as the labels "asthma" and "COPD" are difficult to apply to patients and overlap between these diagnoses exist inspiring key respiratory researchers to believe that there should be less emphasize on the old labels. Instead they make a call for the identification of "treatable traits" in patients [52], [53].

Monitoring and treatment of COPD

In both mild and moderate COPD, exhaled breathprints (both eNose and GC-MS) have shown to be associated with differential cell counts and with soluble sputum markers of activated neutrophils and eosinophils [54]. This may be an indication that exhaled breathprints can be used in monitoring airway inflammation in COPD. A study that included both the Cyranose and the Tor Vergata eNose, showed a difference in breathprints after treatment with different combinations of bronchodilators and inhaled corticosteroids (ICS), but the eNoses were not able to discriminate breathprints after bronchodilator alone and combination of bronchodilator and ICS [55]. Exacerbations in COPD have a large impact on the (irreversible) deterioration of lung function in patients, therefore they have been the subject of multiple studies that applied exhaled breath analysis. The SpiroNose has shown the ability to discriminate between patients that did/did not experience an exacerbation ≤ 3 months prior to measurement [56]. Other studies showed differences in exhaled breathprints between stable COPD patients and frequent exacerbating COPD patients [57] and a moderate discriminatory ability between viral and bacterial infections in stable COPD patients [58]. These studies show the potential for breathomics in monitoring of COPD patients and might even suggest a role in guiding treatment.

Cystic fibrosis

Monitoring of CF

Exhaled breath analysis in CF patients is less relevant for diagnostic purposes, since current diagnostic tools are sufficient; new-borns are accurately screened for CF using neonatal heel pricks followed by genealogical DNA tests and sweat chloride testing [59], [60]. However, with the recent developments in treatments for CF patients, there is a growing demand for non-invasive methods to monitor disease development, activity and progression.

As a first attempt, several studies have tried to distinguish CF from both healthy controls as other chronic airway diseases, such as asthma, using exhaled breath analysis. The distinction between CF patients and healthy controls, based on both MS and eNose technology, showed moderate to excellent accuracy (AUROC 0.77–0.96) [40], [61]–[64]. However, in every study a different technique was used and, in all the MS based studies, different VOCs for this discrimination were found, making validation studies of high importance. When compared to asthmatics, CF patients had different exhaled breath profiles based on broadband quantum cascade laser-based spectroscopy [65], as well as eNose technology (AUROC of 0.90) [40]. In the study of Paff et al. eNose technology (i.e., Cyranose) was able to distinguish CF from primary ciliary dyskinesia (PCD) patients with a good sensitivity (89%), but with a low specificity (56%) [64]. Taking all these studies together, it seems that not only inflammatory processes occurring in chronic airway diseases can be detected in the exhaled breath, but also the specific respiratory disease.

A highly relevant purpose of exhaled breath analysis in CF could be the monitoring of disease instability, preferably before clinical symptoms or exacerbations occur. Therefore, several studies have tried to detect exacerbations in CF patients using exhaled breath. In 2006, Barker *et al.* showed that pentane levels measured by GC-MS were elevated in CF patients with exacerbation compared to stable patients [61]. In the study by Paff *et al.* differences existed between patients with and without exacerbations for both CF patients (sensitivity 89%, specificity 56%) as PCD patients (sensitivity 100%, specificity 90%) using eNose technology (Cyranose 320) [64]. For future research, it is highly relevant to investigate the potential of exhaled breath analysis for exacerbation detection and prediction in a longitudinal manner.

Detection of respiratory infections

Patients with chronic airway diseases can be burdened with respiratory infections. Due to their disease, they may have more complaints which may persist for a longer period when compared to healthy people. Currently, airway infections are detected by sputum culture. Sputum is a thick fluid produced by the lower airways during infections, not to be confused with saliva. Culturing of this sputum allows for bacteria and fungi to grow and become visually detectable under the microscope. Unfortunately, the culturing commonly takes a day or several days and lacks both sensitivity and specificity. Moreover, expectorating sputum is unpleasant and not always possible for patients to do. Therefore, different methods for detection of respiratory infections are studied, among which exhaled breath analysis. It is known that bacteria themselves can

produce volatiles, making exhaled breath analysis an interesting non-invasive and possibly real-time tool for detection of respiratory infections. Moreover, VOCs in exhaled breath may potentially be a more accurate detection method than sputum culture, since sputum often come from only one part of the lungs while exhaled breath may represent the whole lung.

Infections in CF

Cystic fibrosis is one of the foremost chronic airway diseases suffering from respiratory infections. Patients with CF have thickened mucus production, which makes it hard for them to clear respiratory infections. Often, CF patients eventually get infected chronically, which has a big impact on their lung function both short-term and long-term. More than other chronic airway disease patients, it is hard for CF patients to expectorate sputum, especially in the early stage of the disease. This makes the detection of respiratory infections in sputum challenging leading to possible treatment delay, which is known to increase the chance of chronic infections in CF patients. Exhaled breath analysis as an alternative method for infection detection is therefore of special interest for these patients.

Volatiles coming from *Pseudomonas aeruginosa* (*P. aeruginosa*) and *Staphylococcus aureus* (*S. aureus*) have been studied the most in CF, since these bacteria have the highest prevalence. The review of Bos *et al.* [66] gives a clear overview of volatiles associated with six pathogens, among which *P. aeruginosa* and *S. aureus*, found in at least two studies that either used clinical samples or reference strains. Compounds that were specifically found for *P. aeruginosa* were: 1-undecene, 2,4-dimethyl-1-heptane, 2-butanone, 4-methyl-quinazoline, hydrogen cyanide (HCN), and methyl thiocyanide. The volatile biomarkers for identification of *S. aureus* were isovaleric acid and 2-methyl-butanal.

For detection of *P. aeruginosa* multiple techniques have been used already, among which GC-TOFMS showed good accuracy (AUROC of 0.86) [67], as well as eNose technology (i.e., SpiroNose) with a cross-validation value of 82.4% and an AUROC of 0.93 [68]. In another study of Enderby *et al.* [69], SIFT-MS was used to detect *P. aeruginosa* infections in exhaled breath. They specifically measured hydrogen cyanide (HCN) concentrations, which were higher in CF patients infected with *P. aeruginosa* (13.5 ppb) than in asthmatics (2.0 ppb) who were free of any infection. Later, Gilchrist *et al.* [70] investigated whether HCN concentrations, also measured with SIFT-MS, could serve as a screening test for *P. aeruginosa* infections in CF. Compared to most exhaled breath studies in CF, they included a large CF population (n = 233) and had a long follow-up period (i.e.,

two years). At the start of the study all CF children were free from *P. aeruginosa* and at the end 71 of them got infected. They showed that with every 1 ppb increase in exhaled HCN, the odds of *P. aeruginosa* infection increased by 212%. Although this resulted in a high specificity (99%), sensitivity was lacking (33%) and therefore seems to be unsuitable for screening of *P. aeruginosa* infections in CF.

Among other infections investigated in CF, detection of *S.aureus* showed to have an excellent sensitivity (100%) and high specificity (80%) using GC-MS [71], and a high accuracy (AUROC 0.88) using GC-TOFMS [67]. Furthermore, *Aspergillus fumigatus* also seems to alter the exhaled breath profile in CF patient with an AUROC of 0.89 using eNose technology (i.e., Cyranose 230) [72].

Overall, exhaled breath analysis could potentially be an easy and accurate method for detection of respiratory infections. However, so far, most studies examining VOCs from pathogens in CF patients have mainly been rather small and cross-sectional. Moreover, validation of results is often lacking. It is necessary to increase the number of patients in the studies and to externally validate the results in independent research groups to make conclusions about the accuracy and applicability of exhaled breath analysis for infection detection in clinical practice [73].

Future perspectives

Overall, exhaled breath analysis has many advantages: it is non-invasive, allows point-of-care testing and can be easy to perform for both patients as care-givers. It offers opportunities for detection of highly specific and individual biomarkers as well as overall metabolic profiles. However, challenges exist as well. Several technical aspects regarding breath sampling and detection should be overcome to increase the suitability for bed-side or even home monitoring. Regarding future research, it is important to conduct more longitudinal studies and to externally validate results, before clinical implementation can be achieved. For now, it is believed that exhaled breath analysis may be a promising tool in a personalized approach for diagnosing, monitoring and treatment in chronic airway diseases.

References

[1] G. J. Gibson, R. Loddenkemper, Y. Sibille, and B. Lundbäck, Eds., "The burden of lung disease," in *European Lung white book*, 2019th ed., Sheffield: ERS Publications Office, pp. 2–15.

[2] P. Burney, D. Jarvis, and R. Perez-Padilla, "The global burden of chronic respiratory disease in adults.," *Int. J. Tuberc. Lung Dis.*, vol. 19, no. 1, pp. 10–20, 2015.

[3] J. B. Soriano *et al.*, "Global, regional, and national deaths, prevalence, disability-adjusted life years, and years lived with disability for chronic obstructive pulmonary disease and asthma, 1990–2015: a systematic analysis for the Global Burden of Disease Study 2015," *Lancet Respir. Med.*, vol. 5, pp. 691–706, 2017.

[4] E. S. Ford, L. B. Murphy, O. Khavjou, W. H. Giles, J. B. Holt, and J. B. Croft, "Total and state-specific medical and absenteeism costs of COPD among adults aged ≥ 18 years in the United States for 2010 and projections through 2020," *Chest*, vol. 147, no. 1, pp. 31–45, 2015.

[5] P. A. Loftus and S. K. Wise, "Epidemiology and economic burden of asthma," *Int. Forum Allergy Rhinol.*, vol. 5, no. March, pp. S7–S10, 2015.

[6] R. L. Gibson, J. L. Burns, and B. W. Ramsey, "Pathophysiology and Management of Pulmonary Infections in Cystic Fibrosis," *American Journal of Respiratory and Critical Care Medicine*. 2003.

[7] M. Barley *et al.*, "MISSION OF THE CYSTIC FIBROSIS FOUNDATION Annual Data Report 2016 Cystic Fibrosis Foundation Patient Registry," *Int. J. Mol. Sci.*, 2017.

[8] J. Emerson, M. Rosenfeld, S. McNamara, B. Ramsey, and R. L. Gibson, "Pseudomonas aeruginosa and other predictors of mortality and morbidity in young children with cystic fibrosis," *Pediatr. Pulmonol.*, 2002.

[9] L. D. Bos, P. J. Sterk, and S. J. Fowler, "Breathomics in the setting of asthma and chronic obstructive pulmonary disease," *J. Allergy Clin. Immunol.*, vol. 138, no. 4, pp. 970–976, 2016.

[10] I. Horváth *et al.*, "A european respiratory society technical standard: Exhaled biomarkers in lung disease," *Eur. Respir. J.*, vol. 49, no. 4, 2017.

[11] H. D. Bean, J. M. D. Dimandja, and J. E. Hill, "Bacterial volatile discovery using solid phase microextraction and comprehensive two-dimensional gas chromatography-time-of-flight mass spectrometry," *J. Chromatogr. B Anal. Technol. Biomed. Life Sci.*, 2012.

[12] B. Buszewski, M. Kesy, T. Ligor, and A. Amann, "Human exhaled air analytics: Biomarkers of diseases," *Biomedical Chromatography*. 2007.

[13] B. Henderson *et al.*, "Laser spectroscopy for breath analysis: towards clinical implementation," *Appl. Phys. B Lasers Opt.*, vol. 124, no. 8, pp. 1–21, 2018.

[14] A. Hansel, A. Jordan, R. Holzinger, P. Prazeller, W. Vogel, and W. Lindinger, "Proton transfer reaction mass spectrometry: on-line trace gas analysis at the ppb level," *Int. J. Mass Spectrom. Ion Process.*, 1995.

[15] D. Smith and P. Španěl, "The SIFT and FALP techniques; applications to ionic and electronic reactions studies and their evolution to the SIFT-MS and FA-MS analytical methods," *Int. J. Mass Spectrom.*, 2015.

[16] C. Lourenço and C. Turner, "Breath Analysis in Disease Diagnosis: Methodological Considerations and Applications," *Metabolites*, vol. 4, no. 2, pp. 465–498, 2014.

[17] D. J. Beale *et al.*, *Review of recent developments in GC–MS approaches to metabolomics-based research*, vol. 14, no. 11. Springer US, 2018.

[18] P. Španěl and D. Smith, "Quantitative selected ion flow tube mass spectrometry: The influence of ionic diffusion and mass discrimination," *J. Am. Soc. Mass Spectrom.*, 2001.

[19] P. Španěl and D. Smith, "Progress in SIFT-MS: Breath analysis and other applications," *Mass Spectrom. Rev.*, 2011.

[20] D. Smith, P. Španěl, J. Herbig, and J. Beauchamp, "Mass spectrometry for real-time quantitative breath analysis," *Journal of Breath Research*. 2014.

[21] A. B. Kanu, P. Dwivedi, M. Tam, L. Matz, and H. H. Hill, "Ion mobility-mass spectrometry," *Journal of Mass Spectrometry*. 2008.

[22] W. Liu and H. H. Hill, "High-Performance Ion Mobility Spectrometry," in *Comprehensive Analytical Chemistry*, 2015.

[23] H. Borsdorf and G. A. Eiceman, "Ion mobility spectrometry: Principles and applications," *Appl. Spectrosc. Rev.*, 2006.

[24] R. Fernández, "Ion mobility spectrometry: history, characteristics and applications," *Rev. U.D.C.A Actual. Divulg. Científica*, 2012.

[25] F. Röck, N. Barsan, and U. Weimar, "Electronic Nose: Current Status and Future Trends," *Chem. Rev.*, vol. 108, no. 2, pp. 705–725, Feb. 2008.

[26] A. D. Wilson and M. Baietto, "Applications and advances in electronic-nose technologies," *Sensors*. 2009.

[27] M. P. Van Der Schee, T. Paff, P. Brinkman, W. M. C. Van Aalderen, E. G. Haarman, and P. J. Sterk, "Breathomics in lung disease," *Chest*, vol. 147, no. 1, pp. 224–231, 2015.

[28] P. Montuschi, N. Mores, A. Trové, C. Mondino, and P. J. Barnes, "The electronic nose in respiratory medicine," *Respiration*. 2012.

[29] R. D. Anderson, L. F. Roddam, S. Bettiol, K. Sanderson, and D. W. Reid, "Biosignificance of bacterial cyanogenesis in the CF lung," *Journal of Cystic Fibrosis*. 2010.

[30] P. Brinkman *et al.*, "Abstract - Modelling electronic nose sensor deflections by matching Gas Chromatography-Mass Spectrometry exhaled breath samples," *ERS Int. Congr.*, vol. 05.02 Moni, 2019.

[31] H. T. Nagle, S. S. Schiffman, and R. Gutierrez-Osuna, "How and why of electronic noses," *IEEE Spectr.*, 1998.

[32] K. Arshak, E. Moore, G. M. Lyons, J. Harris, and S. Clifford, "A review of gas sensors employed in electronic nose applications," *Sens. Rev.*, vol. 24, no. 2, pp. 181–198, 2004.

[33] S. M. Cristescu, S. T. Persijn, S. Te Lintel Hekkert, and F. J. M. Harren, "Laser-based systems for trace gas detection in life sciences," in *Applied Physics B: Lasers and Optics*, 2008.

[34] D. D. Arslanov, M. Spunei, J. Mandon, S. M. Cristescu, S. T. Persijn, and F. J. M. Harren, "Continuous-wave optical parametric oscillator based infrared spectroscopy for sensitive molecular gas sensing," *Laser and Photonics Reviews*. 2013.

[35] A. Kosterev *et al.*, "Application of quantum cascade lasers to trace gas analysis," *Appl. Phys. B Lasers Opt.*, 2008.

[36] A. Fried and D. Richter, "No TitleInfrared Absorption Spectroscopy," in *Analytical Techniques for Atmospheric Measurement*, 2006.

[37] M. R. McCurdy, Y. Bakhirkin, G. Wysocki, R. Lewicki, and F. K. Tittel, "Recent advances of laser-spectroscopybased techniques for applications in breath analysis," *Journal of Breath Research*. 2007.

[38] S. Dragonieri *et al.*, "An electronic nose in the discrimination of patients with asthma and controls," *J. Allergy Clin. Immunol.*, vol. 120, no. 4, pp. 856–862, 2007.

[39] P. Montuschi *et al.*, "Diagnostic performance of an electronic nose, fractional exhaled nitric oxide, and lung function testing in asthma," *Chest*, 2010.

[40] M. A. G. E. Bannier, K. D. G. van de Kant, Q. Jöbsis, and E. Dompeling, "Feasibility and diagnostic accuracy of an electronic nose in children with asthma and cystic fibrosis," *J. Breath Res.*, vol. in press, 2018.

[41] N. Meyer *et al.*, "Defining adult asthma endophenotypes by clinical features and patterns of volatile organic compounds in exhaled air," *Respir. Res.*, vol. 15, no. 136, 2014.

[42] R. de Vries *et al.*, "Clinical and inflammatory phenotyping by breathomics in chronic airway diseases irrespective of the diagnostic label," *Eur. Respir. J.*, vol. 51, no. 1, p. 1701817, 2018.

[43] P. Brinkman *et al.*, "Identification and prospective stability of eNose derived inflammatory phenotypes in severe asthma," *J. Allergy Clin. Immunol.*, 2018.

[44] V. Plaza *et al.*, "Inflammatory Asthma Phenotype Discrimination Using an Electronic Nose Breath Analyzer.," *J. Investig. Allergol. Clin. Immunol.*, vol. 25, no. 6, pp. 431–7, 2015.

[45] F. N. Schleich *et al.*, "Exhaled Volatile Organic Compounds are Able to Discriminate between Neutrophilic and Eosinophilic Asthma," *Am. J. Respir. Crit. Care Med.*, p. rccm.201811-2210OC, 2019.

[46] M. P. Van der Schee, R. Palmay, J. O. Cowan, and D. R. Taylor, "Predicting steroid responsiveness in patients with asthma using exhaled breath profiling," *Clin. Exp. Allergy*, vol. 43, no. 11, pp. 1217–1225, 2013.

[47] P. Brinkman *et al.*, "Exhaled breath profiles in the monitoring of loss of control and clinical recovery in asthma," *Clin. Exp. Allergy*, vol. 47, no. 9, pp. 1159–1169, Sep. 2017.

[48] C. M. Robroeks *et al.*, "Exhaled volatile organic compounds predict exacerbations of childhood asthma in a 1-year prospective study," *Eur. Respir. J.*, vol. 42, no. 1, pp. 98–106, 2013.

[49] J. J. B. N. Van Berkel *et al.*, "A profile of volatile organic compounds in breath discriminates COPD patients from controls," *Respir. Med.*, vol. 104, no. 4, pp. 557–563, 2010.

[50] S. Dragonieri *et al.*, "An electronic nose in the discrimination of patients with non-small cell lung cancer and COPD," *Lung Cancer*, vol. 64, no. 2, pp. 166–170, 2009.

[51] N. Fens *et al.*, "Exhaled breath profiling enables discrimination of chronic obstructive pulmonary disease and asthma," *Am. J. Respir. Crit. Care Med.*, vol. 180, no. 11, pp. 1076–1082, 2009.

[52] A. Agusti *et al.*, "Treatable traits: Toward precision medicine of chronic airway diseases," *Eur. Respir. J.*, vol. 47, no. 2, pp. 410–419, 2016.

[53] I. D. Pavord *et al.*, "After asthma: Redefining airways diseases," *Lancet*, vol. 6736, no. 17, pp. 1–51, 2017.

[54] N. Fens *et al.*, "Exhaled air molecular profiling in relation to inflammatory subtype and activity in COPD," *Eur. Respir. J.*, vol. 38, no. 6, pp. 1301–1309, 2011.

[55] P. Montuschi *et al.*, "Breathomics for Assessing the Effects of Treatment and Withdrawal With Inhaled Beclomethasone/Formoterol in Patients With COPD.," *Front. Pharmacol.*, vol. 9, p. 258, 2018.

[56] J. J. M. H. van Bragt *et al.*, "Late Breaking Abstract - Detection of clinical instability by eNose in COPD patients," *Eur. Respir. J.*, vol. 52, no. Suppl. 62, PA3849, 2018.

[57] M. T. Gaugg *et al.*, "Real-time breath analysis reveals specific metabolic signatures of COPD exacerbations," *Chest*, no. 2019, 2019.

[58] W. H. van Geffen, M. Bruins, and H. A. M. Kerstjens, "Diagnosing viral and bacterial respiratory infections in acute COPD exacerbations by an electronic nose: a pilot study," *J. Breath Res.*, vol. 10, no. 3, p. 036001, Jun. 2016.

[59] C. Castellani *et al.*, "European best practice guidelines for cystic fibrosis neonatal screening," *Journal of Cystic Fibrosis*. 2009.

[60] P. M. Farrell, "The prevalence of cystic fibrosis in the European Union," *J. Cyst. Fibros.*, 2008.

[61] M. Barker *et al.*, "Volatile organic compounds in the exhaled breath of young patients with cystic fibrosis," *Eur. Respir. J.*, vol. 27, no. 5, pp. 929–936, 2006.

[62] T. Gaisl *et al.*, "Real-Time exhaled breath analysis in patients with cystic fibrosis and controls," *J. Breath Res.*, vol. 12, no. 3, 2018.

[63] C. M. H. H. T. Robroeks *et al.*, "Metabolomics of volatile organic compounds in cystic fibrosis patients and controls," *Pediatr. Res.*, 2010.

[64] T. Paff *et al.*, "Exhaled molecular profiles in the assessment of cystic fibrosis and primary ciliary dyskinesia," *J. Cyst. Fibros.*, vol. 12, no. 5, pp. 454–460, 2013.

[65] E. Van Mastrigt *et al.*, "Exhaled breath profiling using broadband quantum cascade laser-based spectroscopy in healthy children and children with asthma and cystic fibrosis," *J. Breath Res.*, vol. 10, no. 2, p. 26003, 2016.

[66] L. D. J. Bos, P. J. Sterk, and M. J. Schultz, "Volatile Metabolites of Pathogens: A Systematic Review," *PLoS Pathogens*. 2013.

[67] M. Nasir, H. D. Bean, A. Smolinska, C. A. Rees, E. T. Zemanick, and J. E. Hill, "Volatile molecules from bronchoalveolar lavage fluid can 'rule-in' Pseudomonas aeruginosa and 'rule-out' Staphylococcus aureus infections in cystic fibrosis patients," *Sci. Rep.*, vol. 8, no. 1, pp. 1–11, 2018.

[68] A. Lammers *et al.*, "eNose Technology for Detection of Pseudomonas Aeruginosa Infection in Cystic Fibrosis Patients," in *D34. cystic fibrosis and bronchiectasis : clincal and mechanistic studies*, pp. A6181–A6181.

[69] B. Enderby, D. Smith, W. Carroll, and W. Lenney, "Hydrogen cyanide as a biomarker for Pseudomonas aeruginosa in the breath of children with cystic fibrosis," *Pediatr. Pulmonol.*, vol. 44, no. 2, pp. 142–147, 2009.

[70] F. J. Gilchrist *et al.*, " Exhaled breath hydrogen cyanide as a marker of early Pseudomonas aeruginosa infection in children with cystic fibrosis ," *ERJ Open Res.*, vol. 1, no. 2, pp. 00044–02015, 2015.

[71] A. H. Neerincx *et al.*, "Detection of Staphylococcus aureus in cystic fibrosis patients using breath VOC profiles," *J. Breath Res.*, vol. 10, no. 4, 2016.

[72] K. de Heer *et al.*, "Detection of Airway Colonization by Aspergillus fumigatus by Use of Electronic Nose Technology in Patients with Cystic Fibrosis," *J. Clin. Microbiol.*, vol. 54, no. 3, pp. 569–575, 2016.

[73] P. M. Van Oort *et al.*, "The potential role of exhaled breath analysis in the diagnostic process of pneumonia - A systematic review," *J. Breath Res.*, vol. 12, no. 2, 2018.

Part II.

Air pollution

Chapter 3.

Effects of short-term exposures to ultrafine particles near an airport in healthy subjects

Lammers A
Janssen NAH
Boere AJF
Berger M
Longo C
Vijverberg SJH
Neerincx AH
Maitland-van der Zee AH
Cassee FR

Environment International 2020 Aug; 141: 105779

Abstract

Background: Recent studies reported elevated concentrations of ultrafine particles (UFP) near airports. Little is known about the health effects of UFP from aviation. Since UFP can deposit deep into the lungs and other organs, they may cause significant adverse health effects.

Objective: We investigated health effects of controlled short-term human exposure to UFP near a major airport.

Methods: In this study, 21 healthy non-smoking volunteers (age range: 18–35 years) were repeatedly (2–5 visits) exposed for 5 h to ambient air near Schiphol Airport, while performing intermittent moderate exercise (i.e. cycling). Pre- to post-exposure changes in cardiopulmonary outcomes (spirometry, forced exhaled nitric oxide, electrocardiography and blood pressure) were assessed and related to total- and size-specific particle number concentrations (PNC), using linear mixed effect models.

Results: The PNC was on average 53,500 particles/cm^3 (range 10,500–173,200). A 5–95th percentile increase in exposure to UFP (i.e. 125,400 particles/cm^3) was associated with a decrease in FVC of -73.8 mL (95% CI -138.8 – -0.4) and a prolongation of the corrected QT (QTc) interval by 9.9 ms (95% CI 2.0 – 19.1). These effects were associated with particles < 20 nm (mainly UFP from aviation), but not with particles > 50 nm (mainly UFP from road traffic).

Discussion: Short-term exposures to aviation-related UFP near a major airport, was associated with decreased lung function (mainly FVC) and a prolonged QTc interval in healthy volunteers. The effects were relatively small, however, they appeared after single exposures of 5 h in young healthy adults. As this study cannot make any inferences about long-term health impacts, appropriate studies investigating potential health effects of long-term exposure to airport-related UFP, are urgently needed.

Introduction

It has been established that both short- and long-term exposure to air pollution, especially particulate matter (PM), is associated with adverse health effects, prompting air quality regulations. Adverse effects could range from respiratory (e.g. asthma exacerbations and bronchitis) to cardiovascular (e.g. cardiac arrhythmias and heart attacks), which have been associated with more hospitalizations [1]–[7]. In addition, long-term exposure to PM, especially fine particles (i.e. < 2.5 μm), increases the risk of cardiopulmonary mortality by 6–11% per 10 $\mu g/m^3$ [8]–[10].

To date, most studies have focussed on coarse (2.5–10 μm, PM10) and fine (< 2.5 μm, PM2.5) particles, however, concerns about ultrafine particles (< 0.1 μm, UFP) are rising. Compared to larger particles, UFP are potentially more toxic due to their high surface area-to-mass ratio, capability to deposit deep in the lungs, and potential to translocate to other organs [11]–[13] by entering the blood stream [14], [15]. Several *in vitro* and animal studies have shown that UFP can induce inflammation and oxidative stress [16]–[19], raising concerns for possible adverse health effects in humans.

Recently, the U.S. EPA Integrated Science Assessment (ISA) for Particulate Matter (PM) stated that evidence on short-term UFP exposure and both cardiovascular and respiratory effects is suggestive of, but not sufficient to infer, a causal relationship [5]. Moreover, little is known about aviation-related UFP exposure, as most studies focus on road-traffic-related UFP [7]. UFP levels have been shown to be elevated around large airports [20]–[22], reaching similar levels as urbanised areas [23], with different sources influencing UFP composition and size. Aviation-related UFP tend to be smaller (mainly 10–20 nm [21], [24], [25]) than those from road traffic (mainly > 50 nm [26]–[28]), although an overlap in size range exists, especially in the 20–30 nm range [29]. Altogether, this has raised public health concerns for people living near large airports and questions about possible differences in toxicity between UFP sources.

Therefore, we hypothesized that exposure to UFP from aviation acutely affects cardiopulmonary function. Our objective was to assess whether short-term exposure to UFP in healthy individuals next to a major airport, i.e. Schiphol Airport (Amsterdam, the Netherlands), is associated with acute respiratory and cardiovascular effects. Our second objective was to determine the relative contributions of total and size-specific UFP (as indicators for source-specific UFP) to the associations with the health outcomes.

Methods

Study design

This was a prospective, interventional study in which young healthy volunteers were exposed to ambient air near Schiphol Airport (Amsterdam, the Netherlands) and two highways, between April and October 2018. Participants received 5 h exposures (10:00–15:00 h) on at least two and up to five separate visits; while four visits per participant were planned, the number of visits varied as a result of the availabilities of participants and the unpredictability of meteorological conditions (more details in section "number of visits"). The visits were scheduled at least 2 weeks apart to avoid potential carry-over effects. During the exposure, participants performed intermittent cycling on an ergometer for 20 min per hour at low intensity (50–60% of maximal heart rate) based on their age and sex; maximal heart rate was calculated by 220 – age (yrs) for males, and 224 – age (yrs) for females. In between cycling, participants were seated and performed a resting activity of their own choice (e.g. reading a book, watching a movie). Noise-cancelling headphones were handed out to the participants to reduce noise, however, it was not mandatory to wear them. Extensive air monitoring was conducted during the 5 h exposures. Health outcomes were assessed before (07:30–09:30 h) and after (15:30–17:30 h) every exposure, at the Amsterdam UMC (location AMC, Amsterdam, the Netherlands), located 15 km from the exposure site (Figure S1). Participants were transported between locations by a petrol-fuelled hybrid car equipped with a high-efficiency particulate air (HEPA) filter, which took on average 15 minutes.

Restrictions for participants

Participants were asked to refrain from drinking alcohol and caffeine-containing drinks both before (24 and 12 h, respectively) and during all visits. To minimize the influence of nitrate rich food on the fractional exhaled nitric oxide (FeNO) measurement (one of the health outcomes) during study visits, volunteers were not allowed to eat at home in the morning and food and drinks on the exposure day were arranged, however, not standardized. This meant that participants had differences in their breakfast and lunch options, in order to comply with their dietary wishes (e.g. vegetarian), and that participants could choose the time of eating and drinking themselves, except for breakfast. During the whole study period subjects had to refrain from tobacco and drugs. Tobacco use and pregnancy was tested in urine once (at random) during the study and was never positive; urine was collected before and the morning after every exposure as part of the study, however, those results will be described separately.

Ethical approval

The study protocol was reviewed and approved by the Medical Ethical Committee (METC) of the Amsterdam Medical Centre (Amsterdam, the Netherlands) and was registered at the Dutch Trial Register (identifier NTR 6955, www.trialregister.nl).

Study population

Participants were included in the study if they were aged 18–35 years, non-smokers for at least 1 year (< 5 pack years) with normal lung function (predicted forced exhaled volume in 1 s (FEV_1) > 80%). Participants were excluded if they had: any (history of chronic) pulmonary or cardiovascular disease, hay fever, or lived in the vicinity of Schiphol Airport (< 2 km), a highway (< 300 m) or on a busy road (> 10,000 vehicles/day). A list of all in- and exclusion criteria can be found in the supplementary material (Table S1).

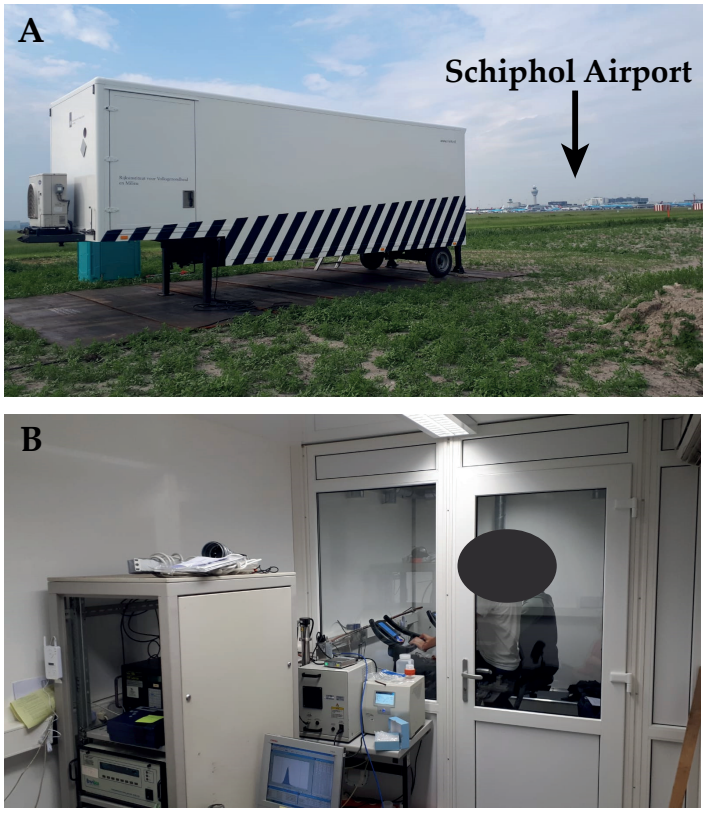

Figure 1. Exposures were conducted in an exposure laboratory right next to Schiphol Airport **(A)**. It consisted of two chambers: one chamber in which subjects were exposed and one for the exposure monitoring equipment **(B)**.

Participants were recruited by online advertisement (i.e. Facebook) and by putting up flyers in schools, universities and student houses in Amsterdam. When interested, volunteers were invited to a screening visit where their health was assessed based on medical history as well as lung (fractional exhaled nitric oxide (FeNO), and spirometry) and heart function measurements (electrocardiography (ECG), blood pressure (BP), heart rate, and oxygen saturation). The ECG was checked by a cardiologist for abnormalities. No strict criteria existed for FeNO, blood pressure and the resting heart rate, but all had to be within or close to normal ranges (see supplementary material Table S1). Participants received a travel allowance and a reimbursement of €75,- per study visit. To reward completion of the study, participants received €100,- for the fourth visit instead of €75,-.

Exposure

On each exposure day, two to four participants were exposed simultaneously in a mobile exposure laboratory (Figure 1). This laboratory was positioned northwest of the airport (~300 m away from two runways), near two highways (~500 m away from the A4 and A9) and close to Amsterdam (~10 km) (Figure 2). The mobile exposure laboratory consisted of two chambers, an exposure chamber and a technical chamber with all exposure monitoring equipment and two technicians. In the exposure chamber of 14 m^3, an airflow system with multiple openings at the top (inlet) and the bottom (outlet) was present to ensure air exchange was constant and ambient air flows of approximately ~400 m^3/h were uniform. The walls and door of the exposure chamber were made airtight to prevent air leakage. In this way, a homogenous distribution of incoming air was secured throughout the chamber. The exposure varied between visits due to the meteorological conditions (mainly wind direction) and runway use. We aimed for differences in UFP levels, source contributions (e.g. aviation and road traffic), and compositions between exposure days within each subject, by considering the weather forecast when scheduling their visits.

Exposure monitoring

Air inside the exposure chamber of the laboratory was sampled continuously (in between the two exercise bikes, in the breathing zone) for several exposure outcomes. Next, 5 h averages were calculated for every exposure day. We did not study variation within the 5 h window. The measured exposure variables were: particle number concentrations (PNC); particle mass concentrations (PM); nitrogen oxides (NO_x, NO_2); carbon monoxide (CO); sulphur dioxide (SO_2); ozone (O_3); and black carbon (BC). The PM during the 5 h exposure period were determined by gravimetric analyses using Teflon filters. Albeit there is no size

selective inlet applied, the curvature of the inlet tubing withheld the influx of relatively larger particles and therefore PM can be considered as approximately PM2.5. Furthermore, particle size distributions between 6 and 225 nm were measured using a scanning mobility particle sizer (SMPS); semi continuous (looping) measurements were taken with a frequency of 30 recordings per hour as default. Wind speed and direction were monitored (outside) as well as the temperature and relative humidity (in- and outside). All exposure monitoring equipment is listed in Table 1.

Figure 2. The exposure laboratory was located (**X**) near Schiphol's runways (grey lines) and a large highway intersection (pink lines). Amsterdam was to the north-east of the exposure site. The building of Schiphol is marked in blue. The map is positioned towards the north. Adapted image from Wikipedia (CC BY-SA 3.0).

Table 1. Overview of exposure monitoring equipment.

Pollutant	**Device**	City/Country
PNC	Condensation particle counter (CPC) water-based Model 3752, TSI with a d_{50} of 4 nm as lower size limit	Shoreview, MN, USA
NOx, NO2	Chemiluminescence Nitrogen Oxides Analyzer, model 200E, Advanced Pollution Instrumentation (T-API)	San Diego, CA. USA
CO	Gas filter correlation analyzer, model 300E/EM, T-API	San Diego, CA, USA
SO2	Pulsed fluorescence analyzer, model 43A, Thermo Enivornmental Instruments (TEI)	Franklin, MA, USA
O3	UV photometric analyzer, model 49, TEI	Franklin, MA, USA
BC	Optically absorbing suspended particulates in a gas colloid stream using a aethalometer: microAeth® Model AE51, ETS	San Francisco, CA, USA
Size distribution	Scanning mobility particle sizer (SMPS) TSI Model 3936, using a Model 3080 Electrostatic Classifier with a "Long-DMA" model 3081 and a Nano water-based TSI Model 3788 CPC. Particle size range between 6 (d_{50}) and 225 nm.	Shoreview, MN, USA
PM	Tapered Element Oscillating Microbalance (TEOM) Series 1400a Ambient Particulate Monitor, Rupprecht & Patashnick, Teflo 2.0 μm 47 mm (R2PJ047), PALL Life Sciences, USA	Albany, NY USA
Temperature inside Humidity inside	digital temperature/relative humidity probe: Vaisala HMP115Y	Vaisala, Finland
Temperature outside Humidity/ outside wind speed wind direction	Davis Advantage Pro 2 weather station	Hayward, CA

Missing exposure data

Due to instrument failure, some of the exposure data was estimated. Temperature and relative humidity in the exposure chamber from the first five exposure days were missing and therefore calculated based on the correlation with outdoor temperature and humidity using a Mollier calculation and diagrams. The recorded NO_2 data were consistently too low when compared to a nearby National Air Quality Network monitoring station (Badhoevedorp). This was

a consequence of a wrong conversion from the voltage that was recorded. The actual concentrations were calculated by adjusting the recorded data with a fixed equation that was derived from a side by side comparison between the applied monitor and the daily calibrated NOx monitor of the National Air Quality Network. On the 12th of June, data of the exposures were not automatically stored and therefore CO, SO_2 and O_3 levels were estimated based on the manual reading and logging of the monitors by the technicians instead of the continuous data that were logged by a computer. The NO_x/NO_2 values for that day were estimated based on the consistent correlation between BC and NO_2 and the nearby NO_x/NO_2 monitor of the National Air Quality Network (Badhoevedorp).

Exposure during transport

To minimize exposure to motorway emissions during transport between the exposure and health assessment location (~15 km), participants were transported by a petrol-fuelled hybrid car (Toyoya Auris and CHR) with closed windows and equipped with a high-efficiency particulate air (HEPA) filter. To test whether the air filter was effective, the particle number concentrations (PNC) was measured using a Philips Nanotracer (in fast mode) in the car with both the windows closed and open while driving on the motorway. A clear difference in PNC levels between both situations occurred; 1,500–25,000 and 80,000–130,000 particles/cm^3 for windows closed and open, respectively.

Number of exposure visits

In the first period of study, we had exceptional weather, in which the wind direction was hardly ever coming from the airport to the exposure site, resulting in low UFP exposures. Therefore, some of the visits were postponed to days with wind directions coming from the airport. Furthermore, participants included at the beginning of the study who received several low UFP exposures, were asked to perform a fifth visit to increase the individual contrast in exposure levels over all study visit.

Health outcomes

Respiratory outcomes: FeNO in ppb was measured using NIOX VERO® (Circassia Pharmaceuticals Inc, USA) according to the manufactures instructions. Lung function was assessed by a spirometer (Jaeger Masterscreen™ software, Erich Jaeger GmbH, Germany) in accordance with current ERS/ATS guidelines [30]. Retrieved outcomes were: forced vital capacity (FVC), forced expiratory volume in 1 s (FEV_1), and peak expiratory flow rate (PEF). Calibration of the spirometer was conducted before each subject, according to the 'three flow'-protocol as described in the manufactures instructions.

Cardiovascular outcomes: non-invasive BP, heart rate and oxygen saturation measurements were performed in sitting position three times with 2-min intervals (Datascope Duo, Mindray, Shenzhen, China). Before starting the BP measurement, participants were seated for 1 min, to stabilize their BP. The cuff was placed around the upper arm, 2–3 cm above the elbow. For BP, the average of the three measurements was used for the analysis. Heart rate and oxygen saturation of the first measurement was used for the analysis. The resting ECG was performed in supine position using a 12-lead MAC™ 5500 HD (GE Healthcare, Chicago, USA). Retrieved outcomes were: PR (onset atrial depolarization until onset ventricular depolarization), QRS (duration of ventricular depolarization) and corrected QT (QTc) intervals (duration of ventricular repolarization corrected for heart rate), as well as heart rate.

The order of the measurements was: FeNO, ECG, BP (including heart rate and oxygen saturation) and spirometry. In the morning, participants ate their breakfast between the FeNO and ECG measurements. Investigators assessing the health outcomes were never informed about the exposure levels on the exposure day, to minimize measurement bias.

Sample size

The sample size was based on the study by Strak et al. [3], in which they used a similar study design (healthy volunteers, 5 h exposures and 20 min exercise each hour). They exposed 31 subjects to ambient air at 5 locations with different PM characteristics and were able to detect increased FeNO and decreased lung function measures (FVC and FEV1), immediately and 2 h after exposure. Associations with PNC remained statistically significant when the analysis was restricted to observations (n = 60) from the continuous traffic (mean 66,500 particles/cm^3; range 60,000–74,000) and urban background site (mean 9,100 particles/cm^3; range 7,000–11,800). Therefore, we assumed that 80 observations (20 healthy volunteers, exposed four times) was sufficient to answer our research question.

Statistical analysis

Differences in health outcomes between post- and pre-exposure ($Y_{post\text{-}pre}$) for each individual (i) and exposure day (j) were modelled using linear mixed effect models. The unadjusted model was:

$$Y_{ij,post-pre} = \beta_0 + Y_{ij,pre} + \beta_1 E_j + U_{0i} + \varepsilon_i$$

where E_j represents a vector of the exposure variable(s) and $Y_{ij,pre}$ the pre-exposure health measurement [31]. The U_{0i} represents the patient-specific deviation from the average change in the outcome parameters of interest in the study sample (i.e. a random intercept) and ε_i the error term. The β's represent population-average fixed effects, with β_0 representing the study sample average change in the outcome parameters when all other covariates are zero and β_1 the average change in the outcome relative to a 5-95th percentile (5-95p) increase in exposure.

The adjusted and main model was:

$$Y_{ij,post-pre} = \beta_0 + Y_{ij,pre} + \beta_1 E_j + \beta_2 V_j + \beta_3 Z_i + U_{0i} + \varepsilon_i$$

where V_j represents a vector of covariates that varied at each visit and Z_i a vector of covariates that were fixed (age, sex and BMI). Covariates that varied at each visit include the temperature and relative humidity in the exposure laboratory and the respiratory symptoms (i.e. cough, dyspnea, blocked nose or sputum production) that participants may have had before exposure (as a binary indicator yes/no). We have only described the results of the adjusted models. All results of the unadjusted models are presented in Tables S7–10 of the supplementary material.

UFP and co-pollutants

Multiple pollutants and combinations of them were examined using this model. First, PNC and all co-pollutants (i.e. BC, NO_2, PM, CO and O_3) were investigated separately using single-pollutant models. Next, two-pollutant models containing PNC and one of the other co-pollutants were conducted, to explore the independency of the effects associated with PNC [7].

UFP size ranges as source indicators

To have an indication of aviation and road-traffic-related UFP, different size ranges of PNC (measured by SMPS) were examined. First, a single-pollutant model was performed for particles ≤ 20 nm, mainly representing aviation-related UFP [21], [24], [25]. As an sensitivity analysis, single-pollutant models for particles ≤ 30 nm, ≤ 50 nm and ≤ 100 nm were conducted. Next, a two-pollutant model (≤ 20 nm vs. > 50 nm) was performed, in which particles ≤ 20 again mainly represented aviation-related UFP and particles > 50 nm represented other sources of UFP, mainly road traffic [26]–[28].

Statistics were performed in R (version 3.5.1) and R studio (Version 1.1.453). For the linear mixed effect models the R package "lme4" was used and the fit of the models was examined by confirming a normal distribution of the residuals using Q-Q plots. Exposure variables included in the same model were not collinear (R < 0.4), as verified using Pearson correlation coefficients.

Results

Participants

In total, 21 of the 23 exposed participants were included in the analysis; two volunteers withdrew after the initial visit due to lack of time for participation (Figure S2). The median age was 23 years (interquartile range (IQR): 20 – 23) and the majority was female (n = 17, 81%). Most participants were students and lived in Amsterdam. Participants had a normal BMI (22.6 kg/m^2, ± 2.4) and all measured health outcomes (i.e. FVC, FEV_1, PEF, FeNO, BP, heart rate and oxygen saturation) were within normal ranges during the screening visit (Table 2). There was no missing data regarding the health outcomes throughout the study.

Exposures

During the study period, 32 exposure days with a total of 86 visits were conducted; participants attended two, four or five exposure days (n = 2, n = 13, n = 6, respectively) (Figure S2). Per day, 5 h averages were calculated for every exposure variable (Table 3). Taking all exposure days together, PNC (measured by a condensation particle counter (CPC)) was on average 53,500 particles/cm^3 (range 10,500–173,200). The highest PNC levels occurred when the wind direction was coming from the airport. Exposure levels per day are shown in the supplementary material (Table S2). At an individual level, the minimal and maximal PNC exposure participants received, was on average 21,300 (range 10,600 – 38,400) and 101,400 (range 28,900 – 173,200) particles/cm^3, respectively (Table S3). The maximal contrast in PNC exposure that participants received (i.e. maximal – minimal exposure), was on average 80,000 particles/cm^3 (range 8,800–152,500) (Table S3).

The PNC measured by SMPS showed that concentrations mainly represented small-sized particles of 6–20 nm and 20–30 nm, covering around 50% and 30% of the total PNC, respectively. Apart from four exposure days, SO_2 levels were below the detection limits, and therefore not included in the analysis. Pearson correlation analysis showed low correlations between all pollutants (R < 0.6), except for BC and NO_2 (R = 0.79) (supplement, Table S4).

Table 2. Baseline participant characteristics.

	Participants (n = 21)
Age (years)	23 (20 – 23)
Sex (female)	17 (81%)
BMI (kg/m^2)	22.6 (± 2.4)
FVC (% of predicted)	113 (± 11)
FEV_1 (% of predicted)	106 (± 13)
PEF (% of predicted)	99 (± 12)
FeNO (ppb)	15 (11 – 23)
Blood pressure	
Systolic (mmHg)	123 (± 12)
Diastolic (mmHg)	77 (± 9)
Heart rate (c/min)	65 (± 8)
Saturation (%)	99.0 (98 – 100)

Data are presented as mean (SD), median (IQR) or n(%). BMI= body mass index; FVC = forced vital capacity; FEV_1 = forced expiratory volume in 1s; PEF = peak expiratory flow; FeNO = fractional exhaled nitric oxide; All health outcomes were measured during the screening visit.

Table 3. Exposure variables of all exposure days based on 5 h averages.

	Exposure days (n = 32)		
Pollutant	**Mean**	**5-95th percentile**	**Min-max**
PNC (particles/cm^3)[a]	53,500	16,100 – 141,500	10,500 – 173,200
6 – 20 nm[b]	17,700	2,500 – 55,200	1,400 – 77,300
20 – 30 nm[b]	10,400	1,600 – 32,100	1,000 – 33,100
30 – 50 nm[b]	4,200	1,400 – 8,900	1,000 – 12,900
50 – 70 nm[b]	1,100	400 – 1,700	300 – 2,400
70 – 100 nm[b]	800	200 – 1,400	180 – 1,700
100 – 200 nm[b]	800	180 – 1,700	150 – 2,200
>200 nm[b]	100	30 – 220	10 – 270
PM (μg/m^3)	23.1	14.1 – 40.6	10.6 - 47.5
BC (μg/m^3)	0.6	0.14 – 1.42	0.12 - 1.94
NO_2 (μg/m^3)	28.2	12.5 – 46.9	12.4 – 60.2
CO (μg/m^3)	638	525 – 780	494 – 830
O_3 (μg/m^3)	35.7	17.5 – 57.3	8.8 – 78.6
Temperature (°C)	23.3	19.2 – 26.6	15.7 – 28.6
Relative humidity (%)	54	43 – 65	40 – 66

PNC = particle number concentration; PM = particulate matter; BC = black carbon; NO_2 = nitric oxide; CO = carbon monoxide; O_3 = ozone; a= measured by condensation particle counter; b = measured by a scanning mobility particle sizer;

Health effect models

No multicollinearity occurred between pollutants that were combined in the two-pollutant models; PNC and all other pollutants (R = 0.08 – 0.37) and the UFP size range of < 20 and > 50 nm (R = 0.12).

UFP and co-pollutants (adjusted models)

The total PNC (5-95p: 125,400 particles/cm^3) was significantly associated with a decrease in FVC of -73.8 mL (95% confidence interval (CI): -138.8 – -0.4) and a trend towards a reduction in FEV_1 of -50.6 mL/s (95% CI: -117.1 – 29.8). Furthermore, PNC was correlated with an prolongation of the QTc interval by 9.9 ms (95% CI: 2.0 – 19.1) (Table 4). Adjustment for co-pollutants (i.e. two-pollutant models) led to similar results (supplement, Table S5).

For the other pollutants (Table 4), BC and NO_2 were associated with an increase in systolic and diastolic BP. No significant associations were found for PM and CO exposure. Effects found for O_3 should be interpreted carefully, since O_3 exposures were low and negatively correlated with NO_2 (R = -0.53). In general, PEF, FeNO, oxygen saturation and QRS intervals were not significantly associated with any of the exposure variables.

UFP size ranges as source indicators (adjusted models)

For the PNC data measured by SMPS, exposure to particles ≤20 nm (5-95p: 52,700 particles/cm^3) showed a trend towards a decrease in FVC of -69.3 mL (95% CI: -135.8 – 1.0) and a significant prolongation of the QTc interval by 9.6 ms (95% CI: 1.9 – 18.4) relative to pre-exposure levels. The sensitivity analysis (i.e. single-pollutant models with particles ≤ 30, ≤ 50 and ≤ 100 nm) showed no substantial changes in these effects (supplement, Table S6).

For the two-pollutant model (consisting of two size fractions, i.e. PNC ≤ 20 nm and PNC > 50 nm), exposure to particles ≤ 20 nm (5-95p: 52,700 particles/cm^3) was associated with lower FVC (-72.1 mL, 95% CI: -140.2 – -2.8), FEV_1 (-49.6 mL, 95% CI: -117.0 – 27.1) and longer QTc intervals (9.9 ms, 95% CI: 2.1 – 18.7). Particles > 50 nm (5-95p: 3,600 particles/cm^3) were associated with an increase in systolic (2.9 mmHg, 95% CI: -0.7 – 6.8) and diastolic BP (3.7 mmHg, 95% CI: 0.1 – 7.5). All other health outcomes were unaffected (Table 5).

Table 4. Single-pollutant models (adjusted).

Outcome	PNC		BC		NO_2	
	Est.	**95% CI**	**Est.**	**95% CI**	**Est.**	**95% CI**
FVC (mL)	**-73.8**	**(-138.8 – -0.4)**	39.0	(-23.7 – 101.6)	2.0	(-71.3 – 75.2)
FEV_1 (mL)	-50.6	(-117.1 – 29.8)	27.7	(-29.0 – 100.5)	-38.0	(-105.6 – 57.6)
PEF (mL/s)	-61.6	(-349.0 – 210.4)	160.4	(-77.9 – 420.0)	-155.6	(-424.5 – 170.6)
FeNO (ppb)	0.3	(-1.1 – 1.7)	0.2	(-1.0 – 1.6)	1.0	(-0.4 – 2.5)
$HR_{sitting}$ (bpm)	-1.1	(-4.6 – 2.4)	-1.4	(-4.4 – 2.4)	-1.4	(-5.0 – 2.8)
Saturation (%)	0.0	(-0.5 – 0.6)	0.1	(-0.5 – 0.6)	-0.1	(-0.7 – 0.5)
BP_{sys} (mmHg)	-1.8	(-4.7 – 1.1)	**3.2**	**(0.5 – 5.7)**	2.8	(-0.4 – 5.9)
BP_{dia} (mmHg)	-1.7	(-4.7 – 1.2)	**2.9**	**(0.2 – 5.6)**	**3.9**	**(0.8 – 7.0)**
ECG - HR (bpm)	3.4	(-0.3 – 7.6)	0.8	(-3.0 – 4.6)	0.2	(-4.0 – 4.6)
ECG - PR (ms)	-2.2	(-7.3 – 1.8)	**4.8**	**(1.4 – 10.2)**	3.4	(-1.2 – 8.7)
ECG - QRS (ms)	1.3	(-1.3 – 3.8)	-1.2	(-3.5 – 1.1)	0.2	(-2.5 – 3.0)
ECG - QTc (ms)	**9.9**	**(2.0 – 19.1)**	0.4	(-7.3 – 9.0)	-0.2	(-9.1 – 9.7)
Outcome	**PM**		**CO**		**O_3**	
	Est.	**95% CI**	**Est.**	**95% CI**	**Est.**	**95% CI**
FVC (mL)	60.2	(-18.4 – 138.8)	10.5	(-346.0 – 366.9)	11.9	(-70.5 – 94.2)
FEV_1 (mL)	69.7	(-6.3 – 154.2)	7.7	(-355.7 – 377.4)	26.7	(-61.1 – 106.4)
PEF (mL/s)	41.0	(-257.7 – 370.6)	-371.8	(-1859.4 – 924.4)	129.7	(-209.3 – 430.3)
FeNO (ppb)	-0.8	(-2.3 – 0.8)	-0.5	(-7.3 – 6.7)	-1.4	(-3.0 – 0.2)
$HR_{sitting}$ (bpm)	0.5	(-3.5 – 4.2)	2.8	(-15.1 – 20.2)	**4.6**	**(0.4 – 8.3)**
Saturation (%)	0.0	(-0.6 – 0.6)	0.5	(-2.3 – 3.3)	-0.4	(-1.1 – 0.3)
BP_{sys} (mmHg)	-0.5	(-3.9 – 2.5)	10.6	(-4.7 – 24.4)	-0.9	(-4.3 – 2.4)
BP_{dia} (mmHg)	0.1	(-3.2 – 3.3)	11.6	(-3.5 – 25.6)	**-4.3**	**(-7.7 – -1.1)**
ECG - HR (bpm)	1.0	(-3.9 – 5.0)	8.7	(-11.5 – 28.3)	0.0	(-4.7 – 4.4)
ECG - PR (ms)	0.3	(-5.1 – 4.7)	2.3	(-20.5 – 23.7)	-0.5	(-8.1 – 4.2)
ECG - QRS (ms)	0.3	(-2.6 – 3.1)	1.0	(-12.0 – 14.0)	-0.9	(-3.9 – 2.0)
ECG - QTc (ms)	1.6	(-8.4 – 10.6)	16.2	(-24.9 – 61.5)	3.3	(-7.0 – 12.9)

Data are presented as estimates (est.) and 95% confidence intervals (CI) intervals. All effect estimates are scaled to the 5-95th percentile change in the exposure of interest and are adjusted for age, sex, BMI, respiratory symptoms, room temperature and room humidity. Numbers in **bold** are significant effects ($p < 0.05$). *Exposures*: PNC = particle number concentration; PM = particulate matter; BC = black carbon; NO_2 = nitric oxide; CO = carbon monoxide; O_3 = ozone. *Health outcomes*: FVC = forced vital capacity; FEV_1 = forced expiratory volume in 1s; PEF = peak expiratory flow rate; FeNO = fractional exhaled nitric oxide; HR = heart rate; BPsys = systolic blood pressure; BPdia = diastolic blood pressure; ECG = electrocardiography; QTc = corrected QT. PNC was detected by a condensation particle counter (CPC) with d_{50} = 4 nm.

Unadjusted models

All results of the unadjusted single- and two-pollutant models based on PNC, co-pollutants and particle size fractions, are presented in the supplementary material (Tables S7–10).

Table 5. Two-pollutant model consisting of two particle size fractions (adjusted).

Outcome	PNC ≤20 nm Adjusted for PNC >50 nm		PNC >50 nm Adjusted for PNC ≤20 nm	
	Est.	**95% CI**	**Est.**	**95% CI**
FVC (mL)	**-72.1**	**(-140.2 – -2.8)**	37.2	(-47.7 – 124.5)
FEV_1 (mL)	-49.6	(-117.0 – 27.1)	16.0	(-69.9 – 110.7)
PEF (mL/s)	-19.2	(-310.7 – 248.3)	71.3	(-272.0 – 421.3)
FeNO (ppb)	0.0	(-1.3 – 1.4)	-0.7	(-2.4 – 1.1)
$HR_{sitting}$ (bpm)	-1.5	(-5.1 – 1.8)	1.8	(-2.9 – 6.1)
Saturation (%)	0.1	(-0.4 – 0.8)	-0.4	(-1.1 – 0.4)
BP_{sys} (mmHg)	-1.9	(-4.8 – 0.8)	2.9	(-0.7 – 6.8)
BP_{dia} (mmHg)	-2.3	(-5.2 – 0.5)	**3.7**	**(0.1 – 7.5)**
ECG - HR (bpm)	3.0	(-0.7 – 7.0)	-1.1	(-6.1 – 3.8)
ECG - PR (ms)	-3.3	(-8.3 – 0.5)	0.5	(-5.8 – 5.8)
ECG - QRS (ms)	1.1	(-1.5 – 3.6)	0.9	(-2.3 – 4.1)
ECG - QTc (ms)	**9.9**	**(2.1 – 18.7)**	-3.4	(-13.5 – 8.0)

Data are presented as estimates (est.) and 95% confidence intervals (CI) intervals. All effect estimates are scaled to the 5-95th percentile change in the exposure of interest and are adjusted for age, sex, BMI, respiratory symptoms, room temperature and room humidity. Numbers in **bold** are significant effects ($p < 0.05$). PNC = particle number concentration; FVC = forced vital capacity; FEV_1 = forced expiratory volume in 1s; PEF = peak expiratory flow rate; FeNO = fractional exhaled nitric oxide; HR = heart rate; BPsys = systolic blood pressure; BPdia = diastolic blood pressure; ECG = electrocardiography; QTc = corrected QT. PNC size fractions were measured by a scanning mobility particle sizer (SMPS) with a limit of detection of 6-225 nm.

Discussion

In this cross-over intervention study including 21 healthy participants, we found that exposure to UFP near a large airport was correlated with lung (FVC) and cardiac function (QTc and BP). The reduction in FVC and prolongation of QTc were associated with total PNC and particles ≤ 20 nm (as a proxy for UFP from aviation). The increase in BP was associated with primarily road–traffic-related pollutants (i.e. BC, NO_2) and particles > 50 nm (as a proxy for UFP from other sources, mainly road traffic).

To our knowledge, this is the first human controlled laboratory based study, that has investigated the effects of (short-term) UFP exposure near a large airport on both lung and heart function. Furthermore, participants were exposed on multiple days in which variation in pollutant levels and sources was achieved due to meteorological conditions (mainly wind direction), instead of exposing subjects at different locations.

The relationship between UFP and respiratory outcomes is in accordance with previous literature [32], however, previous studies did not find an association with aviation derived UFP or did not take this source of UFP into account [3], [33], [34]. Habre et al., exposed 22 patients with mild/moderate asthma for 2 h to both aviation and road-traffic-related UFP in a park downwind of the Los Angeles International Airport (LAX) [33]. In that study, road traffic derived UFP exposure was associated with a reduced FEV_1, but there was no association with aviation derived UFP exposure. Another study (by Strak et al.) found an effect on respiratory outcomes after UFP exposure, but did not assess UFP from aviation [3]. Strak et al. exposed 31 healthy young adults for 5 h to UFP at five different locations: an underground train station, two busy roads, a livestock farm and an urban background location. They found a reduction of FVC after road-traffic-related UFP exposures. In contrast to both our study and the study of Habre et al., Strak et al. did also find an increase in FeNO in individuals exposed to higher levels of UFP. Discrepancies between the findings of our study and the study of Habre et al. and Strak et al. may be due to differences in the location of exposure, which is known to affect the UFP levels, sources and chemical composition. In most studies, road traffic is the most important source of UFP, a source also associated with emissions of other components (e.g. NO_2 and BC). In our study, aviation was the most important source of UFP, which is known to minimally contribute to other components than UFP (hence our low correlations between pollutants).

Potential mechanisms for lung function decline could be that UFP exposure induces pulmonary oxidative stress leading to generation of reactive oxygen species [35]–[37] and pro-inflammatory cytokines [38]. This can alter the barrier function of the respiratory tract and antioxidant defences, which could lead to airway inflammation and decreases in lung function [39]. Another possible mechanism, is the activation of (M_3) muscarinic receptors, controlling the smooth muscle tone [40], resulting in airway constriction and therefore lung function decline. This mechanism was also shown in rat bronchi segments exposed to PM2.5 [41].

For cardiovascular outcomes, the association between air pollution and prolongation in QTc has been shown before, but mainly involved long-term effects in human or short-term effects in animals [42]–[44]. Moreover, these studies only considered exposure to PM2.5 (expressed in mass) and not UFP (expressed in particle number). Furthermore, we found that exposure to BC, NO_2 and relatively larger particles were associated with higher BP, which is consistent with previous literature. In multiple studies, short-term effects on BP have been found before and were mainly associated with BC, PM10 (mass concentrations) and SO_2, but less consistently with PM2.5 (mass concentrations), and UFP (PNC), as summarized by the review of Li et al. [45]. Since our SO_2 levels were almost always under the limits of detection, we could not investigate this relation.

A possible explanation for the cardiovascular effects could be that UFP can easily transfer into the blood stream, possibly inducing oxidative stress and inflammation directly in the vessels and myocardial substrate [46]. This has shown to alter cardiac autonomic control [46] which prolongs ventricle polarization due to changes in sodium and calcium channels [47], [48]. According to the Food and Drug Administration (FDA), an extension of the QTc interval by > 5 ms can already increase the risk of cardiac arrhythmias in sensitive individuals, such as patients with heart disease [49]. One of the possible arrhythmias related to QTc prolongation, is *torsade de pointes*, which can eventually evolve in ventricle fibrillation. The possible mechanism for increases in blood pressure after short-term UFP exposure, could be the acute imbalance of the autonomic nervous system possibly prompted by lung irritant sensory receptors and afferent nerve stimulation [50].

An important strength of this study, is the prospective interventional nature of the study, in which subjects were exposed multiple times at the same location in a highly-controlled environment. The use of the mobile exposure laboratory was a form of blinding for the participants, reduced noise from traffic and prevented measurement error due to wind or rain. In addition, it allowed for air pollution classification on site, which minimized possible exposure misclassification when compared to most observational studies that rely on central site monitoring. Furthermore, low correlations existed between almost all pollutants, which is uncommon for air pollution studies. This makes the independency of the association we found between health outcomes and UFP exposure more likely when compared to other studies [7]. On top of that, we achieved a high contrast in UFP exposure (on average 80,000 particles/cm^3) when compared to previous studies, in which the average contrast ranged from ~20,000 to ~55,000 particles/cm^3 [3], [33], [34], [51]. Although we did not have a "control" exposure, the

lowest exposure that participants received (on average 21,300 particles/cm^3) is comparable to the "control" exposure sites of other studies (i.e. 6,000–19,600 particles/cm^3) [3], [33], [34], [51]. Finally, both drop-outs and missing data were limited.

This study also had several limitations. First, we only included one time-point both before and after the exposure. Therefore, we may not have always captured the maximal response to the exposure, as effects may have recovered rapidly or developed slowly (such as certain inflammatory pathways). Secondly, we had no information about the exposure of the participants before each visit. This may have affected the before-exposure cardiopulmonary measurements. However, we have tried to reduce the residential exposure, by excluding people living < 2 km from Schiphol Airport, < 300 m from high way and on busy roads (5,000–10,000 vehicles/day). A possible confounder, we did not adjust for, was noise. However, the fact that the volunteers were inside a mobile exposure laboratory reduced outside (road traffic and aircraft) noise and several pumps inside the laboratory created constant background noise partly drowning out noise from outside. On top of that, participants were often wearing noise-cancelling headphones. Furthermore, the blood pressure results should be interpreted carefully as blood pressure easily fluctuates, however, we did try to stabilize the blood pressure as much as possible by performing three measurements and having resting time before and between measurements. A potential issue in our study is that the multiple comparisons potentially may have led to finding associations by chance. We chose not to apply adjustments for multiple comparisons, such as Bonferroni correction, as this is controversial in epidemiology [52]. Therefore, we have focused on the consistency of the associations and not on single significant associations, and we recommend performing independent replication studies to confirm our findings. Another limitation is our convenience sample (i.e. young and healthy subjects) and small sample size, limiting the inference and generalizability to people living near Schiphol Airport. In addition, the majority of the study population was female, which may have had an influence on the effects, but due to the lack of power, we could not do a sensitivity analysis for. Finally, exposures were short and sometimes extremely high due to the proximity to the airport, which is not representative for normal daily exposures.

The associations reported in this study are small, however, they represent group averages and were found in a young healthy population after very short exposures. Therefore, we think it is of important to investigate the effects in sensitive groups, such as people with cardiopulmonary problems, and potential health effects of long-term exposure to high levels of airport-related UFP.

Conclusion

Short-term exposure to high levels of UFP near Schiphol Airport was, on average, associated with decreased lung function (mainly FVC) and prolonged repolarization of the heart (QTc), directly after exposure in young healthy adults. The effects were relatively small, however, they appeared after single exposures of 5 h in a young healthy population. As this study cannot make any inferences about long-term health impacts, studies investigating potential health effects of long-term exposure to airport-related UFP, are urgently needed.

References

[1] R. D. Brook *et al.*, "Particulate matter air pollution and cardiovascular disease: An update to the scientific statement from the american heart association," *Circulation*, vol. 121, no. 21, pp. 2331–2378, 2010.

[2] T. L. Knuckles, M. J. Campen, and L. W. Stanek, "Air Pollution and Cardiovascular Disease," *Compr. Toxicol. Second Ed.*, vol. 6, no. 5, pp. 465–487, 2010.

[3] M. Strak *et al.*, "Respiratory health effects of airborne particulate matter: The role of particle size, composition, and oxidative potential-the RAPTES project," *Environ. Health Perspect.*, vol. 120, no. 8, pp. 1183–1189, 2012.

[4] M. Kampa and E. Castanas, "Human health effect of air polution-Enviro Polution," *Environ. Pollut.*, vol. 151, pp. 362–367, 2008.

[5] U.S. Environmental Protection Agency, "Integrated Science Assessment (ISA) for Particulate Matter (Final Report, 2019)," Washington, DC, 2019.

[6] H. Khreis, C. Kelly, J. Tate, R. Parslow, K. Lucas, and M. Nieuwenhuijsen, "Exposure to traffic-related air pollution and risk of development of childhood asthma: A systematic review and meta-analysis," *Environment International*. 2017.

[7] S. Ohlwein, R. Kappeler, M. Kutlar Joss, N. Künzli, and B. Hoffmann, "Health effects of ultrafine particles: a systematic literature review update of epidemiological evidence," *Int. J. Public Health*, vol. 64, no. 4, pp. 547–559, 2019.

[8] G. Hoek *et al.*, "Long-term air pollution exposure and cardio-respiratory mortality: A review," *Environ. Heal. A Glob. Access Sci. Source*, vol. 12, no. 1, 2013.

[9] C. A. Pope III, R. T. Burnett, M. J. Thun, E. E. Calle, D. Krewski, and G. D. Thurston, "to Fine Particulate Air Pollution," *J. Am. Med. Assoc.*, vol. 287, no. 9, pp. 1132–1141, 2002.

[10] R. Beelen *et al.*, "Natural-cause mortality and long-term exposure to particle components: An Analysis of 19 European cohorts within the multi-center ESCAPE project," *Environ. Health Perspect.*, vol. 123, no. 6, pp. 525–533, 2015.

[11] H. J. Heusinkveld *et al.*, "Neurodegenerative and neurological disorders by small inhaled particles," *NeuroToxicology*. 2016.

[12] K. S. Hougaard *et al.*, "A perspective on the developmental toxicity of inhaled nanoparticles," *Reprod. Toxicol.*, 2015.

[13] M. R. Miller *et al.*, "Inhaled Nanoparticles Accumulate at Sites of Vascular Disease," *ACS Nano*, 2017.

[14] G. Oberdörster *et al.*, "Extrapulmonary translocation of ultrafine carbon particles following whole-body inhalation exposure of rats," *J. Toxicol. Environ. Heal. - Part A*, 2002.

[15] "Passage of inhaled particles into the blood circulation in humans," *Circulation*, vol. 105, no. 4, pp. 411–414, 2002.

[16] N. Li *et al.*, "Ultrafine particulate pollutants induce oxidative stress and mitochondrial damage," *Environ. Health Perspect.*, 2003.

[17] V. Stone *et al.*, "Ultrafine particle-mediated activation of macrophages: Intracellular calcium signaling and oxidative stress," in *Inhalation Toxicology*, 2000.

[18] H. Traboulsi, N. Guerrina, M. Iu, D. Maysinger, P. Ariya, and C. J. Baglole, "Inhaled pollutants: The molecular scene behind respiratory and systemic diseases associated with ultrafine particulate matter," *International Journal of Molecular Sciences*. 2017.

[19] K. Donaldson, V. Stone, A. Seaton, and W. MacNee, "Ambient particle inhalation and the cardiovascular system: Potential mechanisms," *Environ. Health Perspect.*, 2001.

[20] N. Hudda, T. Gould, K. Hartin, T. V. Larson, and S. A. Fruin, "Emissions from an international airport increase particle number concentrations 4-fold at 10 km downwind," *Environ. Sci. Technol.*, vol. 48, no. 12, pp. 6628–6635, 2014.

[21] M. P. Keuken, M. Moerman, P. Zandveld, J. S. Henzing, and G. Hoek, "Total and size-resolved particle number and black carbon concentrations in urban areas near Schiphol airport (the Netherlands)," *Atmos. Environ.*, vol. 104, pp. 132–142, 2015.

[22] N. Hudda, M. C. Simon, W. Zamore, and J. L. Durant, "Aviation-Related Impacts on Ultrafine Particle Number Concentrations Outside and Inside Residences near an Airport," *Environ. Sci. Technol.*, 2018.

[23] I. Tesseraux, "Risk factors of jet fuel combustion products," *Toxicol. Lett.*, vol. 149, no. 1–3, pp. 295–300, 2004.

[24] B. Stacey, "Measurement of ultrafine particles at airports: A review," *Atmos. Environ.*, vol. 198, no. October 2018, pp. 463–477, 2019.

[25] M. Mazaheri, T. E. Bostrom, G. R. Johnson, and L. Morawska, "Composition and morphology of particle emissions from in-use aircraft during takeoff and landing," *Environ. Sci. Technol.*, 2013.

[26] L. Ntziachristos, Z. Ning, M. D. Geller, and C. Sioutas, "Particle concentration and characteristics near a major freeway with heavy-duty diesel traffic," *Environ. Sci. Technol.*, 2007.

[27] R. M. Harrison, D. C. S. Beddows, and M. Dall'Osto, "PMF analysis of wide-range particle size spectra collected on a major highway," *Environ. Sci. Technol.*, 2011.

[28] L. Liu, B. Urch, R. Poon, M. Szyszkowicz, M. Speck, and D. R. Gold, "Ambient particle sizes and systemic biomarkers," vol. 534, no. 6, p. 6, 2015.

[29] M. Voogt, P. Zandveld, J. Wesseling, and N. A. H. Janssen, "Metingen en berekeningen van ultrafijn stof van vliegverkeer rond Schiphol - Voor onderzoek naar de gezondheid van omwonenden," *RIVM Rapp.*, vol. 0074, 2019.

[30] M. R. Miller *et al.*, "Standardisation of spirometry," *Eur. Respir. J.*, vol. 26, no. 2, pp. 319–338, 2005.

[31] C. E. Werts and R. L. Linn, "A general linear model for studying growth," *Psychol. Bull.*, 1970.

[32] L. Paulin and N. Hansel, "Particulate air pollution and impaired lung function," *F1000Research*, vol. 5, no. 0, p. 201, 2016.

[33] R. Habre *et al.*, "Short-term effects of airport-associated ultrafine particle exposure on lung function and inflammation in adults with asthma," *Environ. Int.*, vol. 118, no. January, pp. 48–59, 2018.

[34] R. Sinharay *et al.*, "Respiratory and cardiovascular responses to walking down a traffic-polluted road compared with walking in a traffic-free area in participants aged 60 years and older with chronic lung or heart disease and age-matched healthy controls: a randomised, crosso," *Lancet*, vol. 391, no. 10118, pp. 339–349, 2018.

[35] F. J. Kelly and J. C. Fussell, "Size, source and chemical composition as determinants of toxicity attribuTable to ambient particulate matter," *Atmos. Environ.*, vol. 60, pp. 504–526, 2012.

[36] N. A. H. Janssen *et al.*, "Associations between three specific a-cellular measures of the oxidative potential of particulate matter and markers of acute airway and nasal inflammation in healthy volunteers," *Occup. Environ. Med.*, vol. 72, no. 1, pp. 49–56, 2015.

[37] J. G. F. Hogervorst, T. M. C. M. De Kok, J. J. Briedé, G. Wesseling, J. C. S. Kleinjans, and C. P. Van Schayck, "Relationship between radical generation by urban ambient particulate matter and pulmonary function of school children," *J. Toxicol. Environ. Heal. - Part A*, vol. 69, no. 3, pp. 245–262, 2006.

[38] K. Donaldson and V. Stone, "Current hypotheses on the mechanisms of toxicity of ultrafine particles," *Ann. Ist. Super. Sanita*, vol. 39, no. 3, pp. 405–410, 2003.

[39] U. S. EPA, "Integrated science assessment for particlate matter (final report)," *U.S Environ. Prot. Agency, Washinton, DC, EPA/600/R-08/139F*, 2009.

[40] A. E. McGovern and S. B. Mazzone, "Neural regulation of inflammation in the airways and lungs," *Auton. Neurosci. Basic Clin.*, 2014.

[41] R. Wang, X. Xiao, Z. Shen, L. Cao, and Y. Cao, "Airborne fine particulate matter causes murine bronchial hyperreactivity via MAPK pathway-mediated M3 muscarinic receptor upregulation," *Environ. Toxicol.*, 2017.

[42] H. Xu *et al.*, "Ambient air pollution is associated with cardiac repolarization abnormalities in healthy adults," *Environ. Res.*, vol. 171, no. January, pp. 239–246, 2019.

[43] S. J. Chung *et al.*, "HHS Public Access disease," vol. 26, no. 7, pp. 1234–1242, 2016.

[44] V. C. Van Hee *et al.*, "Association of long-term air pollution with ventricular conduction and repolarization abnormalities," *Epidemiology*, 2011.

[45] T.-G. Li, B.-Y. Yang, S.-J. Fan, T. Schikowski, G.-H. Dong, and K. B. Fuks, "Outdoor Air Pollution and Arterial Hypertension," in *Blood Pressure - From Bench to Bed*, 2018, pp. 19–42.

[46] B. Z. Simkhovich, M. T. Kleinman, and R. A. Kloner, "Air Pollution and Cardiovascular Injury. Epidemiology, Toxicology, and Mechanisms," *J. Am. Coll. Cardiol.*, vol. 52, no. 9, pp. 719–726, 2008.

[47] A. J. Moss and R. S. Kass, "Long QT syndrome: From channels to cardiac arrhythmias," *Journal of Clinical Investigation*. 2005.

[48] M. J. Utell, M. W. Frampton, W. Zareba, R. B. Devlin, and W. E. Cascio, "Cardiovascular effects associated with air pollution: Potential mechanisms and methods of testing," *Inhal. Toxicol.*, 2002.

[49] FDA, "Guidance for Industry Interval Prolongation and Guidance for Industry. E14 clinical evaluation of QT/QTc interval prolongation and proarrythmic potential for non-antiarrhythmic drugs.," *U.S. Dep. Heal. Hum. Serv. Food Drug Adm. Cent. Drug Eval. Res. Cent. Biol. Eval. Res.*, no. 1–16, 2005.

[50] C. M. Perez, M. S. Hazari, and A. K. Farraj, "Role of Autonomic Reflex Arcs in Cardiovascular Responses to Air Pollution Exposure," *Cardiovasc. Toxicol.*, 2015.

[51] J. McCreanor *et al.*, "Respiratory effects of exposure to diesel traffic in persons with asthma," *N. Engl. J. Med.*, 2007.

[52] D. L. Streiner and G. R. Norman, "Correction for multiple testing: Is there a resolution?," *Chest*. 2011.

Supplementary materials

Table S1. Inclusion and exclusion criteria.

Inclusion criteria	Exclusion criteria
1) 18–35 years	1) (History of chronic) pulmonary or cardiovascular events/diseases
2) Non-smoker for at least 1 year	2) Use of medications that affect pulmonary or cardiovascular parameters
3) Smoking history of < 5 pack years	3) (History of) hay fever
4) Baseline FEV_1 > 80% of predicted value	4) History of bleeding tendency
5) No clinical findings during screening*	5) Regular consumption of greater than three units of alcohol per day
6) Informed consent	6) Administration of any investigational drug within 30 days of study initiation.
	7) Donation of blood within 60 days
	8) Loss or greater than 400 mL of blood within 12 weeks of study initiation
	9) Respiratory tract infection in the last 6 weeks before or during the study
	10) History of serious drug-related reactions, including hypersensitivity
	11) Pregnancy at screening or during the study period
	12) Residency or daily working with estimated annual average contribution of UFP from air traffic of > 3000 particles/cm^3 < 2 km from Schiphol < 300 m from high way On a busy road (5,000–10,000 vehicles/day)

FEV_1 = forced expiratory volume in 1s; *Abnormalities in ECG were assessed by a cardiologist. No strict criteria existed for fractional exhaled nitric oxide (FeNO), blood pressure and the resting heart rate, but all had to be within or close to normal ranges: i.e. FeNO < 50 ppb, blood pressure systolic 90–140 mmHg and diastolic 60–90 mmHg, and the resting heart rate < 80 bmp.

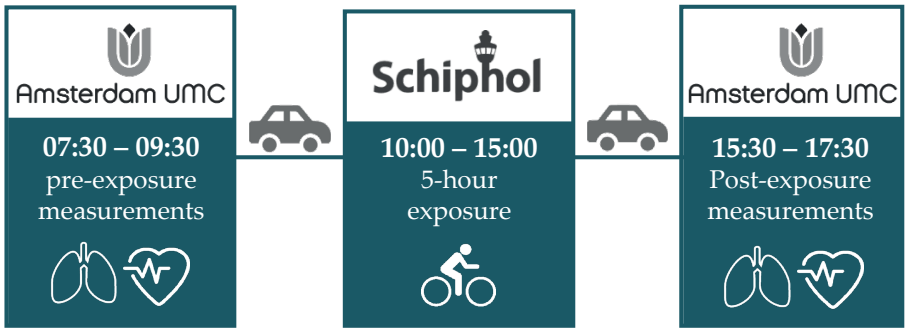

Figure S1. Flow chart of one exposure day: health assessment (lung- and heart function) was performed at the Amsterdam UMC in the morning and afternoon. In between, participants were exposed for 5 h while performing intermittent cycling on an ergometer (20 min per hour). Participants were transported by car between locations.

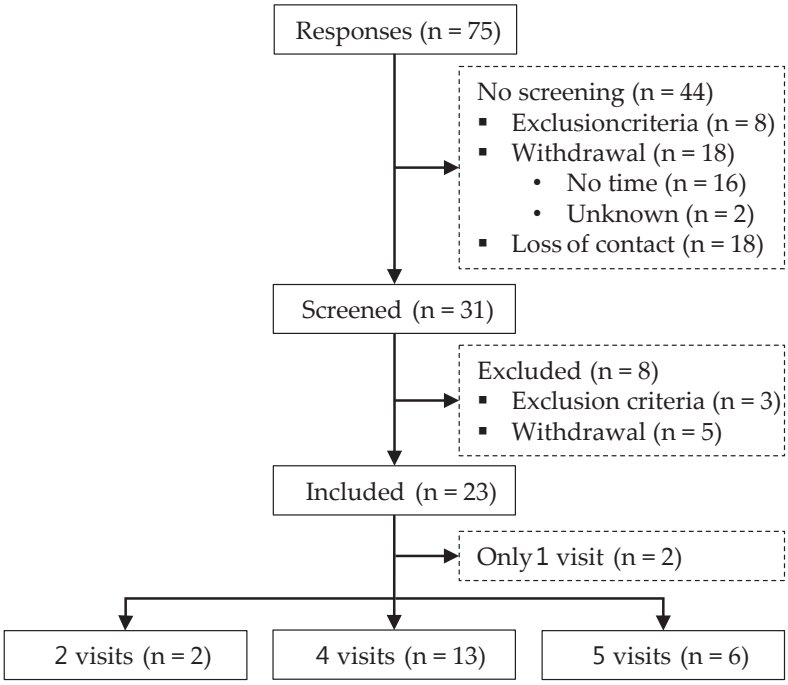

Figure S2. Inclusion chart: in total 75 subjects responded of whom 31 were interested and suitable for screening. Eventually, 23 subjects were exposed. Only subjects who had more than one visit (n = 21) were included in the analysis and were exposed two (n = 2), four (n = 13) or five (n = 6) times.

Table S2. Distribution of exposure variables per exposure day (5 h averages).

Exposure day	PM ($\mu g/m^3$)	PNC ($\#/cm^3$)	BC ($\mu g/m^3$)	NO_2 ($\mu g/m^3$)	CO ($\mu g/m^3$)	SO_2 ($\mu g/m^3$)	O_3 ($\mu g/m^3$)	Temp (^oC)	RH (%)
1	29.9	74,466	0.3	12.4	619	DL	44.5	19.4	43
2	17.0	40,156	0.3	13.3	599	DL	40.6	18.8	44
3	18.8	28,898	0.6	48.4	775	2.0	38.8	22.3	54
4	27.3	22,049	0.8	37.8	650	1.5	38.4	23.9	62
5	22.4	23,356	0.7	28.1	621	3.2	52.1	24.2	51
6	39.4	18,861	1.3	41.4	784	1.2	39.4	22.3	62
7	14.5	27,835	0.5	24.5	619	DL	32.8	21.9	46
8	13.6	30,413	0.3	16.4	587	DL	34.7	21.4	43
9	26.6	134,879	0.7	42.8	569	DL	25.7	24.0	40
10	25.7	32,144	0.5	12.8	510	DL	46.5	24.0	53
11	25.7	23,474	0.2	16.1	691	DL	56.8	24.0	50
12	28.0	35,357	0.4	27.3	667	DL	20.9	25.2	54
13	16.0	24,866	0.3	16.3	494	DL	57.9	24.6	50
14	21.9	12,619	0.4	20.0	579	DL	31.2	24.1	58
15	27.9	20,926	0.1	12.4	537	DL	39.0	25.2	57
16	16.0	52,896	0.3	23.3	611	DL	46.9	26.0	52
17	18.2	39,531	0.3	27.0	568	DL	33.3	26.5	47
18	18.4	38,360	0.4	18.8	557	DL	48.8	25.0	47
19	47.5	46,866	0.8	26.8	616	DL	47.4	26.6	53
20	20.3	45,524	1.0	27.7	603	DL	78.6	28.6	52
21	27.8	64,379	0.5	24.8	670	DL	28.3	24.8	65
22	24.4	139,321	1.0	36.2	705	DL	28.2	25.2	66
23	19.1	173,187	0.6	33.9	597	DL	25.3	21.3	58
24	24.8	128,166	1.1	35.8	681	DL	18.6	24.4	66
25	26.7	80,856	0.6	34.1	744	DL	20.6	26.6	63
26	42.0	20,644	1.6	44.0	830	DL	28.1	22.8	62
27	18.6	42,565	0.1	12.6	744	DL	37.6	21.6	60
28	10.6	144,191	0.9	45.6	744	DL	19.7	21.2	51
29	15.1	28,846	1.9	60.2	696	DL	8.8	22.2	57
30	15.0	25,160	0.1	19.3	620	DL	29.6	20.6	58
31	18.0	79,701	0.3	32.9	550	DL	25.6	20.1	51
32	21.5	10,520	0.5	28.6	585	DL	16.2	15.7	47
mean	**23.1**	**53,469**	**0.6**	**28.2**	**638**	**2.0**	**35.7**	**23.3**	**54**
SD	8.3	43,776	0.4	12.2	83	0.9	14.4	2.7	7
max	47.5	173,187	1.9	60.2	830	3.2	78.6	28.6	66
min	10.6	10,520	0.1	12.4	494	1.2	8.8	15.7	40

Mass concentration based on filter measurements; PM = particulate matter; PNC = particle number concentration measured by a condensation particle counter (CPC) with d_{50} = 4 nm; BC = black carbon; NO_2 = nitric oxide; CO = carbon monoxide; SO_2 = sulfur dioxide; O_3 = ozone; DL= value below detection limit; Temp = temperature; RH = relative humidity; SD = standard deviation.

Table S3. Distribution of particle number concentrations per participant (5 h averages).

Participant	PNC exposure (#/cm³)				Visits
	mean	min	max	contrast	
1	97,200	38,400	144,200	105,800	5
2	93,200	20,700	144,200	123,500	4
3	89,500	20,700	173,200	152,500	4
4	75,300	24,900	144,200	119,300	5
5	68,200	24,900	173,200	148,300	4
6	63,200	25,200	139,400	114,200	5
7	52,600	10,600	139,400	128,800	4
8	52,300	12,700	134,900	122,200	4
9	52,000	22,100	128,200	106,100	5
10	51,400	20,700	134,900	114,200	4
11	50,000	23,500	80,900	57,400	4
12	50,000	23,500	80,900	57,400	4
13	48,200	21,000	79,800	58,800	5
14	42,700	27,900	64,400	36,500	4
15	41,200	12,700	74,500	61,800	4
16	40,500	25,200	74,500	49,300	5
17	35,600	18,900	64,400	45,500	4
18	34,900	18,900	45,600	26,700	4
19	30,400	21,000	46,900	25,900	4
20	27,800	23,400	32,200	8,800	2
21	19,700	10,600	28,900	18,300	2
mean	**53,100**	**21,300**	**101,400**	**80,000**	
min	19,700	10,600	28,900	8,800	
max	97,200	38,400	173,200	152,500	

PNC = particle number concentration measured by a condensation particle counter (CPC) with d_{50} = 4 nm. PNC levels are rounded to hundreds.

Table S4. Correlation matrix for all pollutants, particle size ranges and room conditions measured during 5 h exposures.

	PNC[a]	**PM**	**BC**	**NO_2**	**CO**	**O_3**	**PNC ≤ 20 nm**	**PNC ≤ 30 nm**	**PNC ≤ 50 nm**	**PNC ≤ 100 nm**	**PNC > 50 nm**	**PNC > 100 nm**	**Temp**	**RH**
PNC[a]		-0.11	0.14	0.37	0.08	-0.37	**0.97**	**0.98**	**0.98**	**0.98**	0.11	-0.17	0.01	0.05
PM	-0.11		0.38	0.13	0.33	0.06	-0.13	-0.08	-0.05	-0.04	0.30	0.36	0.26	0.36
BC	0.14	0.38		**0.79**	0.59	-0.28	0.09	0.13	0.14	0.15	0.43	0.50	0.05	0.40
NO_2	0.37	0.13	**0.79**		0.57	-0.53	0.30	0.32	0.32	0.33	0.44	0.42	0.02	0.29
CO	0.08	0.33	0.59	0.57		-0.33	0.07	0.07	0.07	0.08	0.28	0.30	-0.04	0.56
O_3	-0.37	0.06	-0.28	-0.53	-0.33		-0.32	-0.30	-0.27	-0.27	0.07	0.28	0.31	-0.26
PNC[b] ≤ 20 nm	**0.97**	-0.13	0.09	0.30	0.07	-0.32		**0.99**	**0.98**	**0.98**	0.12	-0.15	0.03	0.03
PNC[b] ≤ 30 nm	**0.98**	-0.08	0.13	0.32	0.07	-0.30	**0.99**		**1.00**	**1.00**	0.16	-0.12	0.10	0.06
PNC[b] ≤ 50 nm	**0.98**	-0.05	0.14	0.32	0.07	-0.27	**0.98**	**1.00**		**1.00**	0.19	-0.10	0.13	0.07
PNC[b] ≤ 100 nm	**0.98**	-0.04	0.15	0.33	0.08	-0.27	**0.98**	**1.00**	**1.00**		0.21	-0.08	0.14	0.07
PNC[b] > 50 nm	0.11	0.30	0.43	0.44	0.28	0.07	0.12	0.16	0.19	0.21		**0.81**	0.52	0.22
PNC[b] > 100 nm	-0.17	0.36	0.50	0.42	0.30	0.28	-0.15	-0.12	-0.10	-0.08	**0.81**		0.41	0.29
Temp	0.01	0.26	0.05	0.02	-0.04	0.31	0.03	0.10	0.13	0.14	0.52	0.41		0.29
RH	0.05	0.36	0.40	0.29	0.56	-0.26	0.03	0.06	0.07	0.07	0.22	0.29	0.29	

Pearson correlations with in **bold** R >0.70; PNC = particle number concentration; PM = particulate matter; BC = black carbon; NO_2 = nitric oxide; CO = carbon monoxide; O_3 = ozone; Temp = temperature; RH = relative humidity; a = PNC was detected by a condensation particle counter (CPC) with d_{50} = 4 nm; b = PNC size fractions were measured by a scanning mobility particle sizer (SMPS) with a limit of detection of 6-225 nm.

Table S5. Two-pollutant models (PNC adjusted for co-pollutants).

Outcome	PNC adjusted for BC				PNC adjusted for NO_2				PNC adjusted for PM			
	Est.	95% CI			Est.	95% CI			Est.	95% CI		
FVC (mL)	**-79.2**	**-148.2**	–	**-10.2**	**-83.9**	**-158.1**	–	**-8.4**	-65.1	-132.3	–	5.9
FEV_1 (mL)	-54.4	-121.7	–	24.2	-44.3	-119.8	–	36.3	-41.7	-107.3	–	39.7
PEF (mL/s)	-92.3	-380.0	–	179.0	-3.9	-331.3	–	279.0	-57.6	-346.1	–	220.1
FeNO (ppb)	0.3	-1.1	–	1.7	-0.1	-1.6	–	1.4	0.2	-1.2	–	1.6
$HR_{sitting}$ (bpm)	-0.9	-4.5	–	2.6	-0.7	-4.6	–	2.9	-1.0	-4.6	–	2.5
Saturation (%)	0.0	-0.6	–	0.6	0.1	-0.5	–	0.7	0.0	-0.5	–	0.6
BP_{sys} (mmHg)	-2.4	-5.2	–	0.4	**-3.2**	**-6.3**	–	**-0.2**	-1.9	-4.9	–	1.0
BP_{dia} (mmHg)	-2.3	-5.1	–	0.6	**-3.7**	**-6.7**	–	**-0.7**	-1.7	-4.7	–	1.2
ECG - HR (bpm)	3.3	-0.4	–	7.7	3.9	-0.1	–	8.5	3.5	-0.2	–	7.7
ECG - PR (ms)	-3.5	-8.9	–	0.3	-4.0	-10.5	–	0.0	-2.2	-7.5	–	1.8
ECG - QRS (ms)	1.6	-1.0	–	4.1	1.4	-1.4	–	4.2	1.3	-1.2	–	3.9
ECG - QTc (ms)	**10.1**	**2.1**	–	**19.3**	**11.7**	**3.1**	–	**21.4**	**10.3**	**2.3**	–	**19.4**
Outcome	**PNC adjusted for CO**				**PNC adjusted for O_3**							
	Est.	**95% CI**			**Est.**	**95% CI**						
FVC (mL)	**-74.7**	**-139.5**	–	**-0.9**	**-84.3**	**-157.1**	–	**-3.8**				
FEV_1 (mL)	-50.8	-117.7	–	29.6	-49.4	-124.1	–	38.5				
PEF (mL/s)	-57.0	-341.9	–	218.2	-12.6	-345.8	–	282.8				
FeNO (ppb)	0.3	-1.1	–	1.7	-0.4	-1.8	–	1.2				
$HR_{sitting}$ (bpm)	-1.1	-4.6	–	2.4	0.9	-3.0	–	4.5				
Saturation (%)	0.0	-0.5	–	0.6	-0.2	-0.8	–	0.5				
BP_{sys} (mmHg)	-1.9	-4.8	–	0.9	-2.7	-6.0	–	0.5				
BP_{dia} (mmHg)	-1.8	-4.7	–	1.0	**-4.1**	**-7.2**	–	**-1.1**				
ECG - HR (bpm)	3.3	-0.4	–	7.5	**4.1**	**0.0**	–	**8.9**				
ECG - PR (ms)	-2.2	-7.3	–	1.8	-3.1	-11.4	–	0.7				
ECG - QRS (ms)	1.3	-1.3	–	3.8	1.1	-1.7	–	4.0				
ECG - QTc (ms)	**9.8**	**1.9**	–	**18.9**	**13.5**	**5.0**	–	**23.7**				

Data are presented as PNC estimates (Est.) and 95% confidence intervals (CI). All effect estimates are scaled to the 5-95th percentile change in the exposure of interest and are adjusted for age, sex, BMI, respiratory symptoms, room temperature and room humidity. Numbers in **bold** are significant effects ($p < 0.05$). *Exposures*: PNC = particle number concentration; PM = particulate matter; BC = black carbon; NO_2 = nitric oxide; CO = carbon monoxide; O_3 = ozone. *Health outcomes*: FVC = forced vital capacity; FEV_1 = forced expiratory volume in 1s; PEF = peak expiratory flow rate; FeNO = fractional exhaled nitric oxide; HR = heart rate; BPsys = systolic blood pressure; BPdia = diastolic blood pressure; ECG = electrocardiography; QTc = corrected QT. PNC was detected by a condensation particle counter (CPC) with d_{50} = 4 nm.

Table S6. Single-pollutant models based on particle size fractions.

Outcome	PNC ≤ 20 nm		PNC ≤ 30 nm		PNC ≤ 50 nm		PNC ≤ 100 nm	
	Est.	95% CI	Est.	95% CI	Est.	95% CI	Est.	95% CI
FVC (mL)	-69.3	-135.8 – 1.0	-70.1	-136.6 – 1.3	-67.9	-134.5 – 4.2	-68.0	-134.9 – 4.5
FEV_1 (mL)	-48.1	-114.7 – 28.5	-47.5	-114.3 – 30.7	-44.9	-111.8 – 34.2	-45.1	-112.4 – 34.5
PEF (mL/s)	-12.1	-302.3 – 253.7	-28.6	-320.4 – 239.1	-31.1	-323.8 – 237.9	-30.5	-324.9 – 239.9
FeNO (ppb)	-0.1	-1.4 – 1.4	0.0	-1.3 – 1.5	0.0	-1.3 – 1.5	0.0	-1.3 – 1.5
$HR_{sitting}$ (bpm)	-1.4	-4.9 – 1.9	-1.0	-4.6 – 2.3	-0.8	-4.4 – 2.5	-0.8	-4.4 – 2.6
Saturation (%)	0.1	-0.4 – 0.7	0.1	-0.4 – 0.7	0.0	-0.5 – 0.7	0.0	-0.5 – 0.7
BP_{sys} (mmHg)	-1.6	-4.5 – 1.1	-1.4	-4.3 – 1.4	-1.3	-4.2 – 1.5	-1.3	-4.2 – 1.6
BP_{dia} (mmHg)	-1.9	-4.7 – 1.0	-1.9	-4.7 – 1.0	-1.9	-4.8 – 1.0	-1.8	-4.7 – 1.1
ECG - HR (bpm)	2.9	-0.8 – 6.9	3.4	-0.3 – 7.5	3.6	-0.1 – 7.8	3.6	-0.1 – 7.8
ECG - PR (ms)	-3.2	-8.3 – 0.5	-3.0	-8.0 – 0.9	-2.8	-7.9 – 1.0	-2.8	-8.0 – 1.1
ECG - QRS (ms)	1.2	-1.3 – 3.7	1.2	-1.3 – 3.8	1.3	-1.2 – 3.9	1.3	-1.2 – 3.9
ECG - QTc (ms)	**9.6**	**1.9 – 18.4**	**10.4**	**2.7 – 19.4**	**10.5**	**2.8 – 19.7**	**10.5**	**2.7 – 19.7**

Data are presented as estimates (Est.) and 95% confidence intervals (CI). All effect estimates are scaled to the 5-95th percentile change in the exposure of interest and are adjusted for age, sex, BMI, respiratory symptoms, room temperature and room humidity. Numbers in **bold** are significant effects ($p < 0.05$). PNC = particle number concentration; FVC = forced vital capacity; FEV_1 = forced expiratory volume in 1s; PEF = peak expiratory flow rate; FeNO = fractional exhaled nitric oxide; HR = heart rate; BPsys = systolic blood pressure; BPdia = diastolic blood pressure; ECG = electrocardiography; QTc = corrected QT. PNC size fractions were measured by a scanning mobility particle sizer (SMPS) with a limit of detection of 6-225 nm.

Table S7. Single-pollutant models (unadjusted).

Outcome	PNC		BC		NO_2	
	Est.	**95% CI**	**Est.**	**95% CI**	**Est.**	**95% CI**
FVC (mL)	-66.7	-138.4 – 9.9	46.9	-29.4 – 123.3	16.7	-55.9 – 89.4
FEV_1 (mL)	-57.7	-131.5 – 22.3	40.9	-38.9 – 125.8	-16.3	-94.1 – 71.6
PEF (mL/s)	-53.7	-353.0 – 235.7	195.9	-109.3 – 508.6	-97.8	-387.3 – 212.4
FeNO (ppb)	0.1	-1.3 – 1.6	0.0	-1.5 – 1.6	0.8	-0.7 – 2.3
$HR_{sitting}$ (bpm)	-0.5	-4.0 – 3.0	-1.7	-5.5 – 2.4	-1.4	-5.2 – 2.4
Saturation (%)	-0.1	-0.6 – 0.5	0.3	-0.3 – 0.9	0.0	-0.6 – 0.6
BP_{sys} (mmHg)	-1.9	-4.8 – 1.0	**3.7**	**0.5 – 6.8**	3.0	-0.1 – 6.1
BP_{dia} (mmHg)	-2.3	-5.2 – 0.7	**3.5**	**0.3 – 6.7**	**3.9**	**0.8 – 6.9**
ECG - HR (bpm)	**4.0**	**0.1 – 8.2**	1.0	-3.7 – 5.6	0.1	-4.3 – 4.4
ECG - PR (ms)	-2.6	-7.7 – 2.6	**7.0**	**1.5 – 12.2**	4.8	-0.2 – 10
ECG - QRS (ms)	0.9	-1.7 – 3.5	-1.5	-4.3 – 1.3	0.1	-2.6 – 2.8
ECG - QTc (ms)	**11.6**	**3.1 – 20.8**	-0.5	-10.2 – 9.7	-1.0	-10.2 – 8.6
Outcome	**PM**		**CO**		**O_3**	
	Est.	**95% CI**	**Est.**	**95% CI**	**Est.**	**95% CI**
FVC (mL)	55.4	-20.6 – 131.4	10.4	-65.6 – 86.4	-9.7	-84.8 – 65.4
FEV_1 (mL)	71.4	-6.0 – 150.9	3.5	-76.4 – 83.5	13.6	-68.8 – 90.8
PEF (mL/s)	164.7	-132 – 478.3	-50.3	-357.1 – 247.9	178.2	-122.6 – 470.9
FeNO (ppb)	-0.7	-2.2 – 0.7	-0.1	-1.6 – 1.4	-1.0	-2.5 – 0.5
$HR_{sitting}$ (bpm)	0.8	-2.8 – 4.3	0.1	-3.7 – 3.8	**4.3**	**0.7 – 7.9**
Saturation (%)	0.1	-0.5 – 0.7	0.3	-0.3 – 0.9	-0.4	-1.0 – 0.2
BP_{sys} (mmHg)	-0.4	-3.5 – 2.6	2.1	-1.0 – 5.2	-0.6	-3.7 – 2.4
BP_{dia} (mmHg)	-0.3	-3.4 – 2.8	2.2	-1.0 – 5.2	**-3.8**	**-6.9 – -0.8**
ECG - HR (bpm)	1.7	-2.5 – 5.8	1.0	-3.4 – 5.2	1.2	-3.0 – 5.5
ECG - PR (ms)	0.0	-5.9 – 5.2	2.5	-3.1 – 7.8	-4.7	-9.9 – 0.6
ECG - QRS (ms)	0.4	-2.4 – 3.2	-0.7	-3.4 – 2.0	0.4	-2.3 – 3.1
ECG - QTc (ms)	2.2	-7.2 – 11.2	0.0	-9.3 – 9.7	6.0	-3.3 – 15.0

Data are presented as estimates (est.) and 95% confidence intervals (CI). All effect estimates are scaled to the 5-95th percentile change in the exposure of interest. Numbers in **bold** are significant effects ($p < 0.05$). *Exposures*: PNC = particle number concentration; PM = particulate matter; BC = black carbon; NO_2 = nitric oxide; CO = carbon monoxide; O_3 = ozone. *Health outcomes*: FVC = forced vital capacity; FEV_1 = forced expiratory volume in 1s; PEF = peak expiratory flow rate; FeNO = fractional exhaled nitric oxide; HR = heart rate; BPsys = systolic blood pressure; BPdia = diastolic blood pressure; ECG = electrocardiography; QTc = corrected QT. PNC was detected by a condensation particle counter (CPC) with d_{50} = 4 nm.

Table S8. Two-pollutant models with PNC adjusted for co-pollutants (unadjusted for covariates).

Outcome	PNC adjusted for BC			PNC adjusted for NO_2			PNC adjusted for PM		
	Est.	95% CI		Est.	95% CI		Est.	95% CI	
FVC (mL)	-70.9	-141.8	2.1	**-79.2**	**-155.8**	**-2.0**	-60.5	-129.2	14.6
FEV_1 (mL)	-61.8	-135.9	18.0	-58.6	-138.1	23.8	-50.5	-123.8	29.5
PEF (mL/s)	-78.7	-376.8	208.5	-20.3	-348.9	285.8	-36.7	-333.2	255.0
FeNO (ppb)	0.1	-1.3	1.6	-0.1	-1.7	1.4	0.1	-1.4	1.5
$HR_{sitting}$ (bpm)	-0.3	-3.8	3.2	-0.1	-3.8	3.7	-0.4	-4.0	3.1
Saturation (%)	-0.1	-0.7	0.5	-0.1	-0.7	0.5	-0.1	-0.6	0.5
BP_{sys} (mmHg)	-2.4	-5.2	0.4	-3.3	-6.3	-0.3	-2.0	-4.9	1.0
BP_{dia} (mmHg)	-2.7	-5.5	0.2	-4.0	-7.0	-1.1	-2.3	-5.3	0.6
ECG - HR (bpm)	4.0	0.0	8.2	**4.6**	**0.4**	**9.1**	**4.2**	**0.3**	**8.3**
ECG - PR (ms)	-3.5	-8.5	1.5	-4.9	-10.3	0.5	-2.6	-7.8	2.6
ECG - QRS (ms)	1.1	-1.5	3.8	1.0	-1.8	3.8	1.0	-1.7	3.6
ECG - QTc (ms)	**11.9**	**3.3**	**21.1**	**13.7**	**4.6**	**23.4**	**11.9**	**3.3**	**21.0**

Outcome	PNC adjusted for CO			PNC adjusted for O_3		
	Est.	95% CI		Est.	95% CI	
FVC (mL)	-68.8	-140.5	8.7	-79.8	-156.1	1.2
FEV_1 (mL)	-58.0	-132.1	22.0	-59.9	-139.4	24.2
PEF (mL/s)	-50.8	-350.0	239.5	16.8	-307.5	326.3
FeNO (ppb)	0.1	-1.3	1.6	-0.3	-1.8	1.3
$HR_{sitting}$ (bpm)	-0.5	-4.0	3.0	1.2	-2.4	4.7
Saturation (%)	-0.1	-0.6	0.5	-0.2	-0.8	0.4
BP_{sys} (mmHg)	-2.0	-4.9	0.9	-2.5	-5.6	0.7
BP_{dia} (mmHg)	-2.3	-5.2	0.6	**-4.1**	**-7.0**	**-1.1**
ECG - HR (bpm)	4.0	0.0	8.1	**5.1**	**1.0**	**9.7**
ECG - PR (ms)	-2.7	-7.9	2.4	-4.8	-10.3	0.6
ECG - QRS (ms)	1.0	-1.7	3.6	1.2	-1.6	4.0
ECG - QTc (ms)	**11.7**	**3.1**	**20.8**	**15.5**	**6.7**	**25.1**

Data are presented as PNC estimates (Est.) and 95% confidence intervals (CI). All effect estimates are scaled to the 5-95th percentile change in the exposure of interest. Numbers in **bold** are significant effects ($p < 0.05$). *Exposures*: PNC = particle number concentration; PM = particulate matter; BC = black carbon; NO_2 = nitric oxide; CO = carbon monoxide; O_3 = ozone. *Health outcomes*: FVC = forced vital capacity; FEV_1 = forced expiratory volume in 1s; PEF = peak expiratory flow rate; FeNO = fractional exhaled nitric oxide; HR = heart rate; BPsys = systolic blood pressure; BPdia = diastolic blood pressure; ECG = electrocardiography; QTc = corrected QT. PNC was detected by a condensation particle counter (CPC) with d_{50} = 4 nm.

Table S9. Single-pollutant models based on particle size fractions (unadjusted).

Outcome	PNC ≤ 20 nm		PNC ≤ 30 nm		PNC ≤ 50 nm		PNC ≤ 100 nm	
	Est.	95% CI	Est.	95% CI	Est.	95% CI	Est.	95% CI
FVC (mL)	-61.5	-129.1 – 9.8	-58.1	-123.0 – 10.7	-56.0	-121.1 – 12.9	-56.1	-121.9 – 13.3
FEV_1 (mL)	-52.3	-123.1 – 22.6	-48.5	-116.7 – 23.7	-45.9	-114.3 – 26.5	-45.7	-114.8 – 27.3
PEF (mL/s)	-0.4	-291.0 – 277.8	-1.1	-281.3 – 266.1	3.8	-277.3 – 271.7	8.7	-275.0 – 279.1
FeNO (ppb)	-0.1	-1.5 – 1.3	0.0	-1.3 – 1.3	0.0	-1.3 – 1.3	0.0	-1.4 – 1.3
$HR_{sitting}$ (bpm)	-0.8	-4.2 – 2.5	-0.3	-3.6 – 2.8	-0.1	-3.3 – 3.1	-0.1	-3.3 – 3.2
Saturation (%)	0.0	-0.5 – 0.6	0.0	-0.5 – 0.5	0.0	-0.6 – 0.5	0.0	-0.6 – 0.5
BP_{sys} (mmHg)	-1.6	-4.4 – 1.1	-1.3	-4.0 – 1.3	-1.2	-3.9 – 1.4	-1.2	-3.9 – 1.5
BP_{dia} (mmHg)	-2.2	-5.0 – 0.6	-2.2	-4.8 – 0.5	-2.2	-4.9 – 0.5	-2.2	-4.9 – 0.6
ECG - HR (bpm)	3.4	-0.3 – 7.3	**3.9**	**0.4 – 7.7**	**4.3**	**0.7 – 8.1**	**4.3**	**0.7 – 8.2**
ECG - PR (ms)	-3.9	-8.8 – 1.0	-3.4	-8.1 – 1.3	-3.3	-8.1 – 1.4	-3.3	-8.2 – 1.4
ECG - QRS (ms)	0.8	-1.7 – 3.4	0.9	-1.5 – 3.4	1.1	-1.4 – 3.5	1.1	-1.3 – 3.6
ECG - QTc (ms)	**11.0**	**2.9 – 19.7**	**11.7**	**4.0 – 20.3**	**12.2**	**4.4 – 20.7**	**12.3**	**4.4 – 20.9**

Data are presented as estimates (Est.) and 95% confidence intervals (CI). All effect estimates are scaled to the 5-95th percentile change in the exposure of interest. Numbers in **bold** are significant effects ($p < 0.05$). PNC = particle number concentration; FVC = forced vital capacity; FEV_1 = forced expiratory volume in 1s; PEF = peak expiratory flow rate; FeNO = fractional exhaled nitric oxide; HR = heart rate; BPsys = systolic blood pressure; BPdia = diastolic blood pressure; ECG = electrocardiography; QTc = corrected QT. PNC size fractions were measured by a scanning mobility particle sizer (SMPS) with a limit of detection of 6-225 nm.

Table S10. Two-pollutant model consisting of two particle size fractions (unadjusted for covariates).

Outcome	PNC ≤ 20 nm Adjusted for PNC > 50 nm		PNC > 50 nm Adjusted for PNC ≤ 20 nm	
	Est.	95% CI	Est.	95% CI
FVC (mL)	-66.3	-136.4 – 7.2	29.1	-52.3 – 111.0
FEV_1 (mL)	-57.7	-131.0 – 19.9	33.8	-52.0 – 119.2
PEF (mL/s)	-26.1	-320.0 – 258.3	266.2	-60.9 – 592.6
FeNO (ppb)	-0.1	-1.5 – 1.4	-0.4	-2.0 – 1.3
$HR_{sitting}$ (bpm)	-1.1	-4.6 – 2.3	2.2	-2.0 – 6.3
Saturation (%)	0.0	-0.5 – 0.6	-0.3	-0.9 – 0.4
BP_{sys} (mmHg)	-2.1	-4.9 – 0.8	2.9	-0.4 – 6.4
BP_{dia} (mmHg)	-2.6	-5.5 – 0.3	2.6	-0.8 – 6.0
ECG - HR (bpm)	3.4	-0.5 – 7.5	0.9	-3.8 – 5.6
ECG - PR (ms)	-4.0	-9.0 – 1.2	-0.8	-7.2 – 4.9
ECG - QRS (ms)	0.6	-2.0 – 3.2	2.2	-0.8 – 5.1
ECG - QTc (ms)	**11.1**	**2.7 – 20.2**	1.5	-8.3 – 11.5

Data are presented as estimates (est.) and 95% confidence intervals (CI). All effect estimates were scaled to the 5-95th percentile change in the exposure of interest. Numbers in **bold** are significant effects ($p < 0.05$). PNC = particle number concentration; FVC = forced vital capacity; FEV_1 = forced expiratory volume in 1s; PEF = peak expiratory flow rate; FeNO = fractional exhaled nitric oxide; HR = heart rate; BPsys = systolic blood pressure; BPdia = diastolic blood pressure; ECG = electrocardiography; QTc = corrected QT. PNC size fractions were measured by a scanning mobility particle sizer (SMPS) with a limit of detection of 6-225 nm.

Chapter 4.

The impact of short-term exposure to air pollution on the exhaled breath of healthy adults

Lammers A
Neerincx AH
Vijverberg SJH
Longo C
Janssen NAH
Boere AJF
Brinkman P
Cassee FR
Maitland-van der Zee AH

Sensors, 2021; 21 (7): 2518

Abstract

Environmental factors, such as air pollution, can affect the composition of exhaled breath, and should be well understood before biomarkers in exhaled breath can be used in clinical practice. Our objective was to investigate whether short-term exposures to air pollution can be detected in the exhaled breath profile of healthy adults. In this study, 20 healthy young adults were exposed 2–4 times to the ambient air near a major airport and two highways. Before and after each 5 h exposure, exhaled breath was analyzed using an electronic nose (eNose) consisting of seven different cross-reactive metal-oxide sensors. The discrimination between pre and post-exposure was investigated with multilevel partial least square discriminant analysis (PLSDA), followed by linear discriminant and receiver operating characteristic (ROC) analysis, for all data (71 visits), and for a training (51 visits) and validation set (20 visits). Using all eNose measurements and the training set, discrimination between pre and post-exposure resulted in an area under the ROC curve of 0.83 (95% CI = 0.76–0.89) and 0.84 (95% CI = 0.75–0.92), whereas it decreased to 0.66 (95% CI = 0.48–0.84) in the validation set. Short-term exposure to high levels of air pollution potentially influences the exhaled breath profiles of healthy adults, however, the effects may be minimal for regular daily exposures.

Introduction

Exhaled breath analysis is a topic of research which has gained increased attention in the past few years, especially in the field of respiratory diseases. Important aspects for this interest are the non-invasive nature of breath sampling, and the possibility of analyzing both local and systemic processes. Exhaled breath contains volatile organic compounds (VOCs) that either have an endogenous (e.g., metabolic processes) or exogenous (from ambient air) origin. The endogenous VOCs are the ones of interest regarding biomarker discovery for medical testing purposes, having already shown their potential for discrimination between several respiratory diseases and distinct disease phenotypes [1].

One of the steps towards future clinical implementation of exhaled breath testing is to better understand which exogenous factors could potentially influence the composition of exhaled breath and, thus, should be taken into account when examining exhaled breath.

This holds especially true for electronic nose (eNose) technology, a rapid exhaled breath detection technique based on multiple cross-reactive sensors. Such sensors resemble the powerful mammalian olfactory system [2], in which each sensor can detect multiple VOCs and, vice versa, a VOC can interact with multiple sensors. Therefore, eNose technology does not allow for the detection of individual compounds, making it challenging to identify their source and impossible to delineate their metabolomic pathways. However, by using pattern recognition algorithms, this relatively cheap and easy-to-use technique, is a promising tool for point of care testing, if properly validated and standardized [3]. Regarding validation, knowledge about the possible influences of environmental exposures on the exhaled breath profile is an important aspect [4].

Ambient air is always in direct contact with our respiratory system, making it a part of our exhaled breath but also a continuous exposure, possibly influencing metabolic pathways. Components in the ambient air that can have possible adverse health effects are air pollutants, cigarette smoke, and viral and bacterial agents. With the abundance of road traffic and aviation, air pollution is of increasing concern regarding human health. Previous literature has shown that particulate matter has adverse health effects on the respiratory and cardiovascular system, in which fine and ultrafine particles (UFP) can induce pulmonary as well as systemic inflammation [5–8] and oxidative stress [9,10]. Such processes have been shown to be reflected in exhaled breath patterns of ventilated rats and

patients with asthma or chronic obstructive pulmonary disease (COPD) [11–13]. Therefore, we hypothesize that exposure to air pollution could be detected in the exhaled breath profile.

As part of our study on the effects of short-term exposure to air pollution [14], we collected exhaled breath profiles by an eNose. Our objective was to investigate the effect of short-term exposures of 5 h to air pollution near a major airport and two highways, with a focus on UFP on the exhaled breath profile of healthy young adults. We did this by discriminating pre and post-exposure measurements based on the exhaled breath profile and by testing the associations between individual eNose sensor signals and the exposure measurements.

Methods

Study design

In this prospective study, young healthy adults were exposed to ambient air near Amsterdam Airport Schiphol and two nearby highways (Amsterdam, the Netherlands), between April and October 2018 [14]. Participants were exposed for 5 h on minimally two and maximally four days, with at least two weeks between exposures. During the exposure, participants performed intermittent cycling at low intensity on an ergometer for 20 min/h and were seated in between. Extensive air monitoring was conducted, from which 5 h averages were calculated. Before and after each exposure, exhaled breath was measured using an eNose, at the Amsterdam UMC location AMC (Amsterdam, the Netherlands). A petrol-fuelled hybrid car, equipped with a high-efficiency particulate air (HEPA) filter, was used for transport between the exposure site and the hospital (15 km distance, a 15–20 min drive).

Study population

Participants were young adults, non-smokers for at least 1 year (<5 pack years = number of packs of cigarettes smoked per day * number of years the person has smoked) and had normal lung function (predicted forced exhaled volume in 1 s (FEV_1) > 80%). Subjects were excluded when they had any (history of chronic) pulmonary or cardiovascular disease, hay fever, or when they lived in the vicinity of highly polluted areas: <2 km from Schiphol Airport, <300 m from a highway, or on a busy road (>10,000 vehicles/day). Volunteers were screened for their medical history, as well as lung (spirometry and fractional exhaled nitric oxide

(FeNO)) and heart function (electrocardiography (ECG), blood pressure (BP) and heart rate). More details about the inclusion and exclusion criteria, as well as the screening assessments, were published previously [14].

Exposures

All participants were exposed for 5 h to the ambient air near Schiphol Airport (northwest of two runways, ~300 m away), two highways (~500 m away) and Amsterdam (~10 km). Two to four participants were exposed on the same day, in a mobile exposure laboratory, through which the outside ambient air was circulated. We aimed to expose each participant to different UFP levels, sources (e.g., aviation and road traffic), and compositions between exposure days, by considering the meteorological conditions (mostly wind direction, as the location of the exposure site was fixed) when scheduling their visits.

Exposure parameters

The air inside the exposure chamber was monitored, from which 5 h averages were calculated for the following: particle number concentrations (PNC); particle mass concentrations (PM ≈ PM2.5 meaning particles mainly <2.5 μm); nitrogen oxides (NO_x, NO_2); black carbon (BC); and carbon monoxide (CO). The total PNC was measured by a condensation particle counter (CPC) with d_{50} = 4 nm. Furthermore, we monitored the temperature (temp) and relative humidity (RH) inside the mobile exposure laboratory. More details about the exposure (monitoring equipment) were published previously [14].

PNC sources

Next, we estimated the contribution of different sources to the PNC levels using a positive matrix factorization (PMF) source apportionment model, as extensively described by Pirhadi et al. [15]. In short, the source contribution model was based on the 5 h averages of total PNC (measured by CPC), PNC size fractions (measured by a scanning mobility particle sizer), BC, NOx and CO. The aviation source was labeled as "total aviation" and was also divided into "take-offs" and "landings". Furthermore, two traffic sources were distinguished, "airport traffic" (e.g., passenger busses, baggage trucks) and "road traffic" (e.g., highways around the airport), but were also analyzed as one labeled "total traffic".

Exhaled breath analysis

Exhaled breath analysis was performed using an electronic nose (eNose), the SpiroNose, attached at the rear end of a spirometer (MasterScreen™ PFT, CareFusion) (Figure 1a). The SpiroNose consists of seven different cross-reactive metal oxide sensors: TGS2602 (sensor 1), TGS2610 (sensor 2), TGS2611-COO

(sensor 3), TGS2600 (sensor 4), TGS2603 (sensor 5), TGS2620 (sensor 6), TGS2612 (sensor 7) (Figaro Engineering Inc., Osaka, Japan). Each sensor is present fourfold: twice on the inside, detecting the exhaled breath; and twice on the outer side of the device, detecting the ambient air (Figure 1b).

eNose measurements

First, subjects rinsed their mouth thoroughly three times with water. Subsequently, exhaled breath analysis was performed twice in a row, with a 2 min interval. The maneuver involved five tidal breaths, an inhalation up to total lung capacity, a breath-hold of 5 s and a slow (<0.4 L/s) maximal exhalation towards residual volume. During this maneuver, participants were breathing through a bacterial filter (Lemon Medical GmbH, Hammelburg, Germany) with their noses clipped. Furthermore, complaints of cough, dyspnea, sputum production and a blocked nose were assessed and were labeled as "no" when none and "yes" when one or more of these symptoms occurred.

Data processing

The eNose signals were processed in MATLAB® as described by De Vries et al. [16] and involved filtering, detrending, ambient air correction and peak detection. The highest sensor peak of the duplicate measurements was selected and normalized with respect to the most stable sensor, sensor 2, therefore data from sensor 2 are not presented. Further processing was performed in *R studio* and consisted of two steps in which we aimed to put the eNose sensor data in perspective with subject-specific pre-exposure baselines and fluctuations. First, the mean of all pre-exposure measurements (i.e., baseline) was calculated, after which the deviation from this baseline for all pre and post-exposure measurements, per subject and sensor were determined (Figure 2). The deviation is expressed as a percentage from baseline: (deviation/baseline)×100%.

Statistical analysis

All statistics were performed in R (version 3.6.1) and R studio (version 1.2.1335). The differences in exhaled breath profiles between pre and post-exposure were compared using discrimination analysis (using eNose sensor data) with R packages "mixOmics" and "pROC". Associations between exposure levels and the change in eNose signal (using eNose deviation percentages) were analyzed with linear mixed-effects models using R package "lme4". p-values < 0.05 were considered significant.

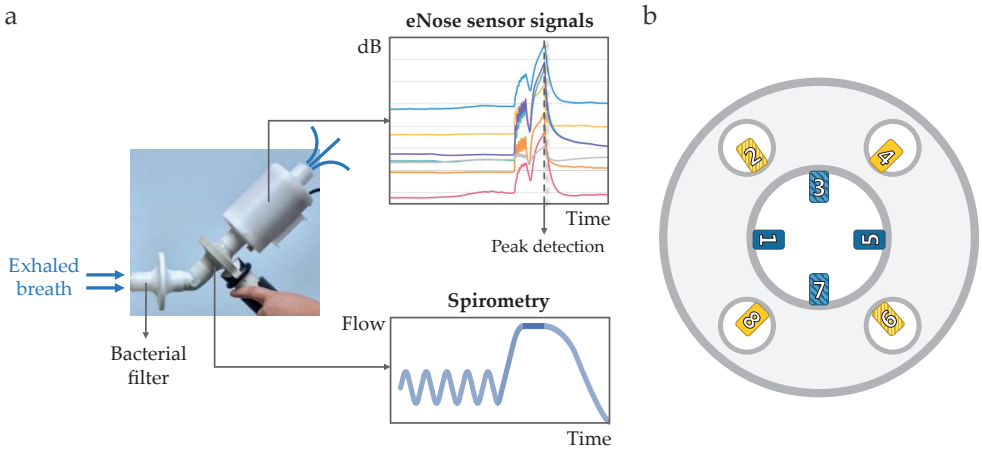

Figure 1. (**a**) The eNose measurement setup consisted of a mouthpiece, bacterial filter, spirometer and the SpiroNose. Participants rinsed their mouths with water three times and clipped their noses before performing 5 tidal breaths, a deep inhalation, a 5 s breath-hold, followed by a slow maximal exhalation (0.4 L/s). (**b**) Schematic overview of the SpiroNose (front view), with four sensor arrays on the outer side that detect the ambient air (**yellow**) and four on the inside that detect the exhaled breath (**blue**). All seven different sensor types are present fourfold, in which the arrays 1, 4, 5 and 8 (filled squares) contain sensors 1–4 (TGS2602, TGS2610, TGS2611-COO and TGS2600, respectively). Sensor arrays 2, 3, 6 and 7 (dashed squares) contain sensors 5–7 (TGS2603, TGS2620 and TGS2612, respectively).

Discriminant analysis

For the discriminate analysis, we performed multilevel partial least square discriminant analysis (PLSDA), in which the pre and post-exposure exhaled breath profiles are compared while taking into account the paired nature of the data (per visit, i.e., pre and post-exposure) to highlight the exposure effects within subjects. Next, the first two components of the PLSDA model were merged into one discriminant score using linear discriminant analysis (LDA). In addition, we stratified the results from the multilevel PLSDA into high (75% percentile, 18 visits) and low (25% percentile, 18 visits) PNC exposures, again followed by LDA, to test whether the discriminant performance was better for higher PNC exposure levels. Finally, we tested the robustness of the model by splitting the eNose sensor data in a training (≈70%) and validation set (≈30%). First, multilevel PLSDA and LDA models were constructed with the training set. Next, these obtained models were tested on the validation set. The performance of all discriminant analyses was determined by receiver operating characteristics (ROC) analysis, for which we reported the area under the ROC curve (AUROCC) with 95% confidence intervals (CI). An overview of the discriminant analysis is shown in Figure 3.

Linear mixed effect models

To take into account the paired data (pre and post), and the multiple visits per participant, we have constructed linear mixed effects models, per individual sensor. These models are suitable for the longitudinal analysis of within-individual change. For this analysis, we used eNose sensor data processed as deviations from a subject-specific mean baseline, expressed as percentages, as described before and depicted in Figure 2.

The associations between the change in eNose deviation percentages and exposure were modelled using a linear mixed-effect model for each individual (i) and exposure day (j):

$$Y_{ij,post-pre} = \beta_0 + Y_{ij,baseline} + \beta_1 E_j + \beta_2 V_j + U_{0i} + \varepsilon_i$$

The deviation percentage from the baseline for all post-exposure measurements ($Y_{ij,\ post}$) was adjusted for the personal baseline ($Y_{ij,\ baseline}$), as two participants with the same deviation but different baselines could have different deviation percentages. E_j represents a vector of the exposure variable(s), U_{0i} the intercept for each participant (i.e., a random intercept) and ε_i the error term. The βs represent population-average fixed effects, with β_0 being the average change in the outcome parameters when all other covariates are zero, and β_1 the average change in the outcome relative to a 5–95th percentile (5–95 p) increase in exposure. The vector V_j represents the covariates that varied at each visit, which included the temperature and relative humidity in the exposure laboratory and the respiratory symptoms (i.e., cough, dyspnea, blocked nose or sputum production) that participants may have had before exposure (as a binary indicator "yes/no").

We examined single-pollutant models for PNC, PM, BC, NO_2 and CO. Next, we conducted two-pollutant models consisting of the PNC exposure adjusted for all other measured pollutants (BC, NO_2, PM and CO) to investigate the independence of the effects associated with PNC [17]. Regarding the PNC sources, we investigated single-source models for take-offs, landings, airport traffic and road traffic, as well as total aviation (take-offs + landings) and total traffic (airport traffic + road traffic). Furthermore, we conducted a two-source model consisting of total aviation and total traffic. The fit of the models was examined by confirming a normal distribution of the residuals using Q–Q plots. Non-collinearity between covariates incorporated in the same model was verified using Pearson correlation ($R < 0.6$).

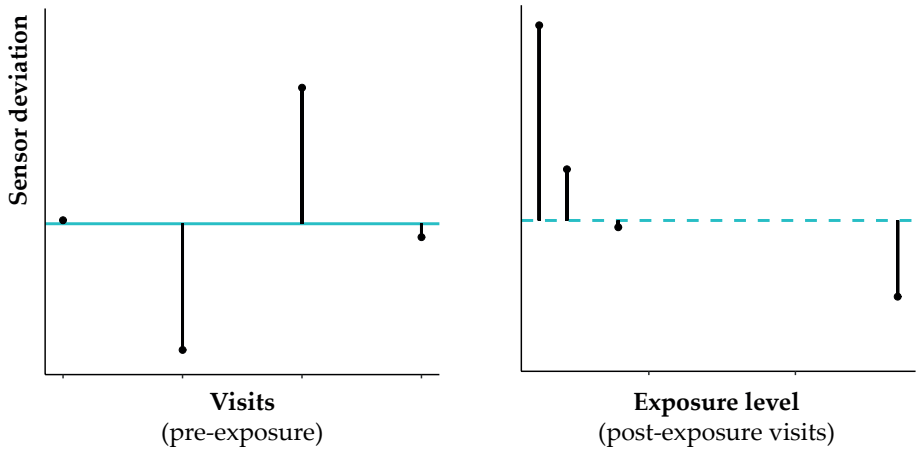

Figure 2. For the deviation percentage calculation, we first determined the individual mean sensor value based on all pre-exposure visits (blue solid line, **left graph**). Next, the deviation percentages from this mean were calculated for both the pre-exposure visits (left graph) and the post-exposure visits (**right graph**, with the blue dashed line representing the mean sensor value based on the pre-exposure visits).

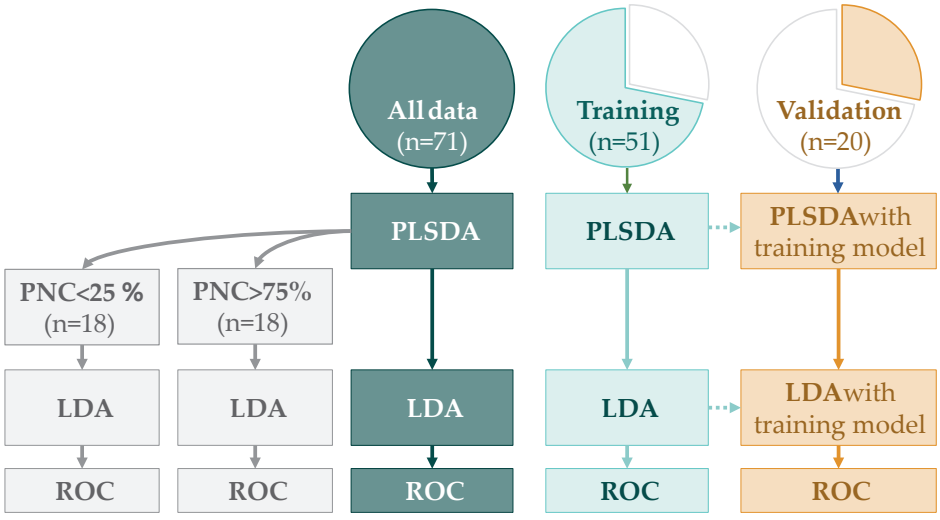

Figure 3. An overview of the discriminant analyses. Multilevel PLSDA and consecutive LDA models were constructed using all eNose sensor data and the training set, separately. The results from the PLSDA model, based on all eNose sensor data, was also used for the stratification analysis, in which high and low PNC exposures were compared. For the validation set, the same models as in the training set were used. The discrimination accuracy of all analyses was determined through ROC analysis. PLSDA = partial least square discriminant analysis ; LDA = linear discriminant analysis; ROC = receiver operating characteristics; PNC = particle number concentration.

To facilitate the interpretation of the results from the linear mixed models, we determined the pre-exposure variability in the deviation percentages. For this, absolute deviation percentages of all pre-exposure measurements were averaged at an individual level and per sensor. Next, the median and interquartile range (IQR) of all participants was determined, again per sensor.

Results

Participants

Complete data were available for 20 out of the 23 participants of our main study. In accordance with our previous paper, we excluded two participants from the analysis because they received only one exposure [14]. In addition, one person was excluded as eNose data was missing for this person due to a sampling error. The participants were young adults (23 years, IQR: 20–23), mainly female (n = 16, 80%), with an average BMI of 22.7 kg/m^2 (±2.4). They had normal lung function (FEV_1 > 80% of predicted), FeNO levels (15, IQR: 12–23) and blood pressure (122 ± 12/77 ± 9 mmHg).

Exposures

In total, we conducted 32 exposure days, however, due to a sampling error, eNose data for 6 exposure days (i.e., 15 visits) were missing. We analysed 26 exposure days and a total of 71 visits, with four (n = 14; 70%), three (n = 3; 15%) or two (n = 3; 15%) visits per participant. The 5 h averages of all exposure variables are summarized in Table 1 and listed per day in Table S1. On average, the total PNC was 53,100 #/cm^3 (range 12,600–173,200). At an individual level, the maximal contrast in PNC exposure that participants received (i.e., maximal–minimal exposure) was, on average, 77,600 #/cm^3 (range 8800–152,600) (Table S2). The source apportionment model revealed that aviation, in particular aircraft take-offs, contributed more to PNCs (26,100 #/cm^3; range 3200–101,800) than traffic-related sources (9100 #/cm^3; range 1700–33,100) (Table 1). No multicollinearity existed between covariates included in the same model (R ≤ 0.58) (Table S3).

Discriminant analysis

The discrimination between pre and post-exposure using multilevel PLSDA combined with LDA reached an AUROCC of 0.83 (CI: 0.76–0.89). With the training set, a similar AUROCC of 0.84 (CI: 0.75–0.92) was reached, whereas the validation set reached an AUROCC of 0.66 (CI: 0.48–0.84) (Figure 4). Furthermore, stratification of the PLSDA components for the 25th and 75th percentiles in total PNC exposure (i.e., <23,800 and >71,900 #/cm^3), showed to have a better

accuracy for discriminating pre and post-exposure when PNC levels were high (AUROCC = 0.98, CI: 0.94–1.00) compared to low PNC levels (AUROCC = 0.77, CI: 0.61–0.93) (Figure 5, Table S4).

Table 1. Exposure variables of all exposure days are based on 5 h averages.

	Exposure Days (n = 26)		
	Mean	**5–95th Percentile**	**Range**
Pollutant			
PNC (# / cm^3)	53,100	19,300 – 138,200	12,600 – 173,200
PM ($\mu g/m^3$)	24.6	14.9 – 41.3	13.6 – 47.5
BC ($\mu g/m^3$)	0.59	0.21 – 1.26	0.13 – 1.55
NO_2 ($\mu g/m^3$)	27	13 – 44	12 – 48
CO ($\mu g/m^3$)	634	516 – 782	494 – 830
PNC sources			
Total aviation (# / cm^3)	26,100	3500 – 84,400	3200 – 101,800
Take-off (# / cm^3)	16,600	700 – 58,800	500 – 62,000
Landing (# / cm^3)	9500	1500 – 26,500	400 – 42,300
Total traffic (# / cm^3)	9100	3600 – 16,700	1700 – 33,100
Airport traffic (# / cm^3)	2400	500 – 4900	100 – 6800
Road traffic (# / cm^3)	6700	2000 – 14,600	600 – 31,100
Weather conditions			
Temperature (°C)	24	20 – 27	19 – 29
Relative humidity (%)	54	43 – 66	40 – 66

PNC = particle number concentration; PM = particulate matter; BC = black carbon; NO_2 = nitric oxide, CO = carbon monoxide; range = min–max. This table has partly been published previously for all exposure days (32 instead of 26) and without the PNC source information (Lammers et al., Environ Int 2020).

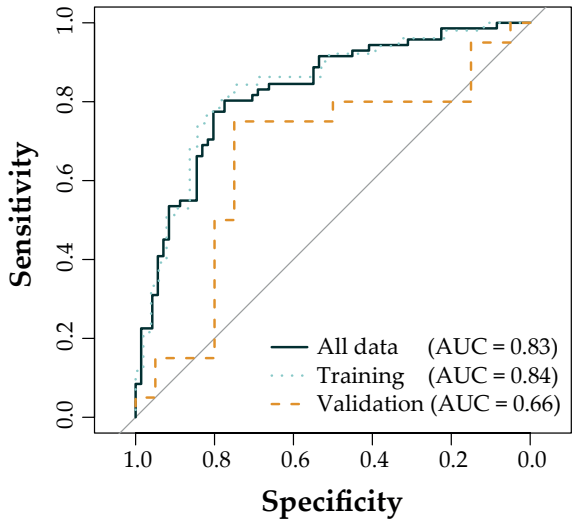

Figure 4. Receiver operating characteristic results from the multilevel PLSDA and LDA models. **Dark blue** solid = all data, 71 visits, **blue** dots = training set, 51 visits, and **orange** dashed line = validation set, 20 visits; PLSDA = partial least square discriminant analysis; LDA = linear discriminant analysis; AUC = area under the curve.

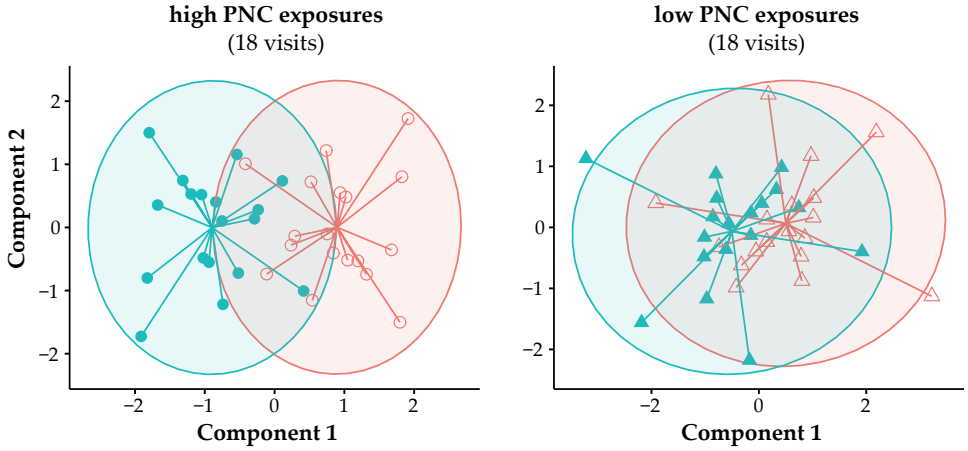

Figure 5. Results of the PLSDA model, stratified for high and low PNC levels, demonstrating that the difference in exhaled breath profiles between pre (& ▲) and post-exposure (○ & △) measurements were larger for high PNC exposures (left) compared to low PNC exposures (right). High levels were defined as PNC levels > 75% percentile (i.e., >71,900 # / cm^3) and low < 25% percentile (i.e., <23,800 # / cm^3). PLSDA = partial least square discriminant analysis; PNC = particle number concentration.

Linear mixed effect models

Pre-exposure variability eNose deviations

The median pre-exposure variation in absolute deviation percentages differed between sensors, ranging between 3.9–13.2% with sensors 1, 5 and 7 having the highest variability; 6.8%, 6.4% and 13.2%, respectively (Table 2).

Associations eNose deviations and pollutants

A significant inverse association was found between PNC and sensor 1 deviation percentages (-7.2% CI: -13.9 – -0.5) (Table S5), which remained significant in all two-pollutant models (i.e., adjusted for PM, BC, NO_2 and CO exposure) (Table S6). Furthermore, the deviation percentages of sensors 4 and 5 were significantly associated with PM exposure; (-5.7% CI: -10.8 – -0.70) and (-12.1% CI: -23.5 – -0.79), respectively. No significant association existed between deviation percentages and BC, NO_2 and CO (Table S5).

Associations eNose deviations and PNC sources

An inverse association was found between road traffic PNC source and sensor 6 deviation percentages (-5.0% CI: -8.2 – -1.9) (Table S7). The total traffic PNC source was also inversely associated with the deviation percentages of sensor 6, both in the single-source (-5.3% CI: -8.9 – -1.8) and two-source model (-5.3% CI: -8.8 – -1.7) (Tables S8 and S9).

Table 2. Pre-exposure variability in absolute eNose deviation %.

Sensor	Deviation Percentage (%) Median (IQR)
1	6.8 (3.3 – 8.8)
3	3.9 (2.7 – 4.9)
4	4.3 (2.5 – 6.9)
5	6.4 (3.6 – 10.8)
6	4.7 (2.6 – 6.5)
7	13.2 (8.4 – 17.7)

At an individual level, the absolute deviation percentages of all pre-exposure measurements were averaged, per sensor. Next, the median, an IQR of all participants was determined, per sensor. IQR = interquartile range.

Discussion

Short-term exposures to air pollution, in particular UFP, near an airport and two highways, appeared to influence the exhaled breath profiles, detected by eNose technology, in young healthy adults. The discriminant analysis with all eNose sensor data and the training set resulted in good discrimination between pre and post-exposure, whereas the validation set reached a poor discriminant accuracy, possibly an indication of overfitting. The stratification analysis for PNC levels did demonstrate an exposure-response relationship, in which a larger difference in exhaled breath profiles existed between pre and post-exposure for higher PNC levels. Furthermore, we found robust associations between the deviation percentages of sensor 1 and total PNC, and between sensor 6 deviation percentages and the PNC sources "road traffic" and "total traffic". However, the change in eNose deviations was in the range of pre-exposure variability. Altogether, air pollution could potentially be of importance as a confounder in exhaled breath analysis, depending on the exposure level and to which extent it affects the disease-related breath profile of patients with chronic airway diseases [4].

To our knowledge, there are no studies that published the effects of controlled exposures to air pollution on exhaled breath profiles detected by eNose technology. The study by Filipiak et al. did focus on (uncontrolled) exogenous factors influencing the composition of exhaled breath, such as smoking habits and exposure to air pollutants, using gas chromatography-mass spectrometry (GC-MS) analysis [18]. They collected breath from 46 healthy volunteers and 69 patients (both groups ≈50/50 smokers and non-smokers), in which the patients had lung cancer, either with or without COPD, or ear-nose-throat (ENT) cancer. The largest influence on exhaled breath was a smoking habit, however, also benzene, a component considered to originate from petrochemical industry products including gasoline, was detected in almost all breath samples. The small effect of air pollutants on the exhaled breath profile in our study can have several explanations. One of them could be that changes occurred in only one or a few VOCs that could not be detected by the eNose, but possibly could have been detected by GC-MS. Another explanation could be that the exposures did not trigger the production of VOCs associated with inflammation and oxidative stress, due to the short duration of the exposures and/or the very healthy and young population we have investigated.

The stratification for high and low PNC exposures in the discrimination analysis demonstrated a potential exposure-response relationship. However, our study involved extremely high PNC levels, up to 170,000 #/cm^3, that are not representative of regular exposures to UFP. In highly urbanized areas or close to airports, PNC levels are commonly in the order of 10,000–20,000 #/cm^3, with maximal PNC levels going up to 30,000–40,000 #/cm^3 [19–21]. Therefore, air pollution may mainly be a possible confounder regarding exhaled breath analysis on days with extremely high levels of air pollution, due to e.g., massive use of fireworks [22–24] or smog. Regarding regular daily exposures to air pollution in urbanized areas, the effects on the exhaled breath profile may be minimal.

This study had several strengths. First of all, we performed multiple exposures in which we reached a large contrast in UFP levels within-subjects. This allowed for the investigation of exposure-response relationships within-subjects and the comparison of these to other participants. Secondly, we controlled air pollution exposures by making use of a mobile laboratory lab. This minimized the measurement error when compared to the commonly used central site monitoring. Thirdly, we used a source apportionment analysis to be able to distinguish UFP from different sources. Regarding the eNose sensor data, we examined normal deviations in exhaled breath profiles to put the effects of air pollution in perspective, as eNose sensor data is challenging to quantify. Finally, our statistical analysis takes into account the longitudinal character of our study, for the whole exhaled breath profile (i.e., discriminant analysis) and per sensor (linear mixed effect models).

Our study also had some limitations. We only compared single pre and post-exposure time points in which we may have captured only a snapshot of the response to the exposure. Furthermore, we had no information about the occupational and pre-visit exposure of the participants, which may have affected the pre-exposure measurement and the response to the exposure. However, we attempted to minimize this confounder by carefully selecting where our healthy volunteers lived; i.e., not near a highway, the airport or a busy street. In addition, the participants were mainly students with generally little occupational exposure. We, therefore, assume that the influence of occupational exposure on our results was minimal. Thirdly, our sample size was relatively small and based on the primary outcomes of the study (i.e., cardiopulmonary function). This possibly explains the issue of overfitting of the discriminant analysis models as demonstrated by the discrepancies between the discriminant accuracy of the training and validation set. Furthermore, our study mainly involved female participants, however, due to a lack of power we could not do a sensitivity

analysis to investigate the influence of gender on our results. Finally, we may have faced the issue of multiple testing in our linear mixed-effect analysis, which has possibly led to finding significant associations by chance. Therefore, we chose to mainly focus on the consistency between the results from our different models [25].

For future research, it could be valuable to either use exhaled breath analysis in air pollution research, or to consider air pollution as a possible confounder in breath research. Exhaled breath analysis is a non-invasive and easy-to-perform method to detect both local and systemic metabolomic processes, making it an interesting tool in air pollution research. Regarding exhaled breath research, not focussing on the effects of air pollution, it could be important to take the air quality of a patient's place of residence into account, mainly for patients living in highly polluted areas (e.g., cities facing recurrent smog). For this, one could make use of air quality data that are constantly monitored in many countries and are publicly accessible.

Conclusion

The short-term exposure of 5 h to air pollution, more specifically UFP, from air and road traffic may influence the exhaled breath profile, detected by eNose technology, of young healthy adults. Our study involved extremely high levels of UFP, as volunteers were exposed in high proximity to a major airport and two highways, which are not representative for regular daily exposures in urbanized areas. Therefore, more insight on air pollution as a possibly important confounder in breath analysis is required to determine to what extent it may influence the exhaled breath profile, especially with respect to the disease-related breath profile of patients with chronic airway diseases.

References

1. Lammers, A.; van Bragt, J.J.M.H.; Brinkman, P.; Neerincx, A.H.; Bos, L.D.; Vijverberg, S.J.H.; Maitland-van der Zee, A.H. Breathomics in Chronic Airway Diseases. In *Systems Medicine*; Elsevier: 2021, *1*, 244-255, doi:10.1016/B978-0-12-801238-3.11589-2.
2. Bushdid, C.; Magnasco, M.O.; Vosshall, L.B.; Keller, A. Humans can discriminate more than 1 trillion olfactory stimuli. *Science (80-.)* 2014, doi:10.1126/science.1249168.
3. Röck, F.; Barsan, N.; Weimar, U. Electronic nose: Current status and future trends. *Chem. Rev.* 2008, *108*, 705-725, doi:10.1021/cr068121q.
4. Brinkman, P.; Zee, A.H.M. Van Der; Wagener, A.H. Breathomics and treatable traits for chronic airway diseases. *Curr. Opin. Pulm. Med.* 2019, *25*, 94-100, doi:10.1097/MCP.0000000000000534.
5. Habre, R.; Zhou, H.; Eckel, S.P.; Enebish, T.; Fruin, S.; Bastain, T.; Rappaport, E.; Gilliland, F. Short-term effects of airport-associated ultrafine particle exposure on lung function and inflammation in adults with asthma. *Environ. Int.* 2018, *118*, 48–59, doi:10.1016/j.envint.2018.05.031.
6. Bendtsen, K.M.; Brostrøm, A.; Koivisto, A.J.; Koponen, I.; Berthing, T.; Bertram, N.; Kling, K.I.; Dal Maso, M.; Kangasniemi, O.; Poikkimäki, M.; et al. Airport emission particles: Exposure characterization and toxicity following intratracheal instillation in mice. *Part. Fibre Toxicol.* 2019, *16*, 23, doi:10.1186/s12989-019-0305-5.
7. Khatri, M.; Bello, D.; Gaines, P.; Martin, J.; Pal, A.K.; Gore, R.; Woskie, S. Nanoparticles from photocopiers induce oxidative stress and upper respiratory tract inflammation in healthy volunteers. *Nanotoxicology* 2013, *7*, 1014–1027, doi:10.3109/17435390.2012.691998.
8. Song, Y.; Li, X.; Du, X. Exposure to nanoparticles is related to pleural effusion, pulmonary fibrosis and granuloma. *Eur. Respir. J.* 2009, *34*, 559–567, doi:10.1183/09031936.00178308.
9. He, R.W.; Shirmohammadi, F.; Gerlofs-Nijland, M.E.; Sioutas, C.; Cassee, F.R. Pro-inflammatory responses to PM 0.25 from airport and urban traffic emissions. *Sci. Total Environ.* 2018, *640-641*, 997-1003, doi:10.1016/j.scitotenv.2018.05.382.
10. Donaldson, K.; Beswick, P.H.; Gilmour, P.S. Free radical activity associated with the surface of particles: A unifying factor in determining biological activity? *Toxicology Letters*; 1996, *88*, 293-298, doi:10.1016/0378-4274(96)03752-6.
11. Albrecht, F.W.; Maurer, F.; Müller-Wirtz, L.M.; Schwaiblmair, M.H.; Hüppe, T.; Wolf, B.; Sessler, D.I.; Volk, T.; Kreuer, S.; Fink, T. Exhaled volatile organic compounds during inflammation induced by TNF-α in ventilated rats. *Metabolites* 2020, *10*, 245, doi:10.3390/metabo10060245.
12. Brinkman, P.; Wagener, A.H.; Hekking, P.P.; Bansal, A.T.; Maitland-van der Zee, A.H.; Wang, Y.; Weda, H.; Knobel, H.H.; Vink, T.J.; Rattray, N.J.; et al. Identification and prospective stability of electronic nose (eNose)–derived inflammatory phenotypes in patients with severe asthma. *J. Allergy Clin. Immunol.* 2019, *143*, 1811–1820.e7, doi:10.1016/j.jaci.2018.10.058.
13. Fens, N.; De Nijs, S.B.; Peters, S.; Dekker, T.; Knobel, H.H.; Vink, T.J.; Willard, N.P.; Zwinderman, A.H.; Krouwelse, F.H.; Janssen, H.G.; et al. Exhaled air molecular profiling in relation to inflammatory subtype and activity in COPD. *Eur. Respir. J.* 2011, *38*, 1301–1309, doi:10.1183/09031936.00032911.
14. Lammers, A.; Janssen, N.A.H.; Boere, A.J.F.; Berger, M.; Longo, C.; Vijverberg, S.J.H.; Neerincx, A.H.; Maitland-van der Zee, A.H.; Cassee, F.R. Effects of short-term exposures to ultrafine particles near an airport in healthy subjects. *Environ. Int.* 2020, *141*, 105779, doi:10.1016/j.envint.2020.105779.
15. Pirhadi, M.; Mousavi, A.; Sowlat, M.H.; Janssen, N.A.H.; Cassee, F.R.; Sioutas, C. Relative contributions of a major international airport activities and other urban sources to the particle number concentrations (PNCs) at a nearby monitoring site. *Environ. Pollut.* 2020, *260*, 114027, doi:10.1016/j.envpol.2020.114027.

16. De Vries, R.; Dagelet, Y.W.F.; Spoor, P.; Snoey, E.; Jak, P.M.C.; Brinkman, P.; Dijkers, E.; Bootsma, S.K.; Elskamp, F.; de Jongh, F.H.C.; et al. Clinical and inflammatory phenotyping by breathomics in chronic airway diseases irrespective of the diagnostic label. *Eur. Respir. J.* 2018, *51*, 1701817, doi:10.1183/13993003.01817-2017.
17. Ohlwein, S.; Kappeler, R.; Kutlar Joss, M.; Künzli, N.; Hoffmann, B. Health effects of ultrafine particles: A systematic literature review update of epidemiological evidence. *Int. J. Public Health* 2019, *64*, 547–559, doi:10.1007/s00038-019-01202-7.
18. Filipiak, W.; Ruzsanyi, V.; Mochalski, P.; Filipiak, A.; Bajtarevic, A.; Ager, C.; Denz, H.; Hilbe, W.; Jamnig, H.; Hackl, M.; et al. Dependence of exhaled breath composition on exogenous factors, smoking habits and exposure to air pollutants. *J. Breath Res.* 2012, *6*, 036008, doi:10.1088/1752-7155/6/3/036008.
19. de Jesus, A.L.; Rahman, M.M.; Mazaheri, M.; Thompson, H.; Knibbs, L.D.; Jeong, C.; Evans, G.; Nei, W.; Ding, A.; Qiao, L.; et al. Ultrafine particles and PM2.5 in the air of cities around the world: Are they representative of each other? *Environ. Int.* 2019, *129*, 118–135, doi:10.1016/j.envint.2019.05.021.
20. Hudda, N.; Simon, M.C.; Zamore, W.; Durant, J.L. Aviation-Related Impacts on Ultrafine Particle Number Concentrations Outside and Inside Residences near an Airport. *Environ. Sci. Technol.* 2018, *52*, 1765–1772, doi:10.1021/acs.est.7b05593.
21. Van Nunen, E.; Vermeulen, R.; Tsai, M.Y.; Probst-Hensch, N.; Ineichen, A.; Davey, M.; Imboden, M.; Ducret-Stich, R.; Naccarati, A.; Raffaele, D.; et al. Land Use Regression Models for Ultrafine Particles in Six European Areas. *Environ. Sci. Technol.* 2017, *51*, 3336–3345, doi:10.1021/acs.est.6b05920.
22. Hoyos, C.D.; Herrera-Mejía, L.; Roldán-Henao, N.; Isaza, A. Effects of fireworks on particulate matter concentration in a narrow valley: The case of the Medellín metropolitan area. *Environ. Monit. Assess.* 2020, *192*, 6, doi:10.1007/s10661-019-7838-9.
23. Lin, C.C. A review of the impact of fireworks on particulate matter in ambient air. *J. Air Waste Manag. Assoc.* 2016, *66*, 1171-1182, doi:10.1080/10962247.2016.1219280.
24. Joly, A.; Smargiassi, A.; Kosatsky, T.; Fournier, M.; Dabek-Zlotorzynska, E.; Celo, V.; Mathieu, D.; Servranckx, R.; D'amours, R.; Malo, A.; et al. Characterisation of particulate exposure during fireworks displays. *Atmos. Environ.* 2010, *44*, 4325–4329, doi:10.1016/j.atmosenv.2009.12.010.
25. Streiner, D.L.; Norman, G.R. Correction for multiple testing: Is there a resolution? *Chest* 2011, *140*, 16-18, 10.1378/chest.11-0523.

Supplementary material

Table S1. Distribution of exposure variables per exposure day (5h averages)

Exposure day	PNC (#/cm³)	PM (μg/m³)	BC (μg/m³)	NO_2 (μg/m³)	CO (μg/m³)	Temp (°C)	RH (%)
1	74,466	29.9	0.3	12.4	619	19.4	43
2	40,156	17.0	0.3	13.3	599	18.8	44
3	28,898	18.8	0.6	48.4	775	22.3	54
4	22,049	27.3	0.8	37.8	650	23.9	62
5	23,356	22.4	0.7	28.1	621	24.2	51
6	18,861	39.4	1.3	41.4	784	22.3	62
7	27,835	14.5	0.5	24.5	619	21.9	46
8	30,413	13.6	0.3	16.4	587	21.4	43
9	134,879	26.6	0.7	42.8	569	24.0	40
10	32,144	25.7	0.5	12.8	510	24.0	53
11	23,474	25.7	0.2	16.1	691	24.0	50
12	35,357	28.0	0.4	27.3	667	25.2	54
13	24,866	16.0	0.3	16.3	494	24.6	50
14	12,619	21.9	0.4	20.0	579	24.1	58
15	20,926	27.9	0.1	12.4	537	25.2	57
16	52,896	16.0	0.3	23.3	611	26.0	52
17	39,531	18.2	0.3	27.0	568	26.5	47
18	38,360	18.4	0.4	18.8	557	25.0	47
19	46,866	47.5	0.8	26.8	616	26.6	53
20	45,524	20.3	1.0	27.7	603	28.6	52
21	64,379	27.8	0.5	24.8	670	24.8	65
22	139,321	24.4	1.0	36.2	705	25.2	66
23	173,187	19.1	0.6	33.9	597	21.3	58
24	128,166	24.8	1.1	35.8	681	24.4	66
25	80,856	26.7	0.6	34.1	744	26.6	63
26	20,644	42.0	1.6	44.0	830	22.8	62
mean	**53,469**	**23.1**	**0.6**	**28.2**	**638**	**23.3**	**54**
SD	43,776	8.3	0.4	12.2	83	2.7	7
max	173,187	47.5	1.9	60.2	830	28.6	66
min	10,520	10.6	0.1	12.4	494	15.7	40

Mass concentration based on filter measurements; PNC = particle number concentration; PM = particulate matter; BC = black carbon; NO_2 = nitric oxide; CO = carbon monoxide; DL = value below detection limit; Temp = temperature; RH = relative humidity; SD = standard deviation. This table has been published previously for all exposure days (32 instead of 26 days) (Lammers *et al.,* Environ Int 2020).

Table S2. Distribution of particle number concentrations per participant (5h averages)

Participant	PNC exposure (#/cm³)				Visits
	mean	min	max	contrast	
1	89,500	20,700	173,200	152,600	4
2	68,200	24,900	173,200	148,400	4
3	52,300	12,700	134,900	122,300	4
4	66,600	21,000	139,400	118,400	3
5	51,400	20,700	134,900	114,300	4
6	72,700	30,500	139,400	109,000	4
7	74,500	20,700	128,200	107,600	2
8	57,800	22,100	128,200	106,200	4
9	85,400	38,400	134,900	96,600	4
10	41,200	12,700	74,500	61,900	4
11	52,200	23,500	80,900	57,400	2
12	52,500	23,500	80,900	57,400	3
13	50,900	24,900	80,900	56,000	3
14	40,300	21,000	74,500	53,600	4
15	44,300	27,900	74,500	46,700	4
16	35,600	18,900	64,400	45,600	4
17	42,700	27,900	64,400	36,600	4
18	34,900	18,900	45,600	26,700	4
19	30,400	21,000	46,900	26,000	4
20	27,800	23,400	32,200	8,800	2
mean	**53,600**	**22,800**	**100,300**	**77,600**	
min	27,800	12,700	32,200	8,800	
max	89,500	38,400	173,200	152,600	

PNC = particle number concentration measured by condensation particle counter (CPC) with d_{50} = 4 nm. PNC levels are rounded to hundreds. Table is order based on the individual contrast in PNC exposure. This table has been published previously for all exposure days (32 instead of 26 days) (Lammers *et al.,* Environ Int 2020).

Table S3. Correlation matrix: For all pollutants, particle size ranges and room conditions measured during 5h exposures

	PNC[a]	**PM**	**BC**	**NO_2**	**CO**	**Total aviation**	Take-off	Landing	**Total traffic**	Airport traffic	Road traffic	**Temp**	**RH**
PNC[a]		-0.03	0.18	0.36	0.00	**0.97**	**0.96**	**0.83**	0.31	-0.18	0.35	0.01	0.09
PM	-0.03		0.59	0.34	0.48	-0.10	-0.05	-0.18	0.46	0.16	0.42	0.14	0.42
BC	0.18	0.59		**0.76**	0.67	0.11	0.19	-0.07	0.31	0.15	0.28	0.04	0.51
NO_2	0.36	0.34	**0.76**		0.67	0.33	0.40	0.12	0.21	0.32	0.14	0.15	0.40
CO	0.00	0.48	0.67	0.67		-0.02	-0.01	-0.03	-0.05	0.20	-0.10	-0.08	0.58
Total aviation	**0.97**	-0.10	0.11	0.33	-0.02		0.97	0.87	0.18	-0.14	0.21	0.05	0.08
Take-off	**0.96**	-0.05	0.19	0.40	-0.01	**0.97**		**0.74**	0.29	-0.01	0.30	0.20	0.12
Landing	**0.83**	-0.18	-0.07	0.12	-0.03	**0.87**	**0.74**		-0.09	-0.39	0.01	-0.26	-0.04
Total traffic	0.31	0.46	0.31	0.21	-0.05	0.18	0.29	-0.09		0.13	**0.97**	0.43	0.10
Airport traffic	-0.18	0.16	0.15	0.32	0.20	-0.14	-0.01	-0.39	0.13		-0.12	0.52	0.20
Road traffic	0.35	0.42	0.28	0.14	-0.10	0.21	0.30	0.01	**0.97**	-0.12		0.30	0.05
Temp	0.01	0.14	0.04	0.15	-0.08	0.05	0.20	-0.26	0.43	0.52	0.30		0.33
RH	0.09	0.42	0.51	0.40	0.58	0.08	0.12	-0.04	0.10	0.20	0.05	0.33	

Pearson correlations with in **bold** R > 0.70; PNC = particle number concentration; PM = particulate matter; BC = black carbon; NO_2 = nitric oxide; CO = carbon monoxide; Temp = temperature; RH = relative humidity; a = PNC was detected by a condensation particle counter (CPC) with d_{50} = 4 nm; b = PNC size fractions were measured by a scanning mobility particle sizer (SMPS) with a limit of detection of 6-225 nm. This table has been partly published previously for all exposure days (32 instead of 26 days) and without the PNC source information (Lammers *et al.*, Environ Int 2020).

Discriminant analysis

Table S4. Discrimination between pre- and post-exposure

	PLSDA multilevel + LDA AUROCC (95%CI)
All eNose sensor data (n=71)	**0.83** (0.76 – 0.89)
PNC level stratification	
PNC < 25 percentile (n=18)	0.77 (0.61 – 0.93)
PNC > 75 percentile (n=18)	**0.98** (0.94 – 1.00)
Internal validation	
Training set (n=51)	**0.84** (0.75 – 0.92)
Validation set (n=20)	0.66 (0.48 – 0.84)

In **bold** AUROCC > 0.80 and p-values < 0.05; PLSDA = partial least square discriminant analysis; LDA = linear discriminant analysis; AUROCC = area under the receiver operating characteristic curve; CI = confidence interval; eNose = electronic nose; n = number of visits; PNC = particle number concentration.

Pollutant models

Table S5. Single-pollutant models: Associations between pollutants and eNose deviation percentages

Sensor		PNC 5-95p = 118,900 #/cm³		PM 5-95p = 26.5 μg/m³		BC 5-95p = 1.05 μg/m³		NO_2 5-95p = 31 μg/m³		CO 5-95p = 265 μg/m³	
		Est. (95% CI)	**R^2**	**Est. (95% CI)**	**R^2**	**Est. (95% CI)**	**R^2**	**Est. (95% CI)**	**R^2**	**Est. (95% CI)**	**R^2**
Deviation % percentage	**1**	**-7.2 (-13.9 – -0.5)**	0.12	5.6 (-2.5 – 13.79)	0.09	4.4 (-3.8 – 12.7)	0.08	1.1 (-7.0 – 9.1)	0.07	5.2 (-4.9 – 15.3)	0.08
	3	1.7 (-1.9 – 5.4)	0.16	-3.6 (-7.9 – 0.71)	0.18	-0.4 (-4.7 – 3.9)	0.15	-1.2 (-5.3 – 2.9)	0.15	2.3 (-3.0 – 7.6)	0.16
	4	1.3 (-3.1 – 5.7)	0.03	**-5.7 (-10.8 – -0.70)**	**0.09**	-1.1 (-6.1 – 4.1)	0.04	-2.3 (-7.2 – 2.6)	0.05	-2.1 (-8.5 – 4.2)	0.03
	5	1.5 (-8.3 – 11.3)	0.19	**-12.1 (-23.5 – -0.79)**	0.24	9.6 (-1.6 – 20.8)	0.22	4.5 (-6.5 – 15.4)	0.20	-3.6 (-17.9 – 10.7)	0.19
	6	-3.0 (-7.6 – 1.5)	0.04	-4.9 (-10.2 – 0.44)	0.06	0.5 (-4.8 – 5.9)	0.02	-0.2 (-5.4 – 4.9)	0.02	3.1 (-3.5 – 9.7)	0.03
	7	-1.0 (-19.0 – 17.0)	0.12	11.4 (-9.8 – 32.71)	0.14	17.1 (-3.4 – 37.5)	0.16	1.5 (-18.5 – 21.4)	0.12	0.7 (-25.2 – 26.6)	0.12

Data are presented as estimates (est.) with 95% confidence intervals (CI) intervals and the conditional explained variance (R^2) by both fixed and random factors (i.e. the entire model). All effect estimates are scaled to the 5-95th percentile change in the exposure of interest and are adjusted for respiratory symptoms, room temperature and room humidity. All results are adjusted for the individual baseline eNose signal (i.e. mean of all pre-measurement per subject and sensor). Numbers in **bold** are significant effects ($p < 0.05$) and/or $R^2 >$ 25%. *Exposures*: PNC = particle number concentration; PM = particulate matter; BC = black carbon; NO_2 = nitric oxide; CO = carbon monoxide.

Table S6. Two-pollutant models: Associations between PNC (corrected for other pollutants) and eNose deviation percentages

	Sensor	PNC (5-95p = 118,900 #/cm³)							
		Adjusted for PM		Adjusted for BC		Adjusted for NO_2		Adjusted for CO	
		Est. (95% CI)	R^2	Est. (95% CI)	R^2	Est. (95% CI)	R^2	Est. (95% CI)	R^2
Deviation %	**1**	**-6.9 (-13.5 – -0.2)**	0.13	**-7.8 (-14.5 – -1.1)**	0.14	**-8.5 (-15.7 – -1.4)**	0.13	**-6.9 (-13.7 – -0.2)**	0.13
	3	1.5 (-2.1 – 5.1)	0.18	1.8 (-1.8 – 5.5)	0.16	2.4 (-1.4 – 6.3)	0.17	1.8 (-1.8 – 5.5)	0.16
	4	0.9 (-3.3 – 5.2)	0.09	1.5 (-2.9 – 5.9)	0.03	2.3 (-2.3 – 7.0)	0.04	1.2 (-3.2 – 5.6)	0.03
	5	0.7 (-8.9 – 10.2)	0.23	0.3 (-9.4 – 10.1)	0.22	0.1 (-10.3 – 10.6)	0.20	1.3 (-8.5 – 11.2)	0.19
	6	-3.4 (-7.8 – 1.0)	0.09	-3.1 (-7.7 – 1.4)	0.04	-3.4 (-8.2 – 1.5)	0.04	-2.9 (-7.4 – 1.6)	0.05
	7	-0.2 (-18.1 – 17.7)	0.14	-3.3 (-21.2 – 14.5)	0.15	-1.7 (-21.1 – 17.7)	0.12	-0.9 (-19.0 – 17.1)	0.12

Data are presented as estimates (est.) with 95% confidence intervals (CI) intervals and the conditional explained variance (R^2) by both fixed and random factors (i.e. the entire model). All effect estimates are scaled to the 5-95th percentile change in the exposure of interest and are adjusted for respiratory symptoms, room temperature and room humidity. The results of the deviation percentages were also adjusted for the individual baseline eNose signal (i.e. mean of all pre-measurement per subject and sensor). Numbers in **bold** are significant effects ($p < 0.05$) and/or $R^2 > 25\%$. *Exposures*: PNC = particle number concentration; PM = particulate matter; BC = black carbon; NO_2 = nitric oxide CO = carbon monoxide. PNC was detected by a condensation particle counter (CPC) with d_{50} = 4 nm.

PNC source models

Table S7. Single-source models: Associations between PNC sources and eNose deviation percentages

	Sensor	Take-off 5-95p = 58,100 #/cm³		Landing 5-95p = 25,000 #/cm³		Airport traffic 5-95p = 4,400 #/cm³		Road traffic 5-95p = 12,600 #/cm³	
		Est. (95% CI)	R^2	Est. (95% CI)	R^2	Est. (95% CI)	R^2	Est. (95% CI)	R^2
Deviation %	**1**	-6.7 (-14.1 – 0.7)	0.10	-5.0 (-11.7 – 1.7)	0.09	6.4 (-1.7 – 14.6)	0.10	-1.9 (-7.1 – 3.2)	0.07
	3	2.0 (-1.9 – 6.0)	0.16	3.1 (-0.4 – 6.7)	0.18	-0.6 (-4.9 – 3.8)	0.15	-1.4 (-4.1 – 1.3)	0.16
	4	2.3 (-2.5 – 7.0)	0.03	1.8 (-2.5 – 6.1)	0.04	-2.7 (-7.8 – 2.5)	0.06	-2.3 (-5.5 – 1.0)	0.08
	5	3.8 (-7.0 – 14.5)	0.20	0.9 (-8.8 – 10.5)	0.19	-3.4 (-15.2 – 8.3)	0.20	-4.9 (-12.2 – 2.4)	0.21
	6	-1.9 (-6.9 – 3.1)	0.03	-1.8 (-6.3 – 2.7)	0.03	3.1 (-2.2 – 8.4)	0.04	**-5.0 (-8.2 – -1.9)**	0.13
	7	4.4 (-15.1 – 24.0)	0.13	-6.9 (-24.7 – 10.8)	0.13	7.9 (-13.4 – 29.3)	0.13	-3.8 (-17.4 – 9.7)	0.13

Data are presented as estimates (est.) with 95% confidence intervals (CI) intervals and the conditional explained variance (R^2) by both fixed and random factors (i.e. the entire model). All effect estimates are scaled to the 5-95th percentile change in the exposure of interest and are adjusted for respiratory symptoms, room temperature and room humidity. The results of the deviation percentages were also adjusted for the individual baseline eNose signal (i.e. mean of all pre-measurement per subject and sensor). Numbers in **bold** are significant effects ($p < 0.05$) and/or $R^2 > 25\%$.

Table S8. Single-source models: Associations between PNC sources (totals) and eNose deviations

	Sensor	Total aviation 5-95p = 81,000 #/cm³		Total traffic 5-95p = 13,100 #/cm³	
		Est. (95% CI)	R^2	Est. (95% CI)	R^2
Deviation %	**1**	-6.4 (-13.7 – 0.8)	0.10	-1.2 (-6.9 – 4.5)	0.07
	3	2.5 (-1.4 – 6.4)	0.17	-1.7 (-4.7 – 1.3)	0.16
	4	2.2 (-2.5 – 6.9)	0.03	-3.1 (-6.6 – 0.5)	0.10
	5	2.9 (-7.6 – 13.4)	0.19	-6.2 (-14.1 – 1.8)	0.22
	6	-1.9 (-6.8 – 2.9)	0.03	**-5.3 (-8.9 – -1.8)**	0.13
	7	0.6 (-18.6 – 19.9)	0.12	-3.1 (-17.9 – 11.7)	0.13

Data are presented as estimates (est.) with 95% confidence intervals (CI) intervals and the conditional explained variance (R^2) by both fixed and random factors (i.e. the entire model). All effect estimates are scaled to the 5-95th percentile change in the exposure of interest and are adjusted for respiratory symptoms, room temperature and room humidity. The results of the deviation percentages were also adjusted for the individual baseline eNose signal (i.e. mean of all pre-measurement per subject and sensor). Numbers in **bold** are significant effects ($p < 0.05$) and/or $R^2 > 25\%$. Total aviation = take-off + landing; total traffic = airport traffic + road traffic.

Table S9. Two-source model: Associations between adjusted PNC sources and eNose deviations

	Sensor	Total aviation 5-95p = 81,000 #/cm³ Adjusted for total traffic	Total traffic 5-95p = 13,100 #/cm³ Adjusted for total aviation	
		Est. (95% CI)	Est. (95% CI)	R^2
Deviation %	**1**	-6.4 (-13.7 – 1.0)	-0.3 (-6.0 – 5.3)	0.10
	3	3.0 (-0.8 – 6.9)	-2.2 (-5.2 – 0.8)	0.19
	4	2.9 (-1.6 – 7.7)	-3.5 (-7.0 – 0.1)	0.10
	5	4.7 (-5.8 – 15.2)	-6.9 (-15.0 – 1.2)	0.22
	6	-0.6 (-5.4 – 4.1)	**-5.3 (-8.8 – -1.7)**	0.13
	7	1.3 (-18.2 – 20.9)	-3.3 (-18.3 – 11.7)	0.13

Data are presented as estimates (est.) with 95% confidence intervals (CI) intervals and the conditional explained variance (R^2) by both fixed and random factors (i.e. the entire model). effect estimates are scaled to the 5-95th percentile change in the exposure of interest and were adjusted for respiratory symptoms, room temperature and room humidity. The results of the deviation percentages were also adjusted for the individual baseline eNose signal (i.e. mean of all pre-measurement per subject and sensor). Numbers in **bold** are significant effects ($p < 0.05$) and/or $R^2 > 25\%$. Total aviation = take-off + landing; total traffic = airport traffic + road traffic.

Chapter 5.

Alterations to the urinary metabolome following semi-controlled short exposures to ultrafine particles at a major airport

Selley L *
Lammers A *
Le Guennec A
Pirhari M
Sioutas C
Janssen N
Maitland - van der Zee AH
Mudway I
Cassee F

International Journal of Hygiene and Environmental Health, 2021; 237: 113802

** both authors contributed equally to this work.*

Abstract

Background: Inflammation, oxidative stress and reduced cardiopulmonary function following exposure to ultrafine particles (UFP) from airports has been reported but the biological pathways underlying these toxicological endpoints remain to be explored. Urinary metabolomics offers a robust method by which changes in cellular pathway activity can be characterised following environmental exposures.

Objective: We assessed the impact of short-term exposures to UFP from different sources at a major airport on the human urinary metabolome.

Methods: 21 healthy, non-smoking volunteers (aged 19-27 years) were repeatedly (2–5 visits) exposed for 5h to ambient air at Amsterdam Airport Schiphol, while performing intermittent, moderate exercise. Pre- to-post exposure changes in urinary metabolite concentrations were assessed via ^{1}H NMR spectroscopy and related to total and source-specific particle number concentrations (PNC) using linear mixed effects models.

Results: Total PNC at the exposure site was on average, 53,500 particles/cm^3 (range 10,500 – 173,200) and associated with significant reductions in urinary taurine (-0.262 AU, 95% CI: -0.507 – -0.020) and dimethylamine concentrations (-0.021 AU, 95% CI: -0.040 – -0.067). Aviation UFP exposure accounted for these changes, with the reductions in taurine and dimethylamine associating with UFP produced during both aircraft landing and take-off. Significant reductions in pyroglutamate concentration were also associated with aviation UFP specifically, (-0.005 AU, 95% CI: -0.010 – <0.000) again, with contributions from both landing and take-off UFP exposure. While non-aviation UFPs induced small changes to the urinary metabolome, their effects did not significantly impact the overall response to airport UFP exposure.

Discussion: Following short-term exposures at a major airport, aviation-related UFP caused the greatest changes to the urinary metabolome. These were consistent with a heightened antioxidant response and altered nitric oxide synthesis. Although some of these responses could be adaptive, they appeared after short-term exposures in healthy adults. Further study is required to determine whether long-term exposures induce injurious effects.

Introduction

Global air transport has grown strongly over the past decades [1]. In 2019, scheduled passenger numbers reached more than 4.5 billion and 61.3 million tonnes of cargo were transported by plane [2]. Encouraged by our developing understanding of road emissions toxicity, concern has developed over the impacts that aviation and other airport emissions could have on human health. In addition to manoeuvring aircraft, auxiliary power units, ground service equipment and ground access vehicles are strong sources of nitrogen oxides (NO_x), carbon monoxide (CO), volatile organic compounds (VOCs), sulphur oxides (SO_x) and particulate matter (PM) at airports [3]–[6].

Much of airport-originating PM falls within the ultrafine size range (PM <0.1 μm) [5] and is dominated by particles <20 nm in diameter based on the particle number concentrations (PNC) counts. This fraction is apportioned to primarily aircraft emissions [5], [7]. Concentrations of aviation-related PNCs have been detected at significantly elevated levels as far as 18 km downwind of airports [7]–[10] affecting both total indoor and outdoor PNCs [8], [10]. Resultantly the number of individuals exposed to aircraft -related emissions far exceeds airport personnel and passengers, extending to residents and workers in the urbanisations that neighbour airports.

Historically, studies of PM toxicity have focused primarily on the adverse impacts of exposure to PM10 and PM2.5 [11]–[15]. However, expansion of these studies to incorporate traffic-related UFPs has demonstrated the potential for UFPs to elicit greater toxicity (based on mass concentrations) and a higher likelihood to induce systemic effects compared with larger particles of the same composition. This is due to their small diameter, high surface area- to- mass ratio and high number concentration. These properties allow UFPs to adsorb greater quantities of redox-active metals and organic compounds and to deposit efficiently within the alveoli where they generate oxidative stress and inflammation, inhibit antimicrobial mechanisms and rapidly enter the surrounding tissue, avoiding clearance by airway macrophages [16]–[19]. Furthermore, small quantities of UFPs can cross the alveolar-capillary barrier, enter the bloodstream and translocate to secondary organs within hours of pulmonary exposure [20]–[22].

Consistent with these observations from UFPs emitted by road-traffic, aviation-related UFPs have been shown to induce both airway and systemic inflammation *in vivo*. In mice, particles collected from a commercial airport and non-commercial airfield caused dose-dependent infiltration of the airways

by neutrophils, lymphocytes and eosinophils during the first 24h of exposure [23]. Heightened concentrations of pro-inflammatory mediator IL-6 were also observed in the blood of asthmatic adults following a 2 h walk in the high UFP-zone surrounding Los Angeles International Airport (LAX) [24]. Supported by evidence that exposure to UFP from Amsterdam Airport Schiphol associates with mild reductions in lung and cardiac function (decreased forced vital capacity and prolonged QTc intervals) in healthy young individuals [25]. While studies of adverse health effects and UFP exposure in airport workers remain scarce and inconclusive [26], the adverse effects that we see in these interventional and *in vitro* studies are consistent with those induced by diesel exhaust particles (DEP) [27]. Together with evidence that ultrafine DEP and aviation UFP have similar physicochemical properties [27], these findings confirm the credibility of concern regarding aviation-related UFP exposure and health.

Expanding upon the observations from Amsterdam Airport Schiphol, this study employed untargeted metabolomics to identify response biomarkers that inform identification of potential causal adverse outcome pathways. Metabolomics captures the profile of small molecules that exist within a sample, and has been used to identify changes in cellular activity following exposure to fuel exhausts produced by road vehicles and ships [28]–[31]. Being global in design, these analyses identified components of adverse responses that were not captured previously by hypothesis-driven studies, including fuel- specific differences [32]. For humans, urine is an especially favourable sample for metabolomic study of environmental exposures. As the primary route of excretion for cellular waste, urine is rich in metabolites and inclusive of pathway dysfunction markers from across the body [33]. As a non-invasive and easily accessible sample, it also lends itself well to studies of large cohorts or repeat sampling.

Employing metabolomic urinalysis, this study explored the hypothesis that UFP from different airport-related sources (aviation, ground service vehicles and feeder highways) induces distinct changes to the urinary metabolome. Aiming to identify mechanistically informative markers of cellular responses to airport UFP exposure, we analysed the metabolic content of urine produced before and after short-term exposures to ambient air at Amsterdam Airport Schiphol, Netherlands.

Materials and methods

Study design and population

The design of this prospective, interventional study is detailed in Figure 1. Healthy adults (n=21) underwent 5h exposures to ambient air within a mobile laboratory at Amsterdam Airport Schiphol (Amsterdam, the Netherlands). Two to five repeat visits were made per participant, leaving a minimum of two weeks between visits to enable ablation of biological responses to exposure. Participants were university students, living in Amsterdam, > 2 km away from Schiphol airport and not within 300m away of a highway or road that was trafficked by > 10,000 vehicles per day. Participants were aged between 20 and 23 years, were predominantly female (81%) and had BMIs within healthy range (22.6 $kg/m^2 \pm 2.4$). All participants had normal cardiopulmonary function as determined by measurements of forced expiratory volume (FEV_1), forced vital capacity (FVC), peak expiratory flow (PEF), fractional exhaled nitric oxide (FeNO), blood pressure, heart rate and oxygen saturation (presented previously in Table 2 of Lammers *et al*. [25]). Each participant provided first morning urine samples the day of exposure and again the next morning, an average of 18h after the end of exposure (minimum 12h, maximum 27h). Proton nuclear magnetic resonance spectroscopy (^{1}H NMR) profiles were acquired for each urine sample to characterise changes in the urinary metabolome that related to UFP exposure at the airport.

Exposure

Detailed methods for participant exposures are provided by Lammers *et al*. (2020). Briefly, individuals remained for 5h within a mobile laboratory (14 m^3), situated next to the airside of Amsterdam Airport Schiphol, ~300 m away from two runways, ~500 m from two highways, 10 km from the city and close to several large car parks. The laboratory was fitted with an airflow system to refresh the flow of ambient air in a uniform manner (~400 m^3/h) for the duration of the exposure. Extensive air quality measurements were produced from the flow to characterise exposures for each individual at each visit. This varied due to differences in meteorological conditions (especially wind direction) and in runway use. By considering forecasted weather, we were able to schedule visits to include variation in UFP levels and source contributions (e.g. aviation and road traffic) for each individual. During the exposures, participants cycled at low intensity for 20 min/h and rested for the remainder of the time. Prior to exposures, participants were instructed not to consume alcohol or caffeine (for 24 and 12h respectively) as well as tobacco and non-pharmaceutical drugs for the

duration of the study. Food and drinks were provided on the day of exposure to minimise intake of nitrate-rich foods but individual intake was not standardised or limited.

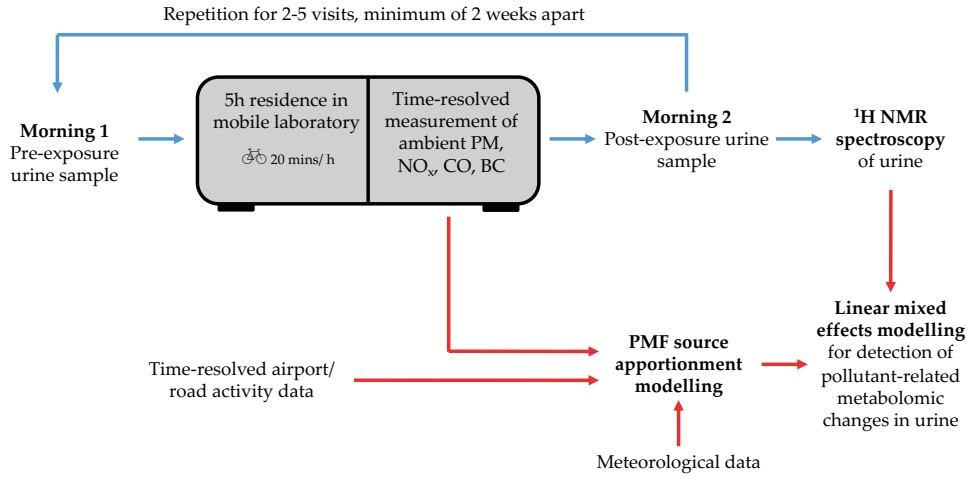

Figure 1. Study design: On 2-5 occasions, participants provided urine samples prior to spending 5h in a mobile laboratory at Amsterdam Airport Schiphol. A second urine sample was given at the 24h time point and the metabolomic content of each sample was characterised via ^{1}H NMR. The output was combined with source apportioned pollutant measurements in a linear mixed effects model to identify changes in urinary metabolic content that relate to different air pollutant exposures at the airport. Exposure and experimental steps are denoted with blue arrows while data interrogation is represented by red arrows.

Exposure characterisation

Individual exposures to UFP emissions from aviation emissions (total, take-off only and landing only), non-aircraft airport vehicles (such as passenger buses, fuel tankers, baggage trucks and local airport traffic) and non-airport (urban background and road) sources were calculated as a 5h average for each exposure date using a Positive Matrix Factorization (PMF) source apportionment model. Details of the model and instruments used to collect the input data are provided by Pirhadi *et al.* (2020) [5] and Lammers *et al.* (2020) [25]. To summarise the sources of the UFP, air within the exposure chamber was sampled continuously and subjected to measurement for particle number concentrations (PNCs) and PM mass (gravimetrically), carbon monoxide (CO), black carbon (BC) and nitrogen oxides (NO_x). A water-based condensation particle counter (CPC) provided PNCs for total PM of ≤ ~2.5 μm in diameter and a scanning mobility particle sizer (SMPS) was fitted to measure PNCs for size fractions between 6 and 225 nm

in diameter. Particle masses were established using a tapered element oscillating microbalance while NO_x was measured with a chemiluminescence NO_x analyzer, CO with a gas filter correlation analyser and BC via optical absorption using an aethalometer. Meteorological conditions (temperature, wind speed and relative humidity) for the times of sampling were provided by the Royal Netherlands Meteorological Institute.

^{1}H NMR spectral acquisition

Samples were prepared by combining 540 µl urine with 60 µl phosphate buffer containing 0.1M trimethylsilylpropanoic acid (TSP) in 5 mm NMR tubes. Spectra were acquired with a 600 MHz AV-NEO spectrometer equipped with a triple resonance cryoprobe with ^{1}H/^{13}C/^{15}N channels and a SampleJet for automation (all Bruker, UK). For each sample, a 1D ^{1}H spectrum was acquired using the presaturation utilising relaxation gradients and echoes (PURGE) pulse sequence, optimised to reduce the effects of non-ideal gradients [34]. 64 scans were used, with an acquisition time of 2.62 s, a spectral width of 20.8 parts per million (ppm), 4 dummy scans and a relaxation delay of 4 s. Additionally, a Total Correlation Spectroscopy (TOCSY) spectrum and a heteronuclear single quantum coherence (HSQC) spectrum were acquired on one of the samples for identification purposes. For TOCSY, the Bruker pulse sequence "dipsi2gpphzs" was used, slightly modified to include presaturation, which 16 scans, 512 t1 increments, a spectral width of 13.7 ppm in both dimensions and a relaxation delay of 2 s. The HSQC spectrum was acquired using the Bruker pulse sequence "hsqcetgpsisp2.2", with 32 scans, 512 t1 increments, a spectral width of 210 ppm in the 13C dimension and 20.8 ppm in the ^{1}H dimension and a relaxation time of 2 s.

^{1}H NMR spectral processing and peak assignment

After acquisition, the 1D ^{1}H spectra were processed with an exponential window function of 0.3 Hz before Fourier Transform, then phasing, calibration of the ppm scale to the TSP peak (0 ppm) and baseline correction with a polynomial function of order 2. Processed spectra were imported into Chenomx Profiler (Chenomx Inc, Canada) for annotation using a peak fitting technique. Statistical total correlation spectroscopy (STOCSY) analyses were performed using Matlab (Version R2019b, Mathworks, USA) to assist this process by identifying peaks that belonged to common parent molecules (r values > 0.8). Annotations were confirmed for feature metabolites by comparing peak signals within the HSQC spectrum with reference values published in the Human Metabolome Database [35]. Integrals were calculated for individual peaks using Matlab, employing code that determined the size of the signal based on the area under the curve between peak minima and maxima. Peak integrals were normalised to those

of creatinine signals from the same spectrum to account for variations in urinary concentration. All Matlab codes were developed within the Section of Computational and Systems Medicine, Imperial College, London.

Statistical analysis

Linear mixed effects models were used to (A) detect confounding variables in the dataset and (B) identify changes in urinary metabolite content that are related to pollutant exposure. These were performed in R Studio (version 1.1.463, USA) using the 'lmer' function of Package 'lme4'. Throughout the analysis, relationships between metabolite signals and variables of interest (presented as regression coefficients) were considered statistically significant where the 95% confidence interval did not contain zero.

Confounding variables

To identify whether use of over-the counter pharmaceuticals (acetaminophen and ibuprofen, as detected within the spectra) induced changes to the urinary metabolome independent of pollutant exposure, pre-exposure data (pre) for each individual (i) and visit (j) was input into the following model:

$$Y_{i,j} = \beta_0 + Y_{i,j,pre} + \beta_1 E_j + U_{0i} + \varepsilon_i$$

With Yi,j referring to the relationships between non-target variable and metabolomic change across the study, Ej represents a vector of the potentially confounding variables and Yi,j ,pre, the metabolite signals produced from the pre-exposure spectra of each participant at each of their visits. β refers to population-average fixed effects; specifically, the average metabolite signal where all other co-variates are zero (β0) and the average signal relative to a 5-95th percentile (5-95p) increase in the variable of interest. The U0i is a random intercept produced from each individual's deviation from the study population's average metabolite signal with ε1 as the accompanying error term.

Pollutant-related metabolomic changes

Alterations were made to the confounding variable identification model to focus on changes in metabolite concentration that were caused by pollutant exposure and to correct for confounding co-exposures.

$$Y_{i,j} = \beta_0 + Y_{i,j,pre\text{-}post} + \beta_1 E_j + \beta_2 V_{1,i,j} + \beta_3 V_{2,j} + \beta_4 V_{3,j} + U_{0i} + \varepsilon_i$$

Here, the model calculated the difference in metabolite signals for each individual at each visit ($Y_{i,j\ ,pre\text{-}post}$) whilst adjusting for vectors of pharmaceutical signals produced from the ^1H NMR spectra ($V_{1,i,j}$), environmental conditions (room temperature and humidity) for different visits ($V_{2,j}$) and where appropriate, concentrations of secondary pollutants during different visits ($V_{3,j}$), β_2, β_3 and β_4 represent population- averages for these variables.

Pearson's correlation analyses were performed using GraphPad Prism 8 (GraphPad, California, USA) to explore the strength of relationships between metabolites that associated with exposure (referred to as feature metabolites). Correlations were considered 'moderate' or 'strong' where the Pearson's r value was ≥ 0.60 and 0.80, respectively [36], and the p value was ≤ 0.05.

Results

Individual particle exposures were predominantly contributed to by aviation emissions

In total, samples from 21 of the exposed participants were included for metabolomic profiling. Spectra from 1 participant were withdrawn from the analysis following peak annotation due to the presence of ethanol peaks in the urine. The remaining samples represented participation on 32 exposure days with each individual undergoing 2–5 exposures during the period between May and October 2018. Only 2 participants undertook two exposures (finishing the study early for personal reasons), with 13 participants undertaking four exposures and 6 participants undertaking five exposures due to extremely low exposures occurring on their first visit.

As documented by Lammers *et al.* and Pirhadi *et al.*, 5h averages of total PNC ranged between 10,500 and 173,200/cm^3 at the exposure site [25], with aviation activity contributing most to PNC exposure for the majority of the study period and individuals (Figure 2A-B) [5] . Pearson's correlation analysis found no significant relationship between PNC from total aviation, airport traffic and non-airport traffic sources but as expected, total aviation PNC correlated strongly and positively with total PNC measurements, take – off PNC and landing PNC (r= 0.97, 0.97 and 0.89 respectively) (Table S1). Moderately strong positive correlations also existed between take-off and landing PNCs (r= 0.76) (Table S1).

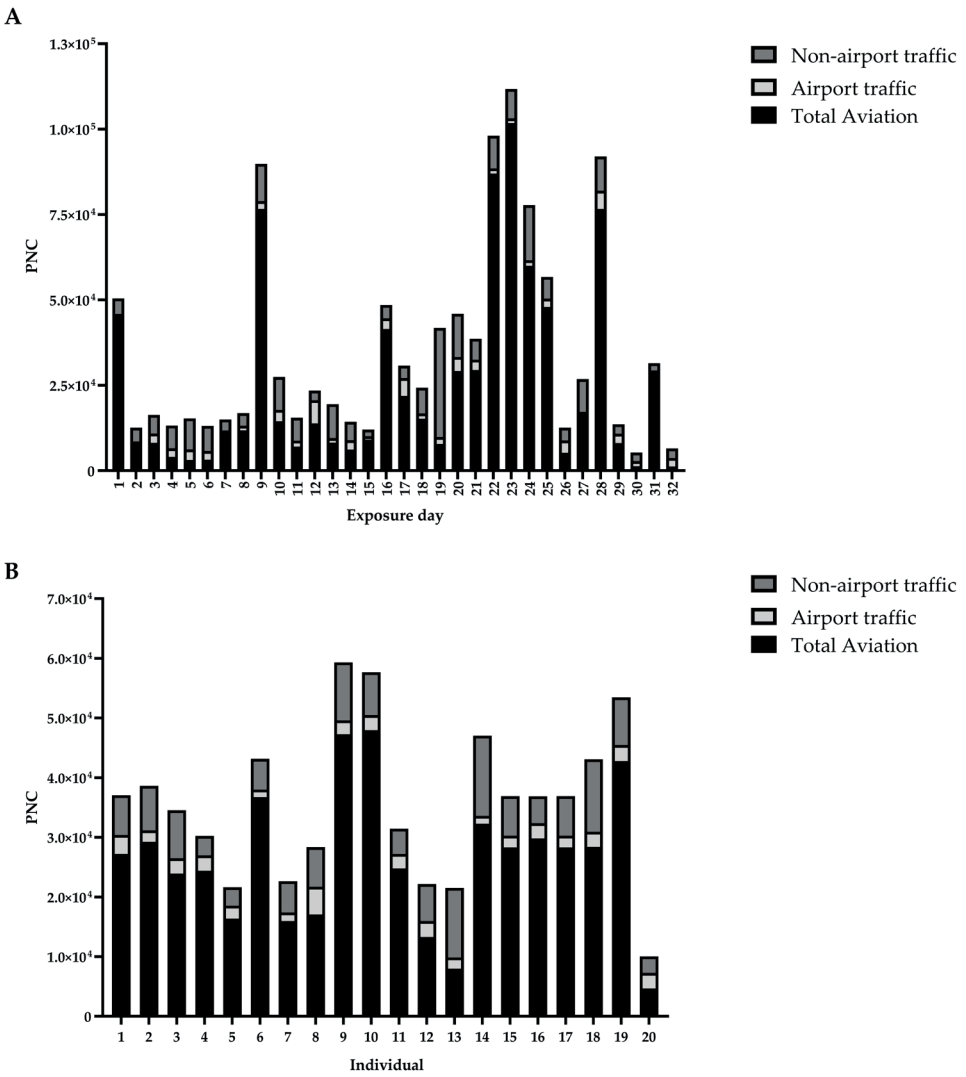

Figure 2. PNC for total aviation, airport traffic and non-airport traffic sources during exposures. Source apportioned 5h mean values are provided for each exposure event **(A)** as determined by PMF modelling [5] and for each participant (presented as the mean of these values across their 2- 5 exposures) **(B)**.

^{1}H NMR spectra revealed substantial use of analgesics within the study population

Peaks from 68 distinct, assignable metabolites were detected within the ^{1}H NMR spectra alongside a further 54 peaks that could not be assigned using Chenomx profiling, HMBD searches or literature searches (Table S2). Of the assignable

metabolites, 9 were produced during metabolism of commonly used, over-the-counter analgesics (ibuprofen and acetaminophen). As use of these analgesics were not exclusion criteria for the study, incidence of use by the study population was assessed using the visibility of the ibuprofen/ibuprofen-glucuronide peak at 0.74 ppm and the acetaminophen- glucuronide peaks at 5.10 ppm as markers of recent ibuprofen and acetaminophen consumption (Figure 3). These peaks were selected because they did not exhibit overlap from other metabolites in the spectra. Visible ibuprofen/ibuprofen-glucuronide peaks, were present in 47 and 50% of pre- and post-exposure spectra (respectively), while visible acetaminophen glucuronide peaks were detected in 20 and 13% of pre- and post-exposure spectra. The presence of both analgesic peaks was detected in 12 and 5% of pre- and post-exposure spectra while only 32 and 41% of pre and post-exposure peaks contained no visible peaks for either metabolite.

Although pharmaceutical use is commonly observed in metabolomic analyses, the impact that therapeutic acetaminophen or ibuprofen use has on the endogenous urinary metabolome in humans has not been published. For the current study, linear modelling of the pre-exposure spectra demonstrated that urinary concentrations of trimethylamine-N-Oxide (TMAO), 3-aminoisobutyrate and glutamine were significantly elevated in association with acetaminophen use, and that citrate, glutamine, threonine, dimethylamine, alanine, TMAO, pyruvate, glutamate, lysine and N-acetylglutamate concentrations were significantly increased with ibuprofen uptake (Table 1). As such, urinary concentrations of acetaminophen and ibuprofen were input as confounding variables during modelling of emissions-related metabolomic change.

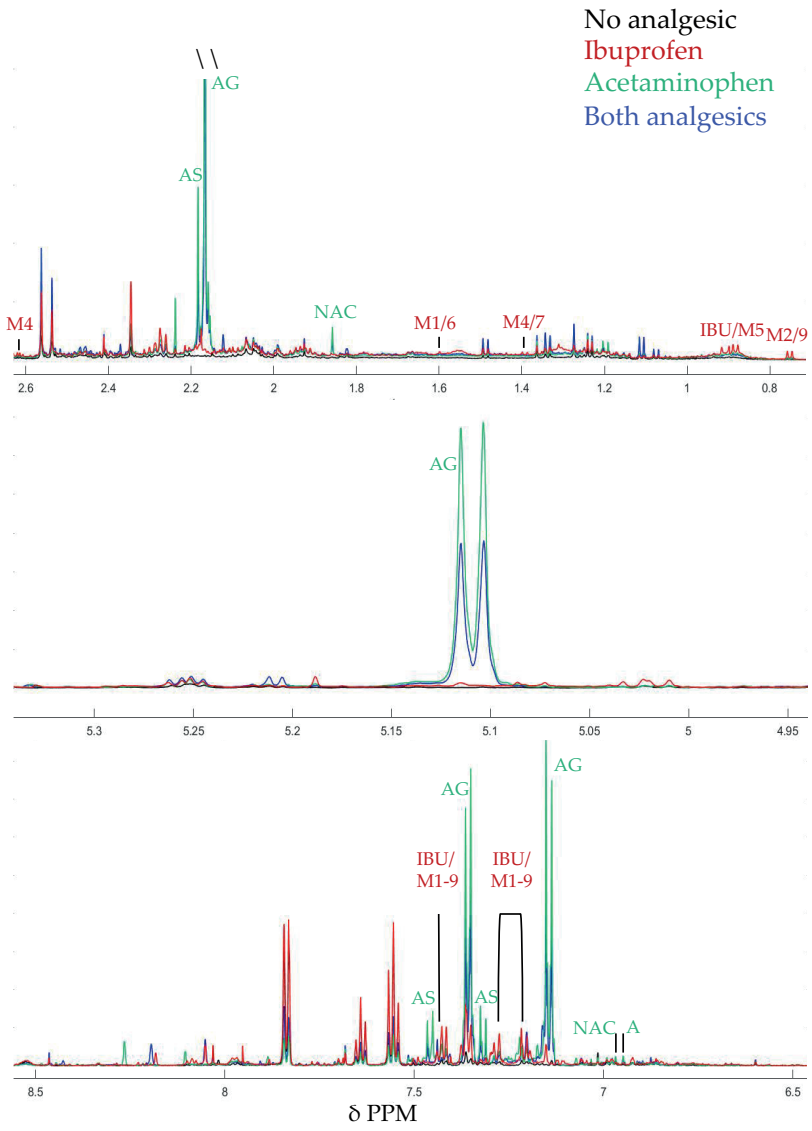

Figure 3. Comparison of selected analgesic peak regions in the urinary ^{1}H NMR spectra of study participants prior to airport exposure. As labelled, these regions display peaks relating to the presence of parent compounds or metabolites of acetaminophen or ibuprofen. Included spectra are representative of those that contain no analgesic peaks (black spectrum), ibuprofen related peaks (red spectrum), acetaminophen related peaks (green spectrum) or peaks relating to both analgesics (blue spectrum). Acetaminophen (A), acetaminophen sulfate (AS), acetaminophen glucuronide (AG), N-acetylcysteine (NAC), Ibuprofen (IBU), 1-hydroxy ibuprofen (Ibuprofen metabolite (M) 2), carboxy ibuprofen (M4), 2-hydroxy ibuprofen glucuronide (M6), carboxy ibuprofen glucuronide (M7), 1-hydroxy ibuprofen glucuronide (M9).

Table 1. Associations between Δ endogenous metabolites and xenobiotic metabolite concentrations.

Metabolite	Ibuprofen	Acetaminophen
	Coef. (95% CI)	Coef. (95% CI)
Citrate	**4.55 (2.30 – 6.90)**	0.17 (-1.63 – 2.03)
Glutamine	**1.69 (1.02 – 2.40)**	**0.866 (0.33 – 1.41)**
Threonine	**1.48 (1.09 – 1.88)**	0.34 (-0.04 – 0.72)
Dimethylamine	**1.48 (0.52 – 2.43)**	0.04 (-0.81 – 0.90)
Alanine	**1.42 (1.04 – 1.80)**	0.19 (-0.19 – 0.16)
TMAO	**1.39 (0.04 – 2.82)**	**1.19 (0.19 – 2.23)**
Unassigned at 2.33 ppm	**0.81 (0.36 – 1.44)**	0.32 (-0.04 – 0.67)
Pyroglutamate	**0.74 (0.45 – 1.05)**	**0.33 (0.11 – 0.56)**
Acetate / Phenylacetylglutamine	**0.54 (0.30 – 0.78)**	0.11 (-0.09 – 0.11)
3-Aminoisobutyrate	0.72 (-0.34 – 1.84)	**1.12 (0.32 – 1.95)**

Data are presented as coefficients (coef.) of the relationship between exposure and Δ in metabolite concentration (post-pre) with 95% confidence intervals (CI) (expressed as the range between lower and upper values). All coefficients are adjusted for room temperature and humidity. Numbers in **bold** represent significant relationships ($p \leq 0.05$).

Exposure to airport-derived particulates causes significant alterations to the endogenous urinary metabolome

Preliminary analysis determined that total PNC exposure was associated with significant reductions in urinary taurine and dimethylamine concentrations (-0.263 arbitrary units (AU, as a ratio with internal creatinine signal), 95% CI: -0.507 - -0.020 and -0.232 AU, 95% CI: -0.396 - -0.670, respectively). Size apportioned PNCs confirmed that these changes associated with exposure to PNC < 20 nm but not PNC > 50 nm. The strength of association between dimethylamine concentration and PNC < 20 nm was of equal size to the relationship between dimethylamine concentration and total PNC, while a 0.035 AU increase in coefficient size was seen for the association between taurine concentration and PNC < 20 nm exposure when compared with total PM exposure (Table 2). These observations indicate that PNC < 20 nm, which associate with airplane emissions, were responsible for the changes. No other changes to the metabolome associated significantly with PNC < 20 nm or PNC > 50 nm or with carbon black exposure specifically (Table 2) but exposure to combustion-associated pollutant gases displayed small but significant associations with changes to the urinary metabolome. NO_2 exposure related to small reductions in urinary 3-hydroxyisovalerate content (-0.005 AU, 95% CI: -0.009 – -0.001) as well as 3-hydroxyisobutyrate (-0.007 AU, 95% CI: -0.013 – -0.001). Exposure to CO also

associated with reductions in 3-hydroxyisobutyrate concentration (-0.009 AU, 95% CI: -0.017 – -0.001) and increases in concentrations of N-acetylglutamine and an unassigned metabolite (0.020 AU, 95% CI: 0.002 – 0.038 and 0.006 AU, 95% CI: 0.001 – 0.010, respectively). Accounting for co-exposures to CO or NO_2 had minimal impact on the strength of association between total PNC, PNC < 20 nm and taurine or dimethylamine. No novel associations between exposure and metabolomic change were identified following the correction (Table S3).

Exposure to UFP from different airport-related sources induces distinct alterations to the endogenous urinary metabolome

The PMF model established that airport activities accounted for 79.3% of total PNC (46.1, 26.7 and 6.5% from aircraft departures, aircraft arrivals and ground service equipment (GSE)/ local airport traffic respectively) while road traffic and urban background sources contributed 18% and 2.7% respectively[5]. Using this data, PNCs were assigned to three general emissions sources at Amsterdam Airport Schiphol; total aviation, airport traffic (from GSE and road traffic within the airport) and non-airport traffic (from the nearby highways and urban background). Consistent with the results above, the largest changes to the urinary metabolome of exposed participants were induced by total aviation PNC (5-95p= 73,485 particles/ cm^3). Here, exposure associated significantly with a 0.26 AU decrease in urinary taurine (95% confidence interval (CI): -0.503- -0.023) as well as smaller but statistically significant decreases in dimethylamine (- 0.021 AU, 95% CI: -0.037 - -0.005) and pyroglutamate concentration (0.005 AU, 95% CI: -0.01- <0.00). Neither PNC produced by airport traffic or non-airport traffic associated with changes in these metabolite concentrations but PNC relating to airport traffic (5-95p= 5077 particles/ cm^3) did associate with significant yet small increases in urinary concentrations of methylguanidine (0.001 AU, 95% CI: >0.000 - 0.002) and decreases in 3-aminoisobutyrate (- 0.010 AU, 95% CI: -0.019 - - 0.001). In contrast, exposure to PNC produced by non-airport traffic (5-95p= 15290 particles/ cm^3) associated with significant increases in urinary 3-aminoisobutyrate concentration (0.010 AU, 95% CI: 0.002 – 0.017) as well as small increases in carnosine/arginine (0.005 AU, 95% CI: 0.001-0.008) and ethanolamine/isethionate concentrations (0.005 AU, 95% CI: 0.001- 0.010) and a reduction in isocitrate concentration (-0.003, 95% CI: -0.005 – -0.001) (Table 3). Adjustment of the single pollutant models to account for co-exposure to UFP from the remaining key sources (total aviation, airport traffic, non-airport traffic, as appropriate), did not cause noteworthy changes to the strength of associations with metabolite features (Table 4). This indicates that the changes to the metabolome that associate with each key feature were unlikely to have been contributed to by co-exposure to the others.

Table 2. Single pollutant models for associations between Δ urinary metabolites and major air pollutants at Schiphol Airport

Metabolite	Total PNC (5-95p = 120,280 # / cm^3)	PNC < 20nm (5-95p = 51,160 # / cm^3)	PNC > 50nm (5-95p = 3,900 # / cm^3)	Black carbon (5-95p = 1.4 μg / cm^3)	NO_2 (5-95p = 33.2 μg / cm^3)	CO (5-95p = 250 μg / cm^3)
	Coef. (95% CI)	**Coef. (95% CI)**	**Coef. (95% CI)**	**Coef. (95% CI)**	**Coef. (95% CI)**	**Coef. (95% CI)**
Taurine	**-0.263**	**-0.298**	-0.044	-0.029	-0.096	-0.113
	(-0.507 – -0.020)	**(-0.550 – -4.709)**	(-0.396 – 0.307)	(-0.349 – 0.290)	(-0.351 – 0.158)	(-0.436 – 0.211)
Dimethylamine	**-0.023**	**-0.023**	0.006	0.003	-0.001	-0.003
	(-0.040 – -0.067)	**(-0.040 – -0.067)**	(-0.018 – 0.029)	(-0.018 – 0.024)	(-0.018 – 0.016)	(-0.025 – 0.019)
Unassigned at 2.85 ppm	0.000	-0.001	0.000	0.000	0.001	0.000
	(-0.002 – 0.002)	(-0.002 – 0.001)	(-0.002 – 0.003)	(-0.002 – 0.002)	(-0.003 – 0.002)	(-0.002 – 0.002)
3-Hydroxyisovalerate	-0.001	0.000	-0.002	-0.004	**-0.005**	-0.005
	(-0.005 – 0.004)	(0.000 - 0.000)	(-0.008 – 0.004)	(-0.009 – 0.001)	**(-0.009 – -0.001)**	(-0.010 – 0.001)
3-Hydroxyisobutyrate	-0.002	-0.002	-0.002	-0.001	**-0.007**	**-0.009**
	(-0.005 – 0.001)	(-0.005 – 0.002)	(-0.006 – 0.002)	(-0.005 – 0.003)	**(-0.013 – -0.001)**	**(-0.017 – -0.001)**
N-Acetylglutamine	0.000	0.002	0.001	-0.007	0.000	**0.020**
	(-0.015 – 0.015)	(-0.014 – 0.017)	(-0.022 – 0.023)	(-0.029 – 0.013)	(-0.001 – 0.000)	**(0.002 – 0.038)**
Unassigned at 1.99 ppm	-0.001	-0.001	0.003	0.003	0.001	**0.006**
	(-0.004 – 0.002)	(-0.004 – 0.003)	(-0.002 – 0.008)	(-0.001 – 0.000)	(-0.002 – 0.005)	**(0.001 – 0.010)**

Data are presented as coefficients (coef.) of the relationship between exposure and Δ in metabolite concentration (post-pre) with 95% confidence intervals (CI) (expressed as the range between lower and upper values). All coefficients are adjusted for urinary ibuprofen and paracetamol markers, room temperature and humidity. Total PNC refers to particles smaller than 2.5μm in diameter, with a lower limit of 4nm, as measured by a condensation particle counter and SMPS. Numbers in **bold** represent significant relationships ($p \leq 0.05$).

Table 3. Single pollutant models for associations between Δ urinary metabolites and UFP from airport-related sources

Metabolite	**Total aviation PNC** (5-95p= 73485 # / cm^3)	**Airport traffic PNC** (5-95p= 5077 # / cm^3)	**Non-airport traffic PNC** (5-95p= 15290 # / cm^3)
	Coef. (95% CI)	**Coef. (95% CI)**	**Coef. (95% CI)**
Taurine	**-0.263 (-0.503 – -0.023)**	0.035 (-0.271 – 0.342)	-0.029 (-0.269 – 0.211)
Dimethylamine	**-0.021 (-0.037 – -0.005)**	0.010 (-0.011 – 0.030)	-0.002 (-0.018 – 0.014)
Pyroglutamate	**-0.005 (-0.010 – < 0.000)**	-0.003 (-0.009 – 0.004)	0.003 (-0.002 – 0.008)
3-aminoisobutyrate	0.002 (-0.006 – 0.010)	**-0.010 (-0.019 – -0.001)**	**0.010 (0.002 – 0.017)**
Methylguanidine	-0.001 (-0.001 – < 0.000)	**0.001 (> 0.000 – 0.002)**	-0.001 (-0.001 – 0.000)
Isocitrate	0.001 (-0.001 – 0.003)	0.002 (< 0.000 – 0.004)	**-0.003 (-0.005 – -0.001)**
Carnosine/arginine	0.002 (-0.002 – 0.006)	0.001 (-0.004 – 0.006)	**0.005 (0.001 – 0.008)**
Ethanolamine/ isethionate	0.002 (-0.003 – 0.007)	0.002 (-0.004 – 0.008)	**0.005 (0.001 – 0.010)**

Data are presented as coefficients (coef.) of the relationship between exposure and Δ in metabolite concentration (post-pre) with 95% confidence intervals (CI). All coefficients are adjusted for urinary ibuprofen and paracetamol markers, room temperature and humidity. Numbers in **bold** represent significant relationships ($p \leq 0.05$).

Table 4. Two pollutant models for associations between Δ urinary metabolites and UFP from key sources, accounting for co-exposures to UFP from the remaining key sources

PNC source of interest:	**Total aviation** (5-95p= 73485 # / cm^3)		**Airport traffic** (5-95p= 5077 # / cm^3)		**Non-airport traffic** (5-95p= 15290 # / cm^3)	
Co-exposing PNC source accounted for :	**Airport traffic**	**Non-airport traffic**	**Total aviation**	**Non-airport traffic**	**Total aviation**	**Airport traffic**
Metabolite	**Coef. (95% CI)**	**Coef. (95% CI)**	**Coef. (95% CI)**	**Coef. (95% CI)**	**Coef. (95% CI)**	**Coef. (95% CI)**
Taurine	**-0.262**	**-0.270**	0.021	0.026	0.023	-0.027
	(-0.502 – -0.022)	**(-0.516 – -0.024)**	(-0.276 – 0.319)	(-0.291 – 0.343)	(-0.195 – 0.241)	(- 0.253 – 0.198)
Dimethylamine	**-0.021**	**-0.022**	0.008	0.008	0.001	-0.002
	(-0.037 – -0.005)	**(-0.038 – -0.006)**	(-0.012 – 0.028)	(-0.012 – 0.030)	(-0.014 – 0.015)	(-0.017 – 0.013)
Pyroglutamate	**-0.005**	**-0.006**	-0.003	-0.002	0.004	0.003
	(-0.010 – < 0.000)	**(-0.011 – -0.001)**	(-0.009 – 0.003)	(-0.008 – 0.004)	(<0.000 – 0.009)	(-0.002 – 0.007)
3-Aminoisobutyrate	0.002	0.000	**-0.015**	**-0.015**	**0.010**	**0.009**
	(-0.006 – 0.009)	(-0.008 – 0.004)	**(-0.030 – -0.001)**	**(-0.030 – <-0.000)**	**(0.004 – -0.017)**	**(0.003 – 0.016)**
Methylguanidine	-0.001	0.003	**0.001**	0.001	<0.000	<0.000
	(-0.001 – >0.000)	(-0.008 – 0.014)	**(>0.000 – 0.002)**	(<0.000 – 0.002)	(-0.001 – >0.000)	(-0.012 – >0.000)
Isocitrate	0.001	0.002	0.002	0.001	**-0.003**	**-0.003**
	(-0.001 – 0.003)	(0.000 – 0.004)	(<0.000 – 0.004)	(-0.001 – 0.003)	**(-0.005 – -0.002)**	**(-0.004 – -0.001)**
Carnosine/arginine	0.002	0.001	0.001	0.002	**0.004**	**0.004**
	(-0.002 – 0.006)	(-0.003 – 0.005)	(-0.004 – 0.006)	(-0.003 – 0.007)	**(>0.000 – 0.008)**	**(>0.000 – 0.009)**
Ethanolamine/ isethionate	0.002	0.001	0.002	0.004	**0.004**	**0.005**
	(-0.003 – 0.007)	(-0.004 – 0.006)	(-0.004 – 0.008	(-0.003 – 0.010)	**(>0.000 – 0.008)**	**(>0.000 – 0.009)**

Data are presented as coefficients (coef.) of the relationship between exposure to key PNC sources and Δ in metabolite concentration (post-pre) following adjustment of the model for co-exposure to the remaining two key sources of PNC at the airport. Data are presented with 95% confidence intervals (CI). All coefficients are adjusted for urinary ibuprofen and paracetamol markers, room temperature and humidity. Numbers in **bold** represent significant relationships ($p \leq 0.05$).

Landing and take-off- related UFP both contribute to changes in the urinary metabolome

Using the PMF source apportionment model, it was possible to explore relationships between urinary metabolomic changes and individual aircraft behaviours. Single pollutant models demonstrated that total PNCs for UFPs produced during take- off (5-95p = 56,130 particles/ cm^3) and landing (5-95p = 31,200 particles/cm^3) could be associated with the significant changes in urinary dimethylamine concentration (-0.019 AU, 95% CI: -0.037- -0.001 for take-off and -0.031 AU, 95% CI: -0.012 - -0.001 for landing). Compared to the relationship with total aviation PNC, reductions in urinary taurine concentrations were larger when associated with landing PNC specifically (-0.413 AU, 95% CI: -0.689 – -0.136). While not statistically significant, due to variation in response levels, reductions in urinary taurine concentration were also present overall, following association with take-off PNC (-0.224 AU, 95% CI -0.495 – 0.047). Similarly, reductions in urinary pyroglutamate associated significantly with take-off PNC (-0.006 AU, 95% CI: -0.012 – -0.001) but their association with landing PNC displayed too much variability to be considered statistically significant (-0.004 AU, 95% CI: -0.001 – 0.003) (Table 5). These associations remained robust following adjustment of the models for co-exposure to airport or non-airport traffic UFP (Table S4).

Table 5. Single pollutant models for associations between Δ urinary metabolites and PNC produced through take-off and landing

Metabolite	**Take-off PNC** (5-95p= 56130 # / cm^3)	**Landing PNC** (5-95p = 31200 # / cm^3)
	Coef. (95% CI)	**Coef. (95% CI)**
Taurine	-0.224 (-0.495 – 0.047)	**-0.413 (-0.689 – -0.136)**
Dimethylamine	**-0.019 (-0.037 – -0.001)**	**-0.031 (-0.049 – -0.013)**
Pyroglutamate	**-0.006 (-0.012 – -0.001)**	-0.004 (-0.010 – 0.002)

Data are presented as coefficients (coef.) of the relationship between exposure and Δ in metabolite concentration (post-pre) with 95% confidence intervals (CI). All coefficients are adjusted for urinary ibuprofen and paracetamol markers, room temperature and humidity. Numbers in **bold** represent significant relationships ($p \leq 0.05$).

Features of the metabolomic response to aviation UFP exposure may contribute to common biological processes.

In order to assign mechanistic meaning to metabolomic change, it is necessary to explore relationships between feature metabolites. With the three metabolites that associate with aviation UFP exposure, there was not sufficient input data

to perform an appropriately powered pathway analysis. As such, Pearson's correlation analyses were performed to identify metabolites that could contribute to or be products of common biological processes. This method identified a strong, positive correlation ($r = 0.88$, $p \leq 0.001$) between Δ dimethylamine and Δ taurine concentrations in post- and pre-exposure samples (Figure 4). No strong nor significant correlations were found between Δ in taurine and Δ pyroglutamate concentration ($r = 0.02$) or between Δ dimethylamine and Δ pyroglutamate concentration ($r = 0.02$) (data not shown).

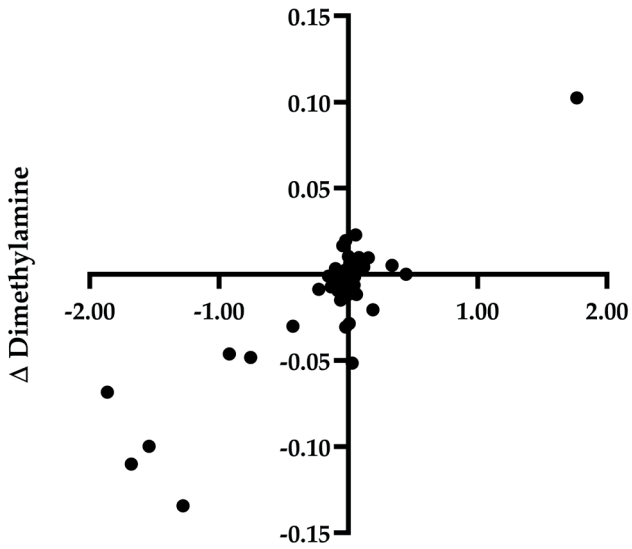

Figure 4. Pearson correlations between Δ feature urinary metabolite concentrations after total aviation emissions exposure. R and significant p values are displayed for all key metabolite pairings (A) alongside a scatterplot of individual data points for dimethylamine and taurine (B). Analysis was performed using post- exposure minus pre- exposure values. *** p = < 0.001.

Discussion

Combining our cross-over intervention study of 21 healthy young adults with source apportionment modelling, we identified acute changes to the urinary metabolome that associate with exposure to UFP from distinct emission sources at Amsterdam Airport Schiphol. Metabolic signatures associating with aviation emissions dominated the response to total PNC and were characterised by

significant reductions in urinary taurine, dimethylamine and pyroglutamate concentrations, consistent with increased utilisation or decreased synthesis of these metabolites.

Previously, exposure to airport UFPs has been associated with pulmonary and systemic inflammation [23], [24], oxidative stress [37] and reductions in cardiopulmonary function [25]. To our knowledge, this study is the first to assess responses to airport emissions at a global, biochemical level. Consistent with observations that airport UFPs have oxidative potential and induce reactive oxygen species (ROS) synthesis *in vitro* [37], several of the metabolites that associated with exposure to aviation UFPs in this study have been related to antioxidant responses to the imposition of oxidative stress.

The most pronounced of these changes was the reduction in urinary taurine which associated with UFP produced during aircraft landing and possibly take-off. The β-amino acid taurine, which is abundant in the cytosol of inflammatory and metabolically active cells, has been proposed to act as an indirect antioxidant via enhancement of classical antioxidant concentrations [38] and modulation of mitochondrial ROS generation [39]. It also acts as an anti-inflammatory agent through its capacity to react with neutrophil-derived hypochlorous acid (HOCl) to form taurine chloramine [40]. When taken up into cells at sites of inflammation, taurine chloramine promotes a broad spectrum xenobiotic and antioxidant response through activation of the Nuclear factor erythroid 2-related factor 2, (Nrf2) transcription factor [40].

Decreased taurine concentrations have been measured in the BALF of rats following ZnO inhalation, reflecting enhanced antioxidant activity within the pulmonary tissue. Supporting the suggestion that landing UFPs also triggered this protective response, taurine has been shown to alleviate oxidative stress, pro-inflammatory cytokine secretion, inflammatory cell recruitment, mitochondrial dysregulation, autophagy and emphysema in mouse lung following exposure to DEP or 1-nitropyrene [41], [42]. It is difficult to hypothesise why the observed change in taurine concentration associated more robustly with landing UFP. To date, no considerable differences have been reported in the composition of emissions produced during take-off and landing [43]. Although landing particles did account for the majority of UFP < 20 nm at our sampling site [5], their concentrations were strongly correlated with those of take-off particles ($r=0.76$), creating the possibility that the observed differences in effect size and significance were artefacts of collinearity within the model. While individuals

are unlikely to only be exposed to landing UFP at an airport, confirming this observation and understanding its cause, could have bearing on future aviation engineering.

Exposure to both landing and take-off related UFPs induced reductions in urinary pyroglutamate. Pyroglutamate is produced in the γ-glutamyl cycle as a precursor to glutathione (GSH) [44]. A decrease in urinary pyroglutamate is therefore consistent with increased cellular GSH synthesis as an adaptive response to the imposition of oxidative stress. This aligns with a potential role for taurine chloramine in promoting GSH synthesis through Nrf2-mediated up-regulation of glutathione synthase expression [45] (Illustrated in Figure 5). This hypothesis does require experimental confirmation, but in the context of the previous literature demonstrating the capacity for UFP to initially deplete antioxidants [29] and subsequently induce protective, adaptive responses [46], the observed relationships do illustrate the utility of metabolomics in generating novel, testable hypotheses to explore causal links between pollutants and adverse responses. It is important to note however, that our results reflect only responses to short term exposures in healthy individuals and there remains a need to understand the impact of recurrent or longer exposures in relation to chronic disease development and exacerbation [47].

As well as pyroglutamate, UFPs produced during take-off and landing were also associated with reductions in urinary dimethylamine. In humans, dimethylamine is produced endogenously by the enzyme dimethylarginine dimethylaminohydrolase (DDAH) during hydrolysis of asymmetric dimethylarginine (ADMA) [48] and through microbial catabolism of dietary choline [49]. In health, dimethylamine is excreted via the urine in the upper μM range [48], with a small fraction converted to dimethylnitrosamine (DMNA). Reduced urinary dimethylamine concentrations may therefore reflect enhanced DMNA synthesis or reduced DDAH activity. As DMNA exerts genotoxicity in mammalian cell lines and rodents and is hypothesised to act similarly in humans [50], [51], this warrants further investigation.

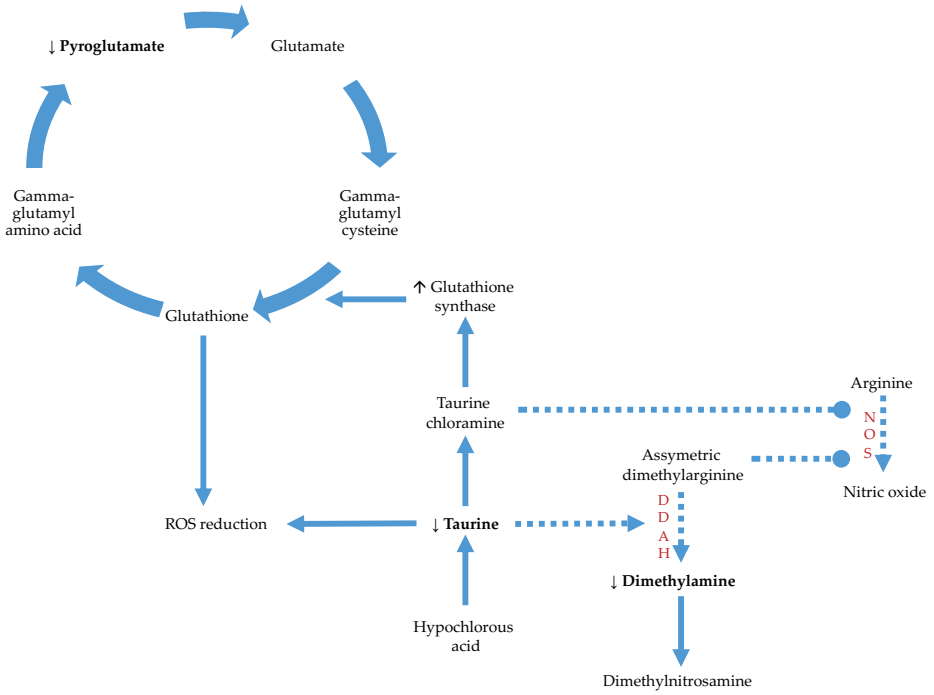

Figure 5. Hypothesised interplay of altered pathway activity following exposure to aviation UFPs. Reductions in urinary pyroglutamate reflect increased demand for glutathione synthesis which is contributed to by conversion of taurine to taurine chloramine with downstream, Nrf2-mediated induction of glutathione synthase expression. Taurine availability also diminishes due to the role of taurine as an inhibitor of ROS generation, leading to decreased DDAH agonism and dimethylamine synthesis. Resultant accumulations of ADMA, combined with increased availability of taurine chloramine inhibit NOS activity, resulting in reduced nitric oxide synthesis. Increased conversion of dimethylamine to nitrosdimethylamine may also contribute to reductions in dimethylamine concentration. Dotted and solid arrows represent reduction and enhancement of reactions (respectively). Dimethylarginine dimethylaminohydrolase (DDAH), nitric oxide synthase (NOS).

As ADMA is an inhibitor of nitric oxide (NO) synthases (NOS), reduced conversion to dimethylamine could also result in decreased NO synthesis. Supporting this hypothesis, increased ADMA and NO precursors have been measured in the plasma of individuals exposed to highway UFPs [29] and reduced NO synthesis has been observed in human aortic endothelial cells following exposure to urban UFPs [52]. As well as impacting vascular tone, airway responsiveness and inflammatory cell function, reduced NO availability results in QT interval prolongation and reduced lung function [23], [24]. While cardiopulmonary function was not measured at the same time as urine sampling

for this study, reductions in FVC and QT interval prolongation did associate with aviation UFP exposure in our cohort 4h post-exposure [25]. Strong positive associations (r=0.88) were observed between the reductions in dimethylamine concentrations and reductions in taurine concentrations, suggesting some degree of interaction between the implicated metabolic pathways (Figure 5). As DDAH is agonised by taurine [55], [56] one explanation could be that the particle-induced decrease in taurine availability led to reduced DDAH activity via less agonism (Figure 5). Like ADMA, taurine chloramine inhibits NOS activity during inflammation [40], [57], supporting the plausibility of interactions between the two pathways following UFP exposure (Figure 5).

Ibuprofen and acetaminophen metabolites were present in approximately 50% of spectra, making correction for their use, a necessity for our model. Like airport UFPs, these metabolites associated with changed urinary concentrations of dimethylamine, pyroglutamate, 3-aminoisobutyrate and mitochondrial metabolism markers, indicating their potential to mask our responses of interest. While many studies prohibit use of analgesics, this was not feasible for our six-month study period. As a result of correcting for their use post-exposure, we add to our outcomes, a preliminary characterisation of how therapeutic doses of ibuprofen and acetaminophen impact the human urinary metabolome. Until now, study of the impacts that these pharmaceuticals have on the human metabolome has been limited to the contexts of overdose and hepatotoxicity [30]–[34].

It must be noted that the participants of this study were predominantly female (81%) and were all young individuals with 'healthy' BMI and cardiopulmonary function who live in areas without high levels of traffic pollution. As such, we cannot presume that the hypothesised mechanisms of aviation UFP toxicity reflect the responses of individuals who do not fit these criteria. As examples, metabolomic responses to traffic-related PM exposure are shown to be influenced by asthmatic status (arginine-related pathways) [58] and by sex and obesity (non-esterified fatty acid metabolism) [59]. It is therefore important that the hypothesised impacts of aviation UFP on the urinary metabolome are validated in larger, more diverse cohorts, especially those that are inclusive of established vulnerable groups.

Conclusions

In this study, we have for the first time, demonstrated a clear distinction between the urinary metabolomic signatures that accompany exposure to aviation UFPs and those that associate with other UFP sources at a major airport. From the metabolic features identified, the direction of their relationship with the exposure estimates and preexisting knowledge base on UFP toxicity, we have elaborated a series of potential testable hypotheses based on the (A) increased utilisation of taurine and induction of an adaptive antioxidant response, including increased synthesis of GSH and (B) modulation of nitric oxide production via enhanced dimethylarginine dimethylaminohydrolase activity.

There remain outstanding questions as to whether the hypothesised responses are informative to an understanding of longer-term or repeat exposures, especially within established vulnerable groups. Considering however, that these responses are consistent with effects induced by road-side levels of traffic particulates [28], [29], [60], which have established links with adverse health [15], [61]–[64], and that airport particulates have been found to induce similar acute phase, inflammatory and genotoxic responses to DEP in mice [23], we believe that the hypotheses merit further exploration. Additionally, our findings, just as previous studies of UFP exposure, emphasise the importance of UFP monitoring networks for a comprehensive examination of long-term UFP exposures and adverse health outcomes, especially in near-source environments such as major airports, to determine threshold levels and support UFP regulations [65].

References

[1] R. Lee, David; Fahey, David; Forster, Piers; Newton, Peter; Wit, Ron; Lim, Liam; Owen, Bethan; Sausen, "Aviation and global climate change in the 21st century | Elsevier Enhanced Reader," *Atmos. Environ.*, vol. 43, no. 2009, pp. 3520–3537, 2009.

[2] International Air Transport Association, "Industry Statistics Fact Sheet," 2020.

[3] X. Yang, S. Cheng, J. Lang, R. Xu, and Z. Lv, "Characterization of aircraft emissions and air quality impacts of an international airport," *J. Environ. Sci. (China)*, vol. 72, pp. 198–207, Oct. 2018.

[4] M. Winther, U. Kousgaard, T. Ellermann, A. Massling, J. K. Nøjgaard, and M. Ketzel, "Emissions of NOx, particle mass and particle numbers from aircraft main engines, APU's and handling equipment at Copenhagen Airport," *Atmos. Environ.*, vol. 100, pp. 218–229, Jan. 2015.

[5] M. Pirhadi, A. Mousavi, M. H. Sowlat, N. A. H. Janssen, F. R. Cassee, and C. Sioutas, "Relative contributions of a major international airport activities and other urban sources to the particle number concentrations (PNCs) at a nearby monitoring site," *Environ. Pollut.*, 2020.

[6] I. Simonetti, S. Maltagliati, and G. Manfrida, "Air quality impact of a middle size airport within an urban context through EDMS simulation," *Transp. Res. Part D Transp. Environ.*, vol. 40, pp. 144–154, Oct. 2015.

[7] M. P. Keuken, M. Moerman, P. Zandveld, J. S. Henzing, and G. Hoek, "Total and size-resolved particle number and black carbon concentrations in urban areas near Schiphol airport (the Netherlands)," *Atmos. Environ.*, vol. 104, pp. 132–142, 2015.

[8] N. Hudda, T. Gould, K. Hartin, T. V. Larson, and S. A. Fruin, "Emissions from an international airport increase particle number concentrations 4-fold at 10 km downwind," *Environ. Sci. Technol.*, vol. 48, no. 12, pp. 6628–6635, 2014.

[9] I. Rivas *et al.*, "Source apportionment of particle number size distribution in urban background and traffic stations in four European cities," *Environ. Int.*, vol. 135, p. 105345, Feb. 2020.

[10] N. Hudda, M. C. Simon, W. Zamore, and J. L. Durant, "Aviation-Related Impacts on Ultrafine Particle Number Concentrations Outside and Inside Residences near an Airport," *Environ. Sci. Technol.*, 2018.

[11] M. Park *et al.*, "Differential toxicities of fine particulate matters from various sources," *Sci. Rep.*, vol. 8, no. 1, pp. 1–11, Dec. 2018.

[12] M. E. Gerlofs-Nijland *et al.*, "Inhalation toxicity profiles of particulate matter: a comparison between brake wear with other sources of emission," *Inhal. Toxicol.*, pp. 1–10, May 2019.

[13] M. E. Gerlofs-Nijland *et al.*, "Toxicity of coarse and fine particulate matter from sites with contrasting traffic profiles.," *Inhal. Toxicol.*, vol. 19, no. 13, pp. 1055–69, Oct. 2007.

[14] K. H. Kim, E. Kabir, and S. Kabir, "A review on the human health impact of airborne particulate matter," *Environment International*. 2015.

[15] R. K. Khan and M. A. Strand, "Road dust and its effect on human health: a literature review," *Epidemiology and health*, vol. 40. Korean Society of Epidemiology, p. e2018013, 2018.

[16] H. S. Kwon, M. H. Ryu, and C. Carlsten, "Ultrafine particles: unique physicochemical properties relevant to health and disease," *Experimental and Molecular Medicine*, vol. 52, no. 3. Springer Nature, pp. 318–328, Mar-2020.

[17] M. Geiser *et al.*, "Ultrafine particles cross cellular membranes by nonphagocytic mechanisms in lungs and in cultured cells," *Environ. Health Perspect.*, vol. 113, no. 11, pp. 1555–1560, Nov. 2005.

[18] M. Lundborg *et al.*, "Aggregates of ultrafine particles impair phagocytosis of microorganisms by human alveolar macrophages," *Environ. Res.*, vol. 100, no. 2, pp. 197–204, Feb. 2006.

[19] N. Li *et al.*, "Ultrafine particulate pollutants induce oxidative stress and mitochondrial damage," *Environ. Health Perspect.*, 2003.

[20] W. G. Kreyling *et al.*, "TRANSLOCATION OF ULTRAFINE INSOLUBLE IRIDIUM PARTICLES FROM LUNG EPITHELIUM TO EXTRAPULMONARY ORGANS IS SIZE DEPENDENT BUT VERY LOW," *J. Toxicol. Environ. Heal. Part A*, vol. 65, no. 20, pp. 1513–1530, Oct. 2002.

[21] G. Oberdörster *et al.*, "Translocation of Inhaled Ultrafine Particles to the Brain," *Inhal. Toxicol.*, vol. 16, no. 6–7, pp. 437–445, Jan. 2004.

[22] J. S. Brown, K. L. Zeman, and W. D. Bennett, "Ultrafine particle deposition and clearance in the healthy and obstructed lung," *Am. J. Respir. Crit. Care Med.*, vol. 166, no. 9, pp. 1240–1247, Nov. 2002.

[23] K. M. Bendtsen *et al.*, "Airport emission particles: Exposure characterization and toxicity following intratracheal instillation in mice," *Part. Fibre Toxicol.*, 2019.

[24] R. Habre *et al.*, "Short-term effects of airport-associated ultrafine particle exposure on lung function and inflammation in adults with asthma," *Environ. Int.*, vol. 118, pp. 48–59, Sep. 2018.

[25] A. Lammers *et al.*, "Effects of short-term exposures to ultrafine particles near an airport in healthy subjects," *Environ. Int.*, vol. 141, Aug. 2020.

[26] H. Merzenich, N. Riccetti, B. Hoffmann, M. Blettner, F. Forastiere, and E. Gianicolo, "Air pollution and airport apron workers: A neglected occupational setting in epidemiological research," *International Journal of Hygiene and Environmental Health*, vol. 231. Elsevier GmbH, p. 113649, Jan-2021.

[27] K. M. Bendtsen, E. Bengtsen, A. T. Saber, and U. Vogel, "A review of health effects associated with exposure to jet engine emissions in and around airports," *Environmental Health: A Global Access Science Source*, vol. 20, no. 1. BioMed Central Ltd, Dec-2021.

[28] S. Oeder *et al.*, "Particulate Matter from Both Heavy Fuel Oil and Diesel Fuel Shipping Emissions Show Strong Biological Effects on Human Lung Cells at Realistic and Comparable In Vitro Exposure Conditions," *PLoS One*, vol. 10, no. 6, pp. e0126536-, Jun. 2015.

[29] D. I. Walker *et al.*, "Metabolomic assessment of exposure to near-highway ultrafine particles," *J. Expo. Sci. Environ. Epidemiol.*, vol. 29, no. 4, pp. 469–483, Jun. 2019.

[30] I. Surowiec *et al.*, "Multi-platform metabolomics assays for human lung lavage fluids in an air pollution exposure study," *Anal. Bioanal. Chem.*, vol. 408, no. 17, pp. 4751–4764, Jul. 2016.

[31] J. B. Brower, M. Doyle-Eisele, B. Moeller, S. Stirdivant, J. D. McDonald, and M. J. Campen, "Metabolomic changes in murine serum following inhalation exposure to gasoline and diesel engine emissions," *Inhal. Toxicol.*, vol. 28, no. 5, pp. 241–250, Apr. 2016.

[32] L. Selley, D. H. Phillips, and I. Mudway, "The potential of omics approaches to elucidate mechanisms of biodiesel-induced pulmonary toxicity," *Part. Fibre Toxicol.*, vol. 16, no. 1, 2019.

[33] S. Bouatra *et al.*, "The Human Urine Metabolome," *PLoS One*, 2013.

[34] A. Le Guennec, F. Tayyari, and A. S. Edison, "Alternatives to Nuclear Overhauser Enhancement Spectroscopy Presat and Carr-Purcell-Meiboom-Gill Presat for NMR-Based Metabolomics," *Analytical Chemistry*, vol. 89, no. 17. American Chemical Society, pp. 8582–8588, Sep-2017.

[35] "Human Metabolome Database." .

[36] H. Akoglu, "User's guide to correlation coefficients," *Turkish Journal of Emergency Medicine*, vol. 18, no. 3. Emergency Medicine Association of Turkey, pp. 91–93, Sep-2018.

[37] R. W. He, F. Shirmohammadi, M. E. Gerlofs-Nijland, C. Sioutas, and F. R. Cassee, "Pro-inflammatory responses to PM 0.25 from airport and urban traffic emissions," *Sci. Total Environ.*, 2018.

[38] H. Tabassum, H. Rehman, B. D. Banerjee, S. Raisuddin, and S. Parvez, "Attenuation of tamoxifen-induced hepatotoxicity by taurine in mice," *Clin. Chim. Acta*, vol. 370, no. 1–2, pp. 129–136, Aug. 2006.

[39] C. Ju, J. • Junichi, • A., and S. Schaffer, "Mechanism underlying the antioxidant activity of taurine: prevention of mitochondrial oxidant production."

[40] C. Kim and Y. N. Cha, "Taurine chloramine produced from taurine under inflammation provides anti-inflammatory and cytoprotective effects," *Amino Acids*, vol. 46, no. 1. Springer, pp. 89–100, Jan-2014.

[41] J. Kim, C. Cory, J. C. Bouchard, D. R. Beal, L. Vaickus, and D. G. Remick, "Taurine Treatment Reduces Oxidative Stress and Pulmonary Inflammation by Taurine a Murine Asthma Model Asthma Induced by House Dust and Diesel Particulate Matter," *FASEB J.*, vol. 25, pp. 613.5-613.5.

[42] X. Li *et al.*, "Taurine ameliorates particulate matter-induced emphysema by switching on mitochondrial NADH dehydrogenase genes."

[43] F. Shirmohammadi, M. H. Sowlat, S. Hasheminassab, A. Saffari, G. Ban-Weiss, and C. Sioutas, "Emission rates of particle number, mass and black carbon by the Los Angeles International Airport (LAX) and its impact on air quality in Los Angeles," *Atmos. Environ.*, vol. 151, pp. 82–93, Feb. 2017.

[44] R. S. Lord and J. A. Bralley, "Clinical Applications of Urinary Organic Acids. Part 1: Detoxification Markers," 2008.

[45] M. L. Steele, S. Fuller, M. Patel, C. Kersaitis, L. Ooi, and G. Münch, "Effect of Nrf2 activators on release of glutathione, cysteinylglycine and homocysteine by human U373 astroglial cells," *Redox Biol.*, vol. 1, no. 1, pp. 441–445, 2013.

[46] N. Li *et al.*, "Nrf2 is a key transcription factor that regulates antioxidant defense in macrophages and epithelial cells: protecting against the proinflammatory and oxidizing effects of diesel exhaust chemicals.," *J. Immunol.*, vol. 173, no. 5, pp. 3467–81, Sep. 2004.

[47] G. S. Downward *et al.*, "Long-Term Exposure to Ultrafine Particles and Incidence of Cardiovascular and Cerebrovascular Disease in a Prospective Study of a Dutch Cohort," *Environ. Health Perspect.*, vol. 126, no. 12, p. 127007, Dec. 2018.

[48] D. Tsikas, "Urinary Dimethylamine (DMA) and Its Precursor Asymmetric Dimethylarginine (ADMA) in Clinical Medicine, in the Context of Nitric Oxide (NO) and Beyond," *J. Clin. Med.*, vol. 9, no. 6, p. 1843, Jun. 2020.

[49] S. H. Zeisel, K. A. DaCosta, and J. G. Fox, "Endogenous formation of dimethylamine," *Biochem. J.*, vol. 232, no. 2, pp. 403–408, Dec. 1985.

[50] International Agency for Research on Cancer, "IARC Publications Website - Radiation," *Some N-Nitroso Compounds: IARC Monographs on the evaluation of the carcinogenic risk of chemicals to humans, volume 17*, 1978. .

[51] R. G. Liteplo and M. E. Meek, "*N* -NITROSODIMETHYLAMINE: HAZARD CHARACTERIZATION AND EXPOSURE–RESPONSE ANALYSIS," *J. Environ. Sci. Heal. Part C*, vol. 19, no. 1, pp. 281–304, May 2001.

[52] Y. Du *et al.*, "Ambient ultrafine particles reduce endothelial nitric oxide production via S-glutathionylation of eNOS," *Biochem. Biophys. Res. Commun.*, vol. 436, no. 3, pp. 462–466, Jul. 2013.

[53] T. Atabay and M. Uzun, "The correlation between the plasma nitric oxide levels QT/QTc interval in conscious rabbits," *Gen. Physiol. Biophys.*, vol. 28, no. 1, pp. 16–23, Mar. 2009.

[54] M. N. Islam, R. L. Yadav, and P. K. Yadav, "Modulation of lung function by increased nitric oxide production," *J. Clin. Diagnostic Res.*, vol. 11, no. 6, pp. CC09-CC12, Jun. 2017.

[55] O. T. Pasaoglu, N. Turkozkan, M. Ark, B. Polat, M. Agilli, and H. Yaman, "The Effect of Taurine on the Relationship Between NO, ADMA and Homocysteine in Endotoxin-Mediated Inflammation in HUVEC Cultures," *Inflammation*, vol. 37, no. 5, pp. 1439–1443, Oct. 2014.

[56] B. Tan *et al.*, "Taurine protects against low-density lipoprotein-induced endothelial dysfunction by the DDAH/ADMA pathway," *Vascul. Pharmacol.*, vol. 46, no. 5 SPEC. ISS., pp. 338–345, 2007.

[57] M. Barua, Y. Liu, and M. R. Quinn, "Taurine Chloramine Inhibits Inducible Nitric Oxide Synthase and TNF-α Gene Expression in Activated Alveolar Macrophages: Decreased NF-κB Activation and IκB Kinase Activity," *J. Immunol.*, vol. 167, no. 4, pp. 2275–2281, Aug. 2001.

[58] D. Liang *et al.*, "Perturbations of the arginine metabolome following exposures to traffic-related air pollution in a panel of commuters with and without asthma," *Environ. Int.*, vol. 127, pp. 503–513, Jun. 2019.

[59] Z. Chen *et al.*, "Near-roadway air pollution exposure and altered fatty acid oxidation among adolescents and young adults – The interplay with obesity," *Environ. Int.*, vol. 130, p. 104935, Sep. 2019.

[60] H. Törnqvist *et al.*, "Persistent Endothelial Dysfunction in Humans after Diesel Exhaust Inhalation," *Am. J. Respir. Crit. Care Med.*, vol. 176, no. 4, pp. 395–400, Aug. 2007.

[61] R. Sinharay *et al.*, "Respiratory and cardiovascular responses to walking down a traffic-polluted road compared with walking in a traffic-free area in participants aged 60 years and older with chronic lung or heart disease and age-matched healthy controls: a randomised, crossover study," *Lancet*, vol. 391, no. 10118, pp. 339–349, Jan. 2018.

[62] S. D. Adar, D. R. Gold, B. A. Coull, J. Schwartz, P. H. Stone, and H. Suh, "Focused exposures to airborne traffic particles and heart rate variability in the elderly," *Epidemiology*, vol. 18, no. 1, pp. 95–103, 2007.

[63] F. Zhou *et al.*, *Molecular medicine reports.*, vol. 12, no. 2. D.A. Spandidos, 2015.

[64] H. Kan, G. Heiss, K. M. Rose, E. Whitsel, F. Lurmann, and S. J. London, "Traffic exposure and lung function in adults: The Atherosclerosis Risk in Communities study," *Thorax*, vol. 62, no. 10, pp. 873–879, Oct. 2007.

[65] R. W. Baldauf *et al.*, "Ultrafine particle metrics and research considerations: Review of the 2015 UFP workshop," in *International Journal of Environmental Research and Public Health*, 2016, vol. 13, no. 11.

Supplementary material

Table S1. Correlation matrix for all pollutants, particle size ranges and room conditions measured during 5 h exposures

	PNC[a]	PM	BC	NO_2	CO	Total aviation	Take-off	Landing	Total traffic	Airport traffic	Non-airport traffic	Temp	RH
PNC[a]													
PM	-0.12												
BC	0.18	0.45											
NO_2	0.41	0.17	**0.77**										
CO	0.08	0.34	0.60	0.58									
Total aviation	**0.97**	-0.15	0.15	0.37	0.06								
Take-off	**0.95**	-0.09	0.20	0.41	0.05	**0.97**							
Landing	**0.85**	-0.24	0.02	0.23	0.08	**0.89**	**0.76**						
Total traffic	0.34	0.40	0.30	0.19	0.05	0.25	0.33	0.04					
Airport traffic	-0.01	0.09	0.26	0.38	0.26	0.03	0.10	-0.11	0.22				
Non-airport traffic	0.35	0.39	0.24	0.09	-0.02	0.24	0.32	0.07	0.96	-0.04			
Temp	-0.03	0.27	0.08	0.05	-0.05	0.04	0.17	-0.20	0.42	0.42	0.31		
RH	0.04	0.36	0.41	0.29	0.55	0.03	0.08	-0.08	0.09	0.13	0.05	0.29	

Pearson correlations with in **bold** R >0.70; PNC = particle number concentration detected by a condensation particle counter (CPC) with d_{50} = 4 nm; PM = particulate matter; BC = black carbon; NO_2 = nitric oxide; CO = carbon monoxide; Temp = temperature; RH = relative humidity; Total aviation (also subdivided into "take-off" and "landing") and total traffic (also subdivided into "airport traffic" and "road taffic") are different sources of PNC. This table has been partly published previously (Lammers *et al.,* doi.org/10.1016/j.envint.2020.105779).

Table S2. Locations of metabolite peaks within ^{1}H NMR spectra

Peak minimum (ppm)	Peak maximum (ppm)	Metabolite
0.735	0.765	1-hydroxy ibuprofen glucuronide
0.83	0.84	2-hydroxyisovalerate
0.875	0.893	Ibuprofen/ ibuprofen glucuronide
1.035	1.06	Valine
1.06	1.09	Carboxy ibuprofen/ carboxy ibuprofen glucuronide
1.09	1.12	3-hydroxyisobutyrate
1.12	1.13	4-deoxyerythreonic acid
1.134	1.15	Acetaminophen
1.15	1.17	U1
1.27	1.28	3-hydroxyisovalerate
1.32	1.35	Threonine
1.36	1.38	2-hydroxyisobutyrate
1.43	1.44	U2
1.44	1.45	Acetoin
1.46	1.51	Alanine
1.89	1.92	Acetate and phenylacetylglutamine
1.92	1.93	Acetate
1.95	1.97	Isoeugenol
1.98	2	U3
2.02	2.03	U4
2.03	2.05	Pyroglutamate
2.33	2.36	U5
2.43	2.51	Glutamine
2.52	2.57	Citrate
2.6	2.64	3-aminoisobutyrate
2.71	2.74	Dimethylamine
2.78	2.79	2-hydroxyibuprofen
2.795	2.805	2-hydroxyibuprofen glucuronide
2.805	2.815	U6
2.82	2.85	Methylguanidine
2.85	2.86	U7
2.86	2.87	U8
2.88	2.9	U9
2.9	2.91	Trimethylamine
2.91	2.92	U10
2.925	2.94	N,N-dimethylglycine
2.97	2.99	Isocitric acid
2.995	3.01	U11

3.01	3.03	U12
3.044	3.08	Creatine
3.115	3.125	U13
3.125	3.14	U14
3.14	3.17	Ethanolamine and isethionic acid
3.17	3.19	U15
3.19	3.22	N-N-Nitrosodimethylamine
3.22	3.24	Carnitine
3.24	3.25	Carnosine
3.25	3.26	Taurine
3.26	3.29	TMAO
3.29	3.32	U16
3.36	3.366	U17
3.366	3.37	Theophylline
3.38	3.395	U18
3.395	3.405	U19
3.41	3.42	U20
3.45	3.456	U21
3.456	3.464	U22
3.468	3.476	U23
3.476	3.49	U24
3.52	3.526	Caffeine
3.535	3.545	U25
3.545	3.565	U26
3.57	3.58	Glycine
3.58	3.59	U27
3.93	3.945	Creatine phosphate
4.095	4.115	U28
4.16	4.21	N-acetylglutamine
4.215	4.24	U29
4.34	4.355	Tartrate
4.502	4.51	U30
4.51	4.53	Ascorbate
4.53	4.54	U31
4.557	4.57	U32
4.57	4.576	U33
6.28	6.29	U34
6.29	6.3	U35
6.31	6.34	U36
6.34	6.36	U37
6.364	6.38	U38

6.386	6.39	U39
6.39	6.395	U40
6.41	6.419	U41
6.424	6.432	Trans-aconitate
6.425	6.433	Urocanate
6.44	6.46	Chlorogenate
6.473	6.48	U42
6.48	6.494	U43
6.495	6.51	Fumarate
6.52	6.535	U44
6.538	6.544	U45
6.555	6.575	2-furoate
6.58	6.588	U46
6.626	6.69	2-octenoate
6.718	6.728	Homovanillate
6.755	6.78	U47
6.78	6.795	2-hydroxyphenylacetate
6.8557	6.88	P cresol
6.905	6.915	4-aminohippurate
6.915	6.93	3-hydroxymandelate
6.975	6.983	Tyrosine
7.01	7.02	U48
7.05	7.065	U49
7.065	7.08	Histamines
7.27	7.295	U50
7.305	7.335	U51
7.495	7.52	Tryptophan
7.53	7.59	Hippurate
7.67	7.687	U52
7.687	7.72	3-inodoxyl sulfate
8.026	8.034	3-methylxanthine
8.46	8.47	Formate
8.64	8.655	U53
8.67	8.69	U54
8.77	8.8	Pyrimidine
8.798	8.81	Nicotinurate/nicotinamide
8.81	8.87	Trigonelline
8.88	8.91	1-methylnicotinamide

Where multiple peaks were identified for a single metabolite, a representative peak with no/least spectral overlap was selected for inclusion in the analysis. Chemical shifts are displayed in parts per million (ppm) as the range between peak minima and maxima.

Table S3. Two pollutant models exploring the impact of co-exposure to combustion gases on metabolomic responses to airport particle exposure

Metabolite	**Total PNC** (5-95p= 120,280 # / cm^3)	
	Accounting for NO_2 (5-95p = 33.2 $\mu g/cm^3$)	**Accounting for CO** (5-95p = 250 $\mu g/cm^3$)
	Coef. (95% CI)	**Coef. (95% CI)**
Taurine	**-0.300 (-0.569 – -0.031)**	**-0.296 (-0.546 – -0.046)**
Dimethylamine	**-0.027 (-0.044 – -0.009)**	**-0.023 (-0.040 – -0.007)**

Metabolite	**PNC < 20 nm** (5-95p = 51,160 # / cm^3)	
	Accounting for NO_2 (5-95p = 33.2 $\mu g/cm^3$)	**Accounting for CO** (5-95p = 250 $\mu g/cm^3$)
	Coef. (95% CI)	**Coef. (95% CI)**
Taurine	**-0.293 (-0.547 – -0.039)**	**-0.319 (-0.577 – -0.060)**
Dimethylamine	**-0.025 (-0.042 – -0.008)**	**-0.023 (-0.040 – -0.006)**

Data are presented as coefficients (coef.) of the relationship between exposure and Δ in metabolite concentration (post-pre) with 95% confidence intervals (CI) (expressed as the range between lower and upper values). All coefficients are adjusted for urinary ibuprofen and paracetamol markers, room temperature and humidity. Total PNC refers to particles smaller than 2.5μm in diameter, with a lower limit of 4nm, as measured by a condensation particle counter and SMPS. Numbers in **bold** represent significant relationships ($p \leq 0.05$).

Table S4. Two-pollutant models for associations between Δ urinary metabolites and UFP produced through take-off and landing

Metabolite	**Take-off PNC** (5-95p= 56130 # / cm^3)	
	Accounting for airport traffic PNC (5-95p= 5077 # / cm^3)	**Accounting for non-airport traffic PNC** (5-95p= 15290 # / cm^3)
	Coef. (95% CI)	**Coef. (95% CI)**
Taurine	-0.223 (-0.494 - 0.047)	-0.232 (-0.513 - 0.050)
Dimethylamine	**-0.019 (-0.037 - -0.001)**	**-0.020 (-0.038 - -0.001)**
Pyroglutamate	**-0.006 (-0.012 - -0.001)**	**-0.008 (-0.014 - -0.002)**
Isocitrate	0.001 (-0.001 - 0.003)	**0.002 (> 0.000- 0.004)**
2-hydroxyisobutyrate	-0.002 (-0.005 - < 0.000)	**-0.003 (-0.006 - < 0.000)**

Metabolite	**Landing PNC** (5-95p = 31200 # / cm^3)	
	Accounting for airport traffic PNC (5-95p= 5077 # / cm^3)	**Accounting for non-airport traffic PNC** (5-95p= 15290 # / cm^3)
	Coef. (95% CI)	**Coef. (95% CI)**
Taurine	**-0.414 (-0.692 – -0.136)**	**-0.414 (-0.692 – -0.136)**
Dimethylamine	**-0.031 (-0.049 – -0.012)**	**-0.031 (-0.050 – -0.013)**
Pyroglutamate	**-0.002 (-0.004 – < 0.000)**	**-0.002 (-0.004 – < 0.000)**
Isocitrate	0.001 (-0.001 – 0.004)	0.002 (-0.001 – 0.004)
2-hydroxyisobutyrate	-0.001 (-0.004 – 0.002)	-0.001 (-0.004 – 0.002)

Data are presented as coefficients (coef.) of the relationship between exposure and Δ in metabolite concentration (post-pre) with 95% confidence intervals (CI). All coefficients are adjusted for urinary ibuprofen and paracetamol markers, room temperature and humidity. Numbers in **bold** represent significant relationships ($p \leq 0.05$).

5

Part III.

Rhinovirus exposure

Chapter 6.

Increased day-to-day fluctuations in exhaled breath profiles after a rhinovirus challenge in asthma

Lammers A
Brinkman P
Te Nijenhuis LH
De Vries R
Dagelet JWF
Duijvelaar E
Xu B
Abdel-Aziz MI
Vijverberg SJ
Neerincx AH
Frey U
Lutter R
Maitland - van der Zee AH
Sterk PJ
Sinha A

Allergy, 2021, online ahead of print, doi: 10.1111/all.14811

Abstract

Background: Early detection/prediction of flare-ups in asthma, commonly triggered by viruses, would enable timely treatment. Previous studies on exhaled breath analysis by electronic nose (eNose) technology could discriminate between stable and unstable episodes of asthma, using single/few time-points. To investigate its monitoring properties during these episodes, we examined day-to-day fluctuations in exhaled breath profiles, before and after a rhinovirus-16 (RV16) challenge, in healthy and asthmatic adults.

Methods: In this proof-of-concept study, 12 atopic asthmatic and 12 non-atopic healthy adults were prospectively followed thrice weekly, 60 days before, and 30 days after a RV16 challenge. Exhaled breath profiles were detected using an eNose, consisting of 7 different sensors. Per sensor, individual means were calculated using pre-challenge visits. Absolute deviations (|%|) from this baseline were derived for all visits. Within-group comparisons were tested with *Mann-Whitney U* tests and receiver operating characteristic (ROC) analysis. Finally, Spearman's correlations between the total change in eNose deviations and fractional exhaled nitric oxide (FeNO), cold-like symptoms, and pro-inflammatory cytokines were examined.

Results: Both groups had significantly increased eNose fluctuations post-challenge, which in asthma started 1 day post-challenge, before the onset of symptoms. Discrimination between pre- and post-challenge reached an area under the ROC curve of 0.82 (95% CI = 0.65–0.99) in healthy and 0.97 (95% CI = 0.91–1.00) in asthmatic adults. The total change in eNose deviations moderately correlated with IL-8 and TNFα ($\varrho \approx 0.50$–0.60) in asthmatics.

Conclusion: Electronic nose fluctuations rapidly increase after a RV16 challenge, with distinct differences between healthy and asthmatic adults, suggesting that this technology could be useful in monitoring virus-driven unstable episodes in asthma.

Introduction

One of the major burdens in asthma, are episodes of loss of control and exacerbations,[1], [2] characterized by acute flare-ups of respiratory symptoms, such as shortness of breath, cough, wheezing and chest tightness. Commonly, these episodes are triggered by respiratory viral infections [3], especially rhinoviruses [4]–[6], and can potentially lead to emergency visits and hospitalisations, possibly requiring urgent medical interventions [1], [2] and incurring high healthcare expenses.

Unfortunately, episodes of loss of control are hard to detect due to the poor correlation between clinical symptoms and the underlying disease activity [7]. Furthermore, predictors of upcoming exacerbations in an individual patient are currently lacking, except that recent (severe) asthma exacerbations are predictive of future (severe) exacerbations [8], [9]. Moreover, treatment is modestly effective during exacerbations [10], which emphasizes the importance of strategies that limit the development of exacerbations, preferably in the pre-symptomatic phase. Robust biomarkers indicating disease severity and control over time could help predict (the severity of) episodic flare-ups in asthma. A metabolomic approach might be able to sufficiently capture subtle changes in asthma control, possibly before symptoms occur.

Analysis of the exhaled breath's metabolic content (i.e., breathomics) is relatively new and of interest in asthma, because of its non-invasive character and its potential to detect changes of inflammatory profiles in asthmatic patients [11]. Exhaled breath consists of volatile organic compounds (VOCs), which are gaseous organic molecules that originate either from the body itself (endogenous) or from the environment (exogenous). Endogenous VOCs can reflect the metabolic processes occurring in the lungs and beyond [12]. The studies by Brinkman *et al*. [13] and Fens *et al*. [14] showed that exhaled breath could distinguish clinically stable from unstable episodes in asthmatic patients; however, only three time-points (i.e., baseline, loss of control, and recovery) were compared with weeks to months between visits. Moreover, the studies by Robroeks *et al*. [15] and van Vliet *et al*. [16] showed that exacerbations could be predicted based on two-monthly exhaled VOC measurements, using an offline breath analysis technique. Furthermore, our group has previously shown that breath profiles change after an experimental rhinovirus-16 (RV16) infection in healthy and asthmatic adults [17]. However, only single time-point comparisons and group averages were

examined. Now, studies investigating the potential of real-time exhaled breath analysis to monitor and predict such episodes on a day-to-day basis should follow.

It is believed that biological and thereby metabolic processes fluctuate over time to maintain homeokinesis and that external triggers can influence such fluctuations [18]. These metabolic fluctuations may be reflected in exhaled breath metabolites and possibly be of value in detection and prediction of loss of control/exacerbations in asthma. Since most exhaled breath studies are cross-sectional or longitudinal with low temporal resolution, knowledge about the day-to-day fluctuations in exhaled breath profiles, with and without external triggers, in patients and healthy controls, is lacking.

We hypothesized that the day-to-day fluctuations of exhaled breath would change after an external trigger and that this response would differ between healthy controls and asthmatic patients, due to differences in biological processes. Our first objective was to compare the day-to-day fluctuations from personal baselines in exhaled breath profiles between asthmatic and healthy controls, before and after a rhinovirus (RV) challenge. Our second objective was to investigate whether the magnitude of the altered eNose fluctuations was linked to pre-challenge inflammatory markers and was reflected in post-challenge symptoms and inflammation, to identify possible differences in biological processes between and within groups.

Methods

Study design

In this prospective, intervention study, asthmatic patients and healthy controls were followed for 60 days before and 30 days after a RV16 challenge (Figure 1). The study was conducted at the Amsterdam UMC, location AMC (Amsterdam, The Netherlands), from February 2016 till June 2017. Before inclusion, participants were screened and provided informed consent. Prior to the start of the study period, participants went through a run-in phase to familiarize themselves with all the different measurements performed in the study. Exhaled breath analysis was performed 3 times per week using an electronic nose (eNose).

This study, along with the safety of the virus, was approved by the medical ethical committee of the Amsterdam UMC, location AMC (Amsterdam, the Netherlands), and registered at the Netherlands Trial Register (NTR5426).

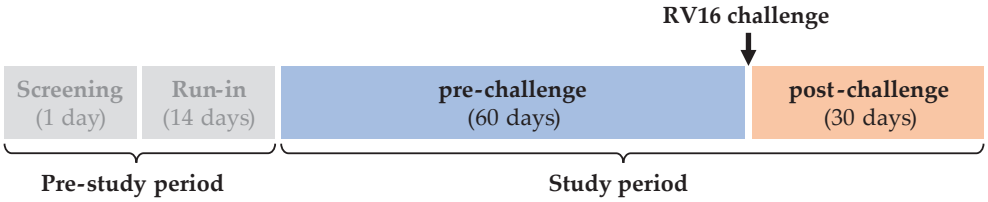

Figure 1. Overview of study design: all participants were screened (1 visit) to test eligibility and had a run-in phase (2 visits) to make participants familiarized with all measurements. During the study period of 90 days, participants had around 2-3 visits per week, with ~20 visits in the pre-challenge phase (60 days) and ~10 visits in the post-challenge phase (30 days).

Study population

In this study, 12 intermittent or mild-to-moderate atopic asthmatics (based on the Global Initiative for Asthma criteria 2014, www.ginasthma.org) and 12 non-atopic healthy controls were included, aged 18–35 years, all non-smokers. Atopy was based on a skin prick test with common aeroallergens (see Supplementary material). Asthmatics had to be clinically stable at inclusion, defined by no use of corticosteroids and no exacerbations, 6 weeks prior to inclusion.

Subjects were excluded when they had a cold (4 weeks prior to screening), a RV16 titer ≥1:8 in serum (at the time of screening and before the RV16 challenge visit), and a positive PCR for any respiratory virus in nasal lavage (at the day before the RV16 challenge) or when they were pregnant. Details about the inclusion and exclusion criteria can be found in the published work by Sinha *et al.* [18]. All participants were recruited via advertisements at the outpatient clinics of various hospitals in Amsterdam and via social media. Furthermore, subjects from previous study cohorts of our hospital were contacted, only when they had provided informed consent to be invited for future research.

Rhinovirus challenge

After the 60-day pre-challenge phase, participants were exposed to RV16 using a standardized and validated challenge approach, as previously described [18], [19]. An experimental RV16 infection was used with a nasal dose of inoculum of 100 TCID50, tissue culture infective dose of the virus required to cause cytopathy in 50% of the cells. This has been considered safe for *in vivo* testing in human volunteers, during a scientific advice meeting at BfArM (Bonn, Germany, April 30, 2013). The RV16 was prepared under good manufacturing practice (GMP), as

part of the U-BIOPRED study, and tested in a dose-dependent manner in healthy individuals and mild asthma patients (manuscript in preparation), which revealed that 100 TCID50 was the lowest dose that effectively infected those exposed and caused expected symptomology.

Exhaled breath analysis

Measurement setup

Real-time exhaled breath analysis was performed using an eNose, the SpiroNose, connected in series with a spirometer (SpiroPerfect™, Welch Allyn) (Figure S1). The SpiroNose consists of seven different cross-reactive metal oxide sensors (Table S1), present in fourfold, twice on the inside and twice on the outside of the device. The mixture of VOCs in exhaled breath is detected by the inner sensors during the exhalation, while ambient VOCs are detected by the outer sensors.

eNose measurement

The eNose measurement was performed as described previously [20]. In short, subjects were asked to rinse their mouth three times thoroughly with water. Subsequently, exhaled breath analysis was performed in duplicate with a 2-min interval. All participants were instructed to perform five tidal breaths, followed by a single inspiratory capacity maneuver up to total lung capacity, a 5-s breath-hold, and slow (<0.4 L/s) maximal expiration toward residual volume, with their nose clipped. A new mouthpiece, bacterial filter, and nose clamp were used for each subject.

Data processing

Processing of the eNose sensor data was performed using MATLAB® as described in De Vries *et al.* [20] and included filtering, detrending, ambient correction, and automated peak detection. The highest sensor peak of each sensor signal was selected as the variable for further analysis. All sensor peaks were normalized to the most stable sensor, sensor 2, to minimize the inter-array differences. Therefore, data from sensor 2 are not included in the fluctuation analysis.

Other outcomes

Home monitoring

During the study, several clinical parameters were monitored at home: spirometry, the Wisconsin Upper Respiratory Symptom Survey (WURSS-21), and Asthma Control Questionnaire (ACQ). Spirometry and the ACQ-6 (six questions, with a score range of 0-6) [21] were monitored daily, in the morning at home, by the volunteers themselves, using a hand-held spirometry device (MicroDiary,

CareFusion). Lung function parameters of interest were the forced vital capacity (FVC), forced expiratory volume in 1 s (FEV_1) and peak expiratory flow (PEF), expressed as percentages of predicted. The WURSS-21 questionnaire (see Supplementary material) monitoring started at the day of challenge.

FeNO

Double fractional exhaled nitric oxide (FeNO) measurements were performed using the NIOX MINO (Aerocrine AB, Sweden) during the study visits (thrice weekly) at the Amsterdam UMC, location AMC (Amsterdam, the Netherlands), according to American Thoracic Society recommendations [22]. We used the average of the two measurements in our analysis.

Nasal lavages

Nasal lavages were collected once weekly pre-challenge and thrice weekly post-challenge during the study visits, as described previously [18]. Standardized washings collected from the nose were used for cytokine analyses by luminex: IFN-γ, IL-1β, IL-6, IL-8, IL-10, IL-13, IL-17A, IL-33, IP-10 and TNF-α (after the cells were removed by centrifugation).

Sample size

This proof-of-concept study had an explorative nature and was based on initial estimates of fluctuating inflammatory biomarkers. Our sample size of 12 individuals per group was based on previous studies by Turner *et al*. [23], [24], in which detection of temporal variability in exhaled VOCs was possible with fewer data points (once weekly, for 6 months). Moreover, our sample size provides adequate power for multi-omics analysis according to the study by Li *et al*. [25].

Statistical analysis

Baseline characteristics and clinical presentation

Baseline characteristics are presented as mean and standard deviation (SD) for normally distributed variables, median and interquartile range (IQR) for skewed data, and n (%) for categorical variables. The distribution of the data was visually examined using histograms and Q–Q (quantile-quantile) plots. Differences between groups were compared using the *Mann-Whitney U* or *Kruskal-Wallis* tests for continuous variables and chi-square test for categorical variables. Lung function, FeNO, WURSS-21 and ACQ scores were summarized by calculating means of the pre- and post-challenge and minima/maxima of the post-challenge at an individual level, followed by medians at group level, to compare baseline (pre-challenge) with the (maximal) response to the RV challenge. For the

WURSS-21 score, data from the day of the RV16 challenge and the first day post-challenge were used for the "pre-challenge" phase, as daily home monitoring started on the day of challenge.

eNose deviations

Fluctuations in the eNose signals were examined for the pre- and post-challenge phase, separately, in both asthmatic and healthy volunteers. For each sensor and subject, means were calculated based on all pre-challenge visits, serving as an individual baseline ($\bar{x}_{baseline}$) (Figure 2A, left graph). Per subject, deviations from this personal baseline were derived for all study visits, expressed as absolute percentages; $|(x - \bar{x}_{baseline})/\bar{x}_{baseline}|$ with $\bar{x}$ being an observation and $\bar{x}$ the sample mean (Figure 2B, right graph). Next, the mean of these absolute deviation percentages was calculated for the pre- ($\bar{x}_{dev,pre}$) and post-challenge ($\bar{x}_{dev,post}$) phase, at individual and group level, consecutively. Within- and between-group comparisons were made using Wilcoxon signed-rank and Mann-Whitney U tests, respectively. Because of multiple testing, False Discovery Rate (FDR) adjusted p-values (q-values) were also calculated [26]. Finally, receiver operating characteristic (ROC) analysis was performed to calculate the discriminative power of the individual sensor fluctuations to distinguish between pre- and post-challenge within and between groups.

Linking change in eNose deviations to inflammatory markers and symptoms

First, we calculated the overall change in eNose fluctuations by summing up all the differences between pre- and post-challenge mean deviation percentages of all sensors (i), at an individual level ($\sum \bar{x}_{i,dev,post} - \bar{x}_{i,dev,pre}$) (Figure 2B, left graph). Next, we explored the link between the magnitude of the change in eNose fluctuations and post-challenge cold-like symptoms (WURSS-21), as well as, pre- and post-challenge inflammatory marker levels (FeNO and cytokines). For this, the FeNO, WURSS-21 and cytokine data were log10-transformed and averaged over the last 10 days pre- ($\bar{x}_{marker,pre}$) and the first 10 days post-challenge ($\bar{x}_{marker,post}$), separately, for each subject (Figure 2B, right graph). Finally, Spearman's rank correlations between the total deviation difference and the mean FeNO, cytokine levels, or WURSS-21 scores, pre- and post-challenge separately, were determined.

Statistics were performed in R (version 3.6.1) combined with R packages "pROC" and "RVAideMemoire". p-values and q-values <0.05 were considered significant.

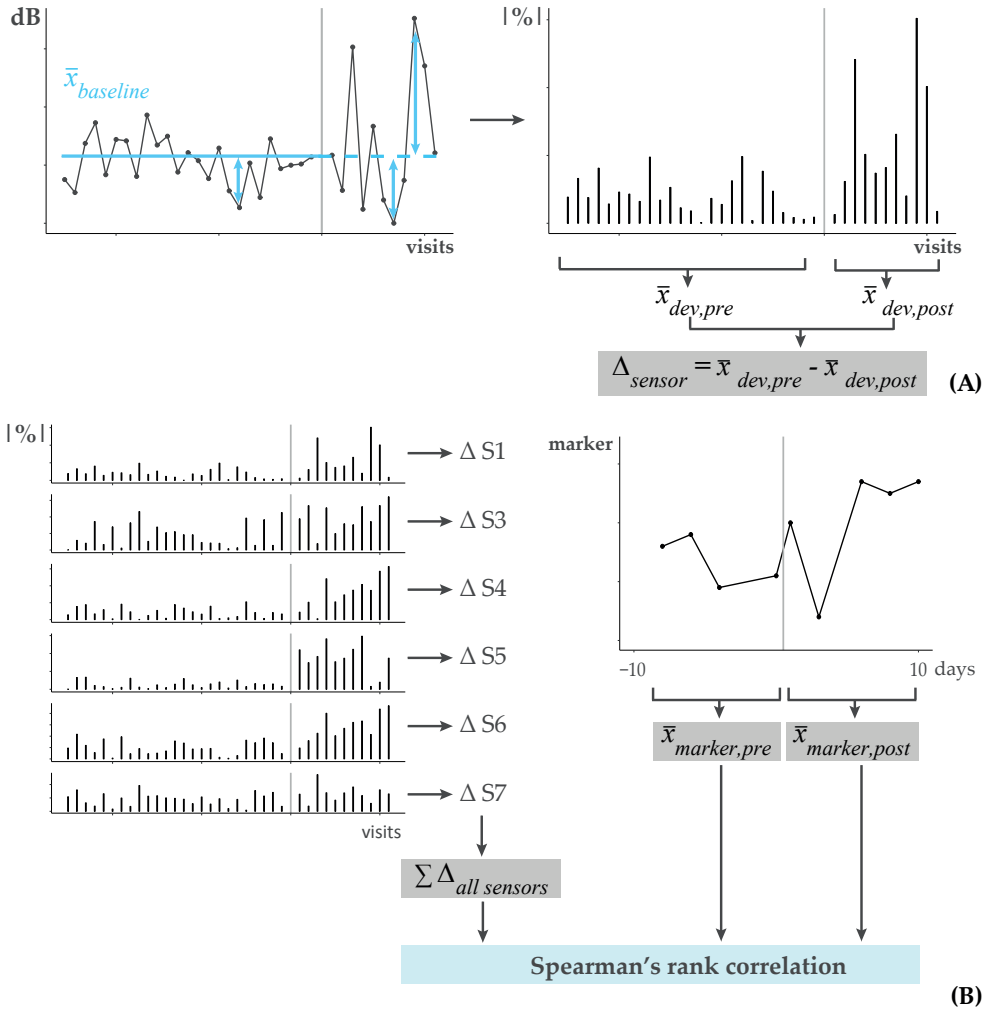

Figure 2. Calculation of eNose deviations. Data from one subject with the vertical gray lines representing the RV challenge. A) The left graph shows the sensor values (dB) of one sensor, for all visits pre- and post-challenge. The mean of the sensor values pre-challenge (blue solid line, $\bar{x}_{baseline}$) served as the baseline, also for the post-challenge phase (blue dashed line). Next, deviations from this personal baseline were calculated (blue double arrows) and expressed as absolute percentages ($|\%|$), as shown on the right. Finally, the average deviation pre- ($\bar{x}_{dev,pre}$) and post-challenge ($\bar{x}_{dev,post}$) was calculated and the difference (Δ_{sensor}) between these, per subject and sensor. B) The left graph shows the deviations from the personal baseline for all sensors (S1, S3-S7), expressed as absolute percentages ($|\%|$). The difference in deviations (Δ_{sensor}) between the pre- and post-challenge phase was calculated for each sensor and summed to determine the total change in deviations ($\sum \Delta_{all\ sensors}$). On the right, data from one of the markers of interest (FeNO, cytokines, and WURSS-21) are shown, from which 10-day averages were calculated for the pre- ($\bar{x}_{marker,pre}$) and post-challenge ($\bar{x}_{marker,post}$) phase (note that 10 days ≠ 10 visits). Finally, Spearman's rank correlations were calculated between the total change in deviation and the pre- and post-averages of the marker of interest, separately.

Results

Study cohort

In total, 24 participants were included in this study; 12 healthy and 12 asthmatic participants (inclusion chart, Figure S2). At baseline, there were no major differences between groups regarding sex, age, ethnicity, body-mass index (BMI), pack years, and lung function (Table 1). Only FeNO was significantly different between groups ($p<0.01$), with a median of 14 ppb (IQR: 12 – 21) in healthy controls and 45 ppb (IQR: 30 – 63) in asthmatics. The number of visits were similar between and within groups, with on average ~23 visits (range 20-29) before and ~11 visits (range 10-16) after the RV16 challenge.

Table 1. Baseline characteristics and the number of visits per group

	Healthy (n=12)	**Asthma (n=12)**
Sex (female)	7 (58%)	8 (67%)
Age (years)	21 (± 1.5)	22.2 (± 2.2)
Ethnicity (Caucasian)	11 (92%)	9 (75%)
BMI (kg/m^2)	22.2 (± 1.6)	22.8 (± 3.1)
Smoking (pack years)	1 (± 0.17)	–
Baseline spirometry		
FEV_1 % of predicted	106 (± 12)	101 (± 10)
FVC % of predicted	104 (± 11)	104 (± 10)
PEF % of predicted	108 (± 14)	105 (± 12)
FeNO (ppb)	14 (12 – 21)*	45 (30 – 63)*
Number of visits (*mean; range*)		
Total	34 (30 – 40)	35 (33 – 38)
Before challenge	23 (20 – 29)	23 (21 – 26)
After challenge	11 (10 – 12)	12 (10 – 16)

Data are presented as mean (±SD), median (IQR), n (%) or else when stated, which have partly been published previously [18]. BMI = body mass index; FEV_1 = forced expiratory volume in 1s; FVC = forced vital capacity; PEF = peak expiratory flow; FeNO = fractional exhaled nitric oxide. Differences in the number of visits were due to personal reasons (i.e., missing visits) or when there was a delay in the RV16 challenge due to logistical reasons (i.e., extra visits). * = significant difference ($p<0.01$)

Clinical presentation (pre- and post-challenge)

Either or a combination of serum antibody tests, along with clinical symptoms and RV Polymerase Chain Reaction (PCR) conducted on nasal lavage samples, confirmed that all the study participants were successfully inoculated with

the RV16, as published previously [18]. During the whole study period, no exacerbations/loss of control, as defined by Reddel *et al.* [1], occurred in the participants. The strongest clinical effect was seen in the WURSS-21 score, which increased after the RV16 challenge in both groups. The maximal WURSS-21 score occurred 3 days post-challenge, with an average score of 35 ±33 in asthmatics and 19 ±9 in healthy participants (Figure S3). Using descriptive statistics, we did not find major changes in lung function, ACQ score, or FeNO (Table S2). However, in-depth analysis on the development of the response to the challenge was carefully studied before using time series analysis, as previously published [18].

eNose deviations

The following comparisons were made regarding the eNose deviations: 1) pre-viral challenge with post-viral challenge states and 2) diseased (asthma) cohort with healthy (control) cohort.

Pre- vs post-challenge

For both groups, the mean deviation of the eNose signals increased after the rhinovirus challenge in the majority of the sensors (Figure 3, Table S3). For healthy subjects, mean deviations increased significantly in sensor 5 ($\Delta = 2\% \pm 2$; $p < 0.05$) and 7 ($\Delta = 8\% \pm 8$; $p < 0.01$) and for asthmatics in sensor 1 ($\Delta = 6\% \pm 7$; $p < 0.05$), 4 ($\Delta = 3\% \pm 4$; $p < 0.05$), 5 ($\Delta = 9\% \pm 7$; $p < 0.001$) and 6 ($\Delta = 3\% \pm 3$; $p < 0.001$) (Figure 3). The change in mean deviations per subject are shown in Figure 4 and S4. The highest area under the ROC curve (AUROCC) for discrimination between pre- and post-challenge was found in sensor 5, for both healthy 0.82 (95% CI: 0.65–0.99) and asthmatic subjects 0.97 (95% CI: 0.91–1.00) (Table 2). The eNose fluctuations of sensor 5 increased (on average) directly one day after the RV challenge in asthmatics (Figure S5). This was less evident in healthy subjects.

Healthy vs Asthma

When comparing the two groups, healthy controls had significantly larger deviations (8% ±6) than asthmatics (6% ±5) before the RV16 challenge in sensor 1 ($p < 0.01$) (Table S3), with an AUROCC of 0.82 (95% CI: 0.65–0.99) (Table 2). Post-challenge, mean deviations were larger in asthmatics compared to healthy controls in sensor 5 (15% ±13 and 6% ±5, respectively; $p < 0.001$) and 6 (6% ±5 and 3% ±3, respectively; $p < 0.01$), and *vice versa* for sensor 7 (17% ±15 and 32% ±26, respectively; $p < 0.01$) (Table S3). The highest AUROCC for discrimination in post-challenge eNose fluctuations between asthma and healthy was 0.94 (95% CI: 0.83–1.00) based on sensor 5 (Table 2).

Table 2. Area under the ROC curves for discrimination between study phase and groups

Sensor	Healthy pre vs. post	Asthma pre vs. post	Pre healthy vs. asthma	Post healthy vs. asthma
1	0.67 (CI: 0.44-0.90)	0.76 (CI: 0.55-0.96)	**0.82** (CI: 0.65-0.99)	0.54 (CI: 0.27-0.81)
3	0.69 (CI: 0.46-0.92)	0.51 (CI: 0.26-0.76)	0.63 (CI: 0.39-0.87)	0.74 (CI: 0.52-0.95)
4	0.64 (CI: 0.40-0.88)	0.67 (CI: 0.43-0.91)	0.61 (CI: 0.37-0.85)	0.52 (CI: 0.27-0.77)
5	**0.82** (CI: 0.65-0.99)	**0.97** (CI: 0.91-1.00)	0.62 (CI: 0.39-0.86)	**0.94** (CI: 0.83-1.00)
6	0.53 (CI: 0.28-0.78)	0.77 (CI: 0.57-0.97)	0.59 (CI: 0.34-0.84)	**0.81** (CI: 0.64-0.99)
7	0.71 (CI: 0.49-0.92)	0.56 (CI: 0.32-0.81)	0.71 (CI: 0.49-0.93)	**0.88** (CI: 0.74-1.00)

The area under receiver operating characteristic curve (AUROCC) for discrimination between pre- and post-challenge, as well as healthy and asthma, using mean sensor deviations. Numbers in **bold** are AUROCC>0.80; CI = 95% confidence interval.

All differences remained (almost) statistically significant ($q \leq 0.051$) after FDR adjustment; all p-values and q-values are shown in Table S4. Individual absolute deviations for all visits and each sensor are depicted in Figures S6–S8. Pearson correlations between eNose sensor peak values are listed in Table S5 and show a strong correlation between sensor 5 and 6 (R = 0.91) due to the cross-reactive nature of the sensors.

Linking change in eNose deviations to inflammatory markers and symptoms

The total change in absolute eNose sensor deviations (i.e., the change in mean deviations summed up for all sensors, per subject) was slightly larger in asthma (20.4%, IQR 7.3–23.5) than in healthy (11.7%, IQR 7.3–21.7), although not statistically significant ($p = 0.48$) (Figure S9). Only for asthma, this total change in deviations moderately correlated (R $\gtrapprox$ 0.50) with four cytokines (Table 3); an increase in eNose fluctuations was inversely correlated with pre- and post-challenge IL-8 levels (pre: $\varrho = -0.50$, $p = 0.10$; post: $\varrho = -0.60$, $p < 0.05$) and post-challenge IL-1β ($\varrho = -0.49$, $p = 0.11$), IL-17A ($\varrho = -0.49$, $p = 0.11$) and TNF-α ($\varrho = -0.55$; $p = 0.07$) levels. For all outcomes (i.e., FeNO, WURSS-21, cytokines) in healthy and asthma (except for the four previously mentioned cytokines), the absolute correlation coefficients were < 0.49 and p-values ≥ 0.14 (Table 3).

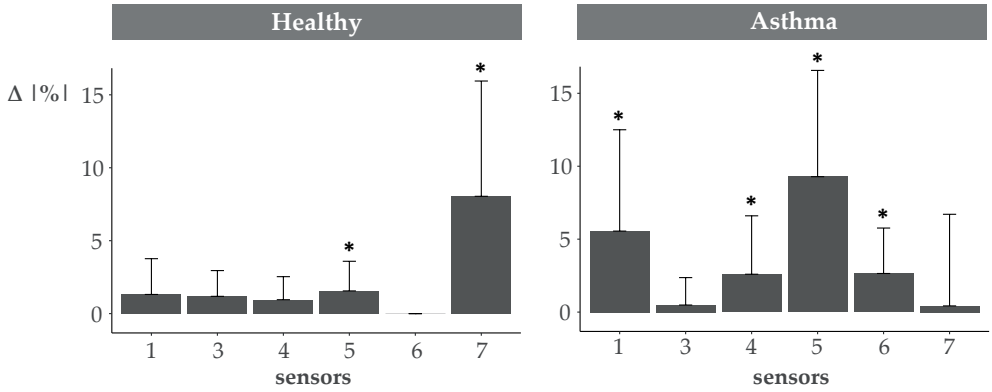

Figure 3. Total change in absolute eNose deviations (per sensor). The change (Δ = post - pre) in eNose fluctuations after the RV16 challenge, expressed as absolute mean deviation percentages (|%|). First, the difference between the personal mean deviations (pre- and post-challenge) was determined (Δ_{sensor}). Next, at group level, the average differences were calculated and are depicted in the graph for each sensor separately. In healthy controls sensor 5 ($p < 0.05$) and sensor 7 ($p < 0.01$) showed significant increases in fluctuations post-challenge, while in asthmatics sensor 1, 4 (both $p < 0.05$), 5 and 6 (both $p<0.01$) were significantly different. * = significant difference ($p < 0.05$).

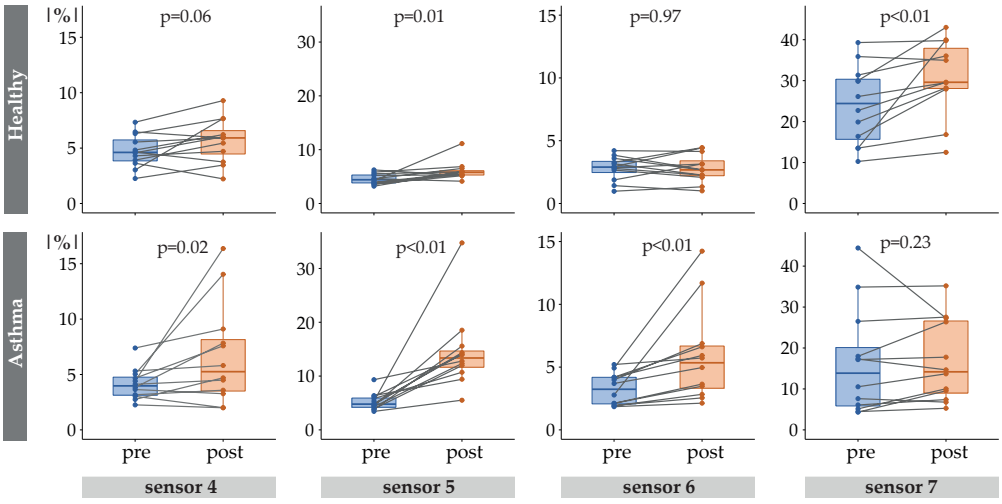

Figure 4. Absolute eNose deviations pre- and post-challenge. Absolute mean deviation percentages (|%|) of all healthy (top) and asthmatic (bottom) participants. Only sensors with significant differences (also after FDR adjustment) between the pre- (**blue**) and post-challenge (**orange**) phase, for either one or both groups, are shown. Each dot represents the personal mean deviation pre- or post-challenge, connected by a line, to visualize individual differences between the two study phases. Note that scales differ between sensors, but not between groups.

Table 3. Correlation between total change in eNose fluctuations and symptoms or inflammation

	Healthy				Asthma			
	Pre		Post		Pre		Post	
	ϱ (95%CI)	p-value	ϱ (95%CI)	p-value	ϱ (95%CI)	p-value	ϱ (95%CI)	p-value
FeNO	-0.16 (-0.64 – 0.47)	0.62	0.20 (-0.52 – 0.73)	0.53	0.00 (-0.73 – 0.61)	1.00	0.03 (-0.72 – 0.61)	0.94
WURSS-21	-	-	0.41 (-0.23 – 0.79)	0.18	-	-	-0.14 (-0.72 – 0.55)	0.67
IFN-γ	-0.15 (-0.71 – 0.52)	0.65	0.19 (-0.45 – 0.76)	0.56	0.12 (-0.59 – 0.68)	0.70	-0.03 (-0.66 – 0.56)	0.92
IL-1β	0.17 (-0.54 – 0.75)	0.60	0.41 (-0.27 – 0.87)	0.18	-0.36 (-0.87 – 0.37)	0.26	-0.49 (-0.89 – 0.21)	0.11
IL-10	-0.13 (-0.77 – 0.63)	0.70	0.30 (-0.41 – 0.83)	0.34	-0.28 (-0.73 – 0.30)	0.38	-0.22 (-0.77 – 0.42)	0.48
IL-13	0.26 (-0.40 – 0.73)	0.42	0.34 (-0.41 – 0.87)	0.28	-0.20 (-0.77 – 0.48)	0.54	-0.49 (-0.82 – 0.12)	0.11
IL-17A	0.06 (-0.55 – 0.62)	0.85	0.14 (-0.53 – 0.72)	0.67	-0.37 (-0.89 – 0.33)	0.24	-0.45 (-0.87 – 0.18)	0.14
IL-33	-0.11 (-0.69 – 0.57)	0.73	-0.05 (-0.61 – 0.51)	0.89	0.00 (-0.70 – 0.66)	1.00	0.01 (-0.67 – 0.80)	0.99
IL-6	0.33 (-0.32 – 0.82)	0.30	0.05 (-0.57 – 0.68)	0.89	-0.26 (-0.81 – 0.44)	0.42	-0.41 (-0.76 – 0.24)	0.18
IL-8	0.29 (-0.40 – 0.80)	0.37	0.29 (-0.33 – 0.81)	0.37	**-0.50** (-0.98 – 0.10)	0.10	**-0.60** (-0.89 – -0.03)	**0.04**
IP-10	-0.38 (-0.93 – 0.41)	0.22	-0.01 (-0.60 – 0.58)	0.97	-0.19 (-0.80 – 0.43)	0.56	-0.36 (-0.89 – 0.38)	0.26
TNF-α	0.22 (-0.45 – 0.73)	0.50	0.25 (-0.41 – 0.83)	0.43	-0.45 (-0.90 – 0.23)	0.14	**-0.55** (-0.92 – 0.01)	0.07

For FeNO, WURSS-21 and the cytokine levels, individual means were calculated based on 10 days pre- or post-challenge; WURSS-21 scores were only available post-challenge. Next, Spearman's rank correlation coefficients (ϱ) and bootstrapped (n=1000) 95% confidence intervals (CI) were calculated between the total change in eNose fluctuations and FeNO, WURSS-21 or cytokines in nasal lavage. Results with p-values <0.05 and/or ϱ≥0.50 are marked in **bold**. FeNO = fractional exhaled nitric oxide; WURSS = Wisconsin Upper Respiratory Symptom Survey.

Discussion

In this prospective 90-day follow-up study, day-to-day fluctuations in exhaled breath signals rapidly increased after a RV16 challenge, in both non-atopic healthy and atopic asthmatic volunteers. We could distinguish between a stable and relatively unstable period with high accuracy, reaching a maximal AUROCC of 0.97 in asthmatics and 0.82 in healthy controls. Asthmatics with a relatively larger increase in eNose fluctuations had (toward) significantly lower IL-1β and IL-17A levels (pre- and post-challenge), and a trend toward lower IL-8 and TNF-α levels (pre-challenge), possibly due to differences in biological processes between groups. In both groups, the change in eNose fluctuations due to RV16 challenge did not correlate with FeNO and cold-like symptoms (WURSS-21).

To our knowledge, we are the first to examine fluctuations in exhaled breath profiles in such an extensive follow-up study, additionally with a highly controlled exposure, in a well-defined study cohort with cases and controls. Our study complements the study of Brinkman *et al.* [13], in which unstable (loss of control induced by steroid withdrawal) and stable (baseline and recovery) asthma periods were correctly classified with 86–95% accuracy, using breath analysis detected by an eNose platform. However, in our study, we did not provoke loss of control, so a direct comparison cannot be made. Our study extends the study of Brinkman *et al.*, as we had a controlled exposure and included more (frequent) time-points (days vs. weeks/months) designed exactly around the viral inoculation event. Moreover, we have improved the accuracy for discriminating pre- and post-challenge phases evidently, when compared to our previous study by Abdel-Aziz *et al.* [17]. In that study, although not the main focus, the discrimination between pre- and post-challenge only reached an AUROCC of 0.79 in asthma and 0.76 in healthy, using single time-point comparisons and "raw" sensor peak values. The improved discriminative accuracy of our current analysis shows the added value of considering all time-points and personal baseline sensor values.

As we had hypothesized, fluctuations in the eNose signals existed regardless of the exposure [27]–[29] and increased after the RV exposure. Fluctuations play an important role in the adaptive capacity of physiological systems to respond to a changing environment and can be too rigid or overly unstable in asthma [30], [31]. Analysis of lung function, nasal eosinophils and neutrophils, and FeNO from the same study as ours, showed that the adaptive capacity was lower in asthma [18], possibly explaining the larger increase in eNose fluctuations after the RV16 challenge in asthmatics compared to healthy controls.

Secondly, the increase in eNose fluctuations after the RV16 challenge was detected by different sensors between the two groups. One explanation could be the cross-reactivity of the sensors, meaning a compound can be detected by several sensors and *vice versa*, which makes it possible that the same or similar compounds were involved between groups. Another explanation could be differences in (patho)physiological mechanisms between healthy and asthmatic participants that become more prominent when local cells are activated (e.g., by viral infection). There are several indications that metabolic activity in local cell asthma differs from that in healthy individuals [32]. These metabolites are often of low molecular weight that can be detected by eNose technology. It is intriguing that we did find moderate inverse correlations between the increase in eNose fluctuations and the cytokine levels of IL-1β, IL-17A, IL-8, and TNF-α, and not for any other mediators. As macrophages are abundantly present in the nasal compartment [33], and M1-like macrophages are activated by RVs [34] at an early stage, it is likely that M1-like macrophages gave rise to these cytokine levels, which can lead to neutrophilic inflammation [35]. Allergic asthmatics have reduced numbers of M1-like macrophages during RV-induced exacerbations [36], which may explain the differences in eNose fluctuations. In addition, airway epithelial cells are activated at an early stage by RV and give rise to mediators like IL-1β and IL-8 [37], [38]. Together, this suggests that the eNose may detect RV-induced metabolic changes.

Finally, we showed that the change in eNose fluctuations was not correlated with FeNO or WURSS-21 scores. It has been shown before that exhaled breath profiles or VOCs minimally correlate with FeNO [13], [39], [40]. This could possibly be explained by eNose signals representing a composite interplay of multiple molecular constituents, making it multidimensional as compared to FeNO. Regarding symptoms, a study by van der Schee *et al*. [41] showed differences in VOC profiles between wheezing and asymptomatic children, regardless of the presence (AUROCC 0.77) or absence (AUROCC 0.81) of a RV. This distinction remained accurate even after symptoms recovered in the RV-positive group (AUROCC 0.84), but not as accurate in the RV-negative group (AUROCC 0.67), illustrating how breath profiles may reflect complex inflammatory processes and/or (pre-existing) biological host-response differences regardless of symptoms.

The first strength of this carefully designed study was the controlled RV exposure and the long follow-up period of 3 months, with multiple measurements per week, throughout the study. On top of that, we included both healthy and asthmatic volunteers, allowing for investigation of differences in response to the RV16 challenge between a diseased and control group. Secondly, we examined

fluctuations at individual level first, using personal baselines, before looking at group averages. This reduced the issue of averaging out individual effects and enabled us to compare normal day-to-day fluctuations with that when triggered with a perturbation. Finally, we made steps toward clinical applicability by using a non-invasive and real-time method, namely eNose technology, for detection of the exhaled breath profiles.

This study also has a few limitations. First of all, the RV16 exposure induced cold-like symptoms, but no loss of control or exacerbation in asthma. This was likely due to our choice to investigate mild asthmatics and a relatively mild RV strain, a choice driven by ethical concerns. Nevertheless, the eNose was capable to detect differences in breath profile fluctuations between the pre- and post-challenge phases, as well as, between groups. Secondly, exhaled breath profiles detected by eNose technology cannot be directly linked to (patho)physiological pathways, as eNose sensors cannot detect and identify single VOCs, due to their cross-reactivity. However, the eNose possibly did reflect macrophage activity or downstream interacting processes. On top of that, it is not easy to delineate differences between groups that arise from disease or atopy, as we included non-atopic healthy and atopic asthmatic volunteers. Nevertheless, the majority of asthmatic subjects in reality also suffer from atopy and hence our study resembled a real-life scenario[42], in which unknown allergic exposures may have influenced the eNose fluctuations. Even so, it would still be of interest to study eNose fluctuations in atopic healthy and non-atopic asthmatics as well, also with respect to the generalizability of our results. Our method of fluctuation analysis (i.e., summarizing all deviations per study phase, at individual and group level) may have caused a loss of temporal and quantitative information on day-to-day fluctuations. Furthermore, we did not perform internal or external validation due to the limited sample size, and the unavailability of comparable data matching the sampling frequency to this intensive study. However, adding multi-omics' analyses offsets the requirement for a large sample size [25], although we admit that it does not exclude the possible risk of overfitting (i.e., unrepresentative AUROCCs) [43], [44]. Consequently, we believe that our data merit a prospective longitudinal study with a larger cohort, preferably in a real-life setting, including daily home monitoring of exhaled breath during stable and unstable periods of asthma. Finally, a sample size estimation was not possible due to the unknown effect sizes of the novel VOC markers, which was compensated by unprecedented high sampling frequency in individuals.

Although these results cannot be directly applied in clinical practice in the current form, they show that exhaled breath analysis could potentially be a useful and additional tool in monitoring disease instability, as it captures a more comprehensive biomarker signal than that merely captured by FeNO and clinical symptoms (WURSS-21). In addition, the increase in eNose fluctuations appeared to start before the onset of cold-like symptoms in asthma, supporting its potential for patient management at the point-of-care. A better understanding of normal and protective homeokinesis vs. diseased and damaging fluctuations is required, to discover how treatment could be guided and the development of exacerbations could be limited, in asthmatic patients. Non-invasive monitoring of exhaled markers using eNose technology can play an important role in this.

Conclusion

Day-to-day fluctuations in exhaled breath profiles rapidly increased after a RV16 challenge with distinct differences between non-atopic healthy and atopic asthmatic volunteers. The increase in fluctuations did not seem to correlate with cold-like symptoms and FeNO, but slightly with some of the investigated pro-inflammatory biomarkers, making it a complementary tool for investigation of disease stability monitoring and possibly treatment adjustment purposes, in a non-invasive manner. Our data justify the design of a longitudinal home monitoring study in a real-life setting and larger population.

References

[1] H. K. Reddel *et al.*, "An official American Thoracic Society/European Respiratory Society statement: Asthma control and exacerbations - Standardizing endpoints for clinical asthma trials and clinical practice," *Am. J. Respir. Crit. Care Med.*, vol. 180, no. 1, pp. 59–99, 2009.

[2] R. Y. Suruki, J. B. Daugherty, N. Boudiaf, and F. C. Albers, "The frequency of asthma exacerbations and healthcare utilization in patients with asthma from the UK and USA," *BMC Pulm. Med.*, 2017.

[3] N. W. Johnston *et al.*, "The September epidemic of asthma exacerbations in children: A search for etiology," *J. Allergy Clin. Immunol.*, 2005.

[4] S. L. Johnston *et al.*, "Community study of role of viral infections in exacerbations of asthma in 9-11 year old children," *BMJ*, 1995.

[5] N. W. Johnston and M. R. Sears, "Asthma exacerbations · 1: Epidemiology," *Thorax*. 2006.

[6] K. G. Nicholson, J. Kent, and D. C. Ireland, "Respiratory viruses and exacerbations of asthma in adults," *Br. Med. J.*, 1993.

[7] P. Haldar *et al.*, "Cluster analysis and clinical asthma phenotypes," *Am. J. Respir. Crit. Care Med.*, 2008.

[8] T. Haselkorn *et al.*, "Consistently very poorly controlled asthma, as defined by the impairment domain of the Expert Panel Report 3 guidelines, increases risk for future severe asthma exacerbations in The Epidemiology and Natural History of Asthma: Outcomes and Treatment Regime," *J. Allergy Clin. Immunol.*, 2009.

[9] T. Haselkorn *et al.*, "Recent asthma exacerbations predict future exacerbations in children with severe or difficult-to-treat asthma," *J. Allergy Clin. Immunol.*, 2009.

[10] R. J. B. Loymans *et al.*, "Comparative effectiveness of long term drug treatment strategies to prevent asthma exacerbations: Network meta-analysis," *BMJ*, 2014.

[11] P. Brinkman *et al.*, "Identification and prospective stability of electronic nose (eNose)–derived inflammatory phenotypes in patients with severe asthma," *J. Allergy Clin. Immunol.*, 2019.

[12] M. P. Van Der Schee, T. Paff, P. Brinkman, W. M. C. Van Aalderen, E. G. Haarman, and P. J. Sterk, "Breathomics in lung disease," *Chest*, 2015.

[13] P. Brinkman *et al.*, "Exhaled breath profiles in the monitoring of loss of control and clinical recovery in asthma," *Clin. Exp. Allergy*, vol. 47, no. 9, pp. 1159–1169, 2017.

[14] N. Fens *et al.*, "Repeated exhaled breath profiling by electronic noses identifies asthma exacerbations," *Am. J. Respir. Crit. Care Med.*, 2014.

[15] C. M. Robroeks *et al.*, "Exhaled volatile organic compounds predict exacerbations of childhood asthma in a 1-year prospective study," *Eur. Respir. J.*, vol. 42, no. 1, pp. 98–106, Jul. 2013.

[16] D. van Vliet *et al.*, "Can exhaled volatile organic compounds predict asthma exacerbations in children?," *J. Breath Res.*, vol. 11, no. 1, p. 016016, Mar. 2017.

[17] M. I. Abdel-Aziz *et al.*, "Cross-sectional biomarker comparisons in asthma monitoring using a longitudinal design: The eNose premise," *Allergy*, vol. 75, no. 10, Oct. 2020.

[18] A. Sinha *et al.*, "Loss of adaptive capacity in asthmatic patients revealed by biomarker fluctuation dynamics after rhinovirus challenge," *Elife*, vol. 8, 2019.

[19] K. F. V. Der Sluijs *et al.*, "Systemic tryptophan and kynurenine catabolite levels relate to severity of rhinovirus-induced asthma exacerbation: A prospective study with a parallel-group design," *Thorax*, 2013.

[20] R. De Vries *et al.*, "Clinical and inflammatory phenotyping by breathomics in chronic airway diseases irrespective of the diagnostic label," *Eur. Respir. J.*, 2018.

[21] E. F. Juniper, P. M. O'Byrne, P. J. Ferrie, D. R. King, and J. N. Roberts, "Measuring asthma control: Clinic questionnaire or daily diary?," *Am. J. Respir. Crit. Care Med.*, 2000.

[22] R. A. Dweik *et al.*, "An official ATS clinical practice guideline: Interpretation of exhaled nitric oxide levels (FENO) for clinical applications," *American Journal of Respiratory and Critical Care Medicine*. 2011.

[23] C. Turner, P. Španěl, and D. Smith, "A longitudinal study of ethanol and acetaldehyde in the exhaled breath of healthy volunteers using selected-ion flow-tube mass spectrometry," *Rapid Commun. Mass Spectrom.*, 2006.

[24] C. Turner, P. Španěl, and D. Smith, "A longitudinal study of breath isoprene in healthy volunteers using selected ion flow tube mass spectrometry (SIFT-MS)," *Physiological Measurement*. 2006.

[25] C.-X. Li, C. E. Wheelock, C. M. Sköld, and Å. M. Wheelock, "Integration of multi-omics datasets enables molecular classification of COPD," *Eur. Respir. J.*, vol. 51, no. 5, p. 1701930, May 2018.

[26] Y. Benjamini and Y. Hochberg, "Controlling the False Discovery Rate: A Practical and Powerful Approach to Multiple Testing," *J. R. Stat. Soc. Ser. B*, 1995.

[27] C. L. Que, C. M. Kenyon, R. Olivenstein, P. T. Macklem, and G. N. Maksym, "Homeokinesis and short-term variability of human airway caliber," *J. Appl. Physiol.*, 2001.

[28] T. A. Tirone and F. C. Brunicardi, "Overview of glucose regulation," *World J. Surg.*, 2001.

[29] B. F. Palmer and D. J. Clegg, "Physiology and pathophysiology of potassium homeostasis," *Adv. Physiol. Educ.*, 2016.

[30] U. Frey, G. Maksym, and B. Suki, "Temporal complexity in clinical manifestations of lung disease," *Journal of Applied Physiology*. 2011.

[31] A. L. Goldberger, L. A. N. Amaral, J. M. Hausdorff, P. C. Ivanov, C. K. Peng, and H. E. Stanley, "Fractal dynamics in physiology: Alterations with disease and aging," *Proc. Natl. Acad. Sci. U. S. A.*, 2002.

[32] C. Michaeloudes *et al.*, "Role of Metabolic Reprogramming in Pulmonary Innate Immunity and Its Impact on Lung Diseases.," *J. Innate Immun.*, vol. 12, no. 1, pp. 31–46, 2020.

[33] G. Ryu *et al.*, "Role of IL-17A in Chronic Rhinosinusitis With Nasal Polyp.," *Allergy. Asthma Immunol. Res.*, vol. 12, no. 3, pp. 507–522, May 2020.

[34] C. Rajput, M. P. Walsh, B. N. Eder, E. E. Metitiri, A. P. Popova, and M. B. Hershenson, "Rhinovirus infection induces distinct transcriptome profiles in polarized human macrophages," *Physiol. Genomics*, 2018.

[35] M. Bullone *et al.*, "Elevated serum IgE, oral corticosteroid dependence and IL-17/22 expression in highly neutrophilic asthma," *Eur. Respir. J.*, vol. 54, no. 5, p. 1900068, Nov. 2019.

[36] A. Nikonova *et al.*, "M1-like macrophages are potent producers of anti-viral interferons and M1-associated marker-positive lung macrophages are decreased during rhinovirus-induced asthma exacerbations," *EBioMedicine*, 2020.

[37] S. C. Piper *et al.*, "The role of interleukin-1 and interleukin-18 in pro-inflammatory and anti-viral responses to rhinovirus in primary bronchial epithelial cells.," *PLoS One*, vol. 8, no. 5, p. e63365, 2013.

[38] M. Yamaya *et al.*, "Clarithromycin decreases rhinovirus replication and cytokine production in nasal epithelial cells from subjects with bronchial asthma: effects on IL-6, IL-8 and IL-33.," *Arch. Pharm. Res.*, vol. 43, no. 5, pp. 526–539, May 2020.

[39] D. Van Vliet *et al.*, "Association between exhaled inflammatory markers and asthma control in children," *J. Breath Res.*, vol. 10, no. 1, 2016.

[40] M. P. Van der Schee, R. Palmay, J. O. Cowan, and D. R. Taylor, "Predicting steroid responsiveness in patients with asthma using exhaled breath profiling," *Clin. Exp. Allergy*, 2013.

[41] M. P. Van Der Schee *et al.*, "Altered exhaled biomarker profiles in children during and after rhinovirusinduced wheeze," *Eur. Respir. J.*, 2015.

[42] A. Bourdin, D. Gras, I. Vachier, and P. Chanez, "Upper airway · 1: Allergic rhinitis and asthma: United disease through epithelial cells," *Thorax*. 2009.

[43] A. Azim, C. Barber, P. Dennison, J. Riley, and P. Howarth, "Exhaled volatile organic compounds in adult asthma: a systematic review," *Eur. Respir. J.*, vol. 54, no. 3, p. 1900056, Sep. 2019.

[44] R. A. Sola Martínez, J. M. Pastor Hernández, Ó. Yanes Torrado, M. Cánovas Díaz, T. de Diego Puente, and M. Vinaixa Crevillent, "Exhaled volatile organic compounds analysis in clinical pediatrics: a systematic review," *Pediatr. Res.*, Sep. 2020.

Supplementary material

Methods

Skin prick test

Participants were considered atopic when allergic to one or more of 12 common aero allergens. The 12 common aero allergens tested were grass mix, tree mix, house dust mite, cat, dog, rabbit, guinea pig, cockroach, alternaria alternata, aspergillus fumigatus, cladosporium herbarum and latex. As a control, histamine and buffer control were tested.

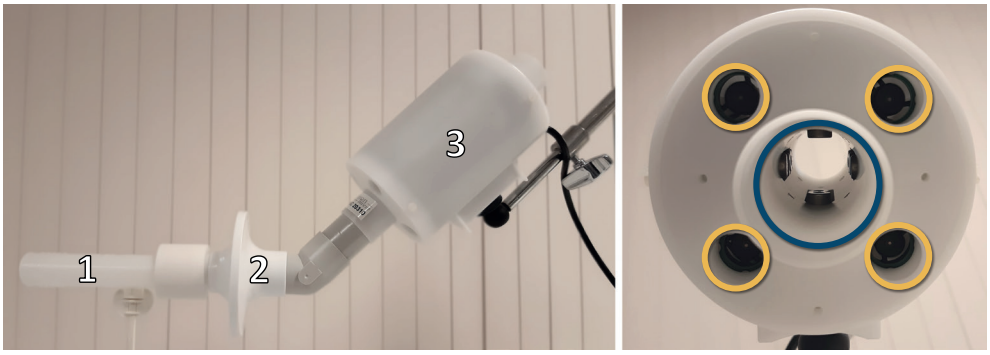

Figure S1. eNose: The eNose (3) was attached to the rare end of a spirometer (1) and a bacterial filter (2) (left, side view). The eNose consists of four sensor arrays (two in duplicate) on the inner side of the eNose (blue circle), detecting the exhaled breath, and four on the outer side for detection of the environment (yellow circles) (right, front view).

Table S1. SpiroNose sensor type, sensitivity and detection range.

Sensor	Type	Highest sensitivity to	Range (ppm)
1	TGS 2602	VOCs (e.g., toluene) and odorous gases (e.g., ammonia and hydrogen sulphide)	1 – 30
2	TGS 2610	Butane and propane	500 – 10,000
3	TGS 2611-COO	Methane and natural gases	500 – 10,000
4	TGS 2600	Hydrogen, carbon monoxide and ethanol	1 – 30
5	TGS 2603	Trimethylamine and methyl mercaptan	1 – 30
6	TGS 2620	Alcohol and solvent vapors	50 – 5,000
7	TGS 2612	Methan, propane and iso-butane	500 – 10,000

ppm = parts per million, VOCs = volatile organic compounds. A similar table has been published previously (Ibrahim *et al.*, Allergy 2020, de Vries *et al.*, Ann Oncol 2019).

Wisconsin Upper Respiratory Symptom Survey – 21 --- *Daily Symptom Report*

Day:	*Date:*	*Time:*	*ID*:

Please fill in one circle for each of the following items:

	Not sick	Very mildly		Mildly		Moderately		Severely
	0	**1**	**2**	**3**	**4**	**5**	**6**	**7**
How sick do you feel **today**?	O	O	O	O	O	O	O	O

Please rate the **average severity of your cold symptoms over the last 24 hours** for each symptom:

	Do not have this symptom	Very mild		Mild		Moderate		Severe
	0	**1**	**2**	**3**	**4**	**5**	**6**	**7**
Runny nose	O	O	O	O	O	O	O	O
Plugged nose	O	O	O	O	O	O	O	O
Sneezing	O	O	O	O	O	O	O	O
Sore throat	O	O	O	O	O	O	O	O
Scratchy throat	O	O	O	O	O	O	O	O
Cough	O	O	O	O	O	O	O	O
Hoarseness	O	O	O	O	O	O	O	O
Head congestion	O	O	O	O	O	O	O	O
Chest congestion	O	O	O	O	O	O	O	O
Feeling tired	O	O	O	O	O	O	O	O

Over the last 24 hours, how much has your cold interfered with your ability to:

	Not at all	Very mildly		Mildly		Moderately		Severely
	0	**1**	**2**	**3**	**4**	**5**	**6**	**7**
Think clearly	O	O	O	O	O	O	O	O
Sleep well	O	O	O	O	O	O	O	O
Breathe easily	O	O	O	O	O	O	O	O
Walk, climb stairs, exercise	O	O	O	O	O	O	O	O
Accomplish daily activities	O	O	O	O	O	O	O	O
Work outside the home	O	O	O	O	O	O	O	O
Work inside the home	O	O	O	O	O	O	O	O
Interact with others	O	O	O	O	O	O	O	O
Live your personal life	O	O	O	O	O	O	O	O

Compared to yesterday, I feel that my cold is…

Very much better	Somewhat better	A little better	The same	A little worse	Somewhat worse	Very much worse
O	O	O	O	O	O	O

WURSS -21© (Wisconsin Upper Respiratory Symptom Survey) 2004
Created by Bruce Barrett MD PhD et al., UW Department of Family Medicine, 777 S. Mills St. Madison, WI 53715, USA

Results

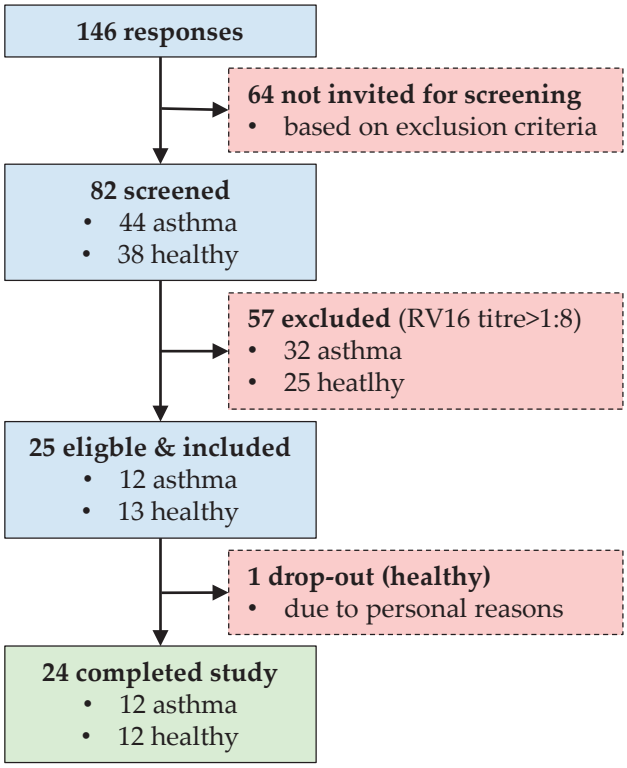

Figure S2. Inclusion flow chart. In total, 146 people were contacted of whom 64 met the exclusion criteria. From the 82 people who were screened, 57 had RV16 antibody levels >1:8 in serum. For the healthy group, we included 13 participants, as one subject had to drop-out because of personal reasons. Eventually 12 asthmatics and 12 healthy individuals completed the study.

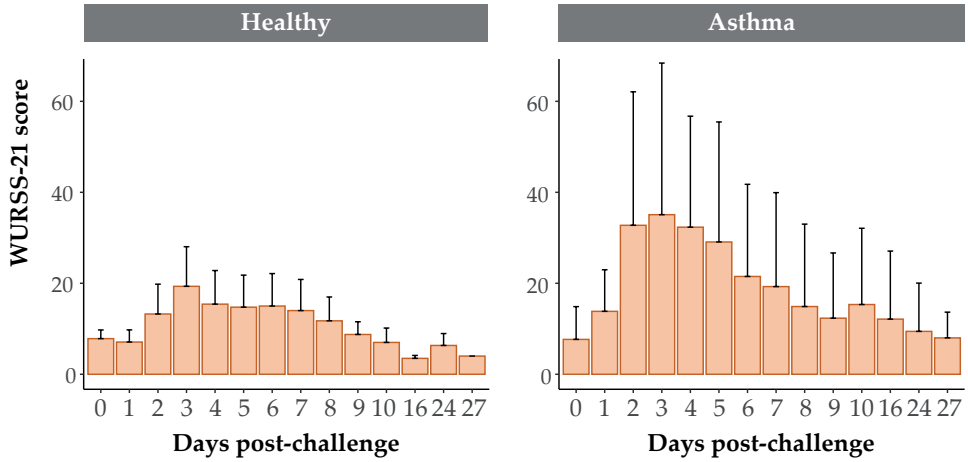

Figure S3. WURSS-21 scores post-challenge (per day). Wisconsin Upper Respiratory Symptom Survey (WURSS-21) scores per day for healthy (left) and asthmatic (right) volunteers expressed as means (±SD). After visit 0, volunteers received the RV16 challenge. The study by Barrett *et al*. reported that the minimal clinical important difference (MCID) of the WURSS-21 score was 10.3 (Barrett, Health Qual Life Outcomes, 2009).

Table S2. Clinical presentation pre- and post-challenge

	Healthy (n=12)			Asthma (n=12)		
	Pre	Post		Pre	Post	
	Median (IQR) of mean	Median (IQR) of mean	Median (IQR) of min/max	Median (IQR) of mean	Median (IQR) of mean	Median (IQR) of min/max
Spirometry						
FVC (%)[a]	80 (78 – 89)	74 (67 – 87)	65 (57 – 81)	89 (77 – 91)	84 (77 – 91)	78 (69 – 85)
FEV_1 (%) [a]	88 (82 – 91)	84 (76 – 90)	76 (68 – 85)	88 (74 – 90)	87 (74 – 90)	81 (68 – 85)
PEF (%)[a]	90 (84 – 100)	92 (77 – 104)	80 (60 – 98)	88 (81 – 93)	88 (78 – 95)	77 (58 – 86)
FeNO (ppb)[b]	14 (13 – 16)	16 (11 – 19)	26 (15 – 31)	46 (36 – 56)	43 (30 - 59)	78 (41 – 86)
WURSS-21 [c]	6 (4 – 10)	9 (6 – 17)	16 (14 – 28)	10 (6 – 18)	18 (8 – 35)	48 (18 – 70)
ACQ[c]	0.3 (0.3 – 0.3)	0.3 (0.3 – 0.3)	0.3 (0.3 – 0.3)	0.3 (0.3 – 0.4)	0.4 (0.4 – 0.4)	0.7 (0.5 – 0.9)

The results are expressed as medians and interquartile ranges (IQR) of the individual means (pre and post) or minima/maxima (post), to compare baseline with the (maximal) response to the RV challenge. First, the mean of all visits pre- and post-challenge and the minimum (spirometry data) or maximum (FeNO, WURSS-21 and ACQ) of the post-challenge were calculated at an individual. Next, the median (IQR) of the means pre- and post-challenge and minima/maxima post-challenge were calculated at group level. A more in depth analysis on this data has been previously published (Sinha *et al.*, eLife 2019).

a = based on daily home monitoring during the whole study period; b = based on clinical visits during the whole study period; c = based on daily home monitoring starting from the day of challenge, in which 'pre' was based on data from the day of challenge and 1 day post-challenge. FVC = forced vital capacity; FEV_1 = forced expiratory volume in 1s; PEF = peak expiratory flow; FeNO = fractional exhaled nitric oxide; WURSS = Wisconsin Upper Respiratory Symptom Survey; ACQ = asthma control questionnaire.

Table S3. Overview of eNose absolute deviation percentages per group and phase

Sensor	Healthy		Asthma	
	pre	post	pre	post
1	8.0 (±5.7)	9.3 (±6.9)	5.6 (±4.8)	11.1 (±12.9)
3	4.5 (±4.0)	5.8 (±4.0)	3.6 (±3.2)	4.0 (±3.5)
4	4.7 (±4.0)	5.7 (±4.9)	4.2 (±3.8)	6.7 (±7.0)
5	4.5 (±3.4)	6.1 (±4.5)	5.3 (±4.5)	14.5 (±13.3)
6	2.8 (±2.6)	2.8 (±2.6)	3.3 (±3.0)	5.9 (±5.4)
7	24.0 (±19.5)	32.1 (±26.2)	16.3 (±19.5)	16.8 (±14.7)

Group averages of absolute deviation percentages (|%|), expressed as mean (±SD), per study phase.

Table S4. P- and q-values for differences in eNose deviation percentages between study phases and groups

Sensor	Healthy pre vs. post		Asthma pre vs. post		Pre healthy vs. asthma		Post healthy vs. asthma	
	p-value	q-value	p-value	q-value	p-value	q-value	p-value	q-value
1	0.077	0.092	0.034	0.051	0.007	0.042	0.755	0.887
3	0.064	0.092	0.677	0.677	0.291	0.454	0.052	0.078
4	0.064	0.092	0.021	0.042	0.378	0.454	0.887	0.887
5	**0.012**	0.036	0.000	0.000	0.319	0.454	0.000	0.000
6	0.970	0.970	0.000	0.000	0.478	0.478	0.008	0.016
7	**0.001**	0.006	0.233	0.280	0.089	0.267	0.001	0.003

P-values and false discovery rate (FDR) adjusted p-values (q-values) of the differences between study phases (pre vs. post) per group and between groups (asthma vs. healthy) per study phase; using *Wilcoxon signed rank* test and *Mann-Whitney U* test, respectively. Numbers in **bold** are significantly different ($p<0.05$).

Table S5. Correlations between eNose sensor peak values

	S1	S3	S4	S5	S6	S7
S1		0.23	0.16	0.00	0.08	-0.41
S3	0.23		-0.42	-0.15	-0.17	0.04
S4	0.16	-0.42		0.35	0.53	-0.34
S5	0.00	-0.15	0.35		**0.91**	-0.56
S6	0.08	-0.17	0.53	**0.91**		-0.63
S7	-0.41	0.04	-0.34	-0.56	-0.63	

Pearson correlations for all eNose measurements, with $R>0.70$ marked in **bold**.

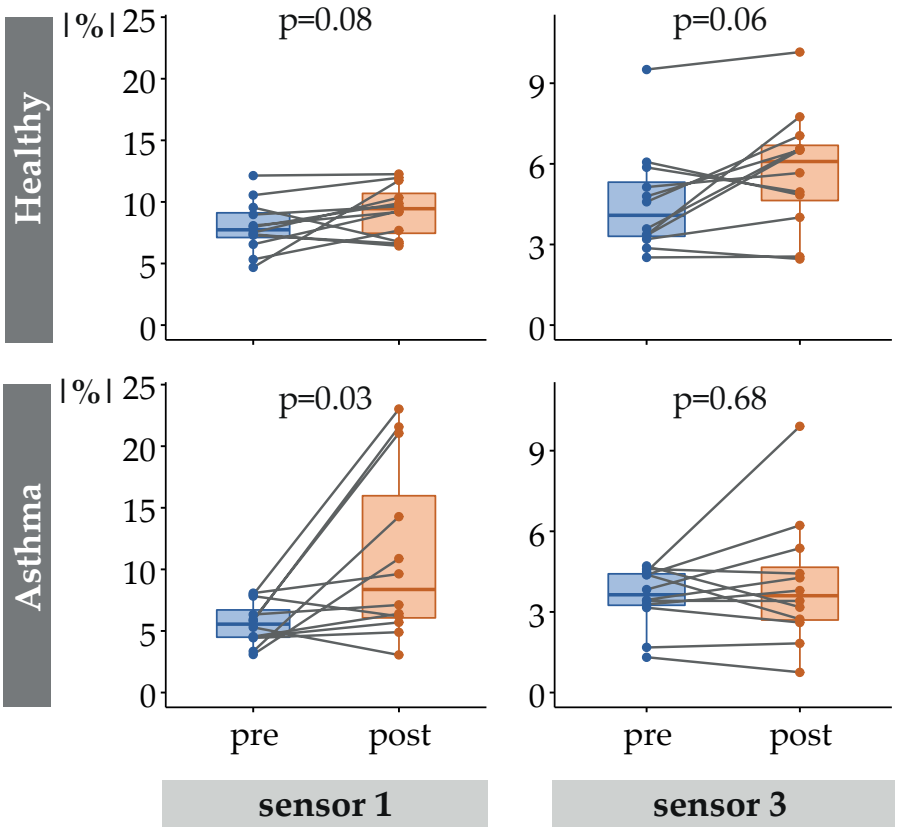

Figure S4. eNose deviations pre- and post-challenge. Absolute mean deviation percentages (|%|) for healthy (top) and asthmatic (bottom) participants. Only sensors that were not significantly different (after FDR adjustment) between the pre- (**blue**) and post-challenge (**orange**) phase for both groups, are shown. Each dot represents the personal mean deviation pre- or post-challenge, connected by a line, to visualize individual differences between the two phases.

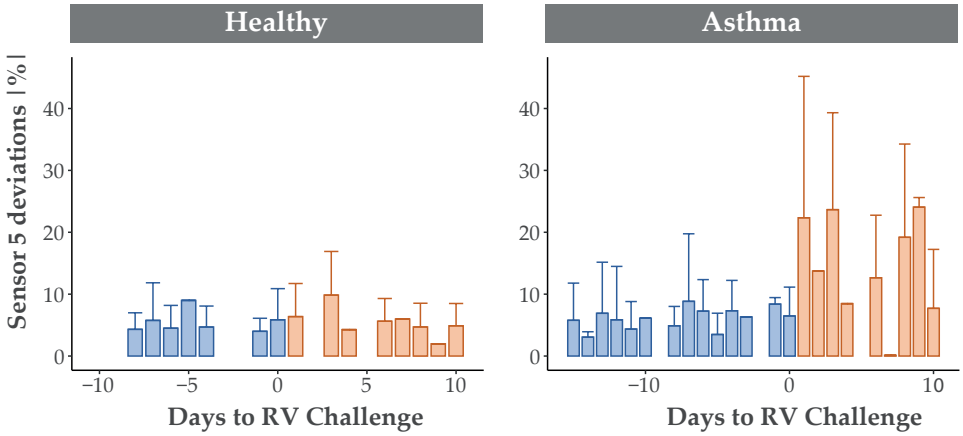

Figure S5. Absolute deviation percentages per day (sensor 5). Deviations in sensor 5 over time (days to or from the RV challenge) expressed as aboslute deviation percentages (mean ±SD). The pre-challenge visit days are markered in **blue** and the post-challenge days in **orange**. For (some) asthma patients, a direct increase in eNose fluctuations is visible one day after the RV challenge. On certain days, eNose measurements were perfomed in one (no SD) or none of the participants (no bar).

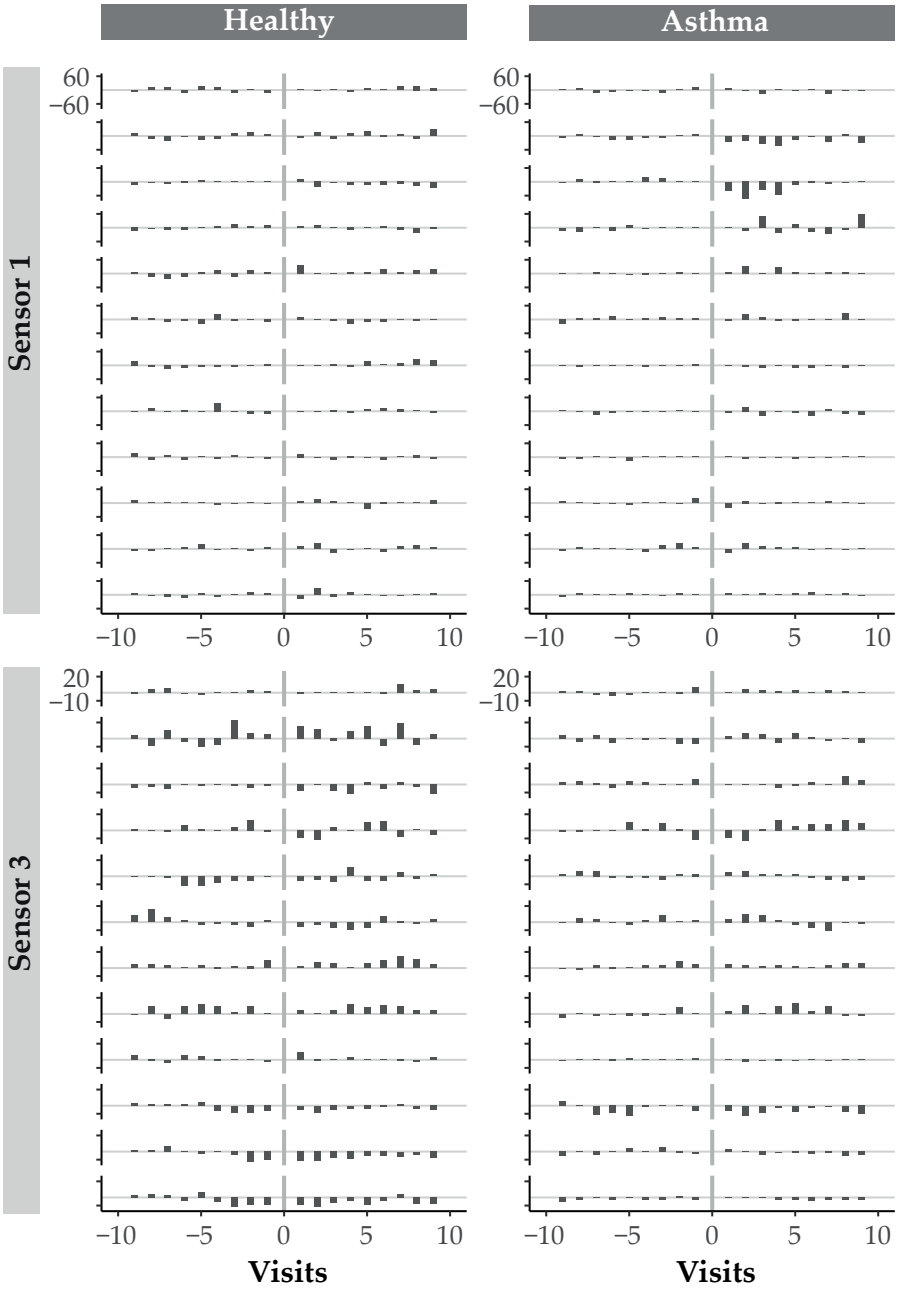

Figure S6. Time series eNose deviations per subject (sensor 1 & 3). Absolute deviation percentages from the individual baselines (horizontal grey lines = 0%) over time (visits) for sensor 1 and 3. Each row is an individual healthy (left) or asthmatic (right) participant. The light gray vertical line, marks the moment of the RV16 challenge. Note that visits are not always at the same day from the RV16 challenge.

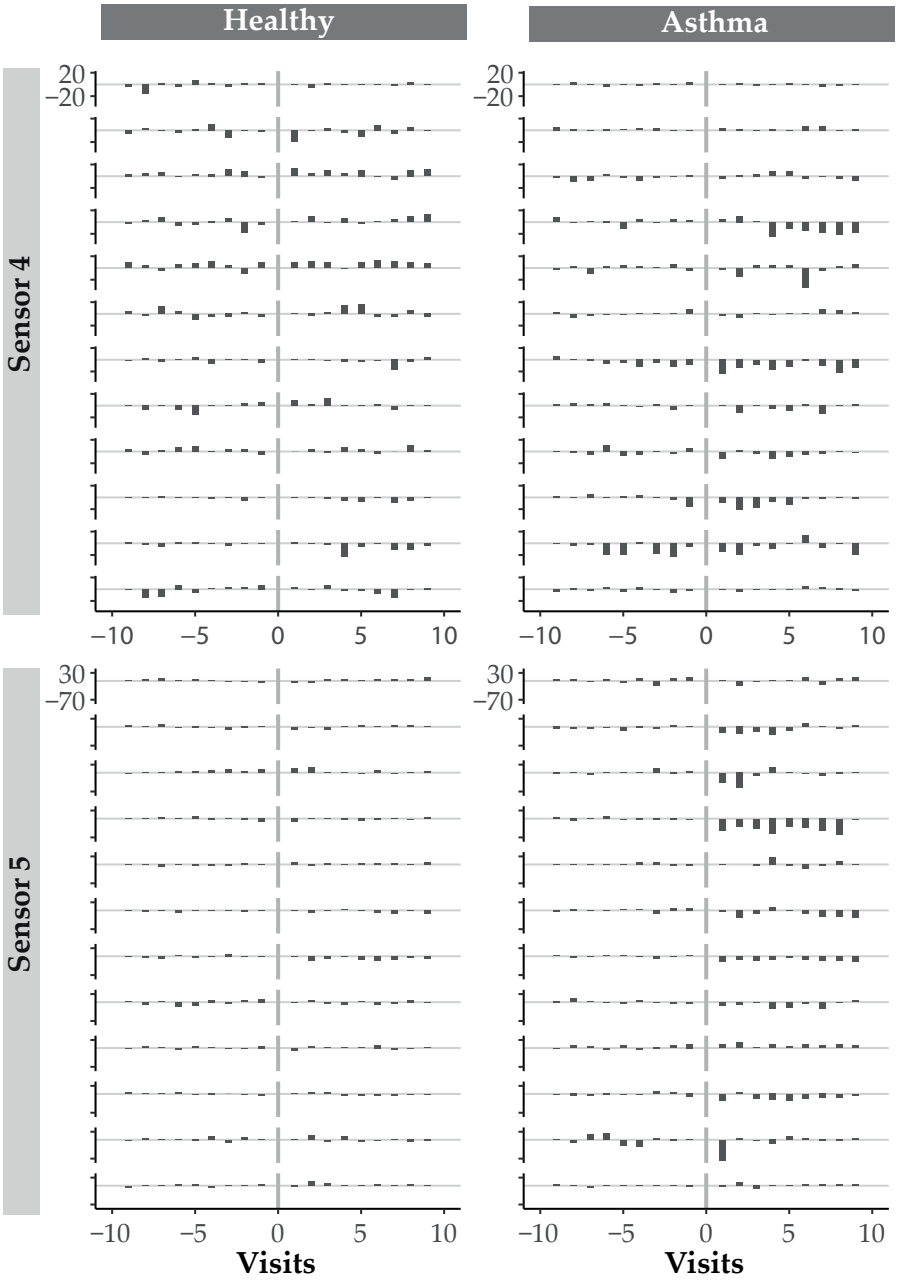

Figure S7. Time series eNose deviations per subject (sensor 4 & 5). Deviation percentages from the individual baselines (horizontal grey lines = 0%) over time (visits) for sensor 4 and 5. Each row is an individual healthy (left) or asthmatic (right) participant. The light gray vertical line, marks the moment of the RV16 challenge. Note that visits are not always at the same day from the RV16 challenge.

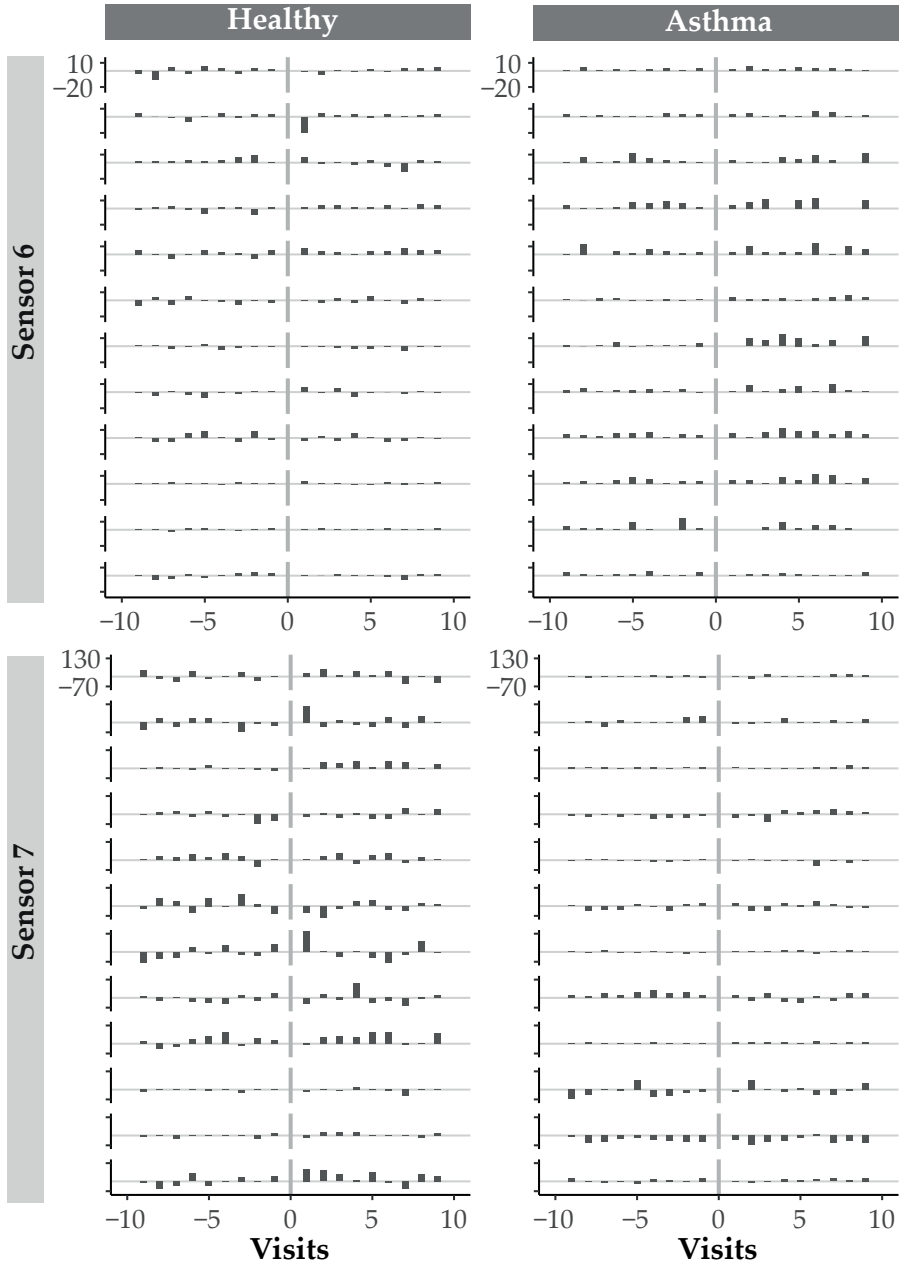

Figure S8. Time series eNose deviations per subject (sensor 6 & 7). Deviation percentages from the individual baselines (horizontal grey lines = 0%) over time (visits) for sensor 6 and 7. Each row is an individual healthy (left) or asthmatic (right) participant. The light gray vertical line, marks the moment of the RV16 challenge. Note that visits are not always at the same day from the RV16 challenge.

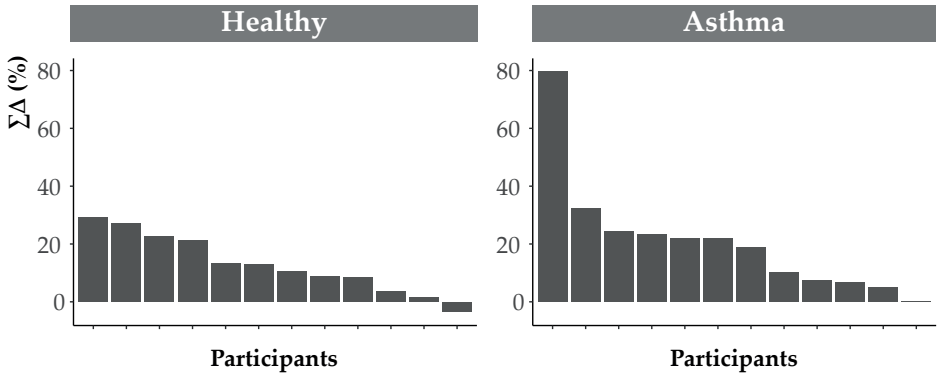

Figure S9. Total change in absolute eNose deviations (per participant). The total change (post – pre) in absolute eNose sensor deviations ($\sum \Delta_{all\ sensors}$). Each bar represents a healthy (left) or asthmatic (right) participant.

Part IV.

Discussion

Chapter 7.
General discussion

General discussion

Environmental factors play an important role with respect to our health and disease prevention [1]–[3]. All environmental factors (e.g. nutrition, physical activity, sleep behaviour, socioeconomic status and environmental exposures) together are called the exposome [2], [4]. Compounds present in environmental air are important contributors to the exposome. The ambient air is in direct contact with our respiratory system, and can contain hazardous agents like air pollutants, tobacco smoke, chemicals and pathogens (including viruses). Such agents possibly induce both short- and long-term health effects. In this thesis we aimed to investigate the short-term effects of exposure to air pollution and rhinoviruses on cardiopulmonary function and the metabolome of the exhaled breath and urine. In this chapter, the main findings of this thesis will be summarized, the main methodological challenges and implications will be addressed and recommendations for future research will be discussed.

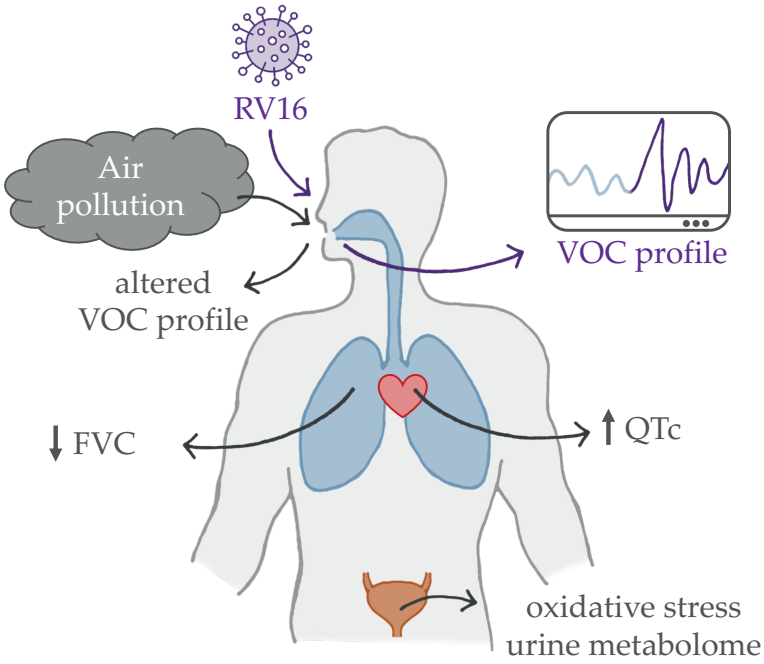

Figure 1. This figure summarizes the main findings of this thesis. Exposure to air pollution near a major airport decreased the forced vital capacity (FVC), prolonged the corrected QT (QTc) interval, induced oxidative stress as detected in the urine metabolome and altered the exhaled volatile organic compound (VOC) profile, in healthy adults. The rhinovirus exposure altered the fluctuations in exhaled breath profile of both healthy adults and mild asthmatics.

Main findings

Short-term exposure to air pollution: cardiopulmonary effects and metabolic changes

In the studies described in **Chapters 3 - 5**, we found that short-term exposure to air pollution, mainly focused on ultrafine particles (UFP), at a major airport had cardiopulmonary effects and altered the breath and urine metabolome in healthy young adults (Figure 1). This was the first study to evaluate this relationship in such a controlled setting. A decreased lung function has been associated with road-traffic related UFP before [5], [6], but we were the first to investigate or find a signification association with aviation-related UFP. Prolonged corrected QT (QTc) intervals have been associated with both short- and long-term exposure to fine particles (PM2.5) in previous literature, but not with (aviation related) UFP [7]–[9]. Even though the observed effects were small, they are important findings for people working at or living close to major airports. As these effects already occurred after exposures of 5 hours and in healthy adults, long-term exposure may have more severe effects, particularly in vulnerable populations with more comorbidities.

Rhinovirus exposure increases exhaled breath profile fluctuations

Furthermore, we showed in **Chapter 6** how a rhinovirus exposure rapidly increases the fluctuations in exhaled volatile organic compound (VOC) profile (Figure 1), in which the magnitude of the change possibly reflected the inflammatory state of the person. As the increase in fluctuations seemed to start before symptoms occurred, exhaled breath might even hold promise for the prediction of virus-induced exacerbations in asthma, which could have serious implications for disease control in severe asthmatics. We were the first to investigate the potential of exhaled breath analysis for monitoring of disease instability in asthma in such an extensive follow-up study, with on top of that, a highly controlled exposure. Previous studies have shown the potential of electronic nose (eNose) technology for the detection of loss of control [10], exacerbations [11], or a recent exacerbation [12] in asthma and chronic obstructive pulmonary disease (COPD), but these studies involved either a retrospective design or a prospective design with weeks to months between measurements.

Methodological challenges and limitations

Air pollution

Exposure assessment

For air pollution research, it is challenging to accurately assess the exposure, both quantitatively (due to measurement errors) and qualitatively (the actual exposure subjects received). Usually, observational studies rely on central site monitoring, which can possibly lead to exposure misclassification. In our study presented in **Part II**, we made use of a mobile exposure laboratory at the exposure location. This allowed us to accurately measure the exposure on site, without measurement errors due to wind (e.g. wind speed) and rain. Although we did exclude people living in highly polluted areas, differences in exposure levels directly before the study visits, both between and within subjects, may have occurred. This has potentially led to differences in the response to the exposure. For future research, the at-home exposure could be estimated or measured, and incorporated as a covariate in the (linear mixed effect) model.

Independence of exposure effects

As air pollution concerns a variety of pollutants, a major challenge is to delineate the independence of the effects from all different exposure components and sources. A suited statistical method to elucidate these independences that we used in our study **(Part II)** is multi-pollutant regression analysis [13]. It is important to recognize that pollutants are often highly correlated, and, when included in the same model, multicollinearity can occur, making the estimates unstable [14]. In that case, one should consider to use more advanced statistical analyses, such as deletion-substitution-addition (DSA) and least absolute shrinkage and selection operator (LASSO) analysis, which are able to capture complex interactions and nonlinear terms of predictors [14]–[16]. Therefore, it is important to check the data for multicollinearity. In our study **(Chapters 3-5)**, multicollinearity did not play a role, as aviation was the main source of UFP and minimally contributes to other pollutants [17].

For distinguishing the effects of different UFP sources, we first split the UFP range in ≤20 nm and >50 nm, as indicators for aviation [17]–[19] and road-traffic [20]–[22] related UFP, respectively. We discarded the particle sizes between 20 and 50 nm, as these particles can originate from both sources [23]. Furthermore, with this method we did not make use of other valuable exposure information, like PM2.5 and black carbon (BC) levels, and the meteorological conditions, in particular wind direction. We overcame these limitations by using positive matrix factorization (PMF) source apportionment models **(Chapter 4 and 5)**. This is an

widely-used and advanced method to identify and quantify the contribution of a source to a specific variable (in our case, total particle number concentrations) [24]–[26], and is recommended for future research on distinguishing the effects of different sources of the same pollutant.

eNose technology

A large diversity of analytical techniques for the detection of VOCs in breath exists **(Chapter 2)**, with the two main approaches being mass spectrometry and sensor-based technology [27], [28]. Mass spectrometry techniques enable the detection of single compounds, making them suitable for biomarkers discovery of distinct metabolic pathways. However, they are costly and cumbersome, and require trained personnel. In contrast, eNose technology has the potential for point-of-care testing, as it an easy-to-perform and relatively cheap method, making it more suitable for clinical practice. A downside of eNose sensors is that they lack specificity, as they cannot detect single compounds, and can therefore not be used to delineate metabolic pathways.

In the studies described in this thesis sensor-based technology was used **(Chapter 4 and 6)**. Therefore, in our rhinovirus exposure study **(Chapter 6)**, we have to be aware that it remains unclear whether the eNose detected the specific effect of the rhinovirus, or a more general response related to a viral infection or external trigger. Nonetheless, eNose technology has shown its potential to distinguish different inflammatory phenotypes [29]–[32] and to detect or predict (recent) exacerbations [10]–[12], in asthma and COPD. This suggests that eNose sensors are able to detect VOCs in exhaled breath that are involved in inflammatory processes. For future studies, it is important to combine the advantages of both techniques, in which we should start with using mass spectrometry techniques for a better understanding of metabolic pathways, to be able to select or develop more specific eNose sensors at a later stage. This would allow us to understand and detect the specific response to environmental exposures and to facilitate the implementation for clinical testing.

Implications

Implications air pollution regarding public health

Currently, the evidence on the health effects of (aviation-related) UFP exposure is inconclusive and inconsistent due to differences in exposure assessment, study design and populations, and confounder adjustments [13], [33]. However, relatively consistent findings have been found regarding pulmonary and systemic

inflammatory and cardiovascular effects (i.e. autonomic tone and blood pressure) [13], and these findings were supported by our study **(Part II)**. Therefore, we believe that our study, and previous studies on air pollution, already merit to monitor and reduce UFP levels, especially in highly polluted areas, e.g. large cities, airports and industrial areas.

The need of a UFP monitoring network

Internationally, a large network of monitoring stations exists, promoted by the the European Environment Agency (EEA, www.eea.europa.eu) and Environmental Protection Agencies (EPA, www.epa.gov), that routinely measure the levels of several air pollutants, like ozon (O_3), coarse particles (PM10) and PM2.5. Currently, such standardized international monitoring does not exist for UFP, partly and ironically, due to the lack of consistent evidence of the adverse health effects of UFP. Thus, long-term epidemiological studies mostly rely on modelled UFP exposures [34]–[36], using land-use regression models [37], [38], instead of measured exposures. However, the spatial and temporal variations in UFP levels are high when compared to more homogenous distributed air pollutants like PM2.5 and PM10 [39]. Therefore, assuming that the temporal changes are evenly distributed across a certain study area, may result in larger estimation errors of UFP exposure when compared to other pollutants. A network for UFP monitoring would facilitate qualitative long-term effects studies; an essential step to substantiate new (inter)national air quality regulations. Moreover, such a network would be required once UFP level regulations have been established, making it of use for the future as well.

Air pollution reduction

The most straightforward solution for minimization of the effects of air pollution, would be to reduce air pollution levels, both indoors and outdoors. This could be realized in several ways; traffic reduction, reduced fuel-combustion and air filtration systems. Traffic reduction in urbanized areas could be achieved by improving public transport (i.e. more frequent and 24-hour services), limiting private automobile traffic, and prohibiting diesel-fuelled vehicles or vehicles that fail emission standards. An interesting example of how these strategies can significantly reduce air pollution levels are the Summer Olympic Games in Beijing of 2008; temporary vehicle restrictions along with restrictions for polluting industries decreased the PM2.5 levels from 78.8 to 45.7 $\mu g/m^3$ [40]. This improved the lung function of healthy and asthmatic adults [41], and reduced the asthma-related outpatient visits [40], cardiovascular mortality [42] and systemic inflammation [43]. The reduction of fuel-combustion could be realized by a transition to electric vehicles, both for private and public transport, and should

be facilitated by governmental regulations and subsidies. Another method is to reduce idling at "kiss-and-ride" zones of train stations, airports and schools. For instance, four urban schools succeeded to reduce PM2.5 levels from 4.11 to 0.99 $\mu g/m^3$ and particle number concentration (PNC) levels from 11,560 to 1,690 particles/m^3 through an anti-idling campaign [44]. Lastly, the installation of soot and High Efficiency Particulate Air (HEPA) filters can significantly reduce the outdoor and indoor levels of air pollution. As an example, the introduction of a high efficiency cabin air (HECA) filtration system reduced levels of BC by 84% and UFP by 88% inside school busses [45].

Overall, air pollution reduction strategies can have beneficial effects on public health and well-being. In the Annals of American Thoracic Society of 2019, Schraufnagel *et al.* state that "reducing pollution at its source can have a rapid and substantial positive impact on our health" [46]. They describe how, within weeks, respiratory symptoms, such as, shortness of breath, cough, and a sore throat, can disappear shortly after air pollution is reduced. On top of that, they state that "school absenteeism, clinic visits, hospitalizations, premature births, cardiovascular illness and death, and all-cause mortality decrease significantly" [46]. The reduction in clinical visits and hospitalizations is also reflected in asthmatics, as exposure to high levels of air pollution is linked to an increased risk of viral infections [47] and (the severity of) virus-induced exacerbations in asthma [48]. The health improvements are most substantial for regions with high air pollution, however interestingly, also occur when air pollution levels decrease below international standards [46]. This highlights the avoidable health risks that could result from air pollution reduction.

Clinical implications

Monitoring individual air pollution levels and effects

Our results on air pollution might have individual implications for vulnerable people, like children and older adults or people with pre-existing respiratory or cardiovascular diseases, a genetic predisposition and/or a low socioeconomic status [49]–[51]. Such people are more prone to the adverse effects of air pollution and could possibly benefit from monitoring their individual exposure levels and its' effects. This could be achieved by introducing an app that includes a map showing the air quality at somebody's home, work and/or school and certain main roads; e.g. the AirVisual app of IQAir (Staad, Switzerland) or the Clean Air Route Finder maps by Cross River Partnership (London, United Kingdom). This may assist people in reducing their air pollution exposure, as people could choose to not exercise during times with high levels of air pollution (e.g. rush hours) and to avoid routes to work/school with poor air quality. Some people

might also benefit from monitoring the effects of air pollution exposure, as this could raise awareness of both the adverse and beneficial effects of air pollution exposure and avoidance, respectively. This could be based solely on clinical symptoms on disease control, like the MASK-air app (Argentina) for self-monitoring of allergic rhinitis and asthma control [52], [53]. For a more biological approach, urine and exhaled breath testing might hold promise, however, this would require new detection methods that enable at-home testing, as described in the section 'future research' of this chapter.

Monitoring of asthma exacerbations

Monitoring of environmental triggers, including air pollution and exposure to rhinoviruses, is of high interest regarding asthma exacerbations. Especially with respect to rhinoviruses, as strategies to reduce rhinovirus exposure and its spread, remain limited to e.g. washing hands regularly, not shaking hands, and staying home when sick. Therefore, minimizing the impact of rhinovirus infections, mainly concerns improved exposure assessment, in which exhaled breath analysis might be a promising new approach for this. Our proof-of-concept study **(Chapter 6)** demonstrates the potential of non-invasive monitoring of the effect of an external (viral) trigger on the stability of the exhaled breath profile, possibly before symptoms occur [54]. The prediction of exacerbations has been studied before by Vliet *et al*. and Robroeks *et al*., in which exacerbations in children with asthma were predicted within days of onset, using exhaled breath analysis detected by gas chromatography-time-of-flight mass spectrometry (GC-TOF-MS) [55], [56]. Furthermore, multiple studies have shown there are significant associations between exhaled breath profiles and inflammatory cells in sputum or blood in patients with chronic airway diseases [29], [31], [57]–[59]. This shows how exhaled breath analysis reflects the biological processes involved in disease (in)stability, and could therefore have more potential to monitor exacerbations when compared to clinical symptoms or lung function testing. Eventually, exhaled breath monitoring could possibly assist in timely treatment adjustments and therefore limit (the severity of) exacerbations. This can have clinical benefits for asthma patients, especially for the frequent exacerbators, as (severe) exacerbations are a major cause of disease morbidity, in some cases leading to loss of lung function [60].

Future research

Validation cohorts

For both our studies **(Part II and III)**, the study cohorts were relatively small ($n \leq 24$) and homogeneous; we only included healthy young adults and mild asthmatics. For future research, we recommend to include more representative and larger cohorts, with a greater age range and (more) co-morbidities, to make the results more generalizable.

Long-term effects of air pollution exposure and reduction

As we found adverse health effects after only 5 hour exposures to air pollution in a very healthy population, we believe that studies investigating the long-term health effects of (aviation-related) UFP should follow. Although some literature exists on the long-term effects, consistent evidence is still lacking, mainly due to differences in exposure assessment and the methods for controlling confounders, especially with respect to adjustments for co-pollutants [13]. Future research on the long-term effects should be facilitated by a large UFP monitoring network and enhanced spatiotemporal models, to improve the accuracy of the exposure estimations. Moreover, researchers might want to also focus on the beneficial effects of air pollution reduction, both short- and long-term; e.g. in schools, work places, cities or areas where air pollution reduction strategies have been implemented. This would provide more evidence regarding why and how we should solve the health issues related to air pollution.

Steps towards monitoring of exposure-related metabolites

This thesis describes how the exposome has an impact on the metabolic content of the exhaled breath and urine. As these biological specimen can be easily sampled, they might be useful methods to monitor the effects of the exposome, not limited to a clinical setting, but also in an at-home setting. However, we believe this requires three main steps regarding validation and implementation: (1) validation of specific biomarkers, (2) selection or development of new, easy-to-perform and non-invasive detection methods, and finally, (3) testing these biomarkers and detection methods in an at-home setting (Figure 2).

Validation biomarkers

First, the robustness and preferably causality of new discovered biomarkers should be determined through adequate validation; an essential step for clinical implementation. Currently, most metabolic biomarkers in breath or urine are not properly validated nor are they proven to be truly specific to a certain disease [61], [62]. Therefore, the issue of false biomarker discovery should

be minimized through the use of stringent statistical approaches, for both individual metabolites and metabolic profiles. This involves an adequate sample size, avoidance of multiple hypotheses testing, and minimization of overfitting through proper internal and external validation, as well as, cross-validation [63].

For the external validation, it is important to standardize the statistical methodology and to accurately report findings, as this facilitates the comparison between studies. For this, authors could follow the already existing international standards to accurately report findings of metabolomic experiments [64], for reporting diagnostic accuracy [65], and for developing, validating and updating prediction models [66]. As part of external validation, one could consider to use a more targeted approach. This can be realized by evaluating the performance of individual biomarkers, that were discovered in previous literature, in a large replication study; making eNose data unsuitable for this approach. As an example, the study by Kos *et al*. has used this approach for the detection of *Pseudomonas aeruginosa* in the exhaled breath of cystic fibrosis patients [67]. First, they performed a literature search on VOCs that were associated with *Pseudomonas aeruginosa* infections and listed the VOCs for which multiple consistent notations were found. Next, they analysed the performance of only these biomarkers in their own patient cohort, instead of including all detected exhaled VOCs. This could be a useful approach for future metabolic research, to reduce the issue of false biomarker discovery.

From valid biomarkers towards targeted detection methods

Once specific biomarkers involved in the response to environmental triggers have been validated, steps towards new specific, easy-to-perform and non-invasive detection methods should follow. Regarding biomarkers in exhaled breath, the knowledge about individual VOCs involved in the metabolic processes of interest, as discovered by mass spectrometry techniques, could be used to introduce new and more specific sensors for eNose technology. This may require the development of novel specific nanomaterials for selective detection of breath gasses [68]. Regarding steps towards home-monitoring, the development of a cheap hand-held device would be required, that enables real-time exhaled breath analysis, and is easy-to-perform for patients [68]. Such a device should preferably be combined with an app, to allow direct instructions on how to perform the breath test and to visualize the results in real-time and over time. We do realize, that the potential of exhaled breath monitoring with such a device would mainly be suitable and cost-effective for patients with severe chronic respiratory disease who regularly have exacerbations.

Regarding urine testing, one could think of the development of a urine test strip (i.e. dipstick), most commonly known for their use in pregnancy testing and the diagnosis of urinary tract infections. This would require the development of specific reagents to the biomarkers of interest. For air pollution, this may involve specific oxidative stress markers. The main advantage of this detection method would be the extremely low costs, rapid assessment (seconds or minutes), easy practicability (insert strip into urine) and suitability for monitoring purposes, when compared to Nuclear Magnetic Resonance (NMR) and mass spectrometry techniques.

At-home monitoring studies

Lastly, prospective follow-up studies in an at-home setting should be conducted. With respect to air pollution, an interesting study could be to let people test their urine or breath at home, work or school on days with high and low levels of UFP. This would allow the investigation of long-term health effects in a prospective manner and at a more individual level; particularly of interest with respect to vulnerable people, that live in highly polluted areas.

Regarding monitoring of exacerbations, exhaled breath analysis has already shown its potential to predict exacerbations within days before onset [55], [56]. Together with our results on day-to-day changes in the exhaled breath profiles during stable and unstable periods of asthma **(Chapter 6)**, a study investigating exhaled breath monitoring in a real-life and at-home setting should follow. This could provide information on the optimal time interval between breath sampling. Based on our results and those of Robroeks et al. and Vliet et al. [55], [56], this may need to start with sampling every other day until the occurrence of an exacerbation, and two weeks after, to fully capture the fluctuations in exhaled breath profiles during the development, occurrence and recovery of an exacerbation. Eventually, the sampling frequency could possibly be reduced during stable periods, as exacerbations partly originate from existing loss of asthma control [69], [70], which would increase the convenience for patients. If exhaled breath analysis proves its ability to predict exacerbations, then randomized controlled trials would be essential to investigate whether exhaled breath analysis can assist in the titration of anti-inflammatory treatments, to hopefully supress or prevent exacerbations in asthma.

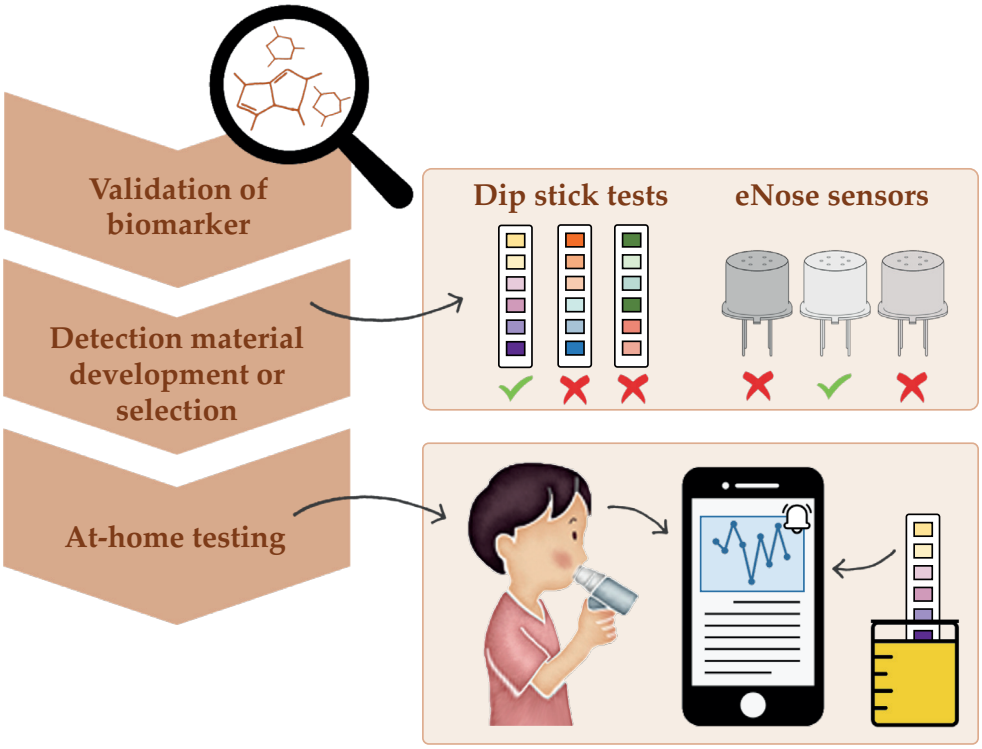

Figure 2. Overview of the next steps towards at-home monitoring of the breath and urine metabolome. First, biomarkers should be adequately validated. Next, new detection methods should be selected or developed. For exhaled breath testing, this requires the selection/development of specific eNose sensors and the development of a hand-held device that is easy to use for patients. For urine testing, dip stick tests could be created. Finally, the added value of these biomarkers and feasibility of these tests, should be investigated in an at-home setting, in which test results could be visualized in real-time, as well as, over time.

Conclusions

This thesis showed how specific parts of the exposome (i.e. air pollution and exposure to rhinoviruses) can have an impact on our health, as reflected in the reduced cardiorespiratory function and alterations in the metabolic content of the breath and urine. The effects occurred after short exposures to air pollution or shortly after exposure to a rhinovirus, even in young healthy adults. Although, future research is needed to determine how detrimental the (long-term) effects are, we do believe that our results emphasize the importance of strategies to prevent or limit these adverse effects through air pollution reduction strategies and monitoring of exposure levels and/or health effects.

References

[1] S. M. Rappaport, D. K. Barupal, D. Wishart, P. Vineis, and A. Scalbert, "The blood exposome and its role in discovering causes of disease," *Environmental Health Perspectives*. 2014.

[2] C. P. Wild, "Complementing the genome with an 'exposome': The outstanding challenge of environmental exposure measurement in molecular epidemiology," *Cancer Epidemiology Biomarkers and Prevention*. 2005.

[3] P. Vineis, P. Schulte, and A. J. McMichael, "Misconceptions about the use of genetic tests in populations," *Lancet*. 2001.

[4] C. P. Wild, "The exposome: From concept to utility," *International Journal of Epidemiology*. 2012.

[5] R. Habre *et al.*, "Short-term effects of airport-associated ultrafine particle exposure on lung function and inflammation in adults with asthma," *Environ. Int.*, vol. 118, no. January, pp. 48–59, 2018.

[6] M. Strak *et al.*, "Respiratory health effects of airborne particulate matter: The role of particle size, composition, and oxidative potential-the RAPTES project," *Environ. Health Perspect.*, vol. 120, no. 8, pp. 1183–1189, 2012.

[7] H. Xu *et al.*, "Ambient air pollution is associated with cardiac repolarization abnormalities in healthy adults," *Environ. Res.*, vol. 171, no. January, pp. 239–246, 2019.

[8] S. J. Chung *et al.*, "Association between particulate air pollution and QT interval duration in an elderly cohort," vol. 26, no. 7, pp. 1234–1242, 2016.

[9] V. C. Van Hee *et al.*, "Association of long-term air pollution with ventricular conduction and repolarization abnormalities," *Epidemiology*, 2011.

[10] P. Brinkman *et al.*, "Exhaled breath profiles in the monitoring of loss of control and clinical recovery in asthma," *Clin. Exp. Allergy*, vol. 47, no. 9, pp. 1159–1169, 2017.

[11] N. Fens *et al.*, "Repeated exhaled breath profiling by electronic noses identifies asthma exacerbations," *Am. J. Respir. Crit. Care Med.*, 2014.

[12] J. J. M. H. van Bragt *et al.*, "Identification of recent exacerbations in COPD patients by electronic nose," *ERJ Open Res.*, 2020.

[13] S. Ohlwein, R. Kappeler, M. Kutlar Joss, N. Künzli, and B. Hoffmann, "Health effects of ultrafine particles: a systematic literature review update of epidemiological evidence," *Int. J. Public Health*, vol. 64, no. 4, pp. 547–559, 2019.

[14] M. Stafoggia, S. Breitner, R. Hampel, and X. Basagaña, "Statistical Approaches to Address Multi-Pollutant Mixtures and Multiple Exposures: the State of the Science," *Current environmental health reports*. 2017.

[15] L. Agier *et al.*, "A systematic comparison of linear regression–Based statistical methods to assess exposome-health associations," *Environ. Health Perspect.*, 2016.

[16] Z. Sun *et al.*, "Statistical strategies for constructing health risk models with multiple pollutants and their interactions: Possible choices and comparisons," *Environ. Heal. A Glob. Access Sci. Source*, 2013.

[17] M. P. Keuken, M. Moerman, P. Zandveld, J. S. Henzing, and G. Hoek, "Total and size-resolved particle number and black carbon concentrations in urban areas near Schiphol airport (the Netherlands)," *Atmos. Environ.*, vol. 104, pp. 132–142, 2015.

[18] M. Mazaheri, T. E. Bostrom, G. R. Johnson, and L. Morawska, "Composition and morphology of particle emissions from in-use aircraft during takeoff and landing," *Environ. Sci. Technol.*, 2013.

[19] B. Stacey, "Measurement of ultrafine particles at airports: A review," *Atmos. Environ.*, vol. 198, no. October 2018, pp. 463–477, 2019.

[20] R. M. Harrison, D. C. S. Beddows, and M. Dall'Osto, "PMF analysis of wide-range particle size spectra collected on a major highway," *Environ. Sci. Technol.*, 2011.

[21] L. Liu, B. Urch, R. Poon, M. Szyszkowicz, M. Speck, and D. R. Gold, "Ambient particle sizes and systemic biomarkers," vol. 534, no. 6, p. 6, 2015.

[22] L. Ntziachristos, Z. Ning, M. D. Geller, and C. Sioutas, "Particle concentration and characteristics near a major freeway with heavy-duty diesel traffic," *Environ. Sci. Technol.*, 2007.

[23] M. Voogt, P. Zandveld, J. Wesseling, and N. A. H. Janssen, "Metingen en berekeningen van ultrafijn stof van vliegverkeer rond Schiphol - Voor onderzoek naar de gezondheid van omwonenden," *RIVM Rapp.*, vol. 0074, 2019.

[24] M. Pirhadi, A. Mousavi, M. H. Sowlat, N. A. H. Janssen, F. R. Cassee, and C. Sioutas, "Relative contributions of a major international airport activities and other urban sources to the particle number concentrations (PNCs) at a nearby monitoring site," *Environ. Pollut.*, 2020.

[25] P. K. Hopke, "Review of receptor modeling methods for source apportionment," *Journal of the Air and Waste Management Association*. 2016.

[26] P. Paatero, S. Eberly, S. G. Brown, and G. A. Norris, "Methods for estimating uncertainty in factor analytic solutions," *Atmos. Meas. Tech.*, 2014.

[27] M. P. Van Der Schee, T. Paff, P. Brinkman, W. M. C. Van Aalderen, E. G. Haarman, and P. J. Sterk, "Breathomics in lung disease," *Chest*, 2015.

[28] P. Brinkman, A. H. M. Van Der Zee, and A. H. Wagener, "Breathomics and treatable traits for chronic airway diseases," *Current Opinion in Pulmonary Medicine*. 2019.

[29] R. De Vries *et al.*, "Clinical and inflammatory phenotyping by breathomics in chronic airway diseases irrespective of the diagnostic label," *Eur. Respir. J.*, 2018.

[30] N. Fens *et al.*, "Exhaled air molecular profiling in relation to inflammatory subtype and activity in COPD," *Eur. Respir. J.*, 2011.

[31] V. Plaza *et al.*, "Inflammatory Asthma Phenotype Discrimination Using an Electronic Nose Breath Analyzer.," *J. Investig. Allergol. Clin. Immunol.*, vol. 25, no. 6, pp. 431–7, 2015.

[32] P. Brinkman *et al.*, "Identification and prospective stability of electronic nose (eNose)–derived inflammatory phenotypes in patients with severe asthma," *J. Allergy Clin. Immunol.*, 2019.

[33] K. M. Bendtsen *et al.*, "Airport emission particles: Exposure characterization and toxicity following intratracheal instillation in mice," *Part. Fibre Toxicol.*, 2019.

[34] S. Weichenthal *et al.*, "Long-term exposure to ambient ultrafine particles and respiratory disease incidence in in Toronto, Canada: A cohort study," *Environ. Heal. A Glob. Access Sci. Source*, vol. 16, no. 1, pp. 1–11, 2017.

[35] L. Bai *et al.*, "Associations of Long-Term Exposure to Ultrafine Particles and Nitrogen Dioxide with Increased Incidence of Congestive Heart Failure and Acute Myocardial Infarction," in *American Journal of Epidemiology*, 2019.

[36] G. S. Downward *et al.*, "Long-term exposure to ultrafine particles and incidence of cardiovascular and cerebrovascular disease in a prospective study of a Dutch cohort," *Environ. Health Perspect.*, 2018.

[37] D. R. Montagne, G. Hoek, J. O. Klompmaker, M. Wang, K. Meliefste, and B. Brunekreef, "Land Use Regression Models for Ultrafine Particles and Black Carbon Based on Short-Term Monitoring Predict Past Spatial Variation," *Environ. Sci. Technol.*, 2015.

[38] S. Weichenthal, K. Van Ryswyk, A. Goldstein, M. Shekarrizfard, and M. Hatzopoulou, "Characterizing the spatial distribution of ambient ultrafine particles in Toronto, Canada: A land use regression model," *Environ. Pollut.*, 2016.

[39] S. Ohlwein, R. Kappeler, M. Kutlar Joss, N. Künzli, and B. Hoffmann, "Health effects of ultrafine particles: a systematic literature review update of epidemiological evidence," *Int. J. Public Health*, vol. 64, no. 4, pp. 547–559, 2019.

[40] Y. Li, W. Wang, H. Kan, X. Xu, and B. Chen, "Air quality and outpatient visits for asthma in adults during the 2008 Summer Olympic Games in Beijing," *Sci. Total Environ.*, 2010.

[41] L. Mu *et al.*, "Peak expiratory flow, breath rate and blood pressure in adults with changes in particulate matter air pollution during the Beijing Olympics: A panel study," *Environ. Res.*, 2014.

[42] C. Su *et al.*, "Assessing responses of cardiovascular mortality to particulate matter air pollution for pre-, during- and post-2008 Olympics periods," *Environ. Res.*, 2015.

[43] D. Q. Rich *et al.*, "Association between changes in air pollution levels during the Beijing olympics and biomarkers of inflammation and thrombosis in healthy young adults," *JAMA - J. Am. Med. Assoc.*, 2012.

[44] P. H. Ryan *et al.*, "The impact of an anti-idling campaign on outdoor air quality at four urban schools," *Environ. Sci. Process. Impacts*, 2013.

[45] E. S. Lee, C. C. D. Fung, and Y. Zhu, "Evaluation of a high efficiency cabin air (HECA) filtration system for reducing particulate pollutants inside school buses," *Environ. Sci. Technol.*, 2015.

[46] D. E. Schraufnagel *et al.*, "Health benefits of air pollution reduction," *Annals of the American Thoracic Society*. 2019.

[47] R. N. Bauer, D. Diaz-Sanchez, and I. Jaspers, "Effects of air pollutants on innate immunity: The role of Toll-like receptors and nucleotide-binding oligomerization domain-like receptors," *Journal of Allergy and Clinical Immunology*. 2012.

[48] A. J. Chauhan *et al.*, "Personal exposure to nitrogen dioxide (NO2) and the severity of virus-induced asthma in children," *Lancet*, 2003.

[49] L. G. Hooper and J. D. Kaufman, "Ambient air pollution and clinical implications for susceptible populations," in *Annals of the American Thoracic Society*, 2018.

[50] M. N. Mead, "Who's at risk? Gauging susceptibility to air pollutants.," *Environmental health perspectives*. 2011.

[51] A. Hüls *et al.*, "Genetic susceptibility to asthma increases the vulnerability to indoor air pollution," *Eur. Respir. J.*, 2020.

[52] J. Bousquet *et al.*, "MASK 2017: ARIA digitally-enabled, integrated, person-centred care for rhinitis and asthma multimorbidity using real-world-evidence," *Clinical and Translational Allergy*. 2018.

[53] J. Bousquet *et al.*, "Allergic Rhinitis and its Impact on Asthma (ARIA) Phase 4 (2018): Change management in allergic rhinitis and asthma multimorbidity using mobile technology," *J. Allergy Clin. Immunol.*, 2019.

[54] A. Lammers *et al.*, "Increased day-to-day fluctuations in exhaled breath profiles after a rhinovirus challenge in asthma," *Allergy Eur. J. Allergy Clin. Immunol.*, 2021.

[55] C. M. Robroeks *et al.*, "Exhaled volatile organic compounds predict exacerbations of childhood asthma in a 1-year prospective study," *Eur. Respir. J.*, vol. 42, no. 1, pp. 98–106, 2013.

[56] D. Van Vliet *et al.*, "Can exhaled volatile organic compounds predict asthma exacerbations in children?," *J. Breath Res.*, 2017.

[57] N. Fens *et al.*, "Exhaled air molecular profiling in relation to inflammatory subtype and activity in COPD," *Eur. Respir. J.*, vol. 38, no. 6, pp. 1301–1309, 2011.

[58] B. Ibrahim *et al.*, "Non-invasive phenotyping using exhaled volatile organic compounds in asthma," *Thorax*, 2011.

[59] M. Basanta *et al.*, "Exhaled volatile organic compounds for phenotyping chronic obstructive pulmonary disease: a cross-sectional study," *Respir. Res.*, 2012.

[60] P. M. O'Byrne, S. Pedersen, C. J. Lamm, W. C. Tan, and W. W. Busse, "Severe exacerbations and decline in lung function in asthma," *Am. J. Respir. Crit. Care Med.*, 2009.

[61] A. H. Emwas *et al.*, "Standardizing the experimental conditions for using urine in NMR-based metabolomic studies with a particular focus on diagnostic studies: a review," *Metabolomics*. 2015.

[62] J. H. Leopold *et al.*, "Comparison of classification methods in breath analysis by electronic nose," *J. Breath Res.*, 2015.

[63] D. I. Broadhurst and D. B. Kell, "Statistical strategies for avoiding false discoveries in metabolomics and related experiments," *Metabolomics*, 2006.

[64] L. W. Sumner *et al.*, "Proposed minimum reporting standards for chemical analysis: Chemical Analysis Working Group (CAWG) Metabolomics Standards Initiative (MSI)," *Metabolomics*, 2007.

[65] P. M. Bossuyt *et al.*, "The STARD statement for reporting studies of diagnostic accuracy: Explanation and elaboration," *Clin. Chem.*, 2003.

[66] G. S. Collins, J. B. Reitsma, D. G. Altman, and K. G. M. Moons, "Transparent reporting of a multivariable prediction model for individual prognosis or diagnosis (TRIPOD): The TRIPOD statement," *BMJ*, 2015.

[67] R. Kos *et al.*, "Targeted exhaled breath analysis for detection of Pseudomonas aeruginosa in cystic fibrosis patients," 2020.

[68] S. Das and M. Pal, "Review—Non-Invasive Monitoring of Human Health by Exhaled Breath Analysis: A Comprehensive Review," *J. Electrochem. Soc.*, 2020.

[69] H. K. Reddel *et al.*, "An official American Thoracic Society/European Respiratory Society statement: Asthma control and exacerbations - Standardizing endpoints for clinical asthma trials and clinical practice," *Am. J. Respir. Crit. Care Med.*, vol. 180, no. 1, pp. 59–99, 2009.

[70] E. D. Bateman *et al.*, "Overall asthma control: The relationship between current control and future risk," *J. Allergy Clin. Immunol.*, 2010.

7

Chapter 8.
Summary

Summary

In this thesis, we investigated the short-term health effects of exposures to air pollution near a major airport and a rhinovirus challenge, in healthy subjects and/or mild asthmatics. In this summary, the main messages of this thesis are described, per chapter.

Chapter 1 is the general introduction of this thesis and describes how our health is not only determined by our genome, but also by environmental factors (i.e. exposome). Environmental exposures can have a major impact on our respiratory and cardiovascular health. This thesis focusses on the effects of air pollution and rhinoviruses. Air pollution, more specifically particulate matter, is associated with cardiopulmonary morbidity and mortality, however, the health effects of the smallest particles (i.e. ultrafine particles (UFP)), are less established, especially the ones related to aviation. Furthermore, this chapter describes how rhinovirus infections do not only have economic consequences due to school and work absenteeism, but also have a great impact on asthma control. There is a need for new biomarkers that can detect or even predict (virus-induced) disease instability in asthma. The non-invasive and easily accessible metabolites in breath and urine might be a promising tool for biomarker discovery and monitoring, as the metabolome is uniquely suited for capturing the impact of environmental factors.

Chapter 2 contains an extensive description of exhaled breath analysis regarding breath sampling, storage and detection techniques, as well as, its potential in chronic airway diseases. It describes how inert and/or disposable devices should be used for sampling, and how exhaled breath manoeuvres and ambient volatile organic compounds (VOCs) can have an impact on the exhaled breath profile. Furthermore, different exhaled breath detection techniques were summarized into three main approaches: (1) separation techniques combined with mass spectrometry for identification and in some cases quantification of multiple VOCs, (2) electronic nose (eNose) technology which is a pattern based technology holding the most potential for online and bed-side monitoring and (3) laser based techniques that are more suitable for quantification of one VOC. Finally, it describes how exhaled breath analysis may potentially improve the healthcare of chronic airway diseases regarding diagnostics, phenotyping, treatment response and detection of exacerbations and infections in asthma, chronic obstructive pulmonary disease (COPD) and cystic fibrosis.

For the investigation of the short-term health effects of exposure to air pollution, we conducted a prospective study **(Part II)**, in which 21 healthy adults were repeatedly (2-5 visits) exposed for 5 hours to the ambient air near a major airport and two highways. Before and directly after each exposure, cardiopulmonary **(Chapter 3)** and exhaled breath measurements **(Chapter 4)** were performed. Furthermore, first morning urine samples were collected the day of exposure and the next morning after **(Chapter 5)**.

Chapter 3 reports the pre- to post-exposure changes in cardiopulmonary outcomes: spirometry, fractional exhaled nitric oxide (FeNO), electrocardiography (ECG), and blood pressure. Using linear mixed effect models, these changes were related to total- and size-specific particle number concentrations (PNC). The total PNC and aviation-related UFP (particles ≤20 nm) were associated with reduced lung function (mainly Forced Vital Capacity) and a prolonged repolarization of the heart (corrected QT interval). Furthermore, we showed that road-traffic-related pollutants (i.e. black carbon, nitrogen dioxide, and particles >50 nm) were associated with increased blood pressure. The health effects were relatively small, however, they appeared after short exposures of 5 hours in a healthy and young population. Therefore, we believe that it is important to investigate the potential health effects of long-term exposure to high levels of (airport-related) UFP, especially in more vulnerable groups.

Chapter 4 reports the effects of these short-term exposures to air pollution on the exhaled breath profile detected by an eNose. Using multilevel partial least square discriminant analysis (PLSDA), linear discriminant and receiver operating characteristic (ROC) analysis, we showed that pre- and post-exposure exhaled breath measurements could be discriminated with good accuracy, especially when UFP levels were (extremely) high. Therefore, exhaled breath analysis might be an interesting and useful tool in air pollution research, as the exhaled breath is easy to collect and reflects both local and systemic metabolomic processes. On the other hand, air pollution could be an important confounder in exhaled breath analysis when exposure levels are high (e.g. smog or massive fireworks), however, to which extent this affects the disease-related breath profile of patients with (chronic airway) diseases should be further investigated.

Chapter 5 involves the results on the pre- and post-exposure changes in the urinary metabolome. Associations between the exposure and changes in the proton nuclear magnetic resonance spectroscopy (1H NMR) profiles of the urine samples were investigated with linear mixed effect models. Exposure to aviation-related UFP was associated with significant reductions in taurine,

pyroglutamate and dimethylamine concentrations. The increased utilization of taurine and synthesis of glutathione (demonstrated by the reduction in pyroglutamate) are both indicative of a heightened antioxidant response. The decrease in pyroglutamate possibly reflects an altered nitric oxide synthesis. Although these oxidative stress responses should be validated in a larger and more heterogeneous cohort, they are consistent with the effects induced by road-traffic particulates in previous literature.

With respect to the influence of viral exposures on our health, an extensive prospective study was conducted to investigate the instability of the respiratory system, and the loss of adaptive capacity in asthma, to changing environmental conditions **(Part III)**. Inflammatory, clinical, and metabolic biomarkers were monitored 60 days before and 30 days after a rhinovirus-16 (RV16) challenge in 12 non-atopic healthy and 12 atopic asthmatic participants. As part of these assessments, exhaled breath profiles were examined 2-3 times a week, using eNose technology. As described in **Chapter 6**, we found that day-to-day fluctuations in the exhaled breath profiles rapidly increased after the RV16 challenge, with distinct differences between atopic mild asthmatics and non-atopic healthy volunteers. Furthermore, the magnitude of the altered eNose fluctuations was modestly correlated with pre- and/or post-inflammatory IL-1β, IL-17A, IL-8 and TNF-α levels in nasal lavages of asthmatics, but not with cold-like symptoms and FeNO. Together, this proof-of-concept study shows the potential of exhaled breath analysis for monitoring of virus-induced exacerbations in asthma at a biological level.

Chapter 7 is the general discussion of this thesis and describes the implications of our main findings and recommendations for future research. The results on the cardiopulmonary effects of air pollution suggest the necessity of monitoring UFP levels (inter)nationally and air pollution reduction strategies. This would facilitate the investigation of long-term adverse effects of UFP exposure and the beneficial effects of air pollution reduction. Furthermore, our findings suggest that metabolites in breath and urine can be used for the detection and monitoring of the exposome's health effects, in which we highlight how exhaled breath monitoring using eNose technology could be of added clinical value regarding exacerbations in asthma. Now, steps towards validation of these biomarkers, the selection or development of specific detection methods and studies in an at-home setting, should follow.

Conclusions

This thesis shows how the exposome can have an impact on our health, as reflected in the reduced cardiorespiratory function and alterations in the metabolic content of the breath and urine. The effects occurred after short exposures to air pollution or shortly after exposure to a rhinovirus, even in young healthy adults. Although, future research is needed to determine how detrimental the (long-term) effects are, we believe our results emphasize the importance of air pollution reduction and the assessment of environmental exposure levels and/or health effects, to hopefully limit the adverse effects.

Chapter 9.

Nederlandse samenvatting

Nederlandse samenvatting

In dit proefschrift hebben we onderzoek gedaan naar de korte termijn gezondheidseffecten van blootstelling aan luchtvervuiling (nabij een groot vliegveld) en een verkoudheidsvirus. Dit hebben we onderzocht bij gezonde proefpersonen en/of astmapatiënten. In deze samenvatting worden de belangrijkste bevindingen en implicaties per hoofdstuk beschreven.

Hoofdstuk 1 is de algemene introductie van dit proefschrift en beschrijft hoe onze gezondheid niet alleen wordt bepaald door onze genen, maar ook door omgevingsfactoren (het exposoom). Blootstelling aan omgevingsfactoren kan een grote impact hebben op het hart en de longen, waarbij dit proefschrift zich richt op de effecten van luchtvervuiling en een verkoudheidsvirus. Luchtvervuiling, met name fijnstof, is geassocieerd met een verhoogde morbiditeit en mortaliteit van hart en longen. Echter, de gezondheidseffecten van de kleinste deeltjes (ultrafijn stof) zijn minder bekend, met name die afkomstig van vliegverkeer. Daarnaast beschrijft dit hoofdstuk hoe het verkoudheidsvirus niet alleen economische gevolgen heeft door school- en werkverzuim, maar ook een grote impact heeft op astma controle. Er is een nieuwe biologische marker (biomarker) nodig om (virus geïnduceerde) instabiliteit in astma te detecteren of zelfs te voorspellen. De non-invasieve en gemakkelijk te verkrijgen metabolieten (metaboloom) in de adem en urine bieden mogelijk potentie voor het ontdekken en monitoren van biomarkers, aangezien het metaboloom erg geschikt is voor het vaststellen van de effecten van omgevingsfactoren.

Hoofdstuk 2 is een uitgebreide omschrijving over uitgeademde lucht analyse, met betrekking tot de afname, opslag en detectie van ademmonsters, en de potentie van het meten van de uitgeademde lucht in chronische luchtwegziekten. Het beschrijft hoe inerte en/of wegwerp apparatuur gebruikt zou moeten worden voor het bemonsteren van adem en hoe adem manouvers en vluchtige organische componenten (VOCs) van de omgeving een impact hebben op het uitgeademde lucht profiel. Daarnaast worden voor de detectietechnieken van de adem drie verschillende benaderingen beschreven: (1) scheidingstechnieken gecombineerd met massa spectrometrie voor de identificatie en in sommige gevallen ook kwantificatie van meerdere VOCs, (2) elektronische neus (eNose) technologie, een patroon gebaseerde technologie vanwege de cross-reactieve sensoren (elke sensor detecteert meerdere VOCs) met de meeste potentie voor online metingen aan het bed, en (3) laser gebaseerde technieken die meer geschikt zijn voor het kwantificeren van één VOC. Ten slotte beschrijft dit hoofdstuk hoe de analyse van uitgeademde lucht mogelijkheden biedt om de gezondheidszorg voor

chronische luchtwegaandoeningen te verbeteren op het gebied van diagnostiek, phenotypering, de respons op behandelingen en de detectie van exacerbaties en infecties, in astma, COPD en taaislijmziekte.

Voor het bestuderen van de korte termijn gezondheidseffecten van blootstelling aan luchtvervuiling, hebben we een studie uitgevoerd **(Deel II)**, waarbij 21 gezonde volwassenen herhaaldelijk (2 tot 5 keer) 5 uur lang zijn blootgesteld aan de omgevingslucht nabij een groot vliegveld en twee snelwegen. Voor en direct na de blootstelling zijn de hart- en longfunctie testen uitgevoerd **(Hoofdstuk 3)** en de stoffen in de uitgeademde lucht gemeten **(Hoofdstuk 4)**. Verder zijn er in de ochtend voor en de na de blootstelling monsters verzameld van de urine **(Hoofdstuk 5)**.

Hoofdstuk 3 beschrijft de verschillen in hart- en long functie: longfunctie (spirometrie), uitgeademde stikstofmonoxide (FeNO), hartfilmpje (ECG) en bloeddruk. Alle ultrafijn stof tezamen (6-100 nm) en dat gerelateerd aan vliegverkeer (deeltjes ≤20 nm) waren geassocieerd met een verminderde longfunctie en een verlengde hersteltijd van een hartslag (QTc interval van het ECG). Daarnaast lieten we zien dat wegverkeer gerelateerde vervuiling (roet, stikstofdioxide en deeltjes >50 nm) geassocieerd waren met een verhoogde bloeddruk. De gemeten effecten waren klein, desalniettemin traden deze op na korte blootstellingen van 5 uur in een gezonde en jonge populatie. Daarom geloven wij dat het belangrijk is om de lange termijn effecten van blootstellingen aan hoge niveaus van (vliegverkeer gerelateerd) ultrafijn stof te onderzoeken, met name in kwetsbare groepen.

Hoofdstuk 4 beschrijft de effecten van deze korte blootstellingen aan luchtvervuiling op het uitgeademde lucht profiel, gedetecteerd door een eNose. We konden een onderscheid maken tussen de ademprofielen van voor en na de blootstelling, vooral wanneer de ultrafijn stof gehaltes (extreem) hoog waren. Hierom denken wij dat uitgeademde lucht analyse een interessante en nuttige methode kan zijn voor luchtvervuilingsonderzoek, aangezien adem makkelijk te verzamelen is en zowel lokale als systemische metabolische processen weerspiegelt. Daartegenover staat dat luchtvervuiling een belangrijke factor kan zijn waarmee rekening gehouden moet worden voor uitgeademde lucht analyses. Bijvoorbeeld wanneer de luchtvervuilingsniveaus hoog zijn, zoals bij smog en veel vuurwerk. Echter, in hoeverre dit het ziekte-gerelateerde ademprofiel van patiënten met (chronische luchtweg) ziekten beïnvloedt, is nog onbekend.

Hoofdstuk 5 beschrijft de resultaten over de veranderingen in de metabolieten in de urine. We vonden dat blootstelling aan vliegverkeer gerelateerde ultrafijn stof was geassocieerd met afnames in taurine, pyroglutamaat en dimethylamine concentraties. Het toegenomen verbruik van taurine en de aanmaak van glutathion (gedemonstreerd door de afname in pyroglutamaat) zijn beide een indicatie voor een verhoogde aanmaak van antioxidanten. Antioxidanten zijn belangrijk voor het onschadelijk maken van vrije radicalen; stoffen die worden aangemaakt tijdens oxidatieve stress en schadelijk zijn voor cellen en weefsels. De afname in dimethylamine concentraties is een indicatie voor een vermindering in stikstofmonoxide vorming. Stikstofmonoxide is een universeel signaalmolecuul betrokken bij veel biologische (ziekte)processen, waarbij een afname in de aanmaak nadelige effecten heeft op de hartfunctie. Hoewel deze effecten nog gevalideerd moet worden in een grotere en meer heterogene groep, zijn ze wel consistent met de effecten die zijn gevonden voor wegverkeer gerelateerde deeltjes in voorgaande literatuur.

Met betrekking tot de invloed van blootstelling aan een verkoudheidsvirus op onze gezond, hebben we een uitgebreide prospectieve studie uitgevoerd. Hierin hebben we de instabiliteit van de luchtwegen onderzocht bij een verandering in omgevingsomstandigheden, namelijk een verkoudheidsvirus **(Deel III)**. Ontstekingsmarkers, metabolieten en klinische gegevens werden gemeten/ verzameld 60 dagen voor en 30 dagen na een gecontroleerde blootstelling aan een verkoudheidsvirus in 12 niet-atopische (geen aanleg voor allergieën) gezonde mensen en 12 atopische (aanleg voor allergieën) astmapatiënten. Hierbij hebben we onder andere uitgeademde lucht profielen gemeten, 2-3 maal per week, door middel van eNose technologie. **Hoofdstuk 6** beschrijft de resultaten van deze studie. We hebben laten zien dat dag-tot-dag fluctuaties in het ademprofiel snel toenam na de blootstelling aan het verkoudheidsvirus, met duidelijke verschillen tussen de astmapatiënten en de gezonde vrijwilligers. Daarnaast was bij de astmapatiënten de grootte van de verandering in deze fluctuaties enigszins gecorreleerd met ontstekingsmarkers, verkregen uit de neus. Deze correlatie vonden we niet met de verkoudheidssymptomen en FeNO (een maat voor ontsteking in de luchtwegen). In deze 'proof-of-concept' studie laten we de potentie zien van uitgeademde lucht analyse voor het monitoring van exacerbaties door virale infecties in astma, op een biologisch niveau.

Hoofdstuk 7 is de algemene discussie van dit proefschrift en beschrijft de implicaties van onze belangrijkste bevindingen en aanbevelingen voor toekomstig onderzoek. De effecten van luchtvervuiling op het hart en de longen die werden gevonden in dit proefschrift impliceren de noodzaak van het (inter)nationaal

monitoren van ultrafijn stof niveaus en strategieën om luchtvervuiling te verminderen. Dit faciliteert het onderzoek naar de nadelige effecten van ultrafijn stof blootstelling op de lange termijn en de gunstige effecten van luchtvervuiling vermindering. Daarnaast suggereren onze bevindingen dat metabolieten in de adem en urine gebruikt kunnen worden voor de detectie en het monitoren van de effecten van omgevingsfactoren. Daarin lichten we toe hoe het monitoren van uitgeademde lucht door eNose technologie klinische toegevoegde waarde kan hebben op het gebied van exacerbaties in astma. Hiervoor moeten nog een aantal stappen genomen worden op het gebied van validatie van deze biomarkers, de selectie of ontwikkeling van specifieke detectie methoden en onderzoek in een thuisomgeving.

Conclusies

Dit proefschrift laat zien hoe het exposoom een impact kan hebben op onze gezondheid, zoals werd gezien in de verminderde hart- en longfunctie, als ook in de veranderingen van de metabolieten in de adem en urine. Deze effecten kwamen tot uiting na korte blootstelling aan luchtvervuiling of kort na blootstelling aan een verkoudheidsvirus, zelfs bij jonge gezonde mensen. Hoewel vervolgonderzoek nodig is om de schadelijkheid van de (lange termijn) effecten te bepalen, geloven we wel dat het belangrijk is om luchtvervuiling te verminderen en de noodzaak van het meten van (de effecten van) omgevingsblootstelling. Hiermee kunnen we mogelijk de nadelige gevolgen op de gezondheid minimaliseren.

Part V.
Appendices

A

Curriculum vitae

Ariana Lammers werd geboren op 23 juli 1991 te Seria, Brunei. Na het behalen van haar vwo-diploma aan het Roelof van Echten college in Hoogeveen, verhuisde zij in 2010 naar Enschede. Daar begon ze aan haar opleiding Technische Geneeskunde aan de Universiteit van Twente. In 2015 startte ze haar vier korte stages van elk 10 weken in het Radboud UMC te Nijmegen, tweemaal in het Amsterdam UMC locatie AMC te Amsterdam en bij Philips Research te Eindhoven. Hierna volgde haar afstudeerstage van een jaar op de intensive care (IC) van het Amsterdam UMC locatie AMC. Ze onderzocht of het ziektebeeld acute respiratory distress syndrome (ARDS) vastgesteld kon worden in de uitgeademde lucht van geventileerde IC-patiënten met behulp van zowel gas chromatografie en massa spectrometrie (GC-MS) als een compacte GC, in samenwerking met Philips Research. Na het behalen van haar masterdiploma in 2017, begon zij aan haar promotietraject op de afdeling longziekten van het Amsterdam UMC locatie AMC, onder begeleiding van prof. dr. A.H. Maitland – van der Zee, dr. A.H. Neerincx en dr. S.J. Vijverberg. Ze was verantwoordelijk voor het opstarten, uitvoeren en coördineren van een onderzoek naar de gezondheidseffecten van luchtvervuiling in samenwerking met het Rijksinstituut voor Volksgezondheid en Milieu (RIVM); de afronding hiervan is te lezen in dit proefschrift. Daarnaast heeft ze de PAPA studie opgestart en gecoördineerd, waarbij wordt onderzocht of luchtweginfecties gedetecteerd kunnen worden in de adem van patiënten met taaislijmziekte; deze studie is nog in uitvoering. Sinds mei 2021 heeft ze haar loopbaan vervolgd bij het bedrijf Quin B.V. te Amsterdam, waar ze werkt als Care Pathway Owner.

A

PhD portfolio

PhD training	Year	ECTS
General courses		
EPIC training	2018	0.1
eBROK	2018	1.0
Practical Biostatistics	2018	1.1
Research Data Management	2018	0.7
AMC World of Science	2018	0.7
Infectious Diseases	2018	1.3
Advanced Topics in Biostatistics	2019	2.1
Project Management	2019	0.6
Seminars, workshops and master classes		
Mini-course Castor EDC	2018	0.1
NRS national lung course	2018	5.0
ERS The impact of air pollution on respiratory health	2018	5.0
3-monthly Amsterdam Mucociliary Disease (AMCD) seminars	2018-2021	0.5
APROVE Career Event	2019	0.1
Precision Medicine seminars	2020	0.2
National conferences & symposia		
Attended		
NRS Young Investigator Symposium	2018-2019	0.4
Breath Summit	2018	0.6
Week van de longen	2018-2019	1.0
Amsterdam Kindersymposium (AKS)	2019	0.6
Presentations		
AKS Oral presentation	2019	0.5
International conferences		
Attended		
European Respiratory Society (ERS)	2018-2020	3.0
American Thoracic Society (ATS)	2019	1.0
UK Cystic Fibrosis Conference (UKCFC)	2019	0.5

Presentations			
ERS	Poster presentation	2018 & 2020	1.0
	Oral presentation	2019	1.0
ATS	Poster presentation	2019	0.5
UKCFC	Poster presentation	2019	0.5

Other		
Weekly Journal Clubs	2017-2021	3.0
Weekly Research Meetings	2017-2021	3.0
Monthly AMCD research meetings	2018-2021	0.5
Coordinator AMCD meetings and seminars	2018-2021	1.0

Teaching		
Supervising		
3rd year Bachelor student Gezondheid en Leven (3 months)	2018	1.0
2nd year Master students Technical Medicine (4 x 3 months)	2018-2019	4.0
3rd year Master student Technical Medicine (10 months)	2020	4.0
Lecturing		
Lecture for Groningen Research Institute for Asthma and COPD	2019	0.1
Lecture for 3rd year medical bachelor students	2019	0.1

Parameters of esteem	
ERS young investigator masterclass presentation prize	2018

Total	45.8

List of publications

1. Selley L, **Lammers A**, le Guennec A, Pirhad M, Sioutas C, Janssen N, Maitland-van der Zee AH, Mudway I, Cassee F. Alterations to the urinary metabolome following semi-controlled exposures to ultrafine particles at a major airport. *International Journal of Hygiene and Environmental Health,* 2021; 237: 113802.

2. Hagens LA, Verschueren ARM, **Lammers A**, Heijnen NFL, Smit MR, Nijsen TME, Geven I, Schultz MJ, Bergmans DCJJ, Schnabel RM, Bos LDJ. Development and validation of a point-of-care breath test for octane detection. *Analyst,* 2021; 146 (14): 4605-4614.

3. Aman J, Duijvelaar E, Botros L, Kianzad A, Schippers JR, Smeele PJ, Azhang S, Bartelink IH, Bayoumy AA, Bet PM, Boersma W, Bonta PI, Boomars KAT, Bos LDJ, van Bragt JJMH, Braunstahl GJ, Celant LR, Eger KAB, Geelhoed JJM, van Glabbeek YLE, Grotjohan HP, Hagens LA, Happe CM, Hazes BD, Heunks LMA, van den Heuvel M, Hoefsloot W, Hoek RJA, Hoekstra R, Hofstee HMA, Juffermans NP, Kemper EM, Kos R, Kunst PWA, **Lammers A**, van der Lee I, van der Lee EL, Maitland-Van der Zee AH, Mau Asam PFM, Mieras A, Muller M, Neefjes ECW, Nossent EJ, Oswald LMA, Overbeek MJ, Pamplona C, Paternotte N, Pronk N, de Raaf MA, van Raaij BFM, Reijrink M, Schultz MJ, Serpa Neto A, Slob EM, Smit MR, Smeenk F, Smit MR, Smits AJ, Stalenhoef JE, Tuinman PR, Vanhove ALEM, Wessels J, van Wezenbeek JCC, Vonk Noordegraaf A, de Man FS, Bogaard HJ. Imatinib in patients with severe COVID-19: a randomised, double-blind, placebo-controlled, clinical trial. *Lancet Respiratory Medicine*, 2021.

4. Kos R, Brinkman P, Neerincx AH, Paff T, Gerritsen MG, **Lammers A**, Kraneveld AD, Heijerman HGM, Janssens HM, Davies JC, Majoor CJ, Weersink EJ, Sterk PJ, Haarman EG, Bos LJD, Maitland-van der Zee AH. Targeted exhaled breath analysis for detection of Pseudomonas aeruginosa in cystic fibrosis patients. *Journal of Cystic Fibrosis*, 2021; S1569-1993(21)00125-9.

5. **Lammers A**, Neerincx AH, Vijverberg SJH, Longo C, Janssen NAH, Boere AJF, Brinkman P, Cassee FR, Maitland-van der Zee AH. The impact of short-term exposure to air pollution on the exhaled breath of healthy adults. *Sensors*, 2021; 21 (7): 2518.

6. **Lammers A**, Brinkman P, Nijenhuis LH, de Vries R, Dagelet YWF, Duijvelaar E, Xu B, Abdel-Aziz MI, Vijverberg SJH, Neerincx AH, Frey U, Lutter R, Maitland-van der Zee AH, Sterk PJ, Sinha A. Increased day-to-day fluctuations in exhaled breath profiles after a rhinovirus challenge in asthma. *Allergy*, 2021.

7. **Lammers A**, van Bragt JJMH, Brinkman P, Neerincx AH, Bos LD, Vijverberg SJH, Maitland-van der Zee AH. Breathomics in Chronic Airway Diseases. *Systems Medicine, Elsevier*, 2021; 1: 244–255.

8. **Lammers A**, Janssen NAH, Boere, AJF, Berger M, Longo C, Vijverberg SJH, Neerincx AH, Maitland-van der Zee, Cassee FR. Effects of short-term exposures to ultrafine particles near an airport in healthy subjects. *Environment International*, 2020; 141: 105779.

9. Abdel-Aziz MI, de Vries R, **Lammers A**, Xu B, Neerincx AH, Vijverberg SJH, Dagelet YWF, Kraneveld AD, Frey U, Lutter R, Sterk PJ, Maitland-van der Zee AH, Sinha A. Cross-sectional biomarker comparisons in asthma monitoring using a longitudinal design: The eNose premise. *Allergy*, 2020; 75 (10): 2690–2693.

Contributing authors

Amsterdam UMC, University of Amsterdam, the Netherlands
Department of Respiratory Medicine
M.I. Abdel-Aziz
M. Berger
J.J.M.H. van Bragt
P. Brinkman
Y.W.F. Dagelet
E. Duijvelaar
C. Longo
A.H. Maitland-van der Zee
A.H. Neerincx
L.H. Nijenhuis
S.J.H. Vijverberg
A. Sinha
P.J. Sterk

Department of Respiratory Medicine & Department of Intensive Care
L.D. Bos

Department of Respiratory Medicine & Department of Experimental Immunology
R. Lutter

Amsterdam UMC, University of Amsterdam, the Netherlands
Department of Respiratory Medicine
Breathomix B.V.
R. de Vries

National Institute for Public Health and the Environment (RIVM)
Centre for Sustainability, Environment and health
A.J.F. Boere
N.A.H. Janssen

National Institute for Public Health and the Environment (RIVM)
Centre for Sustainability, Environment and health
Utrecht University, the Netherlands
Institute for Risk Assessment Sciences
F.R. Cassee

University Children's hospital Basel UKBB, University of Basel, Switzerland
U. Frey

University Montpellier, IMT Mines Ales, France
EuroMov Digital Health in Motion,
B. Xu

University of Cambridge, United Kingdom
MRC Toxicology Unit
L. Selley

King's College London, United Kingdom
Randall Centre of Cell and Molecular Biophysics
A. le Guennec

University of Southern California
Department of Civil and Environmental Engineering
M. Pirhadi
S. Sioutas

Imperial College London, United Kingdom
Faculty of Medicine, School of Public Health: Environmental Research group & National Institute of Health Research, Health Protection Research Unit in Environmental Exposures and Health
I. Mudway

Dankwoord

De laatste pagina's van mijn proefschrift, waarin ik graag iedereen wil bedanken voor zijn/haar hulp, begeleiding en/of samenwerking en voor het meevieren van de mijlpalen van mijn promotietraject. Het is onmogelijk om iedereen bij naam te noemen die een aandeel heeft gehad aan dit proefschrift, dus iedereen die op een manier heeft bijgedragen, ontzettend bedankt!

In het bijzonder wil ik de volgende mensen bedanken:

Alle vrijwilligers van de RIVM, BioFluc en PAPA studie voor al jullie tijd en toewijding.

Mijn promotieteam. Mijn promotor Anke-Hilse Maitland – van der Zee voor het geven van deze unieke kans om zulk divers onderzoek te mogen doen en om zoveel congressen te mogen meemaken. Je pragmatische instelling en enthousiasme heb ik altijd erg gewaardeerd. Stiekem voelt het toch als een eer om begeleid te zijn door een vrouwelijke professor. Mijn co-promoteren Anne Neerincx en Susanne Vijverberg voor al jullie begeleiding. Anne, jij ontzettend bedankt voor de fijne en nauwe samenwerking bij de PAPA studie en de AMCD research group. Ik vond ons altijd een heel goed team samen. Susanne, bedankt voor hoe je me hebt opgevangen aan het begin van mijn PhD en tijdens het opzetten van de RIVM studie.

De leden van mijn promotiecommissie. Erg bijzonder om zo'n belangrijk moment in mijn PhD te mogen delen en mijn werk te mogen bediscussiëren met ervaren wetenschappers.

Mijn paranimfen Annika, Dominic en Demian. First, Annika and Dominic, thank you both so much for being such lovely colleagues but also friends. I enjoyed laughing, talking and of course dancing with you both, very much! Demian, voor alle mooie gesprekken en avonturen die ik steeds meer met je heb mogen delen de afgelopen jaren.

Alle studenten die ik heb mogen begeleiden: Elise, Raymond, Marjolein, Laurien, Jelle en Erik. Jullie hebben echt bijgedragen aan mijn PhD, inhoudelijk maar ook qua gezelligheid.

Alle collega's van het RIVM waarmee ik nauw heb samengewerkt, met in het bijzonder Flemming Cassee en Nicole Jansen. Flemming, het was ontzettend leuk en leerzaam om een kijkje te mogen nemen bij het RIVM. Nicole, bedankt voor alles wat je me hebt geleerd over statistiek en wetenschappelijk denken en schrijven. En verder John, Daan en Jochem.

Het Amsterdam UMC breath research team, met in het bijzonder Yennece voor de (eNose) metingen die ze heeft uitgevoerd voor alle studies. De Amsterdam Mucociliary Disease (AMCD) research group. Ontzettend mooi om gezamenlijk ons in te zetten voor onderzoek naar zeldzame en ernstige luchtwegziekten.

Het PAPA team, met in het bijzonder Renate en Jesper, die hebben gezorgd dat de studie vloeiend door kon gaan. I also would like to thank Jane Davies. Although I was not able to incorporate the work from the PAPA study in my thesis, I really enjoyed working together with you on this relevant and interesting project.

Koos Zwinderman voor alle hulp wanneer ik vastliep met de statistiek.

Alle co-auteurs die hebben meegewerkt aan mijn proefschrift. In particular, Liza Selley, with whom I have worked together very closely on the results of the RIVM study.

De longfunctie afdeling, voor hoe jullie zo ontzettend goed meedenken en -helpen met de onderzoeken van de longziekten afdeling.

Het experimentele lab, met in het bijzonder Tamara Dekker, Barbara Smit en Rene Lutter.

Mijn collega's van F5-260: Job, Levi en Elise, voor alle trein- en autoritjes, borreltjes en het heerlijke geklaag over alles en niets. Pieta, Tess en Katrien, voor jullie gezelligheid en interesse. Paul, voor al je hulp tijdens mijn PhD en voor je mede-enthousiasme omtrent het organiseren van activiteiten. Niloufar, for the lovely sleep-overs and dances. Cristina, for all your help, support and the great parties. En verder Stefania, Anirban, Simone, Rianne, Zulfan, Mahmoud, Luca, Olga, Reim, Kornel, Yolanda, Feiko, David, Yoni, Nadia, Lieke, Hanneke, Julia, Pieter-Paul en Lizzy. Jullie hebben ervoor gezorgd dat ik een ontzettend leuke tijd heb gehad in het AMC.

Jacquelien van der Vlies, Pearl Mau Asam en Marianne van der Pol voor jullie hulp bij de logistiek en ingewikkelde wet- en regelgeving.

Mijn collega's bij Quin met in het bijzonder Marcel, Emiel en het Care Pathway team. Jullie steun tijdens de laatste loodjes van m'n PhD werd erg gewaardeerd.

Iedereen van Divide, met in het bijzonder Annemiek, Carrie, Stefan, Lieke, Rob, Marloes, Kim en Mariëlle. Niet te vergeten, mijn vriendinnetjes van de basis- en middelbare school Judieke, Moniek, Judith, Roemalie, Nori, Iris en Jorien.

Mijn oud-huisgenootjes, Dorith, Wieteke, Lieke, Laura en Sanne en natuurlijk de rest van de Truman groep. Mijn huisgenootje Elke, voor de steun tijdens de laatste maanden van mijn PhD. Bedankt voor al je lieve kaartjes en cadeautjes.

En tenslotte, mijn familie. Mijn lieve broer Erik en zijn vrouw Kim, mijn lieve zus Karin en haar vriend Maaik. Natuurlijk ook mijn neefjes en nichtje Tim, Stan, Juul en Ties, die me altijd zo vrolijk maken. Mijn moeder, voor haar vrije en zorgzame opvoeding en haar steun in al mijn keuzes en mijn vader voor de stimulans, de steun en de eindeloze interesse en trots.

A